Multi-resolution remote sensing data for characterizing tundra vegetation communities on Boothia Peninsula, Nunavut

by

GITA JOAN LAIDLER

Thesis submitted to the Department of Geography
in conformity with the requirements for the degree of
Master of Science

Queen's University
Kingston, Ontario, Canada
July, 2002

Abstract

Arctic tundra environments are thought to be particularly sensitive and responsive to changes in climate, whereby alterations in ecosystem functioning are likely to be expressed through shifts in vegetation phenology and species composition. Due to the remoteness and climatic challenges of the Arctic, remote sensing may provide a viable means for estimating and monitoring these large-scale, potentially rapid changes. Therefore, the objectives of this study are to explore the relationships between conventional and soil-adjusted spectral vegetation indices (VIs), vascular plant biomass, percent vegetation cover, and moisture regimes in a tundra environment where exposed soil and gravel till have significant influence on the spectral response, and hence, the characterization of vegetation communities.

IKONOS multispectral data (4m resolution) were compared to Landsat 7 ETM+ data (30m resolution) for a study area in the Lord Lindsay River watershed on Boothia Peninsula, Nunavut. The former is thought to improve the delineation of tundra vegetation communities, and biophysical properties, characterized by small scale variations in moisture and topographic gradients. Coincident with image acquisition, extensive field data (e.g. percent cover, above-ground biomass, surface spectral characteristics) were collected for twelve 100m x 100m study plots to determine community composition. The normalized difference vegetation index (NDVI), the soil-adjusted vegetation index (SAVI) and the modified soil-adjusted vegetation index (MSAVI) were also investigated to evaluate the utility of soil-adjusted VIs that compensate for high degrees of soil reflectance.

Results suggest that vegetation community composition follows similar trends, but with somewhat lower productivity values, to previous Alaskan and Scandinavian biophysical remote sensing studies. Landsat 7 ETM+ data maintains superior spectral resolution, yet the spatial resolving power of IKONOS data proves useful in delineating within-plot microsite

variations. The utility of soil-adjusted VIs seems limited to moist communities, as there is no significant difference from NDVI over a range of cover types. Vascular plant biomass cannot be related to VIs, but moisture and percent cover are highly correlated with both types (i.e., NDVI and soil-adjusted VIs). Linear regression analysis provides a useful means of modeling percent cover variations over the entire study area. Improving estimates of vegetation community composition, distribution, and biomass are essential to determining a baseline for monitoring or modeling future changes that may follow trends of global climate change.

Dedicated to Joan Guy, and Claire Rondeau…

…in memory of their lifelong perseverance and positive outlook.

Acknowledgements

There were so many people involved in the process of creating this thesis to whom I am forever indebted, and thankful for their time and support.

I wish to thank my supervisor, Dr. Paul Treitz, for providing me the opportunity to work on this project, and to experience the Arctic from a scientific, social scientific, and personal perspective. It was a life-altering experience that I will never forget. Much appreciation is also extended for his generous financial support, his patience, and all the effort he put in to ensure the timely completion of this project. Paul, I can't thank you enough.

I wish to thank Dr. Dennis Jelinski for providing comments from an ecological perspective. I also want to thank Dr. Scott Lamoureux for his suggestions on field campaign planning and providing valuable insight throughout this process. Dr. Gerry Barber and Dr. Mark Rosenberg provided much appreciated help with statistical analyses.

Many thanks go to Craig Sheriff, Andrew Forbes, and Paul Treitz for their field sampling assistance. The Queen's Department of Geography faculty members and students are acknowledged for their support, where notable individuals include: Valerie Thomas, Kevin Lim, Nicole Gombay, Dr. Brandon Beierle, Jaclyn Cockburn, Ian Caldwell, Mark Publicover, Dr. Peter Goheen, Dr. Harry McCaughey, and Dr. Evelyn Peters. The hospitality of Peter and Deborah Maguire and Maureen Tourino made the stay in Taloyoak, Nunavut, delightful, while working with Sarah Takolik, Gina Pizzo, and the Hamlet of Taloyoak was a tremendous learning experience and a great honour. Valuable methodological suggestions were provided by Dr. Phil Teillet (Canada Centre for Remote Sensing), Dr. Jerry Arp (SpaceImaging), Dr. Esther Lévesque (Université de Québec à Trois Rivières), and Dr. Donald Walker (University of Alaska – Fairbanks). Plant identification was greatly improved by Dawn Pier (formerly with Department of National Defense).

Financial support was provided by: a National Science and Engineering Research Council (NSERC) grant (Dr. Paul Treitz), a NSERC PGSA fellowship (Gita Laidler), a Natural Resources Canada (NRCan) Earth Systems NSERC Supplement, the Northern Scientific Training Program (NSTP), and Queen's University TAships. Logistical support was provided by: the Polar Continental Shelf Project (PCSP), and the Nunavut Research Institute (notably Rick Armstrong and John McDonald).

To my family and friends who have encouraged me throughout, thank you. To the Queen's University Women's Varsity Volleyball team, thanks for keeping me sane. To my parents, Chris and Gail Laidler, who have supported me through my loftiest of goals and all related tribulations, I am truly grateful. To Vladimir Ljubicic, who continues to be my rock, thanks for your unwavering support, inspiration, and understanding.

Table of Contents

List of Figures

List of Tables

List of Equations

Chapter 1 – Introduction
An Arctic Initiation

1.1 Introduction

Arctic environments are often erroneously assumed to be barren, unproductive lands, with minimal vegetation cover. Upon greater investigation, it may be seen that these unique environments are fascinatingly complex, maintaining intricate ecosystems and plant community/environment relationships (Laidler and Treitz, 2001). It is difficult to describe a "typical" arctic vegetation, other than one that is low in stature, without trees, and occurring in the Arctic (Shaver and Chapin, 1991). The tundra zone consists of a series of vegetation belts, where succeeding belts experience decreasing diversity with increasing latitude (Young, 1994; Murray, 1997) maintaining progressively lower stature and simpler structure (Longton, 1997). Originating from a Lappish word, likely derived from Finnish *tunturi* (i.e., "treeless heights"), the word tundra reflects the mosaic of compact, wind-sculptured, plant communities usually less than one metre in height that are found within arctic tundra (Stonehouse, 1989). Despite arctic plant growth being constrained spatially, temporally, climatically, and nutritionally, there remains considerable diversity in plant growth pattern, both within and among vegetation types (Shaver and Kummerow, 1992). These characteristics provide a number of challenges, and opportunities, in attempts to determine the current state of tundra ecosystems in arctic Canada, as well as the circumpolar North.

Tundra vegetation covers approximately six million square kilometers of the Earth's surface, and is thus an important consideration in the context of global climate change (Hope *et. al.*, 1993). Arctic vegetation maintains its characteristic low stature, hardiness, resistance to cold, and many other adaptive traits, as a response to, among other things, climate. Climatic elements that most concern living systems around the world include:

ground temperature, air temperature, wind, humidity, precipitation (Stonehouse, 1989), and absorbed photosynthetically active radiation (APAR) (Baret and Guyot, 1991). Global climate change threatens to alter the climatic systems that have dominated arctic latitudes for centuries. Tundra environments are thought to be particularly sensitive and responsive to changes in climate yet it remains unclear as to how these environments will respond (Vierling *et. al.*, 1997; McMichael *et. al.*, 1999; Muller *et. al.*, 1999; Walker, 2000). Predicted rises in arctic mean annual temperatures are significantly greater than predicted global mean annual warming maintaining the potential to greatly affect permafrost – the dominant control over tundra ecosystem processes (Hope *et. al.*, 1995; Vierling *et. al.*, 1997). These forecasted changes may cause a release of previously sequestered carbon to the atmosphere, potentially shifting the global carbon budget because of the vast spatial extent of tundra environments (Vierling *et. al.*, 1997).

Alterations in arctic tundra ecosystem functioning are likely to be expressed through shifts in vegetation phenology and species composition, whereby remote sensing may provide a viable means for estimating and monitoring these large-scale, rapid shifts (Hope *et al.*, 1993; Vierling *et. al.*, 1997). Due to the remoteness and climatic challenges of the Arctic, small-scale vegetation studies may be ideal, but are not always feasible (Stow *et al.*, 1993a; Shippert *et al.*, 1995; Jacobsen and Hansen, 1999), nor necessarily useful in extrapolating to broader expanses of land (Dungan, 1995; Hope *et al.*, 1995; Lobo *et al.*, 1998; Ostendorf and Reynolds 1998; Davidson and Csillag, 2001). Remote sensing techniques maintain the potential to characterize surface variables that control carbon fluxes over landscapes (i.e., $100m^2$ to $100km^2$) or regions (i.e., $>100km^2$) (Hope *et. al.*, 1995). This capability is especially important in arctic environments where it is difficult to move across tundra landscapes on foot or vehicle, and the remoteness of study sites often limits the opportunity for field

campaigns as a function of accessibility, financial cost, and weather conditions (Stow *et. al.*, 1993a; Shippert *et. al.*, 1995; Lévesque, 1996; Jacobsen and Hansen, 1999).

1.2 Rationale

Information regarding the reflectance properties of tundra vegetation communities, and related biophysical components (e.g., leaf area index or biomass) is limited, but the prospect of making large area biophysical estimates using spectral radiance or reflectance characteristics collected from satellites is attractive for regional ecosystem studies (Hope *et. al.*, 1993; Stow *et. al.*, 1993b). The lack of detailed baseline information on tundra vegetation community composition, biomass, health, and distribution at local scales (Bliss and Matveyeva, 1992) suggests that increased attention to these phenomena in Nunavut, and other arctic regions, may be valuable contributions to future ecological modeling and monitoring practices. Canadian tundra vegetation research foci have been placed primarily on the High Arctic (e.g., Wein and Rencz, 1976; Lévesque, 1996; Henry, 1998). One study by Tarnocai and Netterville (1976) mentions Boothia Peninsula, but only reports results from the Pelly Bay study site. The most extensive publications integrating remote sensing and tundra vegetation characterization focus on the North Slope of Alaska (e.g., various publications by Walker, Stow, Hope, and Shippert, among others), sparking the idea to expand investigations into the Canadian Mid-Arctic (i.e., prostrate dwarf-shrub subzone).

Arctic tundra landscapes are characterized by multiple scales of spatial heterogeneity (McFadden *et. al.*, 1998). Scale is also an inherent consideration when selecting remote sensing systems for ecological investigations. Microscale surface irregularities and disturbance produce a fine-grained patchwork of arctic plant distribution (Murray, 1997) that has proven difficult to estimate, much less quantify, without high resolution remote sensing data (Jacobsen and Hansen, 1999). For these reasons, IKONOS high spatial, multispectral

resolution data were incorporated into biophysical remote sensing research of Boothia Peninsula to provide comparisons to the more conventional Landsat data. This work also responds to the reported need for expanding the geographical extent, and detail, of maps displaying biomass and vegetation community distribution/composition in polar regions (Walker, 1995; Walker, 2000). If tundra biophysical characteristics may be accurately estimated from remote sensing data, it provides a valuable starting point from which ecologists/botanists may evaluate soil properties, parent-material and soil moisture factors (Walker, 2000). The catalyst to understanding biophysical trends from remote sensing data is the investigation of relationships between spectral vegetation indices (VIs), how they vary across landscapes, and how these fluctuations are related to vegetation composition, biomass, and ecological site factors (Stow *et. al.*, 1993b; Walker *et. al.*, 1995). The advantages of such data are the non-destructive nature of reflectance measurements, and their recording of the actual, rather than potential, state of ecological variables, including local perturbations (Shippert *et. al.*, 1995). Furthermore, the utility of soil-adjusted VIs is thought to be an important component to investigate in arctic environments, whereby soil reflectance and moisture properties may drastically impact the conventional use of the normalized difference vegetation index (NDVI) (Huete, 1988; Qi *et. al.*, 1994).

1.3 Objectives

It is thought that biophysical remote sensing on Boothia Peninsula will follow similar trends to those established in Alaska, USA, but with lower productivity values resulting from the geographic location (i.e., harsher climate). It is hypothesized that VIs are directly related to above-ground biomass, percent vegetation cover, and surface moisture status, and can be modeled linearly over a larger study area. Soil-adjusted VIs are thought to improve linear biophysical correlations because of their accommodation for soil reflectance and moisture

properties. It is also anticipated that IKONOS data will improve the characterization of tundra vegetation communities, compared to Landsat 7 ETM+ data, through the process of unsupervised classification. To investigate these pre-conceived notions, the objectives of this study are to:

1. characterize tundra vegetation species and community composition for twelve study plots on Boothia Peninsula, Nunavut, by establishing relative species richness and percent cover dominance trends (i.e., for both species and plant functional groupings) across a variety of environments;

2. harvest and evaluate above-ground tundra plant biomass to determine plot-level biomass amounts for functional type groupings, within the same select vegetation communities, for later investigations into the correspondence of biomass to species dominance and moisture regimes;

3. investigate the influence of remote sensing data spatial resolution on plot spectral separability, and unsupervised classification results;

4. evaluate the proficiency of four vegetation indices (i.e., NDVI, SAVI (L=0.5 and L=1), and MSAVI) for distinguishing tundra vegetation communities, employing surface spectro-radiometer, IKONOS, and Landsat 7 ETM+ data;

5. evaluate the relationship of surface and satellite VIs, using linear regression analysis to determine relationships between spectral response and study plot biophysical parameters such as biomass, and percent cover; and

6. employ regression analysis to model biophysical parameters over the larger study area as a preliminary visualization technique.

1.4 Terminology

1.4.1 Arctic delineation

Stonehouse (1989) points out that polar regions are usually poorly represented in atlases, and this is mainly due to the difficulty in determining fixed boundaries to define the circumpolar region. Since the criteria used to define vegetation characteristics result in zonation delineation, and hence artificial boundary formation, Walker's (2000) division of arctic boundaries is adopted for this thesis, as his work is most closely related to current research objectives (Appendix 1).

1.4.2 Plant species identification

When identifying tundra vegetation species in attempts to describe particular community composition, various botanical families and genera will be referenced to depict dominant vegetation types. Within these genera, one, several, or many species may also be present, depending on their tolerance and requirements for soil, drainage, climate, etc., and the particular local environmental conditions (Young, 1994). Because of the analyst's lack of experience with the botany/ecology of arctic environments, descriptions focus primarily on the family or genus level, as opposed to particular species and their minimal differentiating characteristics. For further details corresponding to this depth of knowledge Burt's *Barrenland Beauties* (1991), Pielou's *A Field Guide to Arctic Plants* (1994), and various works by A. E. Porsild should be consulted.

1.4.3 Scalar considerations

Wiens (1989, 385) states that: "The very foundation of geography is scaling. In the atmospheric and earth sciences, the physical processes that determine local and global patterns are clearly linked…and their importance is acknowledged in hierarchies of scale that guide research and define subdisciplines within these sciences." Plant ecologists have long recognized the impact of sampling scale on their descriptions of dispersion/distribution of species, yet field experiments tend to focus on field plots approximately $1m^2$ in diameter (Wiens, 1989). Remote sensing observations are playing an increasing role in the study of landscapes and regions (Jelinski and Wu, 1996), expanding localized results to broader ecological extents while also initiating debates as to appropriate scales of observation.

Remote sensing spatial resolution may be considered analogous to the scale of research observations, as it is fundamentally related to the size of the surface area from which measurements comprising digital image properties are derived (Woodcock and Strahler,

1987). Employing three different remote sensing spatial scales (i.e., spectro-radiometer, IKONOS, and Landsat 7 ETM+) alleviates some of the constraints of spatial scale on the phenomena of investigation; however, including multi-resolution data influences the scale at which ground measurements are made (i.e., must correspond to the coarsest remote sensing scale in order to be informative for all data types). Because scale inherently affects the characterization of tundra biophysical properties, it is important to keep the following components of remote sensing data in mind:

1) the local variance in images is related to the relationship between the size of the objects in the scene and the spatial resolution of the sensor;
2) the spatial resolutions of high local variance change as a function of environment; and
3) multiple scales of variation in an environment will produce multiple ranges of spatial resolution with high local variance. (Woodcock and Strahler, 1987, 329).

The notion of scale offers a framework for ordering nature that may help reveal generalities from a mass of particulars (Hoekstra *et. al.*, 1991), but it is acknowledged that the selected research scale remains an arbitrary decision based on experience, data availability, and practicality. Furthermore, scale is inherently an artificial limitation imposed on natural systems, where scalar impacts on the results of tundra biophysical characterization are difficult to eliminate. The current multi-scale approach is therefore attractive and deemed useful in arctic environments where vegetation properties/distribution are highly influenced by hierarchical data aggregation.

1.5 Thesis Outline

Chapter 2 reviews the key literature involved in biophysical remote sensing of arctic environments, serving as a guide for the methods employed and directions taken in the study on Boothia Peninsula. Moreover, previous studies allow for relative comparisons from which to evaluate the accuracy and utility of, or flaws in, the adopted research approach. Chapter 3 provides a description of the study area and outlines the methods employed for all

study plot investigations: i) field sampling scheme development; ii) quadrat sampling procedures; iii) radiometric sampling; iv) conversion of surface data to plot estimates; v) image rectification; vi) image analysis; and vii) statistical analysis. Chapters 4 and 5 present results and discussion organized according to the two major research themes: i) field sampling; and ii) remote sensing. Results and discussion correspond with the order and topics presented in Chapter 3. The combined results and discussion chapters are thought to enhance the comprehension of results, as well as minimize redundancy and repetition. Discussions are summarized to comprise overarching themes in Chapter 6, reiterating conclusions into a concise synthesis. Concluding statements are supplemented by several recommendations with which future research may be improved. Finally, suggestions to facilitate the expansion of the scope of research are presented to ensure applicability within the broader ecological, political, and social dynamic.

Chapter 2 – Literature Review
Biophysical Remote Sensing Applications in Arctic Environments

2.1 Botany and Vegetation Communities

Arctic tundra vegetation comprises a mosaic of plant communities, usually compact, wind-sculptured, and less than one metre in height (Stonehouse, 1989). Lichens and mosses are prominent growth forms, but tundra communities also include shrubs, sedges, grasses, and forbs (flowering herbs other than grasses). Community composition varies in relation to soil, aspect in relation to sun, drainage, length of snow-cover, and other variables. In other words, the richest soils occur in warm, sheltered spots, providing an environment where tundra can form lush meadows, thickets of tussock grasses, and low shrubs. The poorest soils occur on rocky areas in harsh, unsheltered environments, where only a thin layer of vegetation is able to survive (Stonehouse, 1989).

2.1.1 Sedge meadows

The sedge meadow may be considered the most typical tundra vegetation (Young, 1994). It occurs on almost any flat/rolling terrain in tundra sub-zones 2 – 4 (Appendix 2), and is dominated by a mat of grass-like sedge plants (Young, 1994). This vegetation community becomes increasingly fragmented in more extreme northern areas, but even there it will be the rare greenness amongst exposed rock and gravel. While these communities may be easily distinguished, the "identification of the great majority of grasses, sedges, and rushes, in the Arctic as everywhere else, is not practicable in the field except by people already familiar with them." (Pielou, 1994, 179) There are over 100 species of sedges recorded in the Northwest Territories (Burt, 1991) and they are often confused with grasses and rushes. The number of grass species, along with the intense technicality required for adequate identification, is deemed overwhelming even by Burt (1991) and is thus minimally

documented in her book. This is a definite consideration when attempting to grasp the diversity of arctic flora, and thus aids in delimiting boundaries of detail in vegetation descriptions. Mainly floral families and genera are identified because of the reality that many of the species within a particular genus maintain such subtle differences that only experienced botanists could endeavour to distinguish species. This is an acceptable constraint as it is considered both impractical and unnecessary for this particular investigation.

2.1.2 Shrub tundra

The vegetated tundra shrub cover may range in height from 5cm in the prostrate dwarf-shrub sub-zone to 80cm in the low shrub sub-zone (Walker, 2000) (Appendix 1). Young (1994) characterizes the basic components of this shrub layer as including willow, dwarf birch, and heath, with the relative importance of each varying, but generally dominated by one vegetation type.

Riparian willows are found to follow the smallest tundra rivulets, generally becoming progressively lower in growth as streams become smaller (Young, 1994). When the heads of the streams eventually merge with overall tundra, the low willow shrubs may spread out resulting in hybrid vegetation between riparian willow and tussock tundra. Willows belong to the *Salix* genus (*Salicaceae* family) and display habitat preference variability among plant gender, i.e., females are usually found in moist, fertile, sheltered sites (greatly outnumbering males), whereas males are found in dry, exposed habitats (only slightly outnumbering females) (Pielou, 1994). These plants hybridize frequently, thus making identification difficult and requiring local floral guides for detailed consultation (Burt, 1991).

Heaths belong to the huge, worldwide family of *Ericaceae* (Young, 1994). Although this family is huge and diverse – including such familiar plants as rhododendrons, azaleas,

manzanita, heather, blueberry, cranberry, and mountain laurel – there are many shared characteristics and adaptations that make this group quite well suited to colonize cold acid bogs and tundra areas (Young, 1994). The majority of these species do not extend north of the erect dwarf-shrub sub-zone, but the few that do are usually found in stony uplands far beyond the timberline (Young, 1994; Pielou, 1994). Most heath plants closely associate with *Sphagnum* moss, both tending to invade tussock fields when moisture is abundant and fires have not occurred for long periods of time (Young, 1994). Some of the most commonly found genera and species of the heath family are outlined in Appendix 3.

2.1.3 Fell field

Young (1994) describes the term fell field as being applicable to any stony tundra area where vegetation is thin and discontinuous. Originating from the Norse word *fjell* – stony mountain slopes – fell fields usually supplant heath tundra and tussock tundra in the drier areas along a moisture and exposure gradient (Young, 1994). Among the *Dryas* genus there are a variety of species, but they are essentially a dwarf, creeping, slightly woody shrub in the rose (*Rosaceae*) family. These are so typical of fell field areas that they are almost synonymous (Young, 1994). *Dryas* is also a good indicator of calcium as it grows on calcareous soil, forming mats on gravelly, well-drained soil in areas scoured by steady winds (Burt, 1991). Also referred to as mountain avens, this flora grows in tightly interwoven mats that act as soil stabilizers (Burt, 1991), but should not be confused with plants properly referred to as avens, belonging to the *Geum* genus (Pielou, 1994).

2.1.4 Polar desert

A polar desert is essentially an extreme form of fell field, usually composed of barren areas of bare rock, shattered bedrock, and sterile gravel (Young, 1994) where only a thin, patchy covering of plant life is found (Pielou, 1994). The vegetation cover has seemingly

been reduced to near zero; however, it is difficult to find a square meter of polar desert that is absolutely devoid of any form of vegetation growth (Young, 1994). The vegetation that is present forms a single thin layer, where cryptograms, including algae, lichens (Appendix 4), mosses (Appendix 5), and hepatics, dominate and are increasingly important with increasing latitude (Pielou, 1994).

2.1.5 Landscape patterns and characteristics affecting vegetation distribution

Various landscape spatial characteristics such as tundra polygons (Appendix 6, Figure 1 & 2), and tundra hummocks (Appendix 6, Figure 3), are often called "patterned ground" (Pielou, 1994). Alternate freezing and thawing cause these particular formations, and they develop best in ground where vegetation is sparse or absent (Pielou, 1994). Arctic environments, especially polar desert where colourful flowers are scarce, must not be confused with environments that are devoid of any activity. Some of the most common patterned ground designs are outlined in Appendix 7. It is also important to note the potential effects that permafrost, tundra polygon formation, tundra hummocks, and microtopography may play on the distribution, formation, and composition of vegetation communities (Appendix 6) – all of which influence the available moisture regimes upon which community development are so dependent (Appendix 8).

These general botanical and vegetation community characteristics are important to keep in mind while examining the following sections relating to remote sensing and vegetation spectral response trends. The unique tundra landscape, low stature vegetation, and adherence to microtopographic regimes all impact the manner in which satellite imagery, surface spectra, and vegetation indices may be interpreted.

2.2 Background on Environmental Remote Sensing in Polar Regions

Arctic tundra landscapes are characterized by multiple scales of spatial heterogeneity (McFaddden *et al.*, 1998). These characteristics make them particularly challenging for remote sensing studies as well as for the design of appropriate sampling methods necessary to capture the small scale variability inherent in tundra vegetation studies. Arctic regions such as coastal plains, polar deserts, or arctic foothills are defined by climatic and hydrological influences, and may extend over hundreds of kilometers (McFadden *et al.*, 1998). Each region may be deemed a mosaic where vegetation types are found at scales ranging from 100m to 1km; while microsite variations may occur within centimeters to meters (e.g., changes in relief due to hummocks and frost action in tussock tundra) (McFadden *et al.*, 1998). Hence, spatial variability must be considered when designing sampling methods for relating field data to remote sensing images (e.g., Landsat TM with 30m spatial resolution).

Further considerations, translating into demands for efficient sampling methods, are: the expense of logistical support, the short Arctic growing season, and the inaccessibility of many northern locations (Lévesque, 1996). All things considered, large-scale vegetation diversity and abundance assessments are difficult endeavours due to short visitation time and costly field excursions, emphasizing the critical importance of accurate, efficient, and affordable sampling protocols (Lévesque, 1996) when planning *in situ* data collection for remote sensing data analysis. These same constraints form support for the utility of remotely sensed data acquisition. Remote sensing data, available at a range of spatial and spectral resolutions, offer significant potential for observing, investigating, and analyzing biophysical properties of vegetation at various landscape scales (Tieszen *et. al.*, 1997). Remote sensing data may provide continuous spatial coverage of vegetation and terrain

patterns (Stow *et. al.*, 2000). In polar regions, remotely sensed data have shown potential, depending on sensor capability, to: i) provide baseline information necessary to delineate vegetation communities (Hope *et. al.*, 1995; Spjelkavik, 1995; Rees *et. al.*, 1998); ii) outline vegetation spatial distribution (Walker *et. al.*, 1982; Stow *et. al.*, 1989; Mosbech and Hansen, 1994; Rees *et. al.*, 1998; Muller *et. al.*, 1999); iii) provide a means of estimating above-ground biomass (Hope *et. al.*, 1993; Shippert *et. al.*, 1995; Spjelkavik, 1995; Walker *et. al.*, 1995); and iv) provide input into ecological models (Stow *et. al.*, 1993b; Ostendorf and Reynolds, 1998; McMichael *et. al.*, 1999).

2.3 Satellite Sensors

Optical satellite sensors are often employed for studying various vegetation parameters, regardless of latitude. Rees *et. al.* (1998) highlight several recent investigations showing the usefulness of satellite optical data (e.g. Landsat MSS, TM, and SPOT HRV/XS data) for discriminating different vegetation units in arctic regions. There has been much effort expended in attempting to relate biophysical variables (e.g., leaf area index (LAI) or biomass) to reflectance characteristics recorded in remote sensing images but there remains limited information available on such properties for arctic vegetation communities (Hope *et. al.*, 1993).

A key concern with regards to selecting a sensor type is the spatial resolution – analogous to the scale of observations (Woodcock and Strahler, 1987). Ranging from field spectrometers to space orbiting satellites, the instantaneous field of view (IFOV) is a determining factor in the scale of observation and thus the degree of spectral aggregation occurring in each pixel (Davidson and Csillag, 2001). These discrepancies, along with other constraints (Table 2.1) must be considered when incorporating remotely sensed imagery into biophysical analyses because ecological relationships between pattern and process often vary

with scale; therefore, the selected scale of observation may not necessarily be the most appropriate for the relationship in question (Davidson and Csillag, 2001).

The most extensive tundra investigations employing satellite imagery are localized within a permanent study site initiated in 1984 by the United States Department of Energy (i.e., the *Response, Resistance, Resilience to, and Recovery from, Disturbance in Arctic Ecosystem – R^4D* project) in the Arctic Foothills of Alaska. The R^4D project aims to develop models of tundra ecosystem functioning using remotely-sensed data to provide information regarding vegetation productivity, biomass, and species composition (Hope *et. al.*, 1993). Other studies have been performed in different locations across Canada, Alaska, Europe, and Russia, but with less frequency and permanence than those established on the North Slope of Alaska (Table 2.2).

While these studies have yielded interesting and promising results, there are a few drawbacks to employing satellite imagery with a spatial resolution greater than 10m. Stow *et. al.* (1989; 1993b) found that approximately 30% of mapped vegetation units were less than the 20m nominal spatial resolution of SPOT (usually characterized by spatial scales of less than 45m in at least one dimension). For example, water track vegetation is the most difficult community type to resolve spatially because of its narrow width in the across-track dimension (Stow *et al.*, 1989; Stow *et. al.*, 1993b). This is an important consideration as it implies that SPOT (in

Table 2.1 - Constraints for satellite-based vegetation mapping

Constraint	Description
Separating vegetation classes	It is impossible to separate vegetation classes using vegetation cover characteristics if the classes are minimally vegetated – where the spectral signature is dominated by bare ground
Mixed pixels	It is impossible to map vegetation classes that occur in units of subpixel size
Spectral separability	It is impossible to distinguish vegetation classes if there is no significant difference in spectral signature
Transition zones	Satellite-based mapping does not produce sharp borders between vegetation units that maintain broad transition zones in nature

Adapted from Mosbech and Hansen, 1994

Table 2.2 – Summary of satellite sensor applications in arctic environments

APPLICATION	SENSOR	SOURCE
spectral, spatial and temporal reflectance characteristics of arctic tundra vegetation	SPOT HRV/XS (20m pixels)	Stow *et. al.*, 1993b
vegetation mapping	SPOT HRV/XS (20m pixels)	Stow *et. al.*, 1989; Stow *et. al.*, 1993b; Mosbech and Hansen, 1994
trends in NDVI causes and variations	SPOT HRV/XS (20m pixels)	Walker *et. al.*, 1995; Hope *et. al.*, 1995; Jacobsen and Hansen, 1999
estimating biophysical variables	SPOT HRV/XS (20m pixels)	Shippert *et. al.*, 1995; Walker *et. al.*, 1995
vegetation mapping	Landsat MSS (80m pixels)	Walker *et. al.*, 1982; Muller *et. al.*, 1999
vegetation damage assessment	Landsat MSS (80m pixels)	Rees *et. al.*, 1998
land cover classification	Landsat TM (30m pixels)	Mosbech and Hansen, 1994
correlating field and satellite data	Landsat TM (30m pixels)	Spjelkavik, 1995
biomass estimation	Landsat TM (30m pixels)	Spjelkavik, 1995
comparing vegetation mapping methods	AVHRR (1.1km pixels)	Muller *et. al.*, 1999
spectral-radiometric and spectral-temporal feature extraction	AVHRR (1.1km pixels)	Stow *et. al.*, 2000

multispectral mode) – and by association other coarser resolution sensors – cannot resolve some of the important components of tundra landscapes. Stow *et. al.* (1989; 1993b) then conclude that a spatial resolution of at least 10m would be necessary in order to distinguish between various tundra vegetation communities of interest. This is where advancing technology and higher resolution satellites will become increasingly important in future studies.

2.4 Tundra Spectral Characteristics

Optical remote sensing is a way of passively capturing information about surface reflectance features. Vegetation possesses unique spectral characteristics (Figure 2.1) that aid in vegetation studies and analyses. Chlorophyll molecules preferentially absorb light in the blue (0.45-0.52μm) and red (0.63-0.69μm) regions of the electromagnetic spectrum (i.e., up to 90% of incident light in these regions) (Campbell, 1996; Jensen, 2000). Also, for a typical healthy leaf, the spongy mesophyll cells may cause as much as 76% of incident near infrared (nir) energy (i.e., 0.9μm) to be reflected (Jensen, 2000). These differences in chlorophyll

Figure 2.1 - Typical reflectance characteristics of green grass, dry bare soil, and dead grass

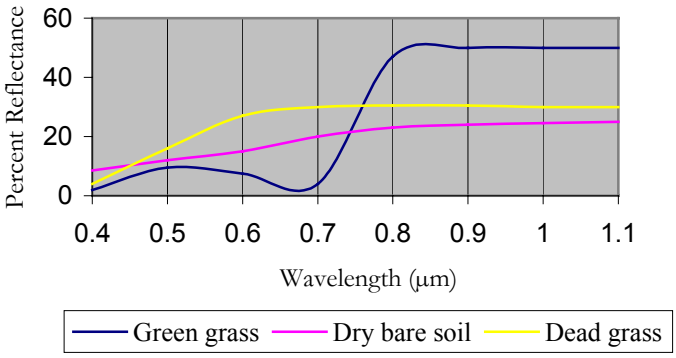

Adapted from Jensen, 1996

absorption of visible wavelengths, and nir reflectance aid in plant type discrimination, plant stress analysis, and plant growth cycle monitoring, while providing useful input parameters into a host of vegetation indices (VIs). Because this characteristic plant spectral signature is related directly to plant physiology, many VIs have been developed as a means of quantitatively measuring certain biophysical parameters of interest (Laidler and Treitz, 2001).

Reflectance measurements from both hand-held radiometers and satellite sensors have been employed in attempts to characterize spectral signatures of particular tundra cover types. Asrar *et. al.* (1989) highlight the value of data acquired from hand-held radiometers to infer plant canopy attributes without destructive sampling. Determining the relationship between vegetation quantities and spectral reflectance can be community specific, which has important implications for dealing with remotely sensed data that may include mixed pixels (Stow *et. al.*, 1993b). Often, the most accurate and informative means of gathering spectral information about a particular tundra vegetation community of interest is to perform *in situ* radiometric measurements and data collection, and even to calculate certain vegetation indices with these data. Hope *et. al.* (1993) describe three main uses of non-imaging hand-held spectral radiometers, reminding readers that this is often the first step in multi-level remote sensing studies (Table 2.3). Tundra vegetation spectral reflectance characteristics recorded using satellite sensors are often similar in trends, but different in intensity, compared to spectra collected by hand-held radiometers in the field. Spectral characteristics

Table 2.3 – Uses of non-imaging hand-held spectral radiometers

1. relationships between biophysical quantities and spectral reflectances can be established without the confounding effects of the atmosphere
2. surface targets can be accurately isolated
3. the area sampled by radiometer is small enough to be able to realistically collect an adequate sample of ground reference data, while still providing the analyst with the flexibility to exploit periods of little or no cloud cover

Source: Hope *et al.*, 1993

derived from ground-level radiometric data provide a preliminary understanding of spectral signatures that may then be expanded to interpretation at satellite imagery scales. The easiest method of comparing surface and satellite spectral reflectance characteristics is to employ ratio-based vegetation indices (VIs). However, the following must be considered when attempting to relate field and satellite reflectance data:

1. time of year and maturity in growing season has a drastic effect on NDVI values for both physiological and illumination reasons (Stow *et. al.*, 1993a; Stow *et. al.*, 1993b; Vierling *et. al.*, 1997)
2. spectral reflectance characteristics of certain vegetation types detailed in one geographic location may vary at another location, due to various local and microtopographical/microclimatological characteristics (Stow *et. al.,* 1989; Spjelkavik, 1995; Stow *et. al.,* 2000)
3. sampling schemes, radiometer height above ground, IFOV, bandwidth and sensitivity, frequency of measurements, averaging of values, calibration techniques, standard deviation of values, etc., must all be factored into analysis of the results – these elements are rarely held constant across studies, and thus must be considered when attempting to compare results (Stow *et. al.*, 1993b; Rees *et. al.,* 1998)
4. vegetation and site familiarity are generally used in spectral analysis, providing invaluable *in situ* experience crucial to producing more accurate, informative, and statistically representative results (e.g., Edwards *et. al.*, 2000)
5. it is important to consider outside factors affecting spectral signature, such as plant structure, soil acidity, geologic formations underlying the soil, site moisture, and preferential plant habitat (Shippert *et. al.,* 1995; Walker *et. al.,* 1995; Vierling *et. al.*, 1997)

2.5 Spectral Vegetation Indices

It has been demonstrated in a range of vegetated ecosystems, that simple transformations of band reflectances are more closely correlated with plant biophysical qualities, and are generally less sensitive to external variables such as solar zenith angle, than individual image bands (Laidler and Treitz, 2001). If biophysical parameters are strongly correlated with remotely sensed reflectance data, then these data maintain the potential to

predict biophysical characteristics for variable scene and sensor characteristics over large areas (for a detailed review see Treitz and Howarth, 1999). Vegetation indices are typically formed from combinations of several spectral values that are mathematically manipulated in a manner designed to provide a single value indicating the amount or vigour of vegetation within a pixel (Campbell, 1996). The most widely used of these transformations is the normalized difference vegetation index (NDVI) (Rouse *et. al.*, 1974) (Appendix 9). NDVI is useful mainly because it normalizes the difference between maximum absorption within the red wavelengths and peak reflectance in the nir. This relationship between the red and near-infrared wavelengths provides the most information regarding vegetative properties (e.g., health, stress level, green biomass, and chlorophyll content). Hence, the most common VIs utilize the information content of the red and near-infrared spectral channels (Appendix 9). The advantage of using ratios of sensitive (nir) and insensitive bands (red) is that the latter functions as a baseline that factors out variability due to causes other than variations in leaf chlorophyll content (Treitz and Howarth, 1999). Vegetation indices have been used to estimate the intercepted, photosynthetically-active radiation (IPAR) of plant canopies (Baret and Guyot, 1991; Sellers *et. al.*, 1992), above ground biomass (Boutton and Tieszen, 1983; vegetation cover (Richardson and Wiegand, 1977; Purevdorj *et. al.*, 1998), chlorophyll content (Tucker, 1977), productivity (Box *et. al.*, 1989), net above-ground primary production (NPP) (Walker *et. al.*, 1995), and leaf area index (LAI) (Baret and Guyot, 1991).

In tundra environments, NDVI is the most commonly employed VI (e.g., Hope *et. al.*, 1993; Stow, *et. al.*, 1993b; Mosbech and Hansen, 1994; Shippert *et. al.*, 1995; Walker *et. al.*, 1995; Rees *et. al.*, 1998). For an extensive review of the results of these studies – both *in situ* (Appendix 10) and remote (Appendix 11) – refer to Laidler and Treitz (2001). More

importantly, VI relations to biophysical parameter estimation such as biomass or percent vegetation cover will be discussed as essential background for later analyses.

2.6 Biophysical Parameter Estimation

Through studies of the relationship between percent vegetation cover, vegetation distribution, biomass, and spectral reflectance (via VIs) several key conclusions have been noted as informing the direction of this thesis, as well as placing results within a broader context.

Rees *et. al.* (1998) suggest that the VI concept, at least at the scale of Landsat MSS (i.e., 80m pixels), is generally of very limited use in arctic environments, and that NDVI alone may be misleading without the availability of a preliminary classification of vegetation groups so that stone, lichen, and dwarf shrub tundra groups can be adequately distinguished. Mosbech and Hansen (1994) analyzed both SPOT and Landsat TM with regards to vegetation spectral characteristics. They found that the delimitation of primary vegetation types (e.g., fen, grassland, scrub heath, copse, and snowbed) was more accurate than subdivided types. Generalized vegetation types at these scales are a function of the "mixed pixel problem", whereby factors other than the presence and amount of green vegetation (i.e., senescent vegetation, soil, gravel, shadow) combine to form composite spectra (Figure 2.2) (Asner, 1998; Davidson and Csillag, 2001). The

Figure 2.2 – Example of background materials confounding VI values

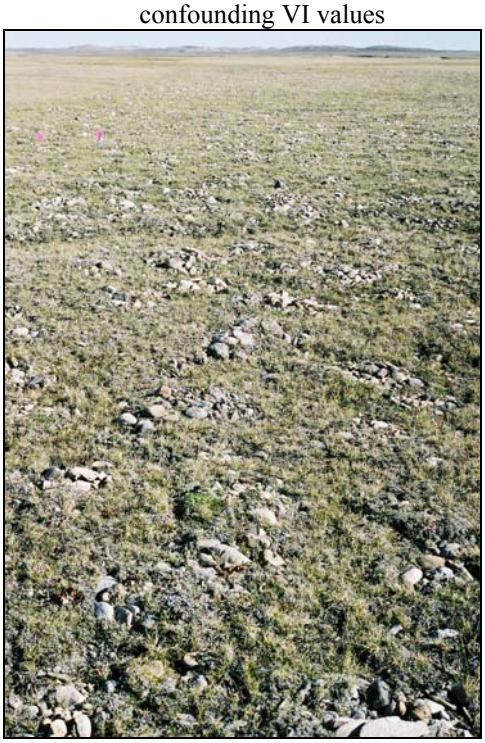

Boothia Peninsula, Nunavut; July, 2001
Exposed soil or rock surfaces tend to alter the spectral reflectance signature of vegetation that is low to the ground or sparsely distributed.

effects of composite spectra on the accurate estimation of biophysical properties over large areas, may be reduced by employing higher spatial resolution data to better depict the spatial variability within vegetation communities.

Stow *et. al.* (1993b) found that SPOT NDVI values were consistently lower than field-derived NDVI, with a slightly compressed range likely caused by atmospheric scattering of red wavelengths. Stow *et. al* (1993b) view SPOT NDVI values as potentially very useful, so long as the errors and nature of the variability are understood. Although they suggest higher spatial resolution (i.e., 9m) data would improve NDVI correlations to biophysical parameters, SPOT data provide the necessary preliminary information to: i) identify initial conditions for patch scale models by inventorying landscape conditions and their relative proportions; ii) stratify landscapes into relatively homogeneous response units for spatially-distributed modeling of material and energy transport; iii) extrapolate results of model simulations by mapping areas that are potentially sensitive to particular disturbances; and iv) assess results of landscape and regional-scale model simulations by comparative spatial pattern analysis.

Walker *et. al.* (1995) investigated the effects of soil acidity and landscape age in a comparative analysis between NDVI derived from field radiometric data and SPOT data. The mean satellite-derived NDVI of mapped acidic dry, moist, and wet vegetation units was consistently higher than those of corresponding non-acidic units; however, satellite-derived NDVI values were about 40% of field-derived NDVI values (likely due to factors associated with sun-target-sensor viewing geometry). They conclude that factors contributing to different NDVI values on different glacial surfaces include: i) a greater abundance of dry, well-drained sites on younger surfaces; ii) more non-sorted circles and stripes on younger hillslopes; and iii) more shrub-rich water tracks on older landscapes.

Many studies have investigated the relationship between VIs and biomass, going on the assumption that a VI is strongly correlated with the "amount" (biomass or LAI) of vegetation present in a given area (Hope *et. al.*, 1993; Stow *et. al.*, 1993b; Mosbech and Hansen, 1994; Shippert *et. al.*, 1995; Walker *et. al.*, 1995; Spjelkavik, 1995; Rees *et. al.*, 1998; McMichael *et. al.*, 1999). Within biophysical remote sensing literature, biomass is often referred to as the total amount of photosynthesizing vegetation present in any one area (Dancy *et. al.*, 1986; Baret and Guyot, 1991; Hope *et. al.*, 1993; Walker *et. al.*, 1995; Davidson and Csillag, 2001). Shippert *et. al.* (1995, 147) define it more formally as "a measure of the amount of carbon stored in the canopy". Vegetation indices have the potential to provide an efficient means of estimating biomass, thereby contributing to various areas of research (e.g., land cover change, vegetation mapping and monitoring, climate change).

Hope *et. al.* (1993) discuss varying degrees of success in relating NDVI values to field biomass measurements. They found that the change in NDVI was very similar to the general pattern of biomass amount, but that biomass was not a significant variable in any of the regression equations. The relationship between biophysical properties and spectral reflectance must be approached with caution because it may be unstable across a growing season due to changes in vegetation phenology, illumination and/or background conditions (Hope *et. al.*, 1993).

As part of an effort to develop multi-scale models of arctic tundra ecosystems to predict disturbance effects related to energy development in Alaska, Stow *et. al.* (1993b) indicate that there is a significant linear relationship between percent shrub cover and NDVI. In addition, they found that NDVI spatial trends along a toposequence corresponded to variations in abundance of green vegetation matter as well as vegetation composition caused by site moisture conditions (Stow *et al.*, 1993b). A related trend

regarding growing season was explored by Mosbech and Hansen (1994). They highlight that great differences in NDVI are seen during the growing season for different vegetation types due to differences in snow cover, water supply, and soil water storage. Based on the fact that peak green biomass occurs in early August, NDVI was found to have a high correlation with soil coverage by green biomass, where increasing NDVI values indicated increasing vegetation coverage along with increasing biomass.

Shippert *et. al.* (1995) describe the relationship between NDVI and biomass for community types as one that is asymptotic. It is thought that as vegetation density increases, absorption of red wavelengths approaches a maximum, beyond which any additional vegetation density would not contribute to an overall change in the reflectance signature (Laidler and Treitz, 2001). This also supports Hansen's (1991) results, which demonstrated an asymptotic relationship between NDVI and biomass for data from many Arctic and sub-arctic vegetation types. One important conclusion is that total above-ground biomass is better correlated to NDVI than green biomass alone. It is often difficult to isolate green biomass as a distinct entity, thus investigations into the utility of separating above-ground biomass into plant functional types such as shrubs (low, erect, prostrate and hemi-prostrate woody vegetation), graminoids (grasses, sedges, and rushes), forbs (various flowering tundra plants), and non-vascular plants (bryophytes and lichens) (after Walker, 2000) (Appendix 12) may provide greater insight into biomass correlations with NDVI (Laidler and Treitz, 2001). Similar to Walker *et. al.* (1995), Shippert *et. al.* (1995) discovered that LAI and biomass images created from SPOT-NDVI, using regression equations, showed trends in LAI and biomass across the North Slope of Alaska landscape that are expected on the basis of local geobotanical maps.

Besides the demonstrated linear asymptotic relationship between NDVI, LAI, and biomass, a new dimension is added by considering that the strength of the relationship is reduced with increasing detail. Shippert *et. al.* (1995) suggest that lowering the resolution of models may increase predictability by averaging out chaotic behaviour, but it will be at the expense of losing detail about the phenomenon of interest. There may not be a strong relation between NDVI and biomass within one vegetation type; however, this same relationship can be quite strong among many vegetation types. Based on this observation, NDVI may not be an appropriate means for estimating biomass if one is interested in detailed variations within a single vegetation type (Shippert *et. al.*, 1995). On the other hand, investigations into particular vegetation combinations may prove fruitful in identifying ecologically significant communities and estimating their contributions to above-ground biomass in tundra environments. If interest lies in broad changes in biomass among differing vegetation types, then NDVI may be an appropriate biomass estimator. SPOT NDVI-derived LAI and biomass images were useful in providing realistic representations of spatial variation and magnitudes of LAI and biomass on the North Slope of Alaska (Shippert *et. al.*, 1995).

2.7 Conclusions

Biophysical remote sensing in arctic environments seems to be in the exploratory stages with many attempts being made to establish methodological protocols and baseline vegetation inventories. Increasing remote sensing investigations, and research into correlation methods with surface variables of interest, are also crucial due to the logistical complexities of conducting arctic field excursions. Contemporary remote sensing research in arctic environments has provided background information on a number of issues related to the research carried out for this thesis.

First, the methodological descriptions of field data collection (e.g., percent cover analysis, biomass harvesting, spectral measurements, etc.) and image analysis (e.g., VI calculation, regression analysis, digital number manipulation, etc.) techniques supported the design of the site-specific data acquisition methods for this research.

Second, despite the fact that authors such as Stow *et. al.* (1993a), Hope *et. al.* (1993), Shippert *et. al.* (1995), and Jacobsen and Hansen (1999) have highlighted the usefulness of the large spatial extent provided by satellite sensors, it is believed that improvements in estimating biophysical aspects of arctic environments would likely result from increased spatial resolving power. Employing IKONOS satellite data (i.e., 4m pixels) represents an attempt to minimize spectral confusion caused by mixed pixels resulting from small-scale tundra vegetation variability.

Third, the narrow realm of investigation into the usefulness of VIs in arctic environments (i.e., simple ratio and NDVI) was unexpected. Thus, the use of other VIs such as the soil-adjusted vegetation index (SAVI) (Huete, 1988) – using different soil correction parameters – as well as the modified soil-adjusted vegetation index (MSAVI) (Qi *et. al.,* 1994) is proposed as an important experiment to determine the effects of exposed soil or rock cover on tundra reflectance characteristics. This may be crucial in allowing for progression towards more representative results in sparsely vegetated areas where bare soil or exposed gravel tills are highly influential on vegetation community spectral response.

Finally, as these key concepts assisted in the formulation of this research, they were also an essential source for raising questions about the results, as well as conventionally accepted findings. The literature review provides a basis for comparison, but keeping in mind the difference in geographical location – and thus vegetation community composition – it does not necessarily provide studies for validation. This is both an exciting and

frustrating aspect of the research, and must not be lost in the evaluation of the following thesis components.

Chapter 3 – Methods
Field Data Collection and Analysis

The field data collection period spanned approximately two months, from June 21st to August 17th, 2001, at a study site located on Boothia Peninsula, Nunavut. Section 3.1 provides a summary of geographic, climatic, and environmental study site conditions. In Section 3.2, the various protocols undertaken to collect estimates of percent cover, biomass, species richness and dominance, site moisture, and surface spectral data are described. Section 3.3 outlines methods employed in the laboratory to determine dry biomass weights, establish percent cover estimates, establish related ecological estimates, calibrate image and field spectral data, calculate spectral vegetation indices, and perform a variety of statistical analyses.

3.1 Study Area Description

The study site on Boothia Peninsula is located in the Kitikmeot Region of Nunavut, within the Lord Lindsay River watershed, just west of Sanagak Lake (70º11'N, 93º44'W; Figure 3.1, Appendix 13). The study area falls within the prostrate dwarf-shrub (Arctic Tundra) sub-zone described by Walker (2000) (Appendix 1). The general characteristics of the four main tundra delineations are summarized in Appendix 14. Despite the main focus remaining on sub-zone 2, it is important to keep the broader context in mind as microsite variability may allow for the presence of several different tundra environments within one sub-zone.

Characteristic of a mid-arctic ecoclimate, vegetation on the peninsula is discontinuous, generally dominated by tundra species such as *Saxifraga oppositfolia*, *Dryas integrifolia*, and *Salix spp.* (Environment Canada, 2000). Wet areas have a continuous cover of

sedges, (e.g., *Eriophorum spp.*, *Saxifraga spp.*) and mosses (Environment Canada, 2000). Boothia Peninsula consists of extensive plateaus, plains, and lowlands, with the Boothia Plateau exhibiting low rolling bedrock hills with summits up to 500m asl (Dyke, 1984). The northern and southeastern ends of the plateau maintain a blocky appearance due to the narrow intersecting valleys excavated along lines of structural weakness in the landscape (Dyke, 1984). The landscape is underlain by crystalline gneiss forming a narrow north-trending prong of the Precambrian Shield, partly covered by outliers of Palaeozoic strata (Environment Canada, 2000). "Bedrock outcroppings are common, and turbic cryosols developed on hummocky, thin, discontinuous sandy moraine are the dominant soils. Permafrost is continuous and of low ice content." (Environment Canada, 2000, 1)

The mean annual temperature for Boothia Peninsula is -15.4°C (Dyke, 1984) but the mean July temperature is 6°C (Walker, 2000). Annual precipitation is approximately 153.4mm (Dyke, 1984). During the two-week sampling period (Section 3.2.4) mean daily temperatures were 14°C with 0 mm of

Figure 3.1 – Study site location on Boothia Peninsula, NU

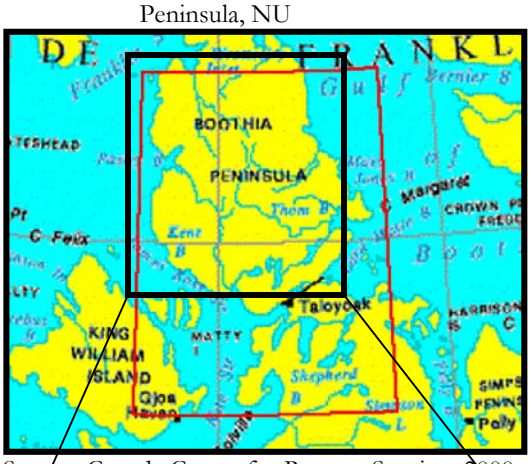

Source: Canada Centre for Remote Sensing, 2000

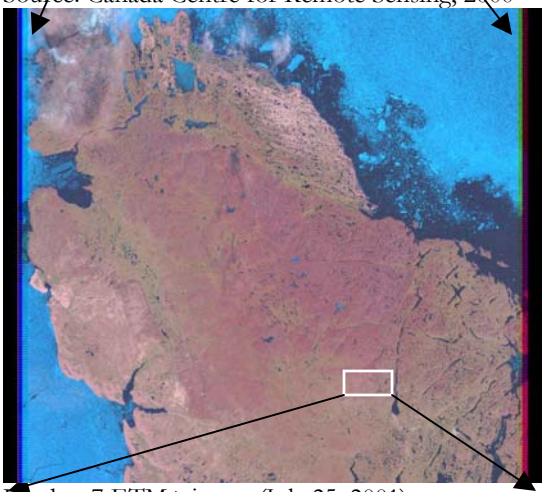

Landsat 7 ETM+ image;(July 25, 2001)

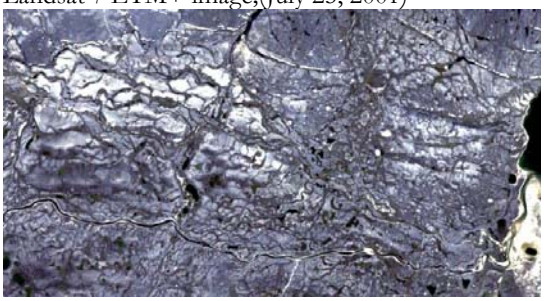

Study site subset of above Landsat 7 image

precipitation (Forbes, 2001). Over the broad study area, non-sorted circles, stripes, and ice-wedge polygons are abundant and frequently interrupt plant cover. Vascular vegetation is often restricted to protected habitats (e.g., cracks and depressions in the polygon network and areas irrigated by runoff from snow patches) (Walker, 2000). Prostrate and hemi-prostrate dwarf shrubs (<10cm) are the dominant growth form on dry and mesic sites, whereas graminoids are more prominent on wet sites. Because sample plot familiarity plays an important role in interpreting both surface and satellite image data it is necessary to consult the summary of plot characteristics in Appendix 15.

3.2 Field Sampling

3.2.1 Sampling protocols

A stratified random sampling design was applied in this study for the following reasons: i) the ease of application in the field; ii) the ability to characterize a variety of community types over their respective environmental gradients; iii) the ability to ensure relative community homogeneity within sample plots; and iv) the ability to ensure plot dimensions identifiable on satellite imagery (Laidler, 2001; Jelinski, 2001). Plots of 100m x 100m were located in what were determined to be relatively homogenous environments, where strata were determined based on spectral class and visual analysis (Section 3.2.2). Quadrats, (i.e., $1m^2$) were randomly sampled within the plot (number of quadrats was to be determined on site). The Braun-Blanquet cover class method was adopted for estimating percent cover in each quadrat, to be later translated into plot %cover values (Table 3.1). This approach is commonly employed in Arctic environments (Wein and Rencz, 1976;

Table 3.1 – Braun-Blanquet cover class estimates

Class	Range of cover (%)	Mean
5	75-100	87.5
4	50-75	62.5
3	25-50	37.5
2	2-25	15.0
1	1-5	2.5
+	<1	0.1
r	<<1	*

* Individuals occurring seldom or only once; cover ignored and assumed to be insignificant

Source: Barbour *et al.*, 1987, 186

Walker *et. al.*, 1994; Lévesque, 1996; Edwards *et. al.,* 2000) and was selected for its ease of application in the field, as well as its class flexibility. Several aspects of the sampling strategy that had to be altered *in situ* include: i) number and location of plots; ii) number, size, and distribution of quadrats within each plot; iii) sampling window duration; iv) biomass sampling procedures; and v) surface radiometric measurements.

3.2.2 Plot selection

Selecting plots of 100m x 100m (1.0 ha) within relatively homogenous areas was priority upon arrival at the field site. A large plot dimension is necessary for the accurate location of the selected areas on the coarsest resolution satellite imagery (i.e., Landsat 7 ETM+, 30m pixels). These plots were delineated in a two-faceted approach following an adaptation of the stratified random sampling method (Mueller-Dombois and Ellenberg, 1974) deemed effective for estimates of vegetated cover and biomass (Gower *et. al.*, 1999).

First, unique spectral classes were outlined using a 20-class unsupervised classification performed on a Landsat TM 5 scene (30m resolution; acquired July 16, 1998). The Isodata classification algorithm in ENVI 3.4 was used to calculate unsupervised spectral class associations. This method was chosen because of the analyst's lack of *in situ* experience (details on the utility and calculations of Isodata are presented in Section 3.3.6c). Selected sample zones were identified within perceived uniform spectral classes of at least 10 contiguous pixels, enabling both image and ground identification. Where possible, three separate plot locations were selected within each zone in an attempt to account for within-community variability. Plots were then outlined on a colour hard copy representation of the classified image to use as a field guide (Appendix 16).

Second, the selected areas were visited to determine vegetation community composition and class similarity. Each plot was located to the best approximation on the

National Topographic Survey (NTS) map sheets (i.e., 57F/2,3,6,7,11 – 1:50 000) to be explored during a site scouting mission on July 5 & 6, 2001. All original sites were observed, geographic coordinates were recorded using a Trimble Geo Explorer II Global Positioning System (GPS) unit, and a pink marker flag was placed on-site for ease of relocation. While many of the selected image classes corresponded visually to unique (between-class) and similar (within-class) communities, a few were extremely difficult to identify. In addition, several seemingly unique environments were found along the way, and were thus added as potential sampling plots. The original 25 plots (Appendix 16) were reduced to twelve (Table 3.2, Figure 3.2, Appendix 17) based on community homogeneity, community uniqueness, environmental gradient (e.g., moisture and elevation status), and accessibility. The rationale for reducing sample plots to twelve included: a) a limited sampling window; b) the duration of within-plot quadrat sampling; c) travel time/distance; d) transportation limitations and; e) sampling intensity (i.e., sufficient within-plot quadrat sample replicates).

Table 3.2 – Sampling plots

Original Plot	Plot Name
VS 1-2	P12
VS 2-1	P2
VS 2-3	P8
VS 4-2	P6
VS 5-1	P7
VS 5-2	P5
VS 6-1	P11
VS 7-2	P10
VS 10-1	P9
VS 12-1	P4
VS 15-1	P1
VS 16-1	P3

The twelve plots were established by recording the corner and centre coordinates for each. Outlining plots necessitated return visits to position corners in a manner that best encompassed the perceived 1.0 ha community homogeneity. To maintain consistency, plots were delineated as squares where corner one (C1) was always at the northwest extremity (facing the East Tributary of the Lord Lindsay River) and corner three (C3) was always at the southeast extremity (Appendix 18). Each corner was marked with an appropriately labeled flag, and coordinates were recorded for later plot identification on satellite imagery (Figure

3.2, Appendix 17). A report of GPS accuracy and coordinate systems is provided in Appendix 19).

Figure 3.2 – Study plot locations

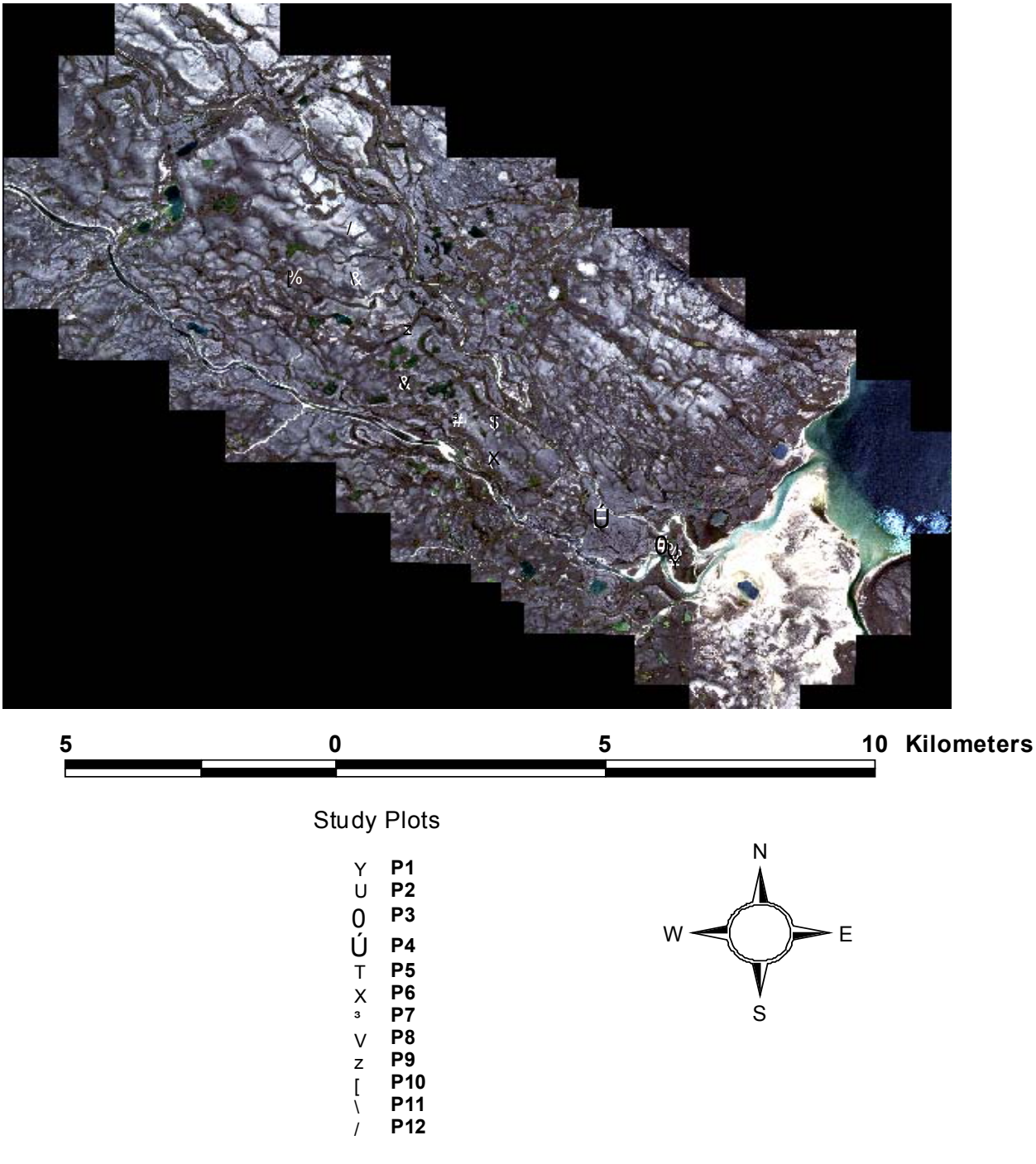

3.2.3 Quadrat number, size, and distribution

The realities of being in the field, and acquiring an understanding of weather and transportation constraints on sampling time and efficiency, led to heeding the advice of Wein and Reincz (1976), who state that a practical number of within-plot replicates be determined based on the maximum number possible within the available time period. A number of issues were considered for determining an appropriate sampling strategy given the time restrictions (de Gruijter, 1999) (Appendix 20). Wein and Rencz (1976) suggest that the number of samples required to measure total cover varies from approximately 10 for meadows to 100 for polar deserts. Quadrat sizes for arctic environments tend to be $<1m^2$ due to the small vegetation stature and local variability (Wein and Rencz, 1976; Shippert *et. al.*, 1995; Walker *et. al.*, 1995; Lévesque, 1996; Edwards *et. al.*, 2000). A variety of sample sizes have also been employed depending on the number of community types selected for analysis, and time available.

Lévesque (1996, 161) suggests that a larger number of smaller, randomly placed quadrats – at least 40-60, 50cm x 50cm quadrats – organized in a stratified random sampling design, "allows for more objective, reliable, and manageable estimates than the survey of fewer larger plots." Therefore, a series of fifty 50cm x 50cm quadrats ($0.25m^2$) were randomly located within each plot (Appendix 21). The $12.5m^2$ total sampling area also complies with the minimum area for tundra environments ($10\text{-}25m^2$) determined by Mueller-Dombois and Ellenberg (1974) and corroborated by Lévesque (1996). This area is considered sufficiently representative of community composition because only two plots could be deemed similar to polar desert cover – which displays much more variable composition than tussock or wet sedge tundra, and tends to require higher aerial coverage to ensure adequate characterization. The number of quadrats was also adopted because of the

time required to sample 50 quadrats for %cover of species – including the biomass and photo samples (Section 3.2.5) – and accounting for travel time (totaling approximately half a day at best). The 0.25m^2 quadrat size was a feasible compromise based on the variety of sizes described throughout the literature. It was also more feasible than the 1m^2 quadrat for estimating %cover because it did not require any movement around the perimeter to maximize the view (Figure 3.3). These quadrat dimensions also facilitated the characterization of microsite variations within each plot representing the local heterogeneity that combines to form a plot-scale homogenous spectral response in satellite imagery.

3.2.4 Sampling window

Figure 3.3 – Visual percent cover analysis using 50cm x 50cm quadrat in P1

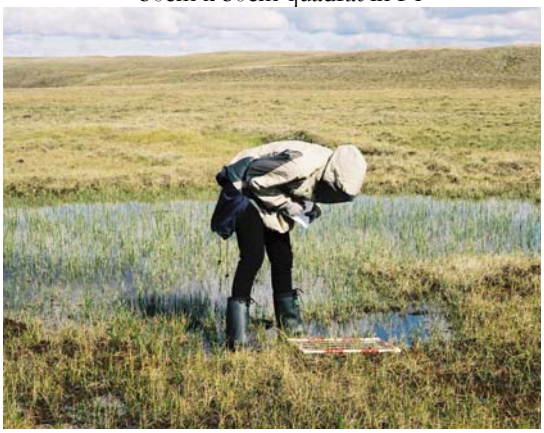

Photo: Craig Sheriff, July 19, 2001

As mentioned previously, the time to complete sampling protocols is a limiting factor in the amount and quality of data acquired in any field campaign (Jacobsen and Hansen, 1999; Shippert *et. al.*, 1995; Stow *et. al.*, 1993a; Lévesque, 1996). The last two weeks of July were pre-selected to fall as closely as possible to peak vegetative development (Shaver and Chapin, 1991; Shaver *et. al.*, 1992) and ensure phenology stage similarity. These efforts aim to minimize sample variance due to external factors associated with temperature, snowmelt, and precipitation. Furthermore, the sampling period corresponded to the IKONOS image acquisition window. Sampling of the twelve study plots was completed between July 17 and July 28, 2001. Radiometric sampling procedures (Section 3.2.6) were completed over a three day period (August 6 – 8, 2001).

3.2.5 Quadrat sampling

A method of data entry into field books was adapted from Edwards *et. al.* (2000). For each quadrat, the microsite, topographic position, and exposure variables were estimated (Appendix 22), as well as %cover using the Braun-Blanquet class estimates (Table 3.1) for each associated species code (Appendix 23). Estimating %cover was performed with the aid of 10cm red and white divisions on the 50cm x 50cm quadrat, as well as a reference grid of string following the same 10cm intervals (Figure 3.4), to allow for more accurate determination of a species' relative abundance. Locational data were collected for each quadrat using the GPS.

Figure 3.4 – Quadrat with 10cm reference grid

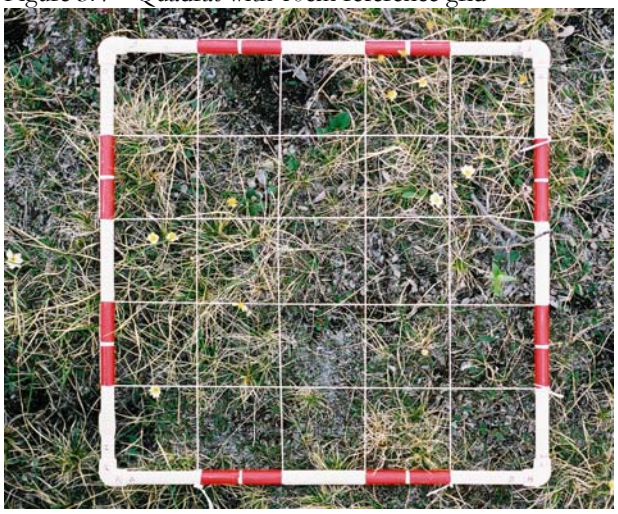

Photo: Gita Laidler, July 17, 2001

Table 3.3 – Relative moisture estimates

Code	Summary	Description
1	Very dry	**Very little moisture**, soil does not stick together
2	Dry	**Little moisture**, soil somewhat sticks together
3	Damp	**Noticeable moisture**, soil sticks together but crumbles
4	Damp to moist	**Very noticeable moisture**, soil clumps
5	Moist	**Moderate moisture**, soil binds, but can be broken apart
6	Moist to wet	**Considerable moisture**, soil binds and sticks to fingers
7	Wet	**Very considerable moisture**, water drops can be squeezed out of soil
8	Very wet	**Much moisture** can be squeezed out of the soil
9	Saturated	**Very much moisture**, water drips out of soil
10	Very saturated	**Extreme moisture**, soil is more liquid than solid

Source: Edwards *et. al.*, 2000

For every fifth quadrat (i.e., 10 in total) the relative soil moisture value was estimated (Table 3.3). The term "relative soil moisture" is employed because the numbers recorded are more a reflection of comparative soil moisture along the described gradient instead of exact estimates. Furthermore, in wet, and sometimes moist plots, the moisture value is a measure

of moisture of the organic layer, as the soil layer may be too deep (Figure 3.5). Qualitative descriptors of overall plot characteristics such as topographic position and exposure (Appendix 22), as well as landform and surficial geomorphology (Appendix 24) were also recorded, to gather as much information as possible about the selected vegetation community. Appendix 25 contains an example of all field book entries for one sample plot.

Similar to relative soil moisture, above-ground biomass was collected for a total of 10 quadrats in each plot (i.e., every fifth quadrat). For reference purposes a photograph was taken of each biomass quadrat, prior to the harvest, using a 52mm Nikon camera mounted on a leveled tripod approximately 1.5m above the quadrat (Figure 3.6).

Figure 3.5 – Generalized view of dry, moist, and wet tundra

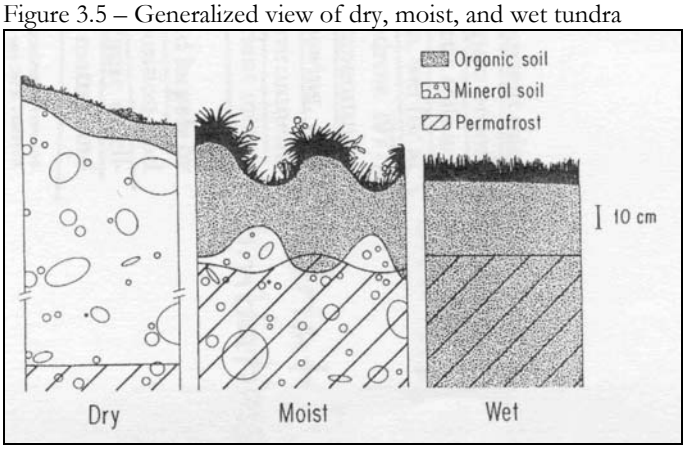

Source: Nadelhoffer *et. al.*, 1992, 282

When harvesting above-ground biomass, plant species were sorted into functional types, forming four sample collection groups: graminoids, forbs, shrubs, and mosses (Table 3.4). These groups were selected for correlation analysis with %cover functional types for greater insight into community composition. Generally, graminoids were first clipped away, then forbs were harvested (usually individually). Following this, shrubs were removed, and mosses were collected within a 10cm x 10cm reference square for later multiplication by %cover area (Figure 3.7). Often vegetation stature was so minimal that hand-picking was

Figure 3.6 – Photograph set-up

Photo: Paul Treitz, August 8, 2001

required to collect the majority of functional types, but in areas of increased moisture, graminoids could be clipped quite efficiently using garden shears.

Biomass samples were weighed wet in the field and air-dried in tents as long as possible (space was a limiting factor). Biomass samples were transferred into paper bags to facilitate air-drying and prevent rotting (Figure 3.8). Samples were later oven-dried to their final dry weight (Section 3.3.1). For all biomass records the appropriate container weight was subtracted from the scale value (Table 3.5).

Table 3.4 – Vegetation functional types and species codes

Vegetation Functional Type	**Code**
Graminoids	**7**
Arctagrostics latifolia	PG
Carex aquatilis	CG
Carex bigelowii	LG
Equistem variegatum	EV
Eriophorum species	ESP
Eriophorum augustifolium	EA, RG
Unidentified grass/sedge	GR
Forbs	**22**
Armeria maritima	AM
Brassica sp.	BS
Cardamine digitata	CD
Cardamine pratensis	CP
Cardamine species	CS
Chrysanthemum integrifolium	CI
Circular leaf plant	CR
Lesqurella arctica	LA
Melandrium apelatum	MA
Oxytropis arctobia	OA
Oxytropis maydelliana	OM
Oxyria digyna	OD
Papaver radicatum	PR
Pedicularis capitata	PC
Pedicularis lanata	PL
Pedicularis sudetica	PS
Potentilla vahliana	Y6
Saxifraga hirculus	SX
Saxifraga oppositifolia	SO
Stellaria longipes	PP, WF
Stellaria species	TF
Undifferentiated leaves	UL

Vegetation Functional Type	**Code**
Shrubs	**6**
Cassiope tetragona	CA
Dryas integrifolia	DI
Erect salix	EW
Prostrate salix	PW
Salix herbacea	SH
Salix reticulata	SR
Bryophytes	**3**
Indistinguishable moss species	MO
Mushroom	MU
Lycopodium species	LS
Lichens	**5**
Cladina species	CL
Thamnolia subliformis sp.	TS
Unknown yellow lichen	YL
Xanthoria elegans	JL
Rock tripe	RT

* Divisions formed after Walker, 2000 (Appendix 12)

Figure 3.7 – Biomass harvest process

a) cutting off shrub layer (P4)

Photo: Paul Treitz, August 8,. 2001

b) Q6 (P9) before biomass harvest

Photo: Gita Laidler, July 28, 2001

c) Q6 (P9) after biomass harvest

Photo: Gita Laidler, July 28, 2001

3.2.6 Radiometric sampling

A portable FieldSpec®Pro spectro-radiometer by Analytical Spectral Devices (ASD) (Boulder, CO) was employed for all surface radiometric measurements. For each spectral sample an 8° field of view (FOV) foreoptic was used to record spectral data for an area approximately 10cm in diameter (with foreoptic mounted at 0.6m above the area of interest) (Figure 3.9). Surface spectra were selected on the basis of their homogeneity, but also as a representation of cover types found in the 12

Figure 3.8 – Biomass sample air-drying

August 12, 2001

Table 3.5 – Container weights and errors

Container	Weight	Error
10" plastic bag	8.1g	+/- 0.2g
Small baking tin	13.8g	+/- 0.3g
Large baking tine	16.7g	+/- 0.1g
Scale	n/a	+/- 0.2g

sample plots (as opposed to pure endmember spectra). Each spectral sample was located in the middle of a 0.25m^2 quadrat where %cover had been estimated. After taking a reference photograph (Section 3.2.5) and collecting surface spectra, aboveground biomass was harvested (Section 3.2.5) from each ASD quadrat for evaluation of relationships between biomass and surface spectral characteristics. A total of 18 quadrats, within 7 study plots, were selected to record spectral data (Table 3.6). For each of these 18 quadrats, spectral reflectance measurements were calculated by averaging a total of 250 individual samples to provide one spectral response curve ranging from visible to mid-infrared wavelengths (0.35 – 2.5μm). To account for in-sensor and atmospheric variations, dark current and white reference (Spectralon Reflectance Target calibrated for an 8° foreoptic by Labsphere®, Sutton, N.H., October 15, 1999) calibration measurements were acquired before and after each reflectance calculation.

Figure 3.9 – Acquiring surface spectral measurements with the portable spectro-radiometer

Photo: Paul Treitz, August 8, 2001

Table 3.6 – Spectral quadrat plot locations

Spectral quadrat	Plot
A1	P1
A2	P1
A3	P1
A4	P2
A5	P2
A6	P2
A7	P3
A8	P3
A9	P4
A10	P4
A11	P5
A12	P5
A13	P5
A14	P5
A15	P6
A16	P6
A17	P9
A18	P9

3.3 Laboratory Analysis

3.3.1 Biomass

For deriving estimates of dry biomass the air-dried biomass samples were oven-dried to ensure complete moisture removal. Samples were dried at 60°C for 4 hours and weighed immediately to ensure minimal moisture accumulation after drying. This method was

applied based on methods presented by Lévesque (2001) after determining the amount of time necessary to provide less than a 3 – 4% change in weight. Therefore, the initial process included the following:

1) Weigh air-dried biomass
2) Dry at 60°C for 4 hours
3) Weigh
4) Dry at 60°C for 4 hours
5) Weigh
6) Determine %change for stage 3 and 5 from original weight (end if <4%)

The above format was conducted for the first 64 samples, and due to small individual sample size and minimal texture variations it was possible to dry remaining samples to a constant weight after only 4 hours. To maintain consistency in biomass records, only the dry weights after 4 hours were included in analysis of plot-level biomass estimates, and appropriate container weights were subtracted from final biomass amounts (Table 3.5).

Because above-ground biomass was only harvested for 10 quadrats per plot, sample size becomes an empirical constraint for all biomass analyses. The final dry weights were documented by plant functional type within each quadrat. Original biomass values are expressed as $g/0.25m^2$, but were converted to g/m^2 values to comply with conventional biomass estimates (Hope *et. al.*, 1993; Shippert *et. al.*, 1995; Walker *et. al.*, 1995; Edwards *et. al.*, 2000). From this point onwards, all biomass values are expressed as g/m^2 values. Plot biomass estimates were made by calculating the mean for each plant functional type (the sum of these values indicate total above-ground plot biomass in g/m^2).

The ten relative moisture estimates associated with each biomass quadrat were combined to form one plot level moisture value using the median of the samples, as is appropriate for ordinal data (Barber, 1988).

3.3.2 Percent cover estimates

Microsite conditions tend to be discontinuous and patchy at the small sampling scale within quadrat dimensions, thus species population densities may exhibit a multimodal distribution over space (Brown, 1984). However, averaging the %cover species data from many replicate sites within the plot causes this pattern to disappear (Brown, 1984), and was therefore selected as the more straightforward method of determining plot-level %cover values. Furthermore, this simplistic approach is deemed more efficient than a hierarchical ecological classification scheme such as the two-way indicator species cluster analysis (TWINSPAN) approach based on previously demonstrated poor correspondence between TWINSPAN hierarchies and spectral classes (Treitz *et al.,* 1992). van Groenewoud (1992) does not recommend TWINSPAN for ecological analyses based on his findings of very erratic results for anything but the simplest ecological gradient. In demonstrating that qualitative dominant cover estimates provide equal validation of image classification compared to complex quantitative analysis, as well as higher correlation between field and remote spectral response (Treitz *et. al.*, 1992), the following methods are deemed appropriate for the current biophysical remote sensing study.

Braun-Blanquet (BB) cover estimates were entered into a spreadsheet for each species in each quadrat of the twelve sample plots. While vegetation cover is conventionally defined as "the vertical projection of the crown or shoot area of vegetation to the ground surface expressed as fraction or percent of the reference area" (Purevdorj *et. al.*, 1998, 3519) its definition changes with the consideration of remote sensing techniques. Therefore, plot %cover is calculated to reflect "the green vegetated area which is directly detectable by the sensor from any view direction" (Purevdorj *et. al.*, 1998, 3519). The following steps were conducted to determine the dominant cover type for each plot:

i) BB class codes were converted to their associated mean value (Table 3.1) for each quadrat;
ii) all species not present in a particular quadrat (but present elsewhere in the plot) were assigned a value of 0;
iii) for all quadrats containing a rare (r) species, %cover was deemed insignificant and was also assigned a %cover value of 0;
iv) species – and their associated quadrat %cover value – were sorted into plant functional groups (i.e., graminoid, forb, shrub, moss, lichen, or non-vegetated cover) (Table 3.4);
v) the %cover of each species within each functional type was summed to form a total %cover value per functional group per quadrat;
vi) the mean total functional type %cover for all 50 quadrats within the plot was calculated to determine the dominant cover type;
vii) the variance of total functional type %cover for all 50 quadrats within the plot was calculated to determine the variability of the dominant cover type; and
viii) the mean and variance of total vegetated %cover (for all 50 quadrats) was calculated to determine total plot %cover.

3.3.3 Species dominance

Estimating species diversity for the twelve study plots is complex due to the author's inexperience in arctic plant identification and the constraints of 50 replicates per plot. Therefore, the distinction between richness, frequency, and dominance must be made in order to represent within-plot species in the most appropriate manner.

The measure of species diversity alone is often unsatisfactory (Goodall, 1970), so species-based analyses will be evaluated from three different perspectives. Here, *richness* refers to the number of species present in a given plot area. To calculate plot richness a species was added to a running plot tally if it was present in any quantity within a %cover quadrat, an ASD quadrat, or if it was seen in passing within the plot. These estimates are thus very conservative and are anticipated to be underestimates of the true biological richness of tundra plants in this region of Boothia Peninsula. Where plants could not be identified to a species, genus, or even family level, a naming convention was assigned that best described their characteristics. Despite species identities being confirmed, and improved, by Ms. Dawn Pier (environmental biologist/plant toxicologist, formerly with the

Department of National Defense) there remains substantial uncertainty in these estimates. Hence, species richness numbers provide a relative estimate for comparison purposes but cannot be taken as quantitative estimates in a botanical or ecological sense.

The *frequency* of species distribution within a plot (only using the 50 quadrats sampled for %cover) adds a new dimension to species analysis. Plot species frequency was calculated by totaling the number of quadrats in which a particular species appeared. Thus, the frequency measure relates to species dispersion around the plot.

The frequency measure denotes a presence or absence characterization of species diversity, but since no relative abundance value is associated with frequency it alone cannot be employed to describe vegetation community *dominance* – the main issue of relevance to remote sensing image analysis. Therefore, species dominance was calculated by averaging the %cover value (within the 50 quadrats) for each species (using species codes in Table 3.4). Plot-level comparisons were made using the aggregated mean functional type %cover values (Table 3.4). Dominance is therefore similar to the abundance terminology employed by Brown (1984).

3.3.4 Surface radiometric measurements

The FieldSpec®Pro Analytical Spectral Devices spectro-radiometer acquired surface spectra within the 0.35 – 2.5μm wavelengths, with a spectral resolution of 0.0014μm (for the 0.35-1.05μm range), and 0.002μm (for the 1.00-2.50μm range) (Analytical Spectral Devices, 2002). Surface spectral reflectance measurements acquired for the 18 selected quadrats were converted to mean values for each wavelength in

Table 3.7 – Satellite band wavelengths

Wavelengths (μm)	IKONOS	Landsat 7 ETM+
Blue	0.445-0.516	0.45-0.52
Green	0.506-0.595	0.53-0.61
Red	0.632-0.698	0.63-0.69
Near Infrared	0.757-0.853	0.78-0.90
Mid-Infrared (SWIR)	N/A	1.55-1.75
Mid-Infrared	N/A	2.09-2.35

Source: SpaceImaging, 2001; Goward *et. al.*, 2001

the spectro-radiometer using Analytical Spectral Devices' software (ASD ViewSpecPro). Surface spectral values for each given ASD quadrat were then averaged to correspond to IKONOS and Landsat 7 ETM+ wavelengths, providing surface spectra that may be related to image bandwidths (Table 3.7).

To evaluate the potential effect of varying IKONOS and Landsat bandwidths on tundra vegetation characterization, simple correlation analysis was employed. From initial inspection of Table 3.7 it is clear that there are inconsistencies between the green and near-infrared (nir) image bands, in that Landsat channels are shifted towards longer wavelengths. The blue and red spectral channels are the same for the two sensors. Results show that green spectral channels are essentially identical ($R=1.000$, $p<0.0001$), while the nir channels are also significantly correlated ($R=0.998$, $p<0.0001$). A one-way analysis of variance also demonstrates no significant difference between sensor bands (i.e., green: $F=0.017$, $p<0.898$; nir: $F=0.100$, $p<0.754$), supporting their functionally equivalent usage. Therefore, only Landsat 7 red and nir bandwidths are used to calculate surface vegetation indices (VIs) from ASD reflectance data.

3.3.5 Image rectification

a) Geometric correction

IKONOS multispectral imagery possesses a spatial resolution of 4m and comes pre-processed with a stated 2m horizontal metric accuracy (SpaceImaging, 2001). The acquired image was provided in the Universal Transverse Mercator (UTM) projection (zone 15) and the World Geodetic System 1984 (WGS84) datum. This image was re-projected to the North American Datum 1927 (NAD27) to correspond to GPS data collected in the field. In order to cover the entire study site, two separate IKONOS overpasses (July 23 and 27, 2001)

were collected. These data were then mosaicked to provide a seamless representation of the 60km^2 area of Boothia Peninsula just west of Sanagak Lake.

Landsat 7 ETM+ imagery (July 25, 2001) acquired for this study possesses a spatial resolution of 30m and six spectral channels (bands 1-5, 7). The original data were radiometrically calibrated (i.e., on-board, full aperture 5% absolute radiometric calibration) and geometrically processed (i.e., +/- 50m) (Radarsat, 2002). Landsat 7 ETM+ data for the study area were georeferenced directly to the IKONOS data. The main difficulty in referencing images of any kind, in such a remote arctic location, is the lack of linear man-made features with which high geometric confidence levels may be associated. In the absence of such features, the most easily employed ground control points (GCPs) were the middle of ponds or sand bars that were broader than 60m x 60m (so as to be clearly identifiable on the Landsat image). It is important to stay away from boundary areas because, although they are easily identified in IKONOS imagery, Landsat's coarse resolution demonstrates spectral mixing and thus spatial inaccuracy for limited extents. Employing 15 GCPs spaced evenly throughout the study site (Appendix 26), a planimetric accuracy of 0.26 pixels (approximately 8m) was obtained and employed to fit the Landsat image to the UTM projection (zone 15) and NAD27 datum.

b) Radiometric correction

As mentioned previously, surface spectral data were radiometrically corrected by calculating reflectance values based on a white reference panel calibration before and after each spectral measurement (Section 3.2.6). Lacking any other *in situ* empirical atmospheric measurements, this represents the most accurate and efficient manner of correcting for unperceivable atmospheric attenuation that would create erratic spectral response (i.e., spectra were only collected on sunny, essentially cloud-free days).

Correcting remote sensing image data to reflectance is more complex than for surface data, and is inherently sensor- and time-specific. Landsat 7 ETM+ data were

Equation 3.1 – Radiance calculation

$$L_\lambda = gain \times DN + offset$$

Equation 3.2 – Reflectance calculation

$$\rho_{TAO} = \frac{(\pi \times L_\lambda \times d^2)}{(ESUN_\lambda \times \cos\theta)}$$

where:
- ρ_{TAO} = unitless planetary reflectance
- L_λ = spectral radiance at the sensor's aperture
- d = earth-sun distance in astronomical units (1.01573) (Smithsonian Meteorological Tables, 2002)
- $ESUN_\lambda$ = mean solar exoatmospheric irradiance
- θ = solar zenith angle in degrees (51.07□)

calibrated to radiance (Equation 3.1), and then reflectance (Equation 3.2), following procedures outlined by NASA (2002). The gain and offset values required in Equation 3.1 are obtained directly from the header information in the Landsat image files, while the mean exoatmospheric irradiance values are provided by NASA (2002) (Appendix 27).

Calibrating IKONOS data to reflectance values to account for atmospheric attenuation was not straightforward. Due to its space orbiting youth (1.5 years), the uncertainty involved in radiance calibration coefficients provided by SpaceImaging (due to sensor and acquisition time dependence), and the lack of published research employing IKONOS imagery, the accuracy of resultant values is very questionable (Arp, 2002). Considering that the IKONOS sensor does not measure exoatmospheric irradiance at the time of image acquisition, calculating reflectance from these radiance values adds increasing error to the equation. Several variations of radiance calculations from IKONOS calibration coefficients were performed following suggestions from Teillet (2002), yet the extremely low resultant reflectance values were considered inaccurate. Upon reflection, and in the case of

IKONOS data, it was deemed preferable to employ digital numbers for this analysis, as the goal is not to solve a sensor radiometric calibration problem but to conduct an ecological investigation of relative vegetation amounts and distribution. The original 11-bit DN values were linearly re-scaled – employing 0.5 – 99.5% of the original image to exclude influential outliers – to range from 0 to 1. While these cannot be referred to as reflectance values, they approximate reflectance trends as closely as possible and are in a useable form for input into soil-adjusted VIs. These results must be interpreted with caution, but they represent the best alternative to having to exclude IKONOS data altogether due to difficulties with absolute radiance and reflectance calculations.

3.3.6 Image analysis

a) Plot spectra

The plot corner coordinates (Appendix 17) were converted to ArcView GIS 3.4 shape files and imported into ENVI 3.4 to be overlain onto both the IKONOS and Landsat images. Corner coordinates were then saved as ENVI vector files for later use. The plot locations were employed to create region-of-interest (ROI) polygons in ENVI for each satellite image. The ROIs were used to calculate the mean of all plot-level image spectral values. Surface ASD measurements were processed to correspond to plot-level surface spectra by combining a manual weighted average of the most representative surface spectral plots based on similarity of %cover functional type from the 50 quadrat estimates (Appendix 28). This was necessary because exact quadrat locations were impossible to accurately identify on images with 4m pixels, much less 30m pixels, and one spectral quadrat cannot accurately represent the microsite variability within a plot.

To investigate whether or not within-plot vegetation communities may be considered distinct "spectral communities", a spectral separability analysis was performed using the

transformed divergence separability measure provided in ENVI 3.4 (excluding blue wavelengths to minimize atmospheric noise). Normally employed to evaluate class separability for supervised classification, transformed divergence is computed for this study using the mean and covariance matrices of ROI statistics outlined on the remote sensing data (Jensen, 1996). The transformed divergence statistic gives an exponentially decreasing weight to increasing distances between ROIs (Jensen, 1996). The output values are scaled from 0 – 2, indicating the statistical separability of input ROIs (field sample plots). Values greater than 1.9 indicate that ROI pairs maintain good separability, while anything above 1.7 is also considered acceptable (Jensen, 1996). ROI values lower than 1.7 are not considered separable, while values less than 1 are very low (ENVI, 2000) and likely indicate no statistical separability between community spectral characteristics.

b) Spectral vegetation indices (VIs)

The normalized difference vegetation index (NDVI) (Rouse *et. al.*, 1974) (Equation 3.3) is the most commonly employed VI in biophysical remote sensing studies in arctic environments (Hope *et. al.*, 1993; Stow *et. al.*, 1993b; Mosbech and Hansen, 1994; Shippert *et. al.*, 1995; Walker *et. al.*, 1995; Rees *et. al.*, 1998). The NDVI was calculated as a basis for comparison to other arctic remote sensing studies. However, it was also deemed important to investigate VIs designed to account for exposed soil characteristics that affect the reflectance of surface vegetated features. The soil-adjusted vegetation index (SAVI) (Huete, 1988) (Equation 3.4) was explored to determine its utility in an arctic environment where exposed soil, and varying soil characteristics, may impact simple ratio indices such as NDVI. The modified soil-adjusted vegetation index (MSAVI) presented by Qi *et. al.* (1994) (Equation 3.5) was also calculated to evaluate the results of a self-adjusting soil correction

factor on the VI values of tundra vegetation on Boothia Peninsula. VIs were calculated for

Equation 3.3 – NDVI

$$NDVI = \frac{nir - red}{nir + red}$$

where: nir = near infrared image band
red = visible red image band

Equation 3.4 – SAVI

$$SAVI = \left(\frac{nir - red}{nir + red + L} \right) \times (1 + L)$$

where: nir = near infrared image band
red = visible red image band
L = constant (0 – 1)*
*usually 0.5 for mid-density cover, but up to 1 for very low density cover

Equation 3.5 – MSAVI

$$MSAVI = \frac{2(nir) + 1 - \sqrt{(2(nir) + 1)^2 - 8(nir - red)}}{2}$$

where: nir = near infrared image band
red = visible red image band

plot-level surface spectra, as well as for each ROI on the two satellite images.

c) Unsupervised image classification

The purpose of image classification, as applied in this study, is to determine the quality of vegetation community delineation using different spatial resolution image data. The process of unsupervised image classification was employed for both Landsat and IKONOS data. The Isodata classification algorithm was employed despite increased familiarity with *in situ* plot characteristics after completing the field season. The unsupervised method remains preferential due to small sample sizes and the reality that training class selection for a supervised classification would be limited to areas surrounding sample plots. The Isodata algorithm calculates class means evenly distributed in data space, then iteratively clusters the remaining pixels using a minimum distance technique (ENVI,

2000). Each iteration recalculates means and reclassifies pixels with respect to the new means. Iterative class splitting, merging, and deleting is done based on input threshold parameters – all pixels are classified to the nearest class unless a standard deviation or distance threshold is specified (some pixels may remain unclassified if they do not meet the selected criteria) (ENVI, 2000). This process continues until the number of pixels in each class changes by less than the selected pixel change threshold or the maximum number of iterations is reached. Isodata was chosen over the K-means clustering algorithm as it has been suggested to be superior in initiating clusters (Jensen, 1996). The initial mean vectors applied in the Isodata algorithm are situated throughout the heart of existing data (as compared to K-means which uses means from the first line of data) (Jensen, 1996).

Three unsupervised classifications were performed – for IKONOS and Landsat – each with a different maximum class specification, but with consistent iterations, threshold values, and minimum pixels in a class – the remainder of options were left as the default settings (Appendix 29). Resultant unsupervised classes were merged/identified using the vector layer of plot locations, supplemented by *in situ* familiarity (e.g., ground photos, and plot descriptions). Plot ROIs were overlaid on the classified image in an attempt to relate spectral classes with ground cover/vegetation community type.

3.3.7 Statistical analysis

a) Data normality

All plot-level data (*in situ* and remote) were assessed using the Shapiro-Wilk test for normality as implemented in STATISTICA v. 5.5. Sample data are considered to follow a normal distribution if the results are *not* significant at the 95% confidence level (STATISTICA Help, 2000). This test is preferred because of its good power properties in comparison to a variety of alternative tests, over numerous sample sizes (Shapiro *et. al.*,

1968), and was performed in order to present multivariate linear regression analysis results using confidence intervals and significance statements. An analysis of regression residuals was also performed to estimate the compliance of variables with assumptions of normality of the error term.

b) Statistical relationships

Elementary statistical analysis employing the mean, median, and standard deviation are the most commonly employed statistics as they are: i) easiest to use and interpret and; ii) considered representative of the biophysical characteristics of interest. An assessment of the Pearson's R product moment correlation coefficient is employed when comparing percent cover estimates from different numbers of quadrats. One-way analysis of variance (difference of means, one-factor ANOVA) F-scores are incorporated to assess the functional equivalence of cover estimates and VIs. If a significant different of means is indicated, then independent sample t-tests are employed to determine which VIs provide unique biophysical information. The Spearman's rank correlation coefficient is incorporated for analysis including the ordinal moisture variable, as non-parametric statistics are essential in this case (Barber, 1988).

Linear bivariate regression analysis is conducted to explore the relationships between VIs and above-ground biomass, as well as %cover. The coefficient of determination (R^2) is of interest in accounting for the degree of variance between within-plot variables. The linear least-squares regression method is adopted because of its popularity and widespread use for estimating the degree of correlation between surface vegetation parameters (Glaser, 1992; Hope *et. al.,* 1993; McMichael *et. al.,* 1999), as well as between surface and image parameters (Tucker *et. al.,* 1985; Merrill *et. al.*, 1993; Shippert *et. al.,* 1995; Galvao *et. al.*, 2000). In order to verify relationships highlighted with regression analysis, an alternative method of

bootstrap resampling is employed. The nonparametric bootstrap method creates a large sampling distribution by resampling the data, with replacement, and calculating a regression coefficient for each new sample through a specified number of iterations (i.e., 1000) (Neter *et. al.*, 1996). The simulated bootstrap distribution can then be compared to the actual intercept and slope coefficients, without the same dependence on assumptions of normality or limitations of small sample size, to determine the accuracy of conventional regression results (Neter *et. al.*, 1996; Barber, 2002).

3.4 Summary

The diversity of both field and laboratory methods in this study make it simultaneously challenging and intriguing. It is impossible to account for all potential inter-relations between vegetation communities (e.g., species composition), their environment (e.g., soil moisture, topography, microsite, geology, or even human/plant or animal/plant interactions), and their resulting empirical characteristics (e.g., %cover, dry biomass weights, surface and remote spectral characteristics). This study represents an attempt to correlate field data, collected within a single growing season, to spectral derivatives of remote sensing satellite data collected over the same growing season. In addition, image analyses attempt to investigate preliminary issues arising from the use of high spatial resolution IKONOS imagery in comparison to its well-established and well-documented Landsat counterpart.

Chapter 4 – Results and Discussion
Plot species, percent cover, biomass, and moisture

4.1 Moisture

A relative moisture term was recorded for each biomass quadrat within each of the twelve plots (Section 3.2.5). The median of this moisture value is taken as an indication of the relative plot moisture status. Figure 4.1 shows the increasing moisture trend for each plot, demonstrating the variety of environments sampled. Plots follow quite closely to an idealized mesotopographic moisture gradient (Figure 4.2) where each plot can be characterized generally according to one of the five major habitat types (Table 4.1). For these reasons, all following graphic depictions of plot species richness, species dominance, %cover, and biomass results will be arranged according to the plot moisture status highlighted in Figure 4.1. Results of the relative moisture estimates show P6 to be the driest site (< 2), while P10 is the wettest community (> 8).

Figure 4.1 - Relative plot moisture

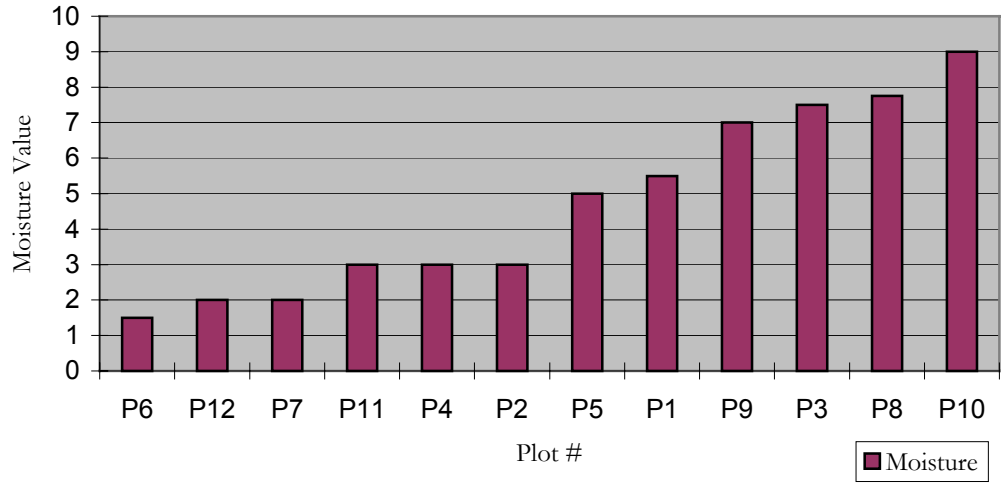

In the majority of arctic locations, the environmental factor most closely correlated with vegetation type is soil moisture (Oberbauer and Dawson, 1992). In areas of high

elevation, water is a limiting factor and an important determinant of vegetation structure, productivity, and composition; in lower areas these aspects may not be directly controlled by soil moisture, but rather by factors correlated with, or affected by, soil moisture (i.e., nutrient availability, thaw depth, soil aeration, redox potential, and pH) (Oberbauer and Dawson, 1992). Microscale moisture gradients (e.g., troughs to high centre polygons, across 2 to 3m from wet meadows to beach ridges, and frost boils/stone stripes) have great influence on the pattern and distribution of vegetation throughout tundra plant communities. This within-plot variability is prominently demonstrated in P6, P5, P8, and P9, whereby small variations in moisture – and likely frost action – impact where vegetation is prolific and where non-

Figure 4.2 – Idealized mesotopographic gradient

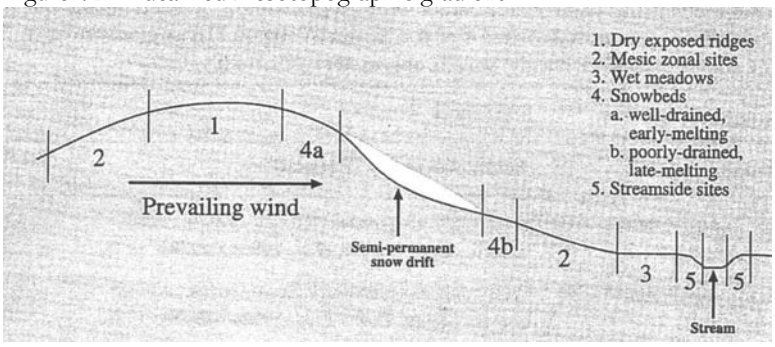

Source: Walker, 2000, 29

*Habitat codes based on Figure 4.2

Table 4.1 – Approximate habitat types*

Plot	Habitat
P1	3
P2	2
P3	3
P4	2
P5	4b
P6	4a
P7	4a
P8	3
P9	5
P10	3
P11	4a
P12	1

vegetated surfaces are exposed (Figure 4.3). Mesoscale soil moisture has an inverse relationship with slope and elevation, whereby fell field ridgetops are the driest environments, increasing downhill to riparian zones in valleys that demonstrate the wettest habitats (e.g., P9 overview, Figure 4.4) (Oberbauer and Dawson, 1992). These trends echo Walker's (2000) depiction of a mesotopographic gradient (Figure 4.3), along which the twelve study plots may be placed (Table 4.1). A variety of physiological factors also play

into the water relations of arctic vascular plants, and readers are referred to Oberbauer and Dawson (1992) for a detailed review.

4.2 Within-plot Species Richness and Dominance

Forbs are a determining factor in species richness (Figure 4.5, Appendix 30), contributing between 35% (P3) and 52% (P8 and P5) to the measure of plot species richness. *Saxifraga oppositfolia* is most prominent on dry and mesic plots, while a variety of *Pedicularis spp.* may be found on moist to wet sites. The most common shrub species include *Dryas integrifolia* and prostrate *Salix spp.*, whilst the most familiar graminoid species include *Eriophorum spp.*, and *Carex spp.*. Bryophytes are limited to one main group, simply labeled moss (MO – likely *Sphagnum spp.*), because of the difficulty in determining subspecies in the field. For similar reasons, lichen species are also described in general terms (Appendix 23). Plot species richness cannot be taken as a measure of cover dominance because the sole measure of species presence in a given quadrat does not ensure correlation to areal coverage (Appendix 31). In fact, the selected plot community types demonstrate only a few dominant species,

Figure 4.3 – Microsite variability

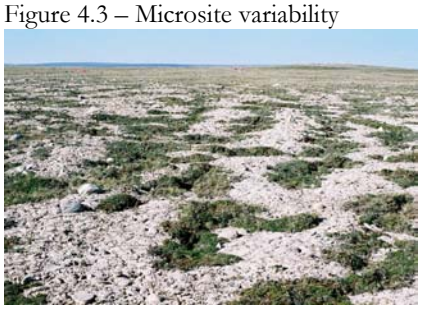

P6: non-sorted stripe and circle formations with vegetation prolific in-between exposed, raised surfaces

P5: exposed dark and light soils create microsite variability

P8: sparse graminoid canopies allow for underlying soils and organics to show through

regardless of total species present. Dominant plant species do, however, correspond to high frequencies within quadrats as may be expected according to Brown (1984) (Figure 4.6). On drier, elevated sites *Dryas integrigolia* is dominant, while rock or exposed soil may be even more prominent. Wetter sites show *Eriophorum spp.* (usually *Eriophorum angustifolium*) as dominant, while *Carex aquatilis* and moss may also play important roles. Soil exposure on these sites is limited, but where present it is of a dark organic nature.

Figure 4.4 – P9 Overview showing mesoscale moisture gradient

July 27, 2001

Figure 4.5 - Plot species richness

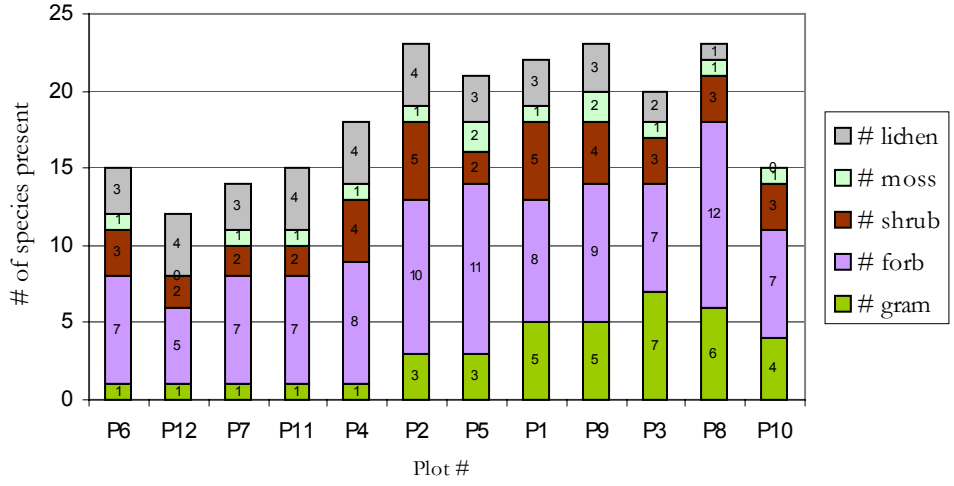

Exploratory regression analysis between vegetated species %cover (including the variety of non-vegetated cover types) and frequency of appearance in quadrats shows a weak linear relationship in most plots for P2, P4, P7, P9, P12 (i.e., $R^2<0.5$), while somewhat stronger relationships are demonstrated in P1, P3, P5, P6, P8, P10, P11 (i.e., $R^2>0.5$)

(Appendix 32). These poor results are a function of the high frequency of *Saxifraga oppositfolia*, *Carex bigelowii*, and prostrate *Salix spp.*, associated with their minimal contribution to overall vegetation cover, which prevents the formation of meaningful intrinsically linear trends. Study plot P7 is an excellent example of how species dominance cannot be determined from species frequency – *Saxifraga oppositfolia, Carex bigelowii,* and lichens are frequently found within random quadrats, yet they occupy very little of the total %cover of quadrats and hence of the overall study plot (Figure 4.6). *Dryas integrifolia* and rock cover types are, however, found frequently and combine to characterize 70% of total plot cover (Figure 4.6). Appendix 32 highlights that no frequency/cover relationships would be found if dominant species were excluded from calculations (i.e., dominant cover types are important influential outliers, essentially determining the cover/frequency relationship). Acknowledging these trends, it is reiterated that plot %cover estimates are grouped into plant functional types reflecting all vegetation cover; however, functional type %cover tends to be determined by one to three dominant species.

Figure 4.6 – Species cover and frequency example

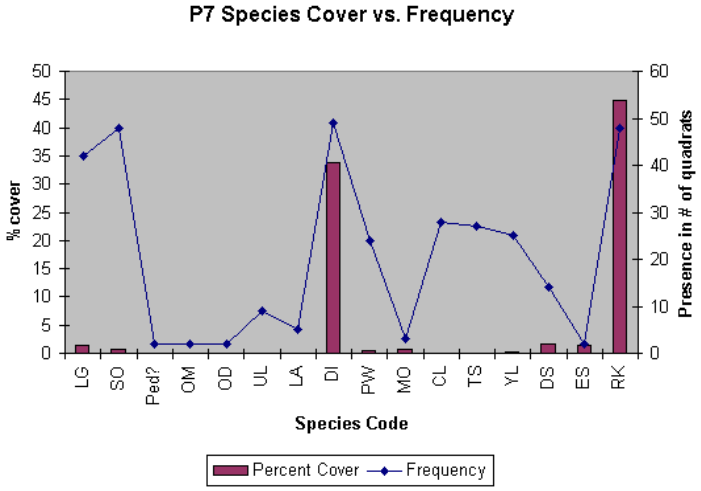

To understand what controls species richness and dominance patterns in arctic environments, "it is necessary to appreciate the environment in which the plants grow, the physical constraints to growth, reproduction, and dispersal, and what the physical conditions mean to spatial organization of habitats, the plant cover, breeding systems, and populations structure." (Murray, 1997, 16) Here, the issues of plant cover, biomass, and moisture are

investigated, as they are believed to be the most directly correlated with tundra vegetation spectral reflectance characteristics.

4.3 Percent Cover

The 50-quadrat visual percent cover estimates made within each plot are considered more representative of community cover types than the ten biomass quadrats alone. To ensure that 50-quadrat cover estimates may be compared to biomass estimates from 10 quadrats, the 10-quadrat %cover values (X) were regressed on the 50-quadrat estimates (Y) (Appendix 33). Because the two cover estimates demonstrate a strong linear relationship (R^2=0.921, p<0.0001), and high degree of correlation (R=0.959, p<0.0001), further analysis employing the 50-quadrat %cover values are considered representative. Despite the two cover estimates being highly correlated, a one-way analysis of variance verifies that there is no significant difference between the two means (F=0.033, p<0.857) (Appendix 33), further justifying the use of 50-quadrat cover estimates. Relatively high standard deviation values for %cover estimates (20 – 40%) (Appendix 34) may be attributed to the flexible BB cover classes where ranges of 25% are common for each category.

Plot %cover estimates include all vegetation functional groups, vascular and non-vascular, as well as non-vegetated cover types. For drier plots, non-vegetated areas dominate the community, while shrubs contribute the most to vegetation coverage. As plot moisture increases, or elevation decreases, shrubs take over as the dominant cover type, while non-vegetated ground continues to contribute about one quarter of %cover – graminoids and forbs are increasingly present. As plot moisture increases further, graminoids become dominant. Non-vegetated cover does not disappear in wet plots, but its characteristics are much different (i.e., dark, absorbent, open organic layer compared to the rocky, baked soil, or sandy exposed surfaces on dry plots). Lichens are listed in many %cover estimates but,

often falling in the <1% category, they do not appear in plot-level %cover graphic summaries for any community type encountered within the study site.

Study plot P12 demonstrates the greatest dominance of exposed soil surfaces (79.15%), P2 shows the greatest coverage of shrubs (52.7%), and P10 depicts the greatest %cover of graminoids (56.9%) (Figure 4.7). Forbs never dominate overall cover, but they are most prominent in P4 (3.5%) (Figure 4.7). Non-vascular plant cover dominates P1 with bryophyte cover of 42.6% (Figure 4.7). As mentioned previously, lichens do not contribute much to overall cover, but they are most prominent in P7 (0.2%). A full listing of %cover values is shown in Table 4.2, while a visual representation of vegetated and non-vegetated plot cover fractions are provided in Appendix 35.

Results presented for plot %cover estimates follow expected trends in vegetation community composition and functional type dominance described in other tundra vegetation research (e.g., Bliss and Matveyeva, 1992; Lloyd *et. al.*, 1994; Walker *et. al.*, 1994; Murray, 1997; Henry, 1998; Young *et. al.*, 1999). Spatial heterogeneity of the study area, regarded as the irregularity of the physical environment that translates into different kinds of plant habitats, demonstrates the importance of local influences on creating a diversity of habitats that can maintain a diversity of species cover (Murray, 1997). Murray (1997, 12) explains that spatial heterogeneity in tundra environments play an important role in defining vegetation composition, for: "[t]he tundra landscape, arctic or alpine, no matter how apparently flat and monotonous, is a series of convexities and concavities. All landscapes are hills and hollows of various sizes, and the differences in plant cover associated with them are often sharply defined." Habitats are colonized by particular species, in relative vegetation cover dominance, following a series of microsite influences: i) topography (Bliss and Peterson, 1992; Schaefer and Messier, 1995; Henry, 1998; Ostendorf and Reynolds, 1998); ii)

Figure 4.7 – Percent cover distribution for select plots

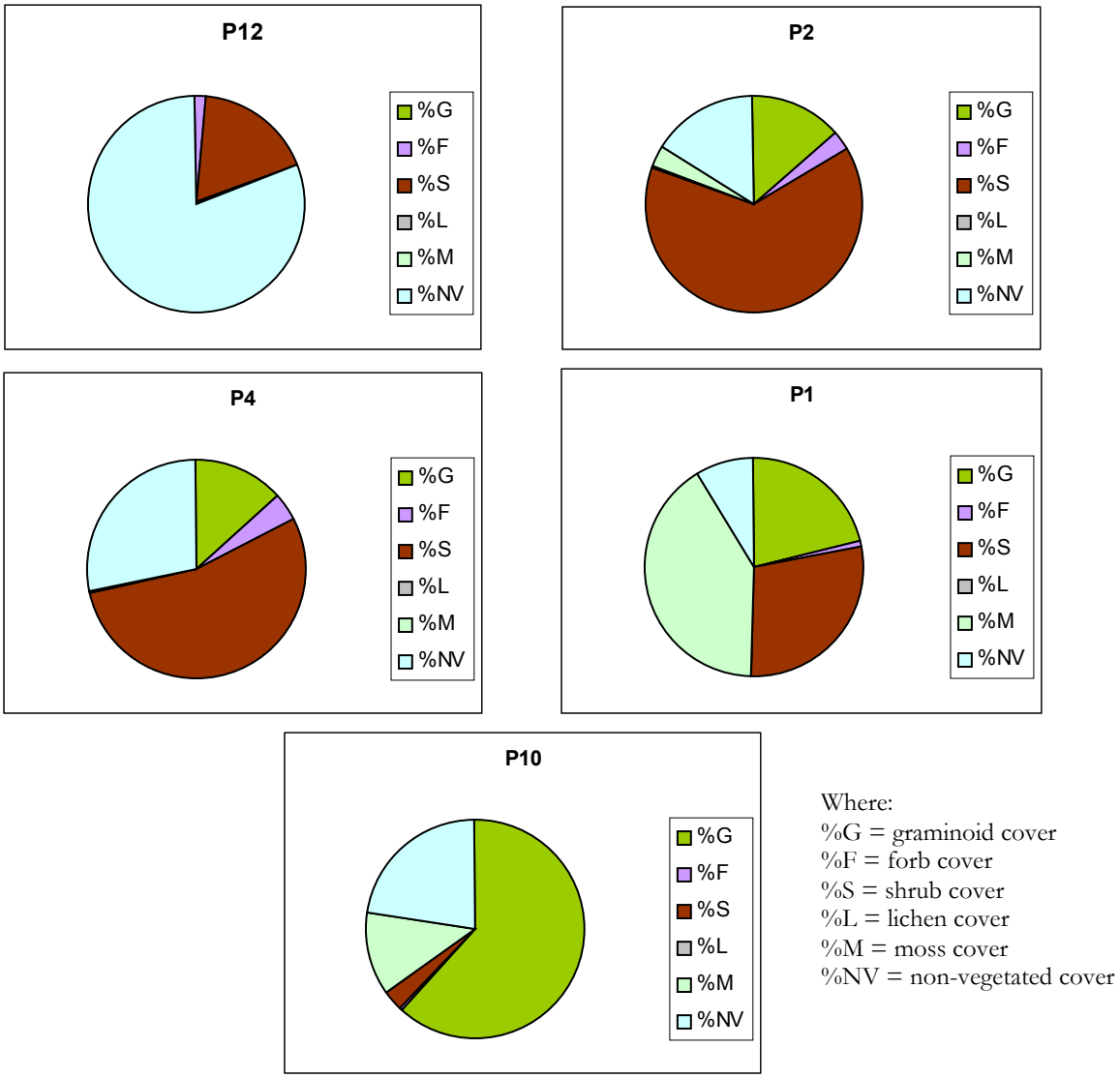

Where:
%G = graminoid cover
%F = forb cover
%S = shrub cover
%L = lichen cover
%M = moss cover
%NV = non-vegetated cover

Table 4.2 – Total vegetation cover and functional type percent cover values for all study plots

Plot	veg cover (50)	Std. Cover (50)	%G	%F	%S	%L	%M	%NV
P6	40.68	28.86	0.57	1.07	31.87	0.07	7.10	47.95
P12	19.00	20.18	0.10	1.60	17.30	0.10	0.00	79.10
P7	36.55	24.18	1.30	1.03	34.32	0.19	0.75	48.15
P11	48.92	29.31	0.30	1.33	44.37	0.07	2.85	46.85
P4	54.06	19.00	10.01	3.51	40.36	0.18	0.00	21.45
P2	69.50	36.45	11.51	2.47	52.66	0.06	2.80	13.41
P5	60.17	34.32	7.77	2.51	38.18	0.06	11.65	26.30
P1	94.61	35.10	22.11	0.96	28.92	0.01	42.60	8.85
P9	85.66	31.61	26.01	0.27	39.42	0.11	19.85	7.45
P3	100.85	27.73	39.96	0.10	20.79	0.00	40.00	3.55
P8	62.98	32.51	30.22	0.89	17.27	0.00	14.60	19.76
P10	71.38	33.87	56.90	0.22	2.95	0.00	11.30	20.95

soil moisture (Oechel, 1989; Bliss and Matveyeva, 1992; Oberbauer and Dawson, 1992; Henry, 1998; Ostendorf and Reynolds, 1998); iii) nutrient availability (Oechel, 1989; Bliss and Peterson, 1992; Henry, 1998); iv) soil pH (Bliss and Peterson, 1992; Yu, 1994; Walker *et. al.*, 1995); v) snow cover (Walker *et. al.*, 1993; Yu, 1994; Schaefer and Messier, 1995); vi) microclimate (Edwards *et. al.*, 2000); vii) grazing intensity (Henry, 1998); and viii) exposure (Larsen, 1964; McFadden and Chapin, 1998). These environmental factors affect study plot tundra vegetation cover distribution and composition; therefore, they are referred to when evaluating plot community types. Little documentation is available describing typical vegetation community composition on Boothia Peninsula, so comparisons with the closest resembling arctic environments are incorporated to evaluate %cover functional type estimates.

Mires are sedge-moss and grass-moss tundra habitats dominated by graminoids – mainly *Eriophorum spp.* and *Carex spp.* (Bliss and Matveyeva, 1992). These environments occur only where water remains on the landscape much of the summer because drainage is blocked at snowmelt by raised ridges (Bliss and Matveyeva, 1992). Mosses tend to establish themselves first, where early graminoid dominance is maintained by *Dupontia fisheri* with *Eriophorum scheuchzeri* as codominant (Bliss and Peterson, 1992). The slower growing *Eriophorum angustifolium* and *Carex aquatilis* establish themselves after vascular plant canopy is more developed, slowly expanding circles of tillers within the vegetation (Bliss and Peterson, 1992). Mires in early successional stage do not appear prominent within the study area, but plots P10, P1, P3, P9 and P8 may be considered later mire successional stage communities according to %cover dominance (Appendix 35) and species composition (Appendix 30). Dominated by graminoids, these plots are thought to be progressing towards the final mire

successional stage in which decreases in availability of phosphorus, as well as decreased pH levels and depth of thaw may be experienced, while accumulation of soil organic matter may become obvious (Bliss and Peterson, 1992). Lacking the prominence of standing water, plots P10, P1, P3, P9, and P8 are therefore considered to range from wet to moist sedge meadow communities, typically underlain by a well-developed bryophyte layer.

Dwarf-shrub heath tundra is dominated by prostrate and hemiprostrate dwarf shrubs (e.g., *Dryas integrifolia*, and *Salix arctica*), as well as cushion forbs (e.g. *Saxifrage oppositifolia, Cerastium alpinum, Papaver radicaturm,* and several *Stellaria spp.*) (Bliss and Matveyeva, 1992). These habitats develop on well-drained, neutral to slightly alkaline soils with limited snow cover (2-10cm) and a relatively deep summer active layer (50-100cm) (Bliss and Matveyeva, 1992). Graminoid species present tend to be dryland *Carex spp.* Study plots associated with this cover type tend to be found on ridge tops, or broad expanses of flat fell field surfaces (e.g., P4, P12, P7, P6, P11). There is significant variety in the appearance of these communities (Appendix 15) but they tend to fall within the dominant species and cover type categories often described as polar semideserts. Study plots P5 and P2 do not fit neatly into sedge meadow or dwarf-shrub heath community descriptions, maintaining unique plant and environmental composition that share microsite similarities to both dwarf-shrub heath and sedge meadow communities. The above discussion is meant as a description of potential community characterization, while further evaluations of biomass will supplement community delineations.

4.4 Biomass

In calculating average above-ground biomass estimates for the twelve sample plots, it became evident that bryophyte biomass results were skewed and inaccurate. Seven of the twelve plots had entries for moss biomass, yet of the ten quadrats within each plot there

were rarely more than three moss collections. Not only are these bryophyte estimates extremely high in comparison to other plant functional type dry weights, there is little confidence in the samples themselves. Because of the methods employed for moss collection (Section 3.2.5), it is impossible to validate bryophyte weights. Reference samples were collected, instead of the entire moss mat (for *in situ* efficiency and time purposes), a protocol that is now deemed ineffective for characterizing bryophyte biomass. In addition to methodological discrepancies, there were additional uncertainties encountered in separating the moss reference layer:

i. Moss carpets were not always harvested if they were not included in visual percent cover analysis (i.e., they were not seen until graminoid layer was clipped away); therefore, the moss dataset is incomplete.
ii. Extrapolating a 10cm x 10cm moss square (2.5 – 3.8cm thick) is very difficult to gain accurate representation of actual moss coverage.
iii. Determining where the moss layer ends and the soil layer begins was extremely challenging – sometimes no soil layer was found, and the bryophyte layer extended deep into the layer of organic material.
iv. While bryophyte biomass is an important component of relatively wet vegetation communities, the uncertainty and error surrounding moss collection (i.e., values appear artificially high in many plots) prevents an accurate assessment of non-vascular plant biomass.

Total aboveground biomass estimates seem greatly impacted by the high moss values (Appendix 36, Figure A). Furthermore, standard deviation values for bryophyte biomass tend to exceed the average plot biomass values in all but one case, which flags these estimates as non-representative (Appendix 36, Figure B). For these unfortunate reasons, it is deemed necessary to exclude non-vascular plant biomass from all further analysis.

For biodiversity studies it is considered prudent to limit studies to vascular plants because of their shared/similar biological attributes (Glaser, 1992); however, despite the necessity involved, restricting aboveground biomass samples to vascular plants does not bode well for establishing relationships between vegetation %cover, spectral reflectance, and biomass.

Some expected vascular plant trends are revealed, whereby shrub biomass forms the majority of aboveground vascular plant matter on drier plots, and decreases in importance along an increasing moisture gradient to the point where graminoids represent the majority of vascular plant biomass (Figure 4.8). Forbs contribute most on dry to moist plots, but never comprise the majority of dry plant matter. Plot 2 reveals the highest vascular plant biomass (514.16 g/m^2) while Plot 10 maintains the lowest vascular plant

Figure 4.8 - Vascular Plant Plot Biomass Estimates

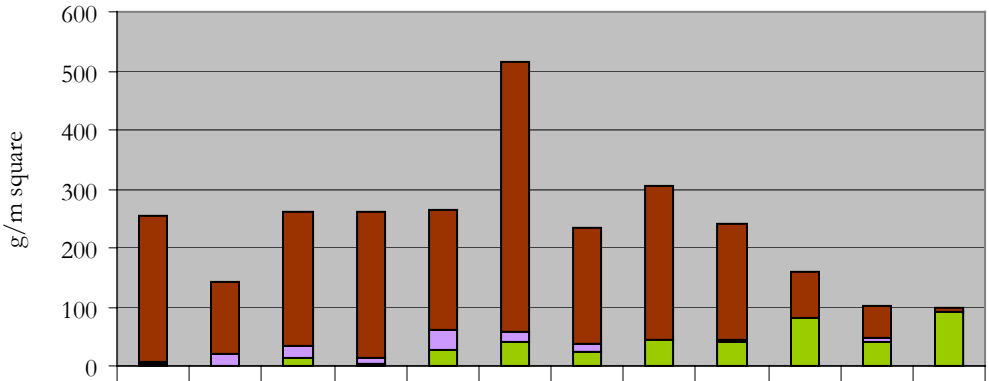

	P6	P12	P7	P11	P4	P2	P5	P1	P9	P3	P8	P10
BS	245.44	121.28	225.6	247.28	201.6	456.76	196.44	259.56	199.64	78.8	55.04	5.08
BF	6.48	19.84	21.88	9.44	33.64	18.4	13.24	0	0.96	2.16	6.68	0.48
BG	1.88	1.12	11.96	3.88	27.72	39	24.16	43.88	41.76	79.68	41	91.12

Plot #

Where: BS = Shrub biomass, BF = Forb biomass, BG = Graminoid biomass.

biomass (99.68 g/m^2) (Figure 4.8). While vascular biomass estimates are much more representative of plot community characteristics, variance within plots remains high (Appendix 37). This trend may be a function of the small within-plot sample size (i.e., 10 quadrats harvested for a 1ha area), resulting from the limited sampling window during a single season field campaign.

Shaver and Chapin (1991, 5) state that "the inclusion of below-ground stems and non-vascular plants in the comparison [tends] to reduce the apparent differences in biomass

among sites." Therefore, having to reduce biomass analysis to above-ground vascular plant dry weight is perhaps not so detrimental to subsequent analyses. The majority of plots (i.e., P6, P12, P7, P11, P4, P2, P5, P1, P9) are dominated by shrub biomass, especially *Dryas integrifolia*, while graminoids are most important in P3, P9, and P10. The contribution of forbs to above-ground biomass is minimal on any site, even though there are more forb species in each plot than any other species (Section 4.2) – a reflection of the presumed correlation between species dominance and biomass. Vascular plant biomass tends to follow trends of relative growth form abundance (Shaver and Chapin, 1991); however, above-ground dry weight results are also reflective of functional type biomass allocation characteristics. For example, approximately 80% of wet graminoid biomass is allocated below-ground, whilst approximately 50% of dry dwarf-shrub biomass is allocated below-ground (Shaver and Chapin, 1991). These aspects may help explain why biomass is lowest on the wettest, graminoid-dominant plot (P10), whereas P12 biomass is higher despite much lower vegetation coverage. Furthermore, enhanced graminoid turgidity and less dense plant fibres, in comparison to prostrate or hemiprostrate shrubs, may lead to lower dry weights for wet sites.

Vascular plant biomass seems to decrease towards moisture level extremes, as evidenced by results showing lowest biomass at the driest (P12) and wettest plots (P8, and P10) (Figure 4.1 and 4.8). Study plot P6 is a notable exception, where exposed soil was hard packed, exhibiting the lowest moisture value, but higher biomass than P12 (Figure 4.1 and 4.8). The increasing importance of moss biomass on wetter sites (i.e., minimum of 30% according to Shaver and Chapin (1991)), is not accounted for in plot biomass results. This absence must be acknowledged as a likely influence in shifting the biomass/moisture relationship towards a more linear trend.

Water interactions affect whole-plant function through multiple direct and indirect linkages, where one of particular interest is the amount of leaf area. Oberbauer and Dawson (1992) suggest that leaf area (commonly measured as the leaf area index – LAI – in remote sensing studies), and hence photosynthetic potential, is regulated by water status. This conclusion has important implications for remote sensing research because if percent cover estimates may be successfully related to spectral vegetation indices (VIs), results may be extrapolated to represent other important tundra biophysical variables (e.g., plant photosynthetic potential, water stress, and plant vigour). In addition, plot moisture, biomass, and percent cover variables serve to define vegetation community types in the current study. Incorporating these plot variables aids the interpretation of results discussed in the following chapter, whereby relationships between biophysical properties and remotely sensed vegetation indices are evaluated.

Chapter 5 – Results and Discussion
Spectral Characteristics of Tundra Vegetation

5.1 Surface Reflectance

Isolating characteristic cover types at ground level is important for later comparisons between surface and satellite plot spectral response. Understanding the spectral nature of vegetation cover from individual quadrats enhances interpretation of plot spectral characteristics that are likely impacted by the amount of gravel till, exposed soil, and/or common occurrence of senescent vegetation properties throughout the growing season. Very few vegetated ASD quadrats display the characteristic vegetation curve (Figure 2.1). Surface spectral curves were calculated by averaging the raw ASD spectra across the appropriate bandwidths, to mimic both IKONOS and Landsat spectral channels (Appendix 38). The purest *Dryas integrifolia* (A13, A17), *Salix spp.* (A3), and *Eriophorum spp.* (A1, A7) radiometric measurements most closely resemble the typical vegetation spectral curve (Figure 5.1, Table 5.1, Appendix 38);

Figure 5.1 – Example of spectral curves derived from ASD measurements

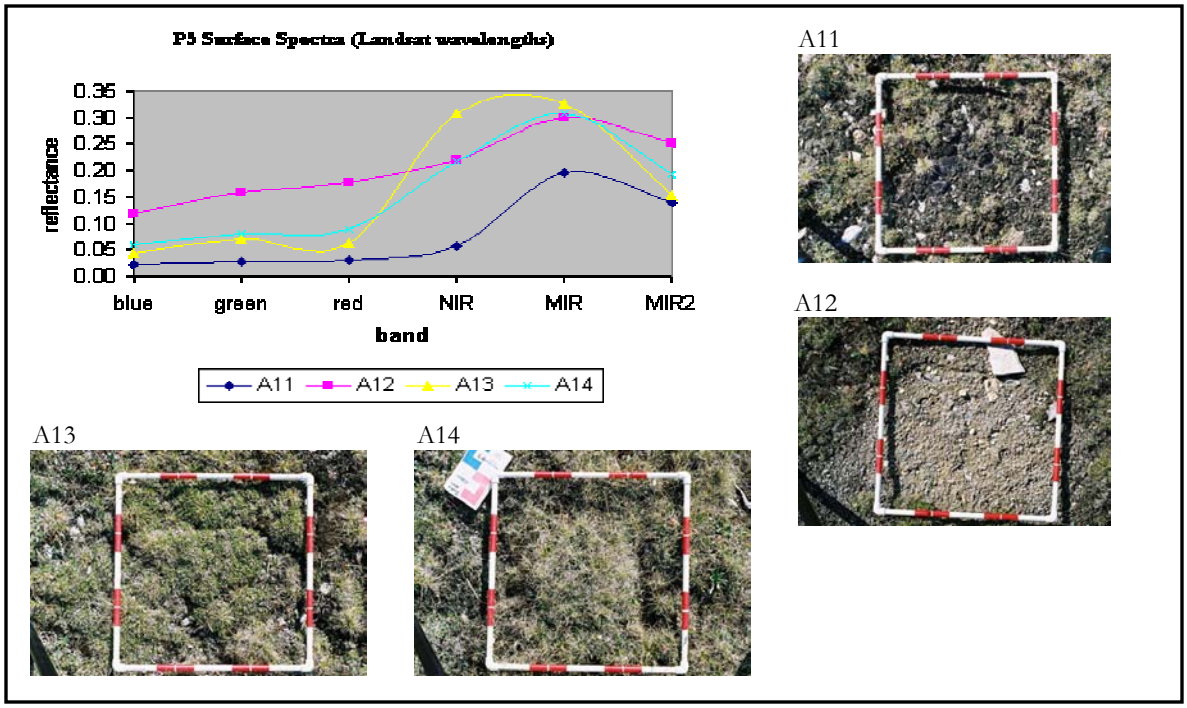

however, the low green peak and low overall reflectance values are unique aspects of tundra vegetation.

The superior spectral range of the Landsat 7 ETM+ simulated data derived from the ASD reflectance data (i.e., 6 spectral channels over visible, nir, and swir) provides increased potential for distinguishing between vegetation cover types (Table 5.1). The addition of the mid-infrared (swir) bandwidths (i.e., corresponding to TM5 and TM7), sensitive to vegetation and soil moisture, provides distinct spectral information for vegetation cover (e.g., between A1 and A3, as well as A5 and A6, where visible and nir spectral trends are almost identical). The swir wavebands also provide increased amplitude differentiation between similar vegetation types in varied moisture environments (e.g., A7 and A8, as well as A17 and A18). Despite the perceived vegetation cover diversity, many of the spectra collected show very similar spectral trends for Landsat channel equivalencies, with a simple magnitude difference depending on the amount of soil exposure or moisture content. For example, the spectra collected at ground level may be divided into approximately five major cover categories through the analysis of their spectral response (Table 5.2). ASD quadrat A2 provides a unique spectral curve whereby the bryophyte vegetative properties, visual colour, and underlying moisture, distinguishes it from any other spectral measurement.

Table 5.1 – ASD quadrat cover descriptions*

ASD Q#	**Spectra descriptions**
A1	ESP mostly, some underlying DI (on moss tussock)
A2	dried out MO (likely *Sphagnum sp.*) reddish/brownish hues
A3	EW, underlying MO, and very sparse ESP
A4	DI, few LG
A5	dead DI, few LG
A6	RK/gravel, some JL and or RT
A7	ESP (likely EA), green and brown
A8	a mix of WA, MO, and ESP
A9	mixed dry vegetation, RK, DI, LG, OM, TS, YL, CL
A10	mixed dry vegetation, LG, little DI, rock, lichens
A11	dark soil, little PW, DI, SO or TF
A12	ES, sandy gravelly surface
A13	DI
A14	mix of DI and LG
A15	ES (baked clay/rock)
A16	combination of DI, dry MO, and maybe little LG (through veg)
A17	SR, DI, and LG mix
A18	ESP (lush green) and WA

* See Appendix 23 for code descriptions.

5.2 Satellite Spectral Response

The spectral separability of study plots was evaluated to determine the natural spectral separability of selected vegetation communities from remotely-sensed data. Section 3.3.6 describes the acceptable level of separability on a 0 – 2 scale, where values above 1.7 are considered acceptable (Appendix 39). Table 5.3 summarizes the spectral communities, which aggregate vegetation communities based on the transformed divergence measure of separability. Contrary to expectations, Landsat data provide more distinct vegetation communities (i.e., 8) than IKONOS (i.e., 3). The higher spatial resolution of IKONOS data was forecasted to provide enhanced plot separability, but this is not the case. The first possible reason may refer back to results presented in Section 5.1. The superior spectral range (i.e., inclusion of swir) of Landsat data was shown to resolve quadrat biophysical characteristics better than visible and

Table 5.2 – Cover types associated with ASD quadrats

Vegetation cover	Environment	ASD quadrats
Healthy green	Moist	A1, A3, A7, A13, A17
Senescent	Dry, exposed	A4, A5, A9, A10
Green, with exposed organic layer	Dry to moist	A11, A14, A15
Exposed sand, gravel till	Dry with microsite moisture	A12, A15
Healthy green	Wet	A8, A18
Reddish bryophyte cover	Dry with underlying wet	A2

Table 5.3 – Plot spectral separability

Spectral Community	IKONOS plots	Vegetation Community	Landsat plots	Vegetation Community
1	P12	Barren, sparsely vegetated	P12	Barren, sparsely vegetated
2	P6, P7, P11, P4	Sparsely vegetated, fell field, patterned ground	P4	Sparsely vegetated, flat dwarf-shrub tundra with evenly interspersed stones
3	P9, P1, P3, P10, P8, P2, P5	Moist to wet sedge meadows	P2	Low ridge-top vegetation, lush in hill dips
4	-	-	P8	Moist sedge meadow
5	-	-	P5	Moist drainage flats, moderately vegetated
6	-	-	P10	Sedge meadow with highest moisture rating
7	-	-	P1, P9, P3	Moist to wet sedge meadows, higher presence of water and frost action formations (i.e. tussocks, polygons)
8	-	-	P7, P6, P11	Fell fields, sparsely vegetated, some patterning, sorted/non-sorted circles

nir wavelengths alone, and may thus be extrapolated to plot properties. Since TM5 is indicative of soil and vegetation moisture content, while TM7 is useful for rock type discrimination (Campbell, 1996), the subtle distinctions between vegetation communities within the visible and nir wavebands seem enhanced by the additional channel capacity of Landsat 7 ETM+.

The spectral nature of P12 is unique for both satellite data types, as it is minimally vegetated, dominated by rock cover, and located on a high ridge-top. Study plot P4 is separated from P6, P7, and P11 by Landsat data, which might be expected based on the fact that P4 is very flat, sparsely but evenly vegetated, with rocks scattered uniformly and frequently throughout. This within-plot vegetation cover and distribution is quite different from the patchy formations found in P7, P11, and even more so in P6. It is perhaps the increased soil/rock exposure and patchy patterned ground formations that maintain the other three as similar to one another, but distinct from P4 in Landsat 7 data. Landsat also shows P2 and P5 to be unique, while they are spectrally aggregated with all other moist to wet sedge meadows in IKONOS data. These two plots (especially P2) possess transformed divergence statistics close to 1.7 for IKONOS data, but maintain enough microsite similarities that they cannot be accurately separated from other, more lush, study plots (Appendix 39). Landsat TM5 sensitivity to moisture is the likely reason for the unique community distinctions of P8 and P10 compared to the general moist to wet sedge meadow grouping in IKONOS data. Study plots P1, P3, and P9 remain grouped by Landsat data, which may be expected based on their moisture ratings (Section 4.1), but not based on visual inspection. The definitive water track characteristics of P9 make it the only plot with well-developed high-centre polygons and a large presence of standing water throughout the summer. However, the stark differences in moisture between polygon centres and troughs

may be aggregated by Landsat to form the spectral similarity to the other moist sedge meadow sites.

In addition to the qualitative assessments of plot spectral separability, based upon vegetation composition and distribution characteristics observed in the field, investigating the mean and standard deviation of plot spectral values provides greater insight into the inability of IKONOS to spectrally separate community types (Figure 5.2, a & b). There are several striking observations that may be taken from satellite plot spectral values: i) IKONOS mean plot spectra tend to have higher converted DNs than Landsat reflectance values (Figure 5.2a) – which may be a function of inability to correct data to reflectance values, or of the capability of IKONOS to distinguish exposed soil reflectance; ii) unconventional vegetation spectral trends appear, whereby several plots demonstrate higher DNs for red wavelengths than for green wavelengths (i.e., P1, P2, P3, P5, P8, P9, P10); iii) there is minimal plot spectral differentiation in IKONOS data throughout the four channels, especially within the nir waveband; and iv) IKONOS standard deviation values are considerably higher (i.e., 0.02 – 0.23) than Landsat standard deviation values (i.e., 0.006 – 0.08) (Figure 5.2b). Therefore, it may be concluded that IKONOS 4m pixels resolve microsite variations, resulting in higher within-plot variance to represent vegetation cover heterogeneity. The higher variance within vegetation communities translates into greater overlap between spectral signatures, hence lowering separability values, which explains the poor characterization of distinct vegetation types (Table 5.3). Landsat data records and represents reflectance data sampled over a 30 m x 30 m surface area (i.e., a single digital value for each channel for a 30 m pixel). As a result, microsite variability is averaged over a 900m^2 area, prior to plot level aggregation, translating into much more homogenous plot spectral response as shown by low within-plot spectral

variance (Figure 5.3a). This coarser spatial resolution, complemented by increased sensor channels, minimizes spectral overlap and improves spectral separability (Figure 5.3b; Table 5.3).

Figure 5.2a – IKONOS mean plot spectra

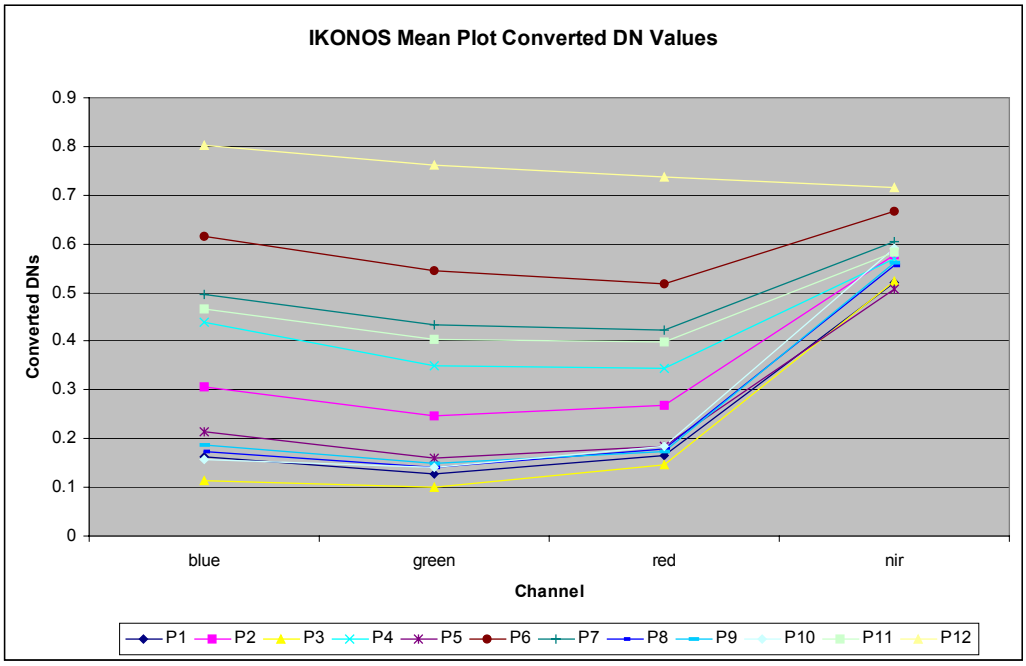

Figure 5.2b – IKONOS plot spectra standard deviation

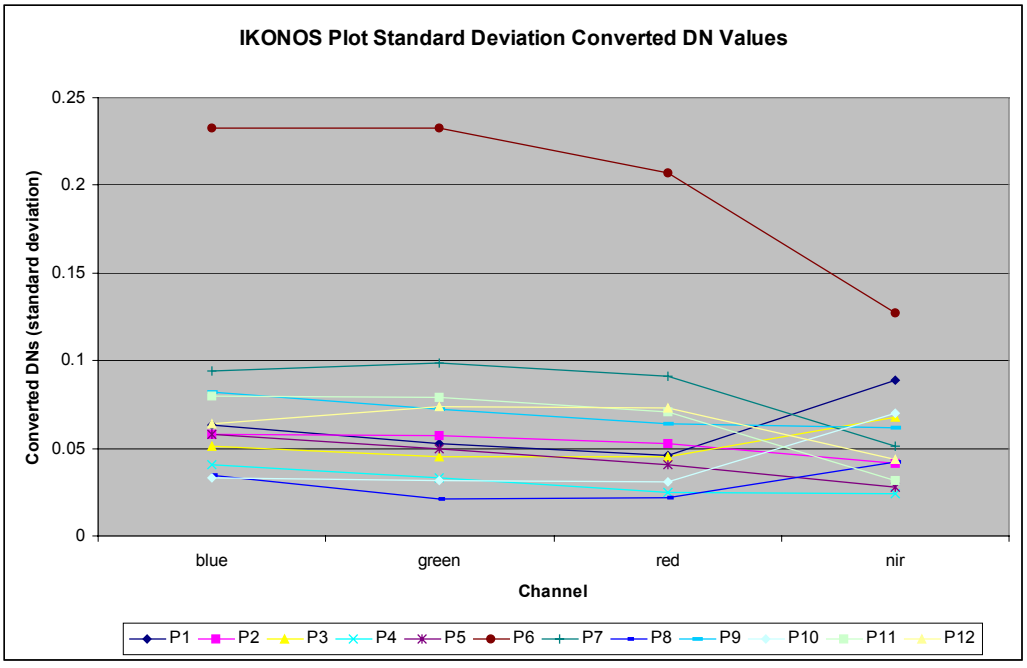

Figure 5.3a– Landsat plot spectra standard deviation

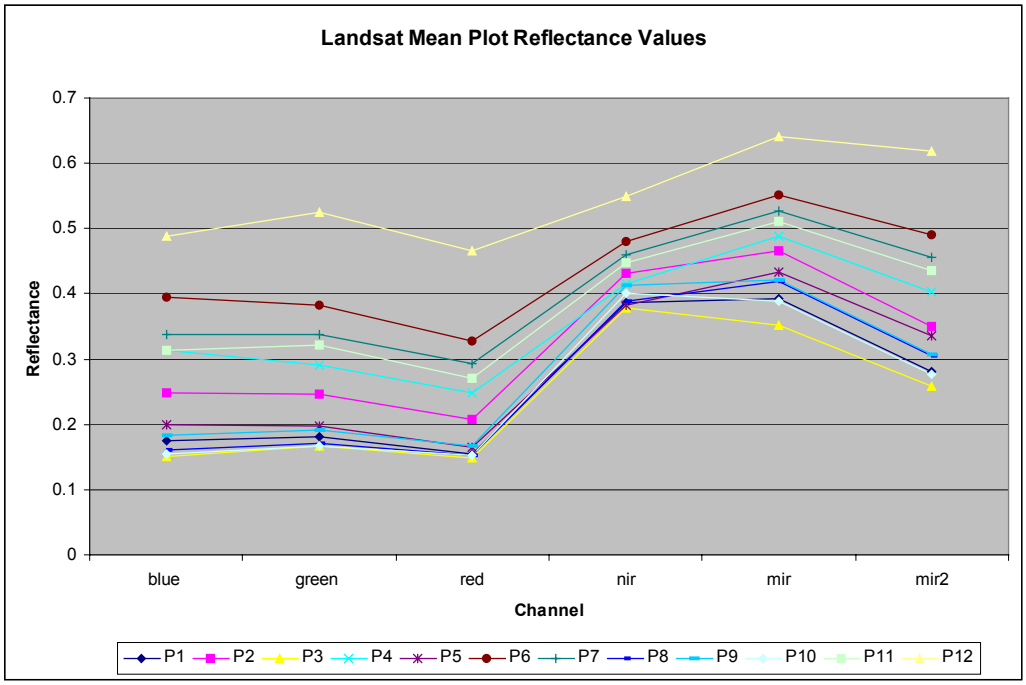

Figure 5.3b – Landsat mean plot spectra

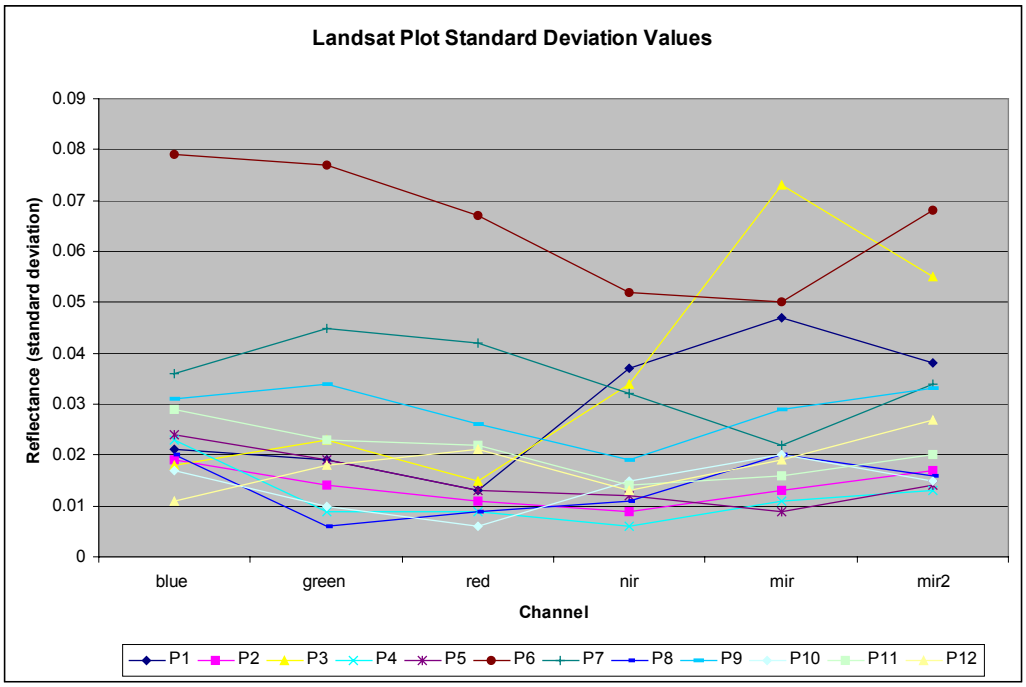

Differing levels of within-plot spectral variance are understandable considering that IKONOS plots contain approximately 625 pixels, while Landsat plots may contain only 9

pixels, depending on plot boundary orientation. Therefore, the enhanced spatial resolution provided by IKONOS serves to delineate microsite characteristics, while also confusing spectral signals at the plot level, forming higher variances where a single vegetation community cannot easily be isolated from other plots. These considerations warrant further study on the quantifiable impact of spatial versus spectral resolution for distinguishing vegetation community types in tundra environments.

5.3 Unsupervised Image Classification

The unsupervised classification of IKONOS data, with a maximum of 10 classes specified for the Isodata algorithm, results in the delineation of six water classes and three vegetation classes (Appendix 40). The 15-class unsupervised classification provides increased distinction between vegetation communities (i.e., five vegetation classes), while water classes increase to eight (Appendix 40). Based on the spectral curves of mean class DNs (Figure 5.4), as well as visual inspection of the 15-class image (Figure 5.5), cover classes are identified as corresponding to particular land cover types (Appendix 40).

Figure 5.4 – IKONOS unsupervised class mean spectral response

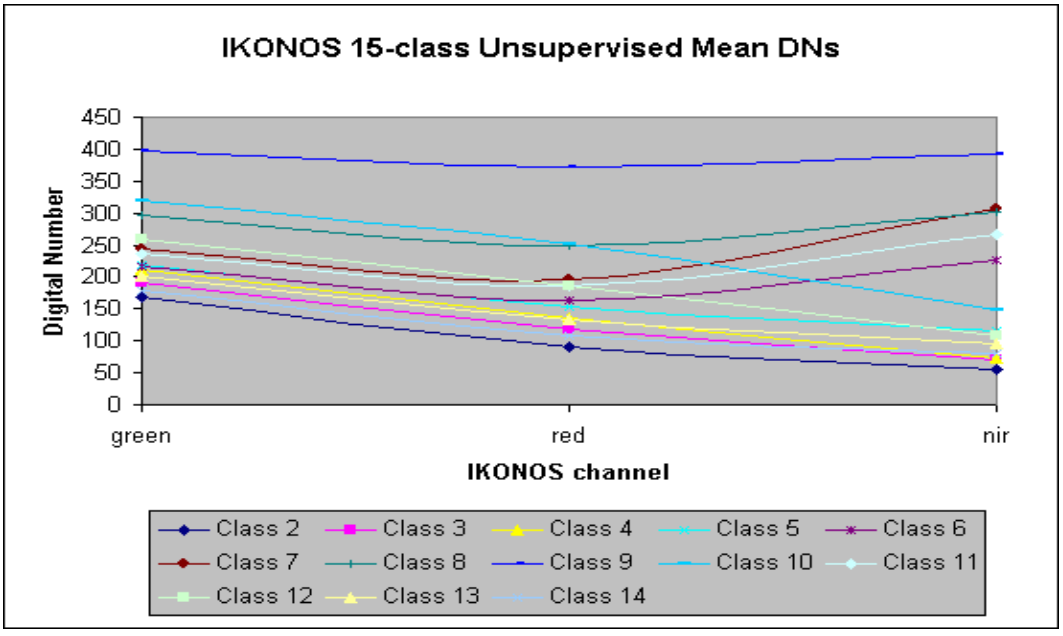

Refer to Classified Images Document (it's own .pdf file)

A specified maximum of 10 classes, for the Isodata algorithm, provides an additional vegetation class for the Landsat 7 ETM+ data compared to those of the IKONOS data (i.e., five water classes and four vegetation classes) (Appendix 40). The classified image comprising a 15-class maximum results in the delineation of six vegetation classes, and eight water classes (Appendix 40). Based on the spectral curves of mean class reflectance values (Figure 5.6), as well as visual inspection of the 15-class image (Figure 5.7), classes are identified as corresponding to particular land cover types (Appendix 40).

Figure 5.6 – Landsat unsupervised class mean spectral response

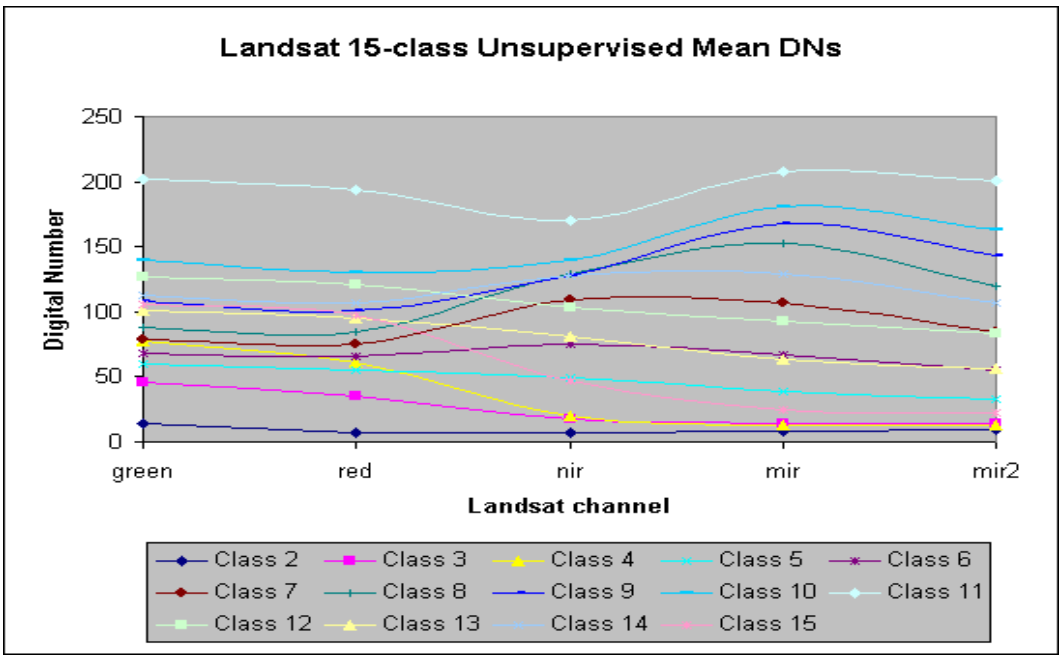

Upon overlaying plot vectors on classification images it becomes apparent that spectral separability (Section 5.2) has an impact on, but is not the sole cause of, class formation. In the IKONOS 10-class image, study plots fit neatly into the same cover classes as those initially defined as spectrally separable (Table 5.4). IKONOS 10-class results almost mirror "spectral communities" identified with the transformed divergence statistic (Table 5.3), while 15-class results provide increased vegetation cover delineation. However, more vegetation classes do not translate into more unique plot adherence to a particular

Refer to Classified Images Document (it's own .pdf file)

community type, rather, study plots are often centered on a particular class with small elements of other classes present within the 1ha plot boundaries. These results indicate that the spatial resolution of IKONOS may be factoring other surface parameters (e.g., texture, microtopography, moisture, etc.) into class distinctions. It also highlights the spatial resolution of IKONOS as being suitable for identifying local microsite variations that reflect small-scale heterogeneity and allows for overlap of land cover classes within different plots.

Table 5.4 – Cover class associations with study plots*

STUDY PLOT	IKONOS 10-CLASS LAND COVER CLASSES	IKONOS 15-CLASS LAND COVER CLASSES	LANDSAT 10-CLASS LAND COVER CLASSES	LANDSAT 15-CLASS LAND COVER CLASSES
P1	5	6, 7	5, 6	7, 8
P2	5, 6	7, 8	6, 7	9, 10
P3	5	6, 7	5	7, 8, 9
P4	6	8	7	10
P5	5	6, 7	6	8, 9
P6	6	8, 9	7, 8	10, 11
P7	6	8	7, 8	8, 9
P8	5	6, 7	6	8
P9	5	7	6	8, 9
P10	5	7	5, 6	8
P11	6	8	7, 8	10, 11
12	7	9	8	11

* Cover class descriptions provided in detail in Appendix 40.

The improved spectral resolution of Landsat data impacts the delineation of unsupervised land cover classes, despite coarser spatial resolution. Compared to IKONOS data, Landsat provides an extra vegetation class in both the 10- and 15-class images. However, the limited spatial resolving power hinders the extent to which cover classes may be defined (i.e., constrained to general, broadly distributed cover types) – an issue lamented by Spjelkavik (1995) and Mosbech and Hansen (1994). Landsat data seems capable of highlighting some within-plot variations as shown by the overlap of plots in different cover classes (Table 5.4), but not with the localized detail of IKONOS data. Spectral superiority may be compensating somewhat for spatial inferiority because the classes are identifiable, yet interpreting the spatial aspects of class distribution is hindered by the pixilated appearance of Landsat cover classes. Despite extra vegetation classes provided by Landsat data, plots are

not found in all classes due to the difficulty of resolving microsite variations that would enhance plot characterization. While both data types experience considerable mixing of plots between classes, there is far less detail provided by Landsat (i.e., one pixel may be different within a Landsat plot, while several pixels may be unique in IKONOS plots – delineating localized cover types).

The spatial attributes of IKONOS classification seem successful, as would be expected based on the suggestion by Stow *et. al.* (1993b) that 10m spatial resolution data are required to adequately resolve tundra land cover heterogeneity. The degree of class overlap exhibited in most study plots suggests that sites are not homogeneous at the 4m scale (Table 5.4). The aggregation of cover types at the 30m scale seems to provide increased plot cover uniformity, but still does not translate into distinct plots corresponding to discrete cover types. These results demonstrate that tundra vegetation cover is far more diverse than initially perceived, but that this diversity may be more a function of local topography, micro-environmental variations, and surface texture than of spectral response or species composition.

The IKONOS unsupervised 15-class data are most appealing (Figure 5.5), where its potential utility for mapping vegetation communities is quite apparent when compared to the 15-class Landsat classification (Figure 5.7). While mapping vegetation distribution is not among the main goals of this study, results do provide an indication of the areal coverage of vegetation classes over the entire study site (Table

Table 5.5 – Image class coverage

CLASS	%IMAGE COVERAGE (IKONOS 15-CLASS)	%IMAGE COVERAGE (LANDSAT 15-CLASS)
2	0.09	1.39
3	0.733	1.02
4	1.37	1.03
5	2.37	0.87
6	**6.30**	1.25
7	**21.21**	**3.28**
8	**26.42**	**15.51**
9	**9.07**	**27.45**
10	1.81	**31.82**
11	**25.65**	**11.37**
12	2.14	0.87
13	2.01	0.83
14	0.30	**2.56**
15	n/a	0.74

* **bold** numbers indicate vegetation classes (rest are water)

5.5). For ease of interpretation, Figure 5.5 shows all land cover types, but combines multiple water classes into one cover type. The IKONOS 15-class image subdivides the initial moist sedge meadow category (from the 10-class IKONOS classification) into three cover classes: water-track vegetation, moist sedge meadow, and snowbed vegetation. Snowbed vegetation comprises a relatively large proportion of vegetation cover types (i.e., 25.7%), shown to predominate at toeslopes, extending further on the northern sheltered sides of ridges. Water track vegetation is highly localized (i.e., 6.3%), while dwarf-shrub heath presides over moist sedge meadow as the dominant study area cover type (i.e., 26.4% vs. 21.2%). The barren/sandy class is localized to high windswept ridge-tops, inseparable from sandy river/lake shores, covering only 9.1% of the study area. Interestingly, the Landsat classification (Figure 5.7) portrays the study area as more barren (i.e., 11.4%), and cannot depict watertrack/snowbed vegetation (i.e., 3.3%) as definitively as IKONOS data. The two sedge meadow classes combine to form the dominant cover type within the study site (i.e., 15.5% and 27.5%), while dwarf-shrub heath is more common in the Landsat classification than for IKONOS (i.e., 31.8%). Landsat 7 ETM+ data seems to be identifying important spectral community components, yet the coarse spatial resolution inhibits accurate interpretation. Distribution patterns shown by the IKONOS classification are much more appealing and easier to confirm based on study site familiarity, but the sensor's spectral limitations suggest that improvements over Landsat are conservative and warrant further quantifiable investigation. The variety of water classes obtained in both data types is an interesting component of the unsupervised classification results; however, it is difficult to accurately interpret these classes, as field data were not collected for varying aquatic habitats.

5.4 Quadrat Vegetation Indices

Prior to interpreting plot VI results, it is important to report preliminary results based only on the original 18 ASD quadrats. As expected from prior experiments by Huete (1988) and Qi *et. al.* (1994), the soil-adjusted VIs yield lower values than NDVI (Figure 5.8, Appendix 41), depending on the amount of exposed soil and plot moisture characteristics. NDVI is highest where vegetative cover is also highest (e.g., A1, A2, A3, A7, A8, A13, A17, A18), ranging from approximately 0.55 – 0.75). ASD quadrats A6, A12, and A15 are essentially non-vegetated and demonstrate the expected low NDVI values (i.e., -0.1).

Figure 5.8 - ASD quadrat VIs

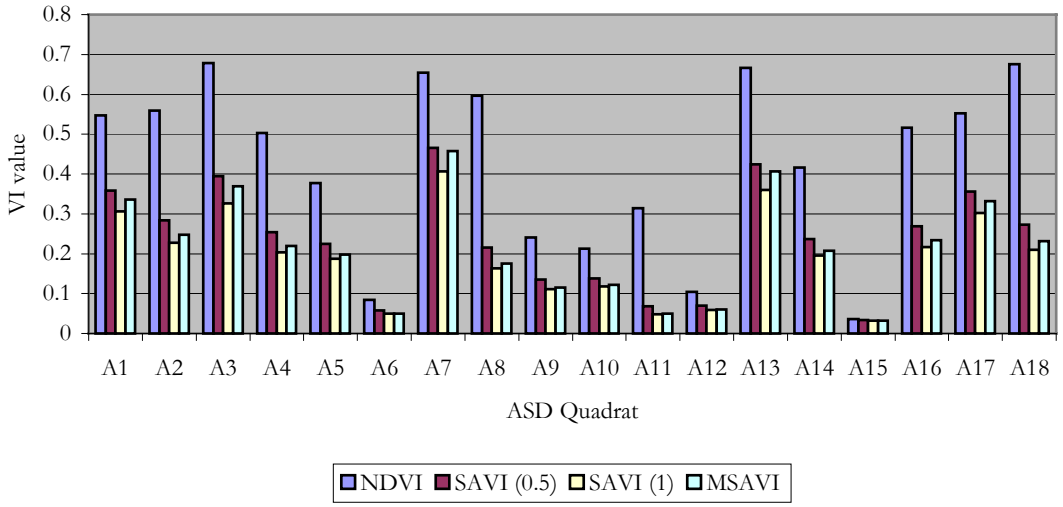

Soil-adjusted VIs tend to decrease VI values by incorporating the impact of soil reflectance on the red and near-infrared wavelengths, resulting in more realistic estimates of plant canopy density and vigour. In areas of low cover the differences are minimal (e.g., A6, A12, A15); however, interesting trends develop when analyzing the effects in relatively high vegetation cover. For example, A7 and A8 are both found within P3, and represent characteristic spectra of *Eriophorum spp.* in a moist to wet environment. While their NDVI values only vary by a magnitude of 0.05, their respective soil-adjusted VIs vary

by approximately 0.25, which can be explained by the amount of exposed (wet) organic layer that predominates A8. There is minimal visual difference among the soil-adjusted VIs, but the trends of SAVI(0.5) being the highest, followed by MSAVI and SAVI(1), remain consistent across cover types (Figure 5.8, Appendix 41). The difference between SAVI responses results from the different adjustment factors (L=0.5 or L=1). Huete (1988) showed L=0.5 to be useful across a wide range of canopy densities, while L=1 is suggested for areas of very low vegetation cover. Both were investigated because the majority of environments seen within the study area were sparsely vegetated and thus L=1 was explored for its appropriateness in a tundra environment. MSAVI is expected to provide a self-adjusting soil reflectance factor (Qi, *et. al.,* 1994), perhaps rationalizing its consistent intermediate response between the SAVI extremes. The minor discrepancies among soil-adjusted VIs catalyze later explorations into their functional equivalence in tundra environments.

5.5 Plot Vegetation Indices

The same four VIs (NDVI, SAVI (L=0.5), SAVI (L=1), and MSAVI) were calculated for surface spectra converted to mean plot values. Similar to the quadrat analysis, NDVI demonstrates considerably higher values than the rest, as it does not account for soil influences on VIs (Figure 5.9). Confounding background effects are a large factor in tundra environments where the vegetation cover, even if 100%, is very low to the ground and wavelengths may easily penetrate the canopy to reflect soil characteristics. VIs are drastically reduced when soil-adjusted calculations are employed. Not only do the soil-adjusted VIs lower values in proportion to the amount of exposed non-vegetated surfaces, they also seem to lower the dynamic range of VIs between plots (Figure 5.9).

Figure 5.9 - Surface VIs derived from ASD spectral measurements

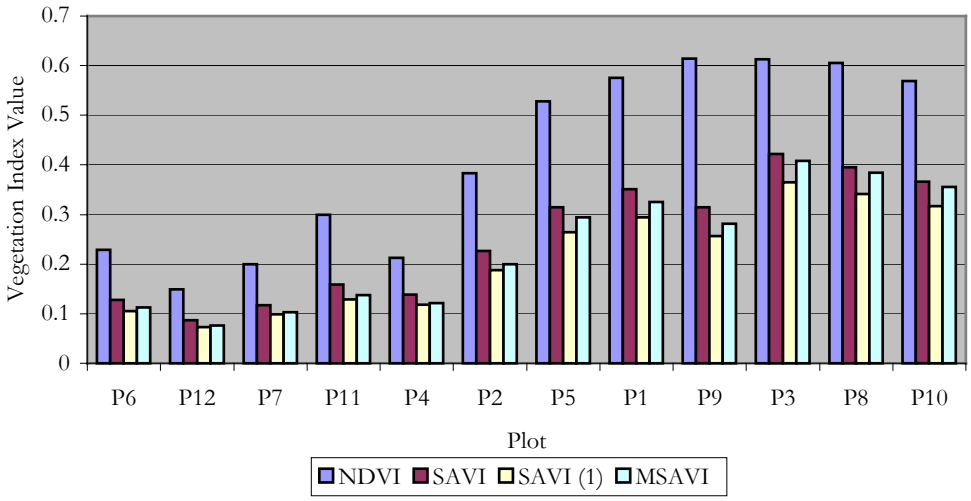

Plot 12 shows the lowest VIs in all cases (i.e., <0.15), not surprisingly since it is the site where non-vegetated cover dominates (Appendix 42). The highest NDVI values are found in P9 and P3, but P3 maintains higher soil-adjusted indices, suggesting that less exposed non-vegetated surfaces are present in this moist sedge-dominated site. Study plots P8 and P10 are the wettest areas, but maintain thinner canopies and prominent patches of dark, moist organics that likely diminishes soil-adjusted VI returns. The very low-lying shrub cover interspersed with rocks and pebbles within P7 and P4 accounts for lower, and similar soil-adjusted VIs; however, P6 exhibits a much different vegetated/non-vegetated configuration (i.e., patches of vegetation in sorted/non-sorted circle formations).

IKONOS plot VIs demonstrate unique findings in relation to both the surface and Landsat VIs (Figure 5.10, Appendix 42). Remote sensing data with 4m resolution provides minimal differentiation between NDVI and the soil-adjusted VIs in areas of low cover (i.e., P4, P6, P7, P11, P12), while areas of higher vegetation cover (i.e., P2, P5, P1, P3, P9, P8, P10) show slight VI decreases when using either SAVI or MSAVI (Figure 5.10). This is

Figure 5.10 - IKONOS VIs

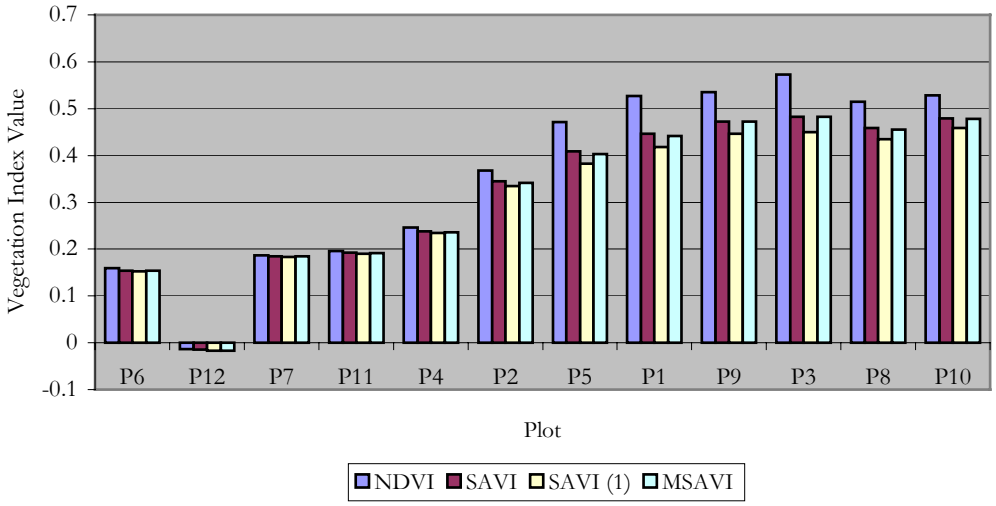

counterintuitive because soil-adjusted VIs tend to deviate minimally from NDVI in areas of very low or very high vegetation cover (Huete, 1988). It is possible, however, that this holds for areas of low cover because IKONOS can accurately resolve the patchy vegetation structure in dry barren sites, while in areas of higher cover this spatial resolution is capable of detecting the non-vegetated, or water-saturated, areas that serve to decrease near infrared reflectance, and thus soil-adjusted VIs. The other consideration is that plots with high percent cover values do not reach the type of cover density demonstrated by grass or cotton canopies shown in the development of soil-adjusted VIs (Huete, 1988; Qi *et. al.*, 1994), and therefore do not demonstrate the expected minimal deviations in areas of higher vegetation cover. The notable exception to this trend is P12, whereby VIs are negative. The barren nature of this plot does not preclude negative VIs, where red DNs are higher than those of nir (Figure 5.4), resulting in slightly negative values. This phenomena may be a function of compression differences due to atmospheric effects, whereby red brightness

values are preferentially elevated, presenting some reasoning for further research into accurate methods of accounting for atmospheric attenuation in arctic environments.

Plot VIs for Landsat 7 ETM+ data follow surface plot VI trends in that soil-adjusted VIs are consistently lower than NDVI (with the exception of P12 where they are equal); however, the decrease is less prominent than for surface VIs (Figure 5.11). With Landsat data, the soil-adjusted VIs seem to minimize the differentiation between plot VIs (Appendix 42). In other words, the similarities between plots reduce the original 12 plots to a loosely defined fourfold grouping:

Figure 5.11 - Landsat VIs

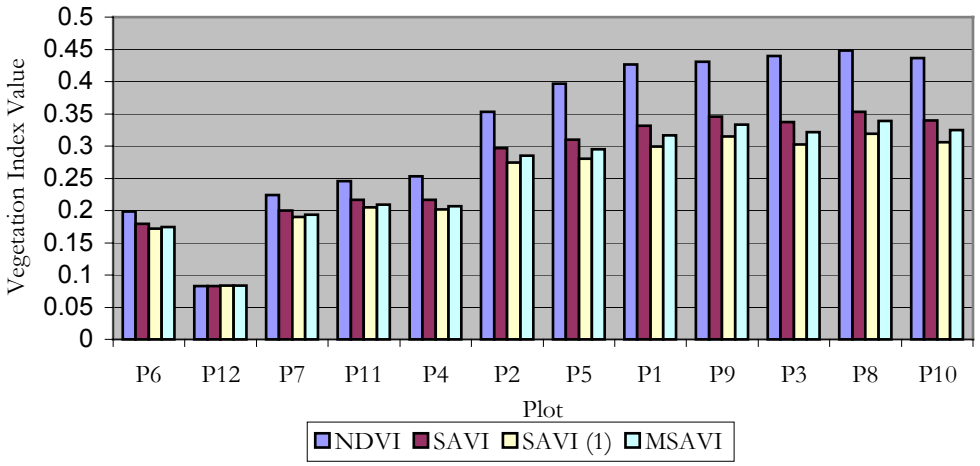

i) VI ≈ 0.075 – P12
ii) VI ≈ 0.175 – P6
iii) VI ≈ 0.19-0.21 – P7, P11, P4
iv) VI ≈ 0.27-0.35 – P2, P5, P1, P3, P9, P8, P10

An initial postulation for these trends of uniformity, as well as decrease in soil-adjusted VIs, is that Landsat's coarse spatial resolution causes the aggregation of numerous within-plot microsite spectral characteristics (of which soil exposure may be quite significant). For these reasons SAVI and MSAVI decrease the VI response, while the spectral mixing at the 30m scale is so great that it renders vegetation communities less distinct.

Surface NDVI values demonstrate similar trends, but slightly lower values, to *in situ* VIs obtained in other arctic environments (Mosbech and Hansen, 1994; Walker *et. al.*, 1995; Rees *et. al.*, 1998) (Appendix 9). The noticeable decrease in surface VIs with the introduction of soil-adjusted VIs provides a preliminary argument for NDVI results being artificially high. Satellite NDVI values also follow similar, but slightly lower, trends to results shown in Walker *et. al.* (1995), showing their dependency on environmental conditions. Compared to results presented by Mosbech and Hansen (1994) and Rees *et. al.* (1998), NDVI results are considerably lower, which may be a function of localized tundra environment or differences in radiometric correction procedures. There are no arctic biophysical remote sensing studies with which to compare soil-adjusted VI results, but the following statistical comparisons between NDVI, SAVI, and MSAVI help evaluate their utility in tundra environments.

Differences in soil moisture content influence soil reflectance, and in turn, vegetation indices (Purevdorj *et. al.*, 1998), providing some insight into decreased soil-adjusted VIs in plots with lush green vegetation underlain by moist or wet organics. Despite the fact that SAVI and MSAVI have been demonstrated to provide unique spectral information regarding vegetation cover (Baret and Guyot, 1991), questions are raised about their functional equivalence within the current study. To investigate the statistical differences between NDVI and soil-adjusted VIs, as well as between soil-adjusted VIs, ANOVA results for each sensor were used to identify a difference of means. Supplementary independent sample t-tests were employed to investigate the difference of means between VI pairs (i.e., all combinations of NDVI, SAVI, and MSAVI) calculated for each type of remote sensing data. ANOVA results suggest that there is a

Table 5.6 – ANOVA results for all VIs

Data Type	ANOVA F	Significance
Surface	5.444	0.003**
IKONOS	0.206	0.892
Landsat	1.876	0.149

** indicates significance at $p<0.01$

significant difference between surface-derived VIs, but not for satellite-derived VIs (Table 5.6). Independent sample t-tests highlight surface soil-adjusted VIs as being significantly different from NDVI ($p<0.01$), but no difference of means is present among soil-adjusted VIs. T-tests also support ANOVA results for satellite data, showing no significant difference of means for IKONOS- or Landsat-derived VIs.

Across a range of vegetation communities the utility of soil-adjusted VIs appears to be minimal; however, when study plots are divided according to moisture status (a division that also reflects plot species composition and functional type cover dominance), results provide new insight into VI dependence on environmental gradients. Because of sample size, further community delineations cannot be made, as difference of means tests cannot be performed on a single variable; however, the dry (i.e., P6, P12, P7, P11, P4, and P2) and moist (i.e., P5, P1, P3, P9, P8, and P10) segregations reflect graphic trends more aptly than statistics incorporating the range of plot types (Figure 5.9, 5.10, and 5.11). ANOVA results for dry plots mirror previous values where a significant difference of means ($p<0.01$) is only found for surface VIs (Table 5.6 and 5.7). In contrast, moist plots demonstrate a significant difference of means present among VIs for all three sensors

Table 5.7 – Independent t-test significance values for dry plots

	SAVI(1)	MSAVI	NDVI
SURFACE			
SAVI	0.363	0.516	0.025*
SAVI (1)	-	0.785	0.007**
MSAVI	-	-	0.01*
IKONOS			
SAVI	0.962	0.985	0.917
SAVI(1)	-	0.977	0.879
MSAVI	-	-	0.902
LANDSAT			
SAVI	0.778	0.911	0.562
SAVI(1)	-	0.391	0.403
MSAVI	-	-	0.464

Table 5.8 – Independent t-test significance values for moist plots

	SAVI(1)	MSAVI	NDVI
SURFACE			
SAVI	0.054	0.001**	0.001**
SAVI (1)	-	0.222	0.001**
MSAVI	-	-	0.001**
IKONOS			
SAVI	0.137	0.894	0.003**
SAVI(1)	-	0.197	0.001**
MSAVI	-	-	0.003**
LANDSAT			
SAVI	0.002**	0.055	0.001**
SAVI(1)	-	0.705	0.001**
MSAVI	-	-	0.001**

** indicates significance at $p<0.01$
* indicates significance at $p<0.05$

($p<0.01$), whereby independent sample t-tests performed on segregated plots provides additional information (Table 5.7 and 5.8). Here, significant differences between NDVI and soil-adjusted VIs are clearly demonstrated for surface, IKONOS, and Landsat VIs (Table 5.8). Furthermore, a significant difference of means is noted between SAVI and MSAVI for surface VIs, as well as for SAVI and SAVI(1) for Landsat VIs (Table 5.8).

Statistical tests support the visual trends noted for surface VIs, whereby soil-adjusted VIs are significantly lower than NDVI (Figure 5.9, Table 5.7, Table 5.8). These results compare to original findings of Huete (1988) where there was a loss of VI signal amplitude between NDVI and SAVI, while discrimination and soil noise levels are supposedly considerably improved. NDVI was also reported as maintaining equal sensitivity to soil darkening as to vegetation development, a phenomenon that SAVI successfully minimized (Huete, 1988). Attempting to improve the stationarity of L in SAVI, Qi *et al.* (1994) proposed the MSAVI to provide a self-adjusting L factor to best account for soil reflectance based on vegetation density. They suggest that MSAVI produces a higher dynamic range and increased reduction of soil background variations than SAVI. These trends are only found within surface VIs of moist plots, and are even less apparent in satellite data. No difference of means between IKONOS VIs may be expected for dry plots, based on the similarity of graphic VI trends (Figure 5.10). T-tests corroborate these observations (Table 5.7), yet soil-adjusted VIs are all significantly different from NDVI within moist plots (Figure 5.10, Table 5.8). Landsat soil-adjusted VIs show similar trends to IKONOS data, where there is no significant difference of means for NDVI of dry plots, but in moist plots they are all highly significant (Figure 5.11, Table 5.8).

Since most early research on soil-adjusted VIs was performed using surface radiometric data, it is difficult to compare satellite VI results to available literature. Landsat

TM data was employed by Gemmell and Varjo (1999), as well as Turner *et. al.* (1999), to investigate relationships between NDVI and SAVI within forest and other temperate zone sites. While the grassland site studied by Turner *et. al.* (1999) may be the closest relation to tundra environments, they found poor LAI/VI relationships. Original soil-adjusted VI experiments were undertaken in grass, cotton, and agricultural crop vegetation covers (Huete, 1988; Qi *et. al.*, 1994), which are also quite distinct from tundra cover. It is therefore suggested that NDVI is adequate for characterizing the sparse vegetation cover within dry study plots (i.e., comparable to low LAI results in the literature), because of an additive spectral reflectance component for low-density canopies. This reflectance trend manifests itself in sparsely vegetated environments due to little soil-vegetation interaction that allows red and nir penetration through the canopy to be nearly equal (Huete, 1988) (Table 5.7). In moist study plots vegetation cover density is greatly increased, along with the difference between red and nir penetration to the soil, causing NDVI to lose its ability to describe soil-vegetation behaviour (Huete, 1988). This observation supports the difference of means (Table 5.8) and lower values of soil-adjusted VIs (Figure 5.9, 5.10, and 5.11) depicted by all sensors for moist vegetation communities. Because there is no consistent difference of means among multi-resolution soil-adjusted VIs, the remaining analyses will only include NDVI and SAVI (L=0.5) to maximize efficiency and minimize redundancy.

The functional VI equivalence between data types, must also be addressed (i.e., differences between VIs obtained from surface, IKONOS, and Landsat data). ANOVA results indicate no significant difference of means between multi-resolution NDVI or SAVI values, across a range of vegetation communities. Pair-

Table 5.9 – Independent t-test significance values for multi-resolution VIs

	LANDSAT	SURFACE
NDVI		
IKONOS	0.658	0.471
Landsat	-	0.191
SAVI		
IKONOS	0.335	0.256
Landsat	-	0.713

** indicates significance at $p<0.01$
* indicates significance at $p<0.05$

wise t-tests for independent samples corroborate ANOVA values, indicating no significant difference of means (Table 5.9) for surface and satellite VIs. In addition, the two satellite sensors seem functionally equivalent for both NDVI and SAVI calculations (Table 5.9). Because of previous findings regarding the influence of plot environmental conditions, as well as visual trends seen in Figure 5.12, it is also worth repeating investigations for dry and moist plots. Again, ANOVA results present no significant difference of means for dry plots ($p<0.7$), yet highly significant difference of means for moist plots ($p<0.01$) (Table 5.10). Findings suggest that the similarities among dry sites are playing down the difference for wet sites when analyzing results across all study plots. In dry, sparsely vegetated plots, (i.e., P6, P12, P7, P11) IKONOS maintains the lowest NDVI, but demonstrates intermediate NDVI values for the remainder of sites. Surface and IKONOS NDVI seem to provide the greatest dynamic range (i.e., 0.15 – 0.61, and –0.01 – 0.57, respectively), while Landsat values are confined between 0.05 and 0.45.

Table 5.10 – Independent t-test significance values for multi-resolution VIs divided by community type

	LANDSAT	SURFACE
NDVI (dry)		
IKONOS	0.580	0.391
Landsat	-	0.705
SAVI (dry)		
IKONOS	0.001*	0.452
Landsat	-	0.132
NDVI (moist)		
IKONOS	0.001**	0.011*
Landsat	-	0.001**
SAVI (moist)		
IKONOS	0.001**	0.001**
Landsat	-	0.221

** indicates significance at $p<0.01$
* indicates significance at $p<0.05$

The minimal NDVI difference for drier plots may be a function of the low vegetation cover, and dominance of soil spectral response, to which all sensors are sensitive. In the wetter areas, soil moisture and canopy density are suggested as the main causes for decreased satellite NDVI values, due to the previously discussed differential reflectance/absorption of nir and red wavelengths. In other words, surface radiometric measurements display high NDVI values from their proximity to the vegetation canopy, as well as their insensitivity to soil moisture at such a fine resolution

(Section 5.4). Coarser satellite resolutions may incorporate influential factors such as broader expanses of exposed organic and moss layers that reduce NDVI values. IKONOS provides mid-range values between surface and Landsat NDVI, which suggests that 4m spatial resolution may be a useful tool for scaling up point measurements without eliminating localized VI characteristics. Study plots P5, P1, P3, P8, P9, and P10 are almost indistinguishable by Landsat NDVI, yet IKONOS maintains noticeable differences in plot characterization (Figure 5.12). These visual trends are supported by t-test results for

Figure 5.12 - Plot NDVI values

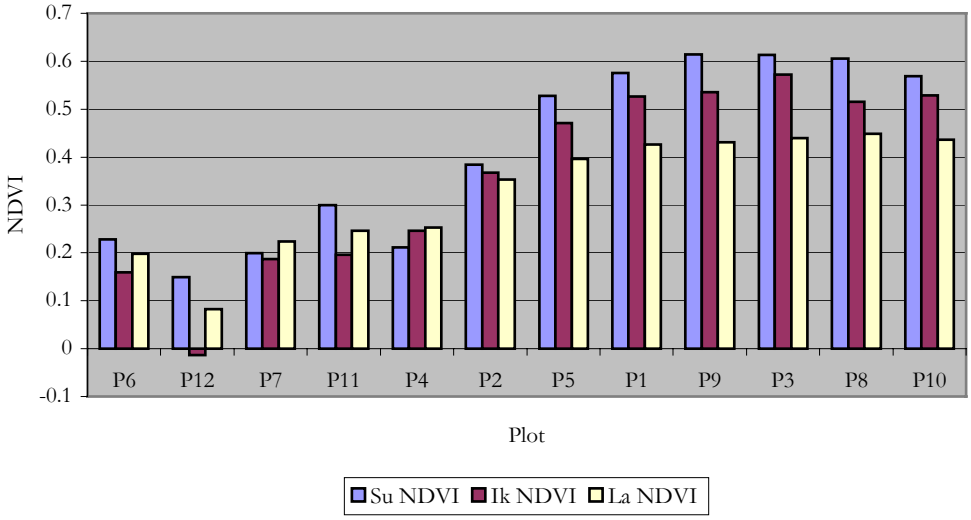

subdivided community types, where there is a significant difference between surface and satellite VIs for moist plots (Table 5.10). In these environments, IKONOS and Landsat NDVI also differ significantly (Table 5.10). Therefore, it would seem that over a range of cover types, any sensor may be employed for biophysical analyses as no significant difference is reported between multi-resolution NDVI values (Table 5.9). When investigating particular community types, however, sensor NDVI values differ greatly (Table 5.10) and must be selected carefully based on a variety of other considerations (i.e., field sampling time, spatial

resolution, and accuracy of biophysical representation of NDVI). Because of intermediary IKONOS NDVI trends it is conservatively suggested that the high spatial resolution satellite would be most useful for characterizing a variety of cover types in tundra environments.

Multi-resolution SAVI results provide much different visual trends (Figure 5.13), but similar statistical results compared to NDVI (Table 5.9). Surface soil-adjusted VIs seem more sensitive to soil reflectance based on the higher observed satellite values for dry sites (with the exception of P12). Study plots P2, P5, P1, P3, P9, P8, and P10 all show IKONOS

Figure 5.13 - Plot SAVI values

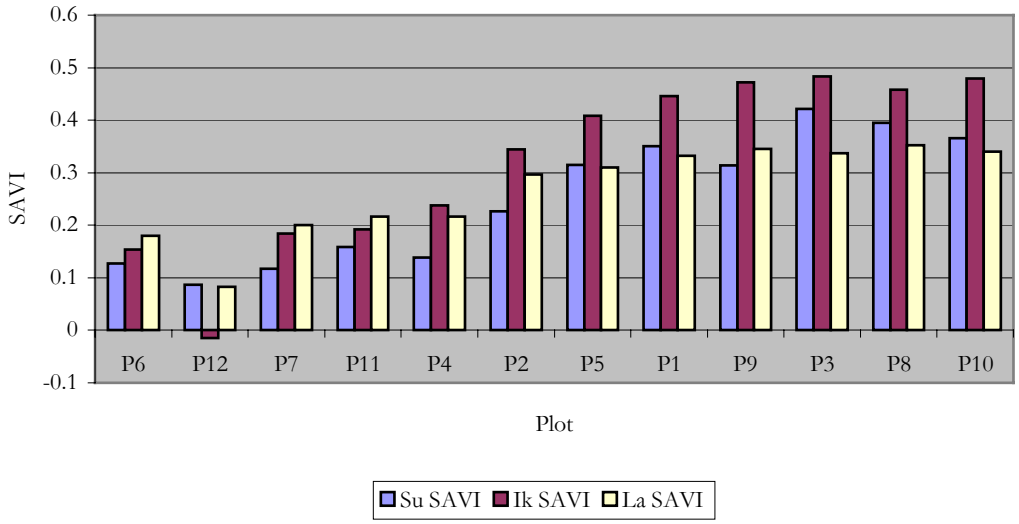

to have the highest SAVI values. This may suggest that the 4m spatial resolution resolves microsite variations, and consequently represents plot vegetation characteristics more accurately. Landsat's spatial aggregation (i.e., regularization of spectral response) seems to minimize plot differentiation using SAVI, while surface values may be overly sensitive to microscale variations in soil moisture/exposure. Over the twelve study plots there remains no statistical difference between multi-resolution SAVI values; however, segregating plots according to dry and moist environments shows all sensors to be significantly different in

SAVI values (excepting surface and Landsat SAVI) (Table 5.10). The similarities among surface and Landsat SAVI results suggest that attempts to calculate reflectance values may be considered relatively successful. SAVI results present support for the argument that soil-adjusted VIs are only useful in environments with moderate to dense vegetation cover. These conclusions present a dilemma for future research, whereby attempts to characterize a range of tundra cover types does not seem to benefit from soil-adjusted VIs, nor a particular remote sensing system. However, if satellite image data is employed to isolate particular cover types, the benefits of a particular VI may become important to assure representative biophysical characterization.

Interesting trends in VI spatial distribution, over the entire study area, may be highlighted by visual representation (Figure 5.14 and 5.15). Image representations of SAVI and other soil-adjusted VIs are not presented, as the visual differences are so minimal they are undetectable by human vision, and thus do not enhance interpretation. Also of note is that subtle gray-tone differences between data types are more a function of viewing tones than of inherent NDVI trends; however, empirical values reported throughout Section 5.5 refer to the actual digital VI values calculated from the surface and satellite reflectance data (Appendix 41 and 42). Dark areas in Figure 5.14 and 5.15 represent regions of low NDVI, while bright areas indicate high NDVI, typically lush green vegetation. Spatial trends of NDVI are similar between images, however IKONOS data can resolve water track vegetation – usually the most productive communities with the highest NDVI values – more accurately than Landsat. As mentioned above, spatial resolution does not seem to factor into VI calculations, but it does factor greatly into the delineation of vegetation communities and patterns of NDVI distribution over the study area (Appendix 43). Noting the spatial

Figure 5.14 – Landsat NDVI Image

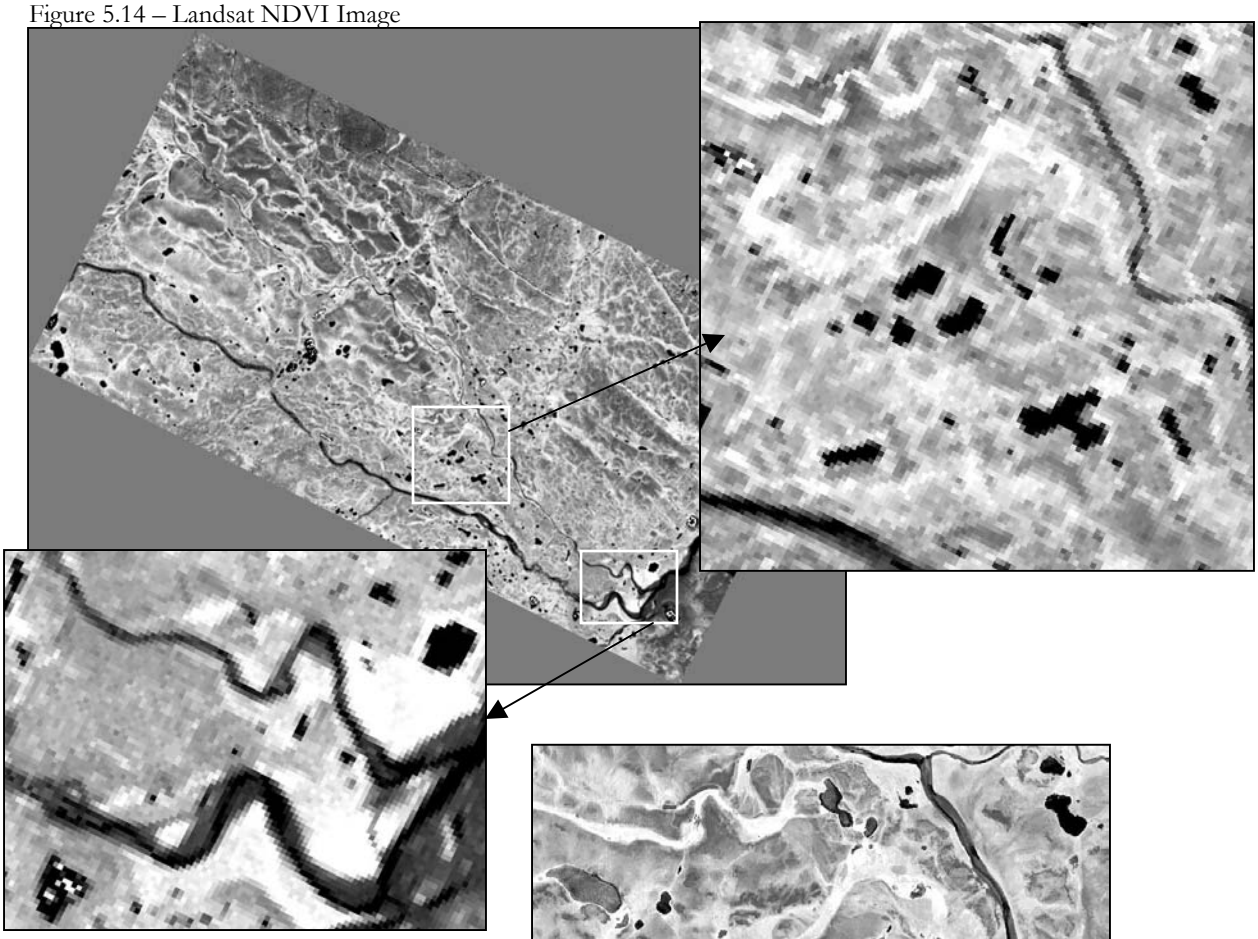

Figure 5.15 – IKONOS NDVI Image

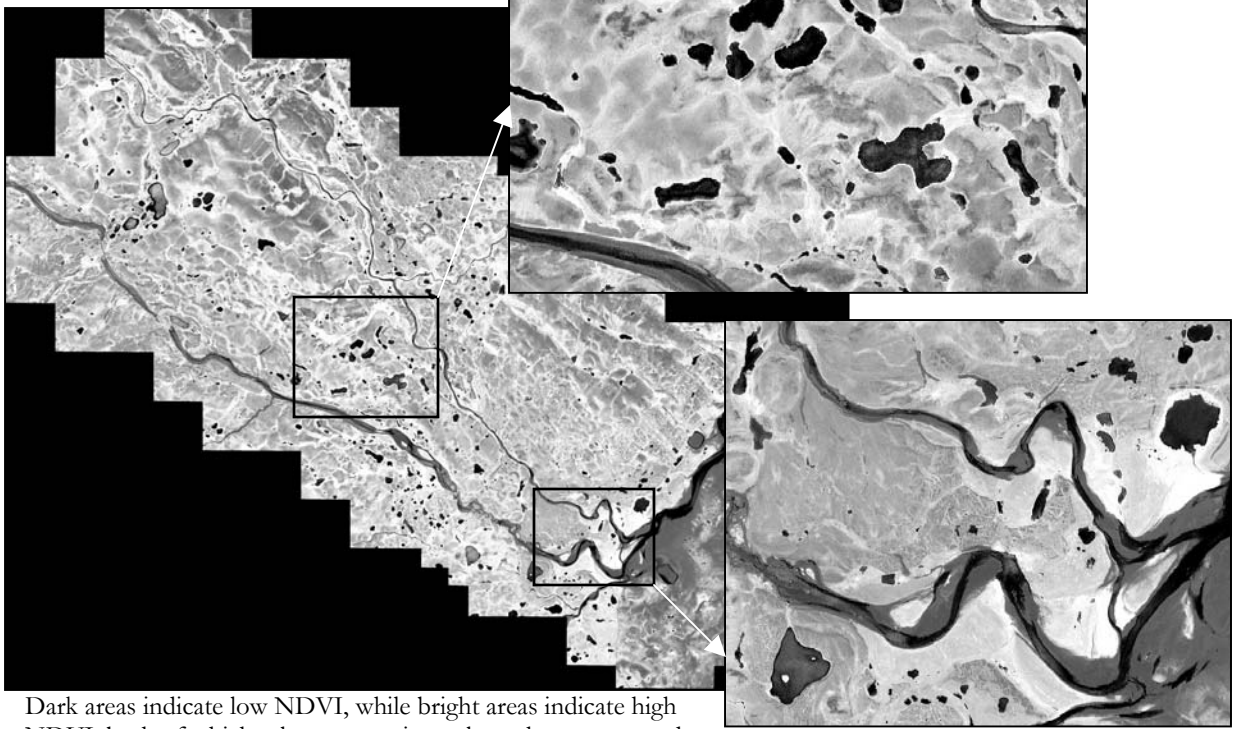

Dark areas indicate low NDVI, while bright areas indicate high NDVI, both of which relate proportionately to the amount and vigour of vegetation cover.

differentiation between images is key for aiding interpretation of moisture and percent cover images calculated from linear regression equations, where both spectral and spatial resolutions factor into the distribution of land cover classes over the entire study area.

5.6 Correlation and Regression Analysis

The Shapiro-Wilk W statistic is used to test for normality of plot variables. All values are not significant at $p<0.05$ (with the exception of surface NDVI $p<0.03$), confirming that biomass, %cover, and VI data employed in regression analyses fit a theoretical normal distribution (Appendix 44). The Shapiro-Wilk test may be the most statistically appealing evaluation of normality, based on its simplicity, but Hair *et. al.* (1998) suggest that the method of constructing histograms (e.g. the number or width of categories) can distort visual portrayal to the point where analysis is useless for small sample sizes (i.e., 12 plots). These difficulties are evident in histograms of study plot variables that often show gaps, or appear bimodal (Appendix 44)**,** whereby these trends may have been proven to be non-normal had they been apparent within a larger sample size. Plots were selected to represent a variety of vegetation environments, but they could not be sufficiently sampled along a continuum. This reality translates into difficulties fitting variables to the theoretical distribution that would be expected from a larger number of plot replicates. Therefore, sample size remains a limiting factor in the interpretation of the normality of the error term in regression analysis and interpretation of results must be conducted with caution. Bivariate regression analyses are performed to determine relationships between biophysical variables and VIs, following warnings that small samples (i.e., <20 observations) are only appropriate for analyses employing simple regression with a single independent variable (Hair *et. al.*, 1998). Despite the unavoidable shortcomings of twelve study plots, regression analysis remains a valuable tool for investigating relationships between tundra biophysical variables

because very strong relationships can still be determined with relative certainty (Hair *et. al.*, 1998). The fact that there are no evident trends of heteroscedasticity in residual plots also indicates the presence of a normal distribution if samples were to be extrapolated to the larger, theoretical population (Appendix 45). These statements suggest that highly significant results warrant more intensive research to investigate whether relationships hold under more robust sampling. Although vegetation indices are usually considered to be a function of vegetation amount, scatterplots and regression equations were constructed with VIs (NDVI or SAVI) as the independent variable in order to calculate biomass, and %cover images from VIs (after Shippert *et. al.*, 1995). In addition to conventional regression analysis, a non-parametric bootstrapping technique is used to reinforce significant relationships in order to alleviate the reliance on error term normality and constraints of a small sample size.

Linear regression analysis produced extremely poor results between VIs and vascular plant biomass (i.e., R^2 <0.1), whereby no appropriate relationship may be determined between the two variables (Figure 5.16). A relationship between vascular biomass and %cover is similarly non-existent. These results are insignificant and thus inadequate for inclusion in further analysis and/or discussion.

A linear relationship between %cover and VIs yields much stronger results than for biomass (i.e., R^2 >0.7) (Table 5.11, Figure 5.17). An interesting addition to regression

Figure 5.16 – Biomass/Surface VI scatterplot

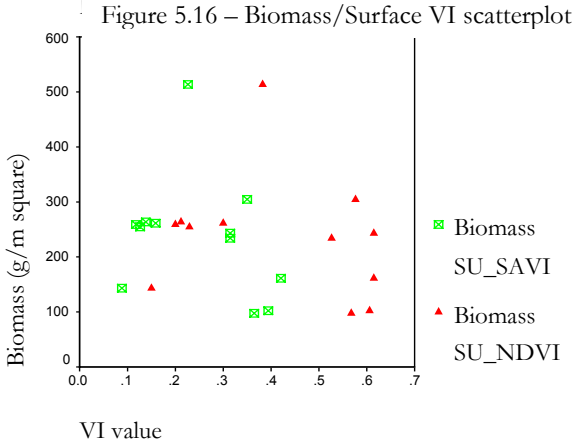

Table 5.11 – Regression results

Y	x	R^2
%cover	Su_NDVI	0.738**
%cover	IK_NDVI	0.825**
%cover	La_NDVI	0.780**
%cover	Su_SAVI	0.716**
%cover	IK_SAVI	0.802**
%cover	La_SAVI	0.767**
%non-veg	Su_NDVI	0.726**
%non-veg	IK_NDVI	0.870**
%non-veg	La_NDVI	0.851**
%non-veg	Su_SAVI	0.688**
%non-veg	IK_SAVI	0.868**
%non-veg	La_SAVI	0.848**

* indicates p<0.05
** indicates p<0.01

Figure 5.17 – Percent cover/NDVI linear relation

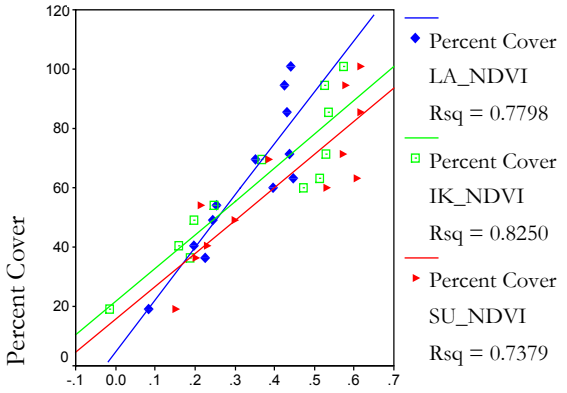

Figure 5.18 - %non-vegetated/NDVI relation

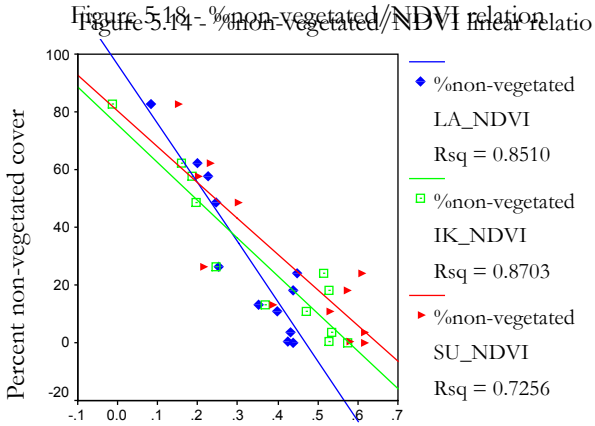

analysis is the investigation into relationships of non-vegetated cover and VIs – as this is often an easier estimate in the field. A negative linear relationship is found between VIs and non-vegetated percent cover estimates (Table 5.11, Figure 5.18), demonstrating stronger linear relationships than %cover values (i.e., $R^2 \approx 0.85$).

Bootstrap resampling is employed to reinforce linear regression results by means of estimating the precision of the regression coefficient (Neter *et. al.*, 1996). The percentile ranges calculated for the intercept (a) and slope (b) coefficients in bootstrap resampling can be compared to regression confidence intervals. If the observed values fall in the middle of the bootstrap calculation percentiles (after 1000 iterations), then regression results are essentially verified with less regard for data normality or sample size. Since the slope (i.e., strength of linear relationship) is of greatest interest, only results for the slope coefficient (b) are reported (Table 5.12). Bootstrap percentiles (Boot 2.5% and 97.5%) provide very similar, but slightly narrower, confidence ranges compared to slope coefficient confidence intervals (Regres. 2.5% and 97.5%) (Table 5.12). These trends reinforce the observed slope coefficients as being representative of linear relationships between biophysical variables and VIs, for both strong and poor results. Poor results (e.g., for biomass and VIs) are confirmed by very broad bootstrap percentiles and confidence intervals. The distribution centered around 0 suggests that the slope is not different from 0 (i.e., no linear relationship).

Regression equations maintaining coefficients with a significant slope (i.e., for %cover and VIs) are reinforced by narrower percentiles/confidence intervals, as well as by values that are all greater than 0 (Table 5.12). This evaluation enables the acceptance of regression slope coefficients, and thus R^2 values, as being representative of trends that may also be prevalent in a larger population.

Table 5.12 – Comparison of regression and bootstrap results

Y	*x*	*Observ. b*	*Boot. 2.5%*	*Regres. 2.5%*	*Boot. 97.5%*	*Regres. 97.5%*
%cover	Su_NDVI	111.27**	68.27	64.54	149.11	157.99
%cover	Ik_NDVI	113.1**	78.36	76.37	138.58	149.75
%cover	La_NDVI	175.19**	116.85	109.60	223.94	240.79
%cover	Su_SAVI	168.61**	96.54	93.86	233.54	243.35
%cover	Ik_SAVI	131.5**	95.93	85.39	168.98	177.60
%cover	La_SAVI	246.44**	175.41	150.84	336.20	342.04

* indicates $p<0.05$
** indicates $p<0.01$

It is postulated that missing bryophyte values greatly impact the observed relationship between biomass and VIs. Currently, no linear trends are displayed, but Figure 5.16 does show the reality that vascular plant biomass is restricted by extremes along the moisture gradient; therefore, peak vascular plant biomass is noticed in mid-range moisture environments (i.e., moist) with moderate VIs (i.e., ≈0.4). Since bryophyte cover tends to increase along with moisture it is likely that linear, or log-transformed, relationships would be enhanced by the inclusion of non-vascular plant biomass (e.g., Hope *et. al.*, 1993). While initial objectives included bryophyte biomass, analysis had to be altered based on results shown in Section 4.4. Shippert *et. al.* (1995) show that grouping biomass plots into physiognomic categories (i.e., dry, moist, wet, etc.) demonstrates strong linear trends. This kind of grouping was not possible for regression analysis employing a 12-plot sample size, but is a valuable consideration for larger data sets, and proved useful in identifying differences in VIs for wetter plots (Section 5.5). The commonly accepted asymptotic relationship between NDVI and biomass for grouped community types (Tucker, 1977;

Hansen, 1991; Shippert *et. al.*, 1995) is also absent from current regression trends, another likely result of missing bryophyte contributions to aboveground biomass. Rees *et. al.* (1998) suggest that VI utility in arctic environments is very limited, based on their poor linear regression results between biomass and NDVI. Difficulties such as spectral mixing and cover type isolation were encountered by Rees *et. al.* (1998) when employing $1m^2$ field plots and Landsat MSS data. It was thought that this study, maintaining larger community characterization (i.e., 1 ha) combined with higher satellite spatial resolution (i.e., Landsat 7 ETM+ and IKONOS), would have improved results; however, it becomes evident that neither data type accurately predicts above-ground vascular plant biomass from vegetation spectral characteristics.

The variance of %cover is best explained by IKONOS NDVI (i.e., 83%). Soil-adjusted VIs do not enhance the linear relationships between %cover and VI response, as may be expected from earlier results showing no significant difference of means between satellite VIs, across a range of tundra environments (Section 5.5). Interestingly, results are slightly improved when incorporating %non-vegetated cover – perhaps the increased simplicity in identifying non-vegetated surfaces improves the accuracy of cover estimates and thus linear relationships. Both IKONOS VIs provide the highest R^2 values when estimating %non-vegetated cover, a possible indication of the utility of high spatial resolution in detecting exposed surfaces. Stow *et. al.* (1993b) found a significant linear relationship between percentage shrub cover and NDVI, while Shippert *et. al.* (1995) showed strong linear relationships between NDVI and LAI when data are grouped into physiognomic categories. Walker *et. al.* (1995) also suggest that areal vegetation coverage is strongly linked to NDVI, as well as other related features such as landscape age and soil pH. Despite the

fact that regression results range from R^2=0.7-0.8, these relationships are linear and significant, corroborating trends reported in other arctic environments.

Figure 5.19 demonstrates the adherence of %cover variations to topographic trends, and corresponding moisture regimes. Stow *et. al.* (1993b) show trends of increasing moisture and NDVI along a toposequence from ridge-top to toeslope, which are visually represented in the %cover image calculated from linear regression (Figure 5.19). Percent cover increases along declining elevations and slope to maintain increased vegetation canopy density in areas of high moisture (i.e., watertracks, drainage channels, and areas with moderate to minimal exposure). Modeling %cover over the entire study site provides an interesting perspective on overall vegetation distribution and cover characteristics that would otherwise be difficult to visualize. Although these values must be interpreted with caution (i.e., IKONOS NDVI only explains 83% of the vegetation cover variance for the study plots), they provide preliminary results with which further, more exhaustive studies may be compared. The high spatial resolving power of IKONOS data shows tremendous potential for tundra vegetation mapping as it is capable of delineating %cover trends throughout the study area, with relative consistency, based only on the detailed vegetation characterization of twelve study plots (Figure 5.19).

Because moisture variables could not be included in regression analysis, a non-parametric Spearman's rank correlation coefficient was employed to investigate the relationships between VIs and plot moisture, as well as moisture and %cover. Results confirm prior qualitative observations that VIs are highest in plots with increased moisture. All results are positively correlated (Table 5.13), yet relations seem slightly improved with the use

Table 5.13 – Spearman's rho

Variable 1	Variable 2	Correlation
Moisture	Su_NDVI	0.843**
Moisture	IK_NDVI	0.903**
Moisture	La_NDVI	0.959**
Moisture	Su_SAVI	0.921**
Moisture	IK_SAVI	0.945**
Moisture	La_SAVI	0.945**
Moisture	%cover	0.801**

* indicates $p<0.05$
** indicates $p<0.01$

of SAVI. Satellite VIs also provide marginal improvements over surface VIs. Moisture and %cover are significantly correlated, but the lower value suggests that VIs may be valuable links with which to characterize tundra biophysical characteristics. Relationships between VIs and moisture have not been directly addressed in arctic biophysical remote sensing studies, perhaps due to the difficulty associated with its quantification, but these elements are always implied where physiognomic and community type divisions are made according to moisture status (e.g., Hope *et. al.*, 1993; Stow *et. al.*, 1993b; Shippert *et. al.*, 1995; Walker *et. al.*, 1995). Remote sensing data may be better correlated with moisture, or %cover, individually through its ability to acquire signals less from vegetation *per se*, and more from associated environmental variables that influence the nature and condition of vegetation. Therefore, the utility of satellite VIs is conservatively suggested to be an important tool in future characterization of vegetation health and spatial arrangements through its ability to account for a variety of influential ecological properties on vegetation vigour.

Figure 5.19 – Percent cover image from IKONOS NDVI*

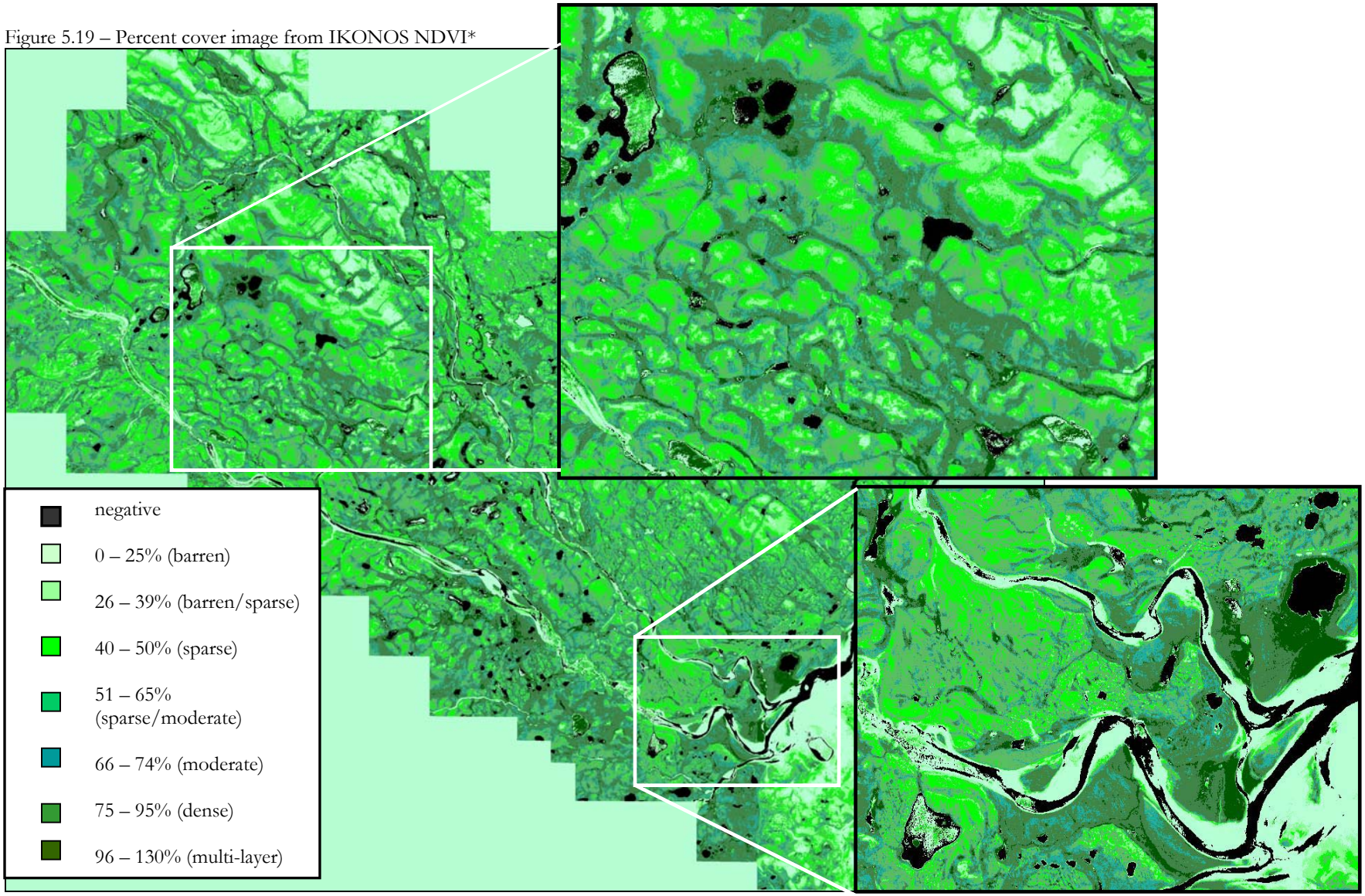

* calculated from regression equation: $Y=6.969+187.586(IK\_NDVI)$ with $R^2=0.825$, $p<0.01$.

Chapter 6 – Conclusions and Recommendations
An Arctic Introspective

6.1 Conclusions

Ordered according to sequence of objectives, the following conclusions may be drawn from results presented in this study:

1. Vegetation communities within the Boothia Peninsula study area demonstrate relatively little variability in trends of species dominance. *Dryas integrifolia* is the dominant species found on both dry and moist sites, where rock cover is also quite prevalent. Wetter sites follow trends towards graminoid dominance by *Eriophorum spp.* and *Carex spp.* with bryophyte cover also prolific underlying the graminoid layer. Plant species richness does not factor into species plot dominance, as forbs contribute substantially to richness measures but minimally to overall vegetation cover. Conservative species richness estimates range from 14 on the most barren ridge-top study plot (i.e., P12) to 23 on moist (i.e., P2) to wet (i.e., P8) plots. These measures likely underestimate actual species richness due to analyst limitations during *in situ* species identification. When species are grouped into plant functional types, %cover trends show that three plots are predominantly non-vegetated (i.e., P6, P7, P12), five plots are dominated by shrub cover (i.e., P1, P2, P4, P9, P11), and graminoids dominate two plots (i.e., P3, P10), while P5 (i.e., mainly shrubs and mosses) and P8 (i.e., almost equal amounts of graminoids, mosses, and non-vegetated cover) demonstrate co-/multiple dominance. Vegetation cover characteristics follow microtopographic gradients which influence soil moisture, nutrient availability, snow cover, exposure, and microclimate differences that define habitats broadly as dwarf-shrub heath or moist to wet sedge meadows. A variety of *in situ* plot differentiations

are also made based on vegetation distribution patterns such as sorted/non-sorted stripes (i.e., P7, P11), sorted/non-sorted circles (i.e., P6), fell fields (i.e., P2, P4), and localized representations of polar desert (i.e., P12), moist sedge meadow (i.e., P1, P8, P10), water-track communities (i.e., P9), and snowbed communities (i.e., P2, P3, P5).

2. Due to difficulties encountered in the field, above-ground biomass collection was limited to vascular plant biomass. Dry weights are relatively consistent with trends in other arctic environments, where the moist study plot (i.e., P2) maintained the highest biomass (514 g/m^2) and the lowest biomass (i.e. $<150g/m^2$) was recorded for the wettest and driest plots (i.e., P10 and P12), respectively. Biomass results tend to reflect relative %cover of plant functional groups; however, when comparing plots with similar amounts of graminoid and shrub cover, biomass is consistently lower for graminoids due to their increased below-ground allocation of biomass and decreased fibre density. The relative moisture term collected within each biomass quadrat resulted in one of the most beneficial variables throughout analysis of results. Scaled from 1 to 10, this qualitative moisture estimate provided valuable insight throughout investigations whereby moisture influences on %cover, biomass, and spectral reflectance were clearly demonstrated.

3. Plot spectral separability proved superior when employing Landsat data, as its higher waveband capacity seems to enhance spectral distinction among cover types that appear similar through the visible and near-infrared wavelengths. The issue of spectral resolution also factors into unsupervised classification analyses; however, as the maximum number of classes allowable is increased, IKONOS proves more useful in delineating tundra vegetation components because of its superior 4m spatial resolution

(compared to 30m for Landsat). IKONOS data can detect microsite variations within plots, and along linear and convoluted topographic features such as watertracks and snowbed vegetation communities.

4. The spectral vegetation indices NDVI, SAVI, and MSAVI were calculated using surface spectro-radiometer, IKONOS, and Landsat 7 ETM+ data. Graphic representation showed common trends of decreased values for soil-adjusted VIs. Statistical comparisons were unexpected in that ANOVA results showed soil-adjusted VIs to be significantly different from NDVI only when analyzing surface VIs, across a range of cover types. Segregating the data into moist and dry plots revealed additional patterns. Observed VIs were identical for dry environments, but soil-adjusted VIs were significantly lower than NDVI for all sensors when analyzing moist plots. Soil-adjusted VIs were concluded to be functionally equivalent for all sensors in the current tundra environment using supplementary independent sample t-tests. This reality led to using only NDVI and SAVI for remaining analysis. Furthermore, no significant difference can be reported when investigating the difference of means for NDVI or SAVI, across a range of environments, using multiple sensors. However, significant differences are found between all but Landsat and surface VIs, within moist plots, when segregating study plots. In other words, spectral vegetation index characterization (using red and near-infrared image bands) of tundra vegetation communities does not seem influenced by spatial resolution, while the utility of soil-adjusted VIs is limited over a range of environments.

5. Linear regression analyses showed strong, significant relationships between VIs and %cover values (i.e. $R^2>0.7$, $p<0.01$). Poor results were determined for vascular plant

biomass (i.e., R^2 <0.1). The missing bryophyte biomass values are thought to be a major cause for these disappointing results. Linear relationships were highest between IKONOS VIs and %cover, followed by Landsat and surface VIs. SAVI did not provide improved linear relations between biophysical variables and remote sensing data, suggesting that soil-adjusted VIs are of limited use in arctic environments as the low stature and canopy density may impart too much soil reflectance to improve NDVI results.

6. Since IKONOS data provided relatively successful linear correlations between NDVI and %cover, the high spatial resolution was deemed the most appropriate when attempting to extrapolate plot-specific results across the entire study area. While image representation of %cover distribution is conservative due to a small sample size, results showing the delineation of environmental gradients experienced during the field campaign are encouraging. Despite not being able to include moisture estimates in regression analysis, strong Spearman's rank correlations are determined between VIs and moisture, where data type again seems of minimal influence. Weaker correlations between %cover and moisture suggest that VIs may be important intermediary variables with which to characterize tundra community types. These results establish preliminary estimates from which future, more exhaustive studies, can build upon to improve the accuracy of spatial and spectral representation of tundra biophysical parameters on Boothia Peninsula, and throughout the Canadian Arctic.

6.2 Recommendations

The following are suggested as means of improving current study results:

1. Collecting bryophyte biomass cannot be done using reference squares. Improving harvesting techniques to include the entire moss mat, with appropriate soil line

delineation, is likely the missing link for developing linear relations between above-ground biomass and VIs. Furthermore, expanding photographic cover and biomass estimates described by Wein and Rencz (1976), to eliminate or minimize destructive biomass harvests, would increase field sampling efficiency while also decreasing environmental impact legacies of scientific field campaigns.

2. Following Spjelkavik's (1995) suggestion to include botanists/field ecologists in field campaigns and satellite interpretation would enhance the representation of species richness and dominance measures, as well as the characterization of vegetation communities.

3. Expanding sample size through more exhaustive field campaigns may characterize biophysical variables more extensively and accurately, but these efforts cannot come at the expense of shrinking within-plot replicates. To accomplish this expansion, future research would require: i) more collaborative researchers (i.e., more people in the field performing a variety of sampling regimes); or ii) multi-year research projects with a longer-term vision (which creates new problems of accounting for seasonal variations). Compromises are inherently necessary since the growing season and transportation factors are so limiting to arctic field studies.

4. Establishing quantitative moisture estimates that may be incorporated into regression analysis may provide an informative additional dimension to biophysical analysis.

5. Developing reliable means of converting IKONOS multispectral data to reflectance values would enhance the interpretation and meaning of IKONOS VIs. In turn, this would increase confidence in the ability of IKONOS to delineate vegetation communities both spectrally and spatially.

6. Establishing reliable methods of calculating atmospheric effects at the time of remote sensing data acquisition could improve the representation of VIs by correcting for atmospheric effects that influence digital brightness values (Stow *et. al.,* 1993b; Shippert *et. al.,* 1995; Jacobsen and Hansen, 1999) and may lead to stronger correlations between biophysical parameters and VIs (Turner *et. al.*, 1999).

7. More research incorporating the utility of soil-adjusted VIs in arctic environments is warranted to determine the accuracy of current conclusions regarding their functional equivalence for estimating tundra biophysical properties.

6.3 Future Directions for Arctic Research

Global warming is expected to be most pronounced at high latitudes (Edlund, 1991; Shaver *et. al.*, 1992; Chapin *et. al.*, 1995); therefore, estimating the sensitivity of tundra environments to potential variations in precipitation and temperature is one of the most prominent research foci in recent and ongoing arctic research. Time series satellite data has

the potential to play a large role in the monitoring of predicted vegetation changes, and hopefully, distinguishing natural variation from industrial human impacts that threaten arctic ecosystems (Spjelkavik, 1995). The need for increased baseline studies is pressing, because natural and human impacts may soon become inseparable, and potential global climate changes are currently unpredictable (Bliss and Matveyeva, 1992). Much important research has been conducted to determine the degree to which tundra vegetation stores/releases carbon dioxide (Oberbauer and Dawson, 1992; Shaver *et. al.*, 1992; Chapin *et. al.*, 1995; Oechel *et. al.*, 1997) but there remains little consensus on the short- or long-term biosphere impacts of these relations. If these shifts are translated into variations in vegetation cover and species composition (as indicated by McFadden *et. al.*, 1998) then the utility of biophysical remote sensing becomes apparent in its ability to characterize large, remote expanses of arctic tundra (Nemani and Running, 1995). Because there are inherent risks involved in using simplified, aggregated models to represent vegetation and ecosystem processes at the scale of a landscape (Ostendorf and Reynolds, 1998), remote sensing can never replace detailed ecological studies, but it may be the link for extrapolating these results to estimate broader implications of locally modified phenomena. Increased collaboration across previously independent research disciplines may provide the most efficient means of tackling the complexity of issues in need of investigation (Chapin *et. al.*, 1992a).

Northern Canada is the dominant national areal component and is important for a variety of political, environmental, economic, and social reasons (Dey and Richards, 1981). Despite the fact that it is unlikely to become home for millions of people (Dey and Richards, 1981), the Arctic is the cherished home of approximately 50 000 Inuit Canadians. Many of these permanent residents still rely heavily on local biological resources and would be greatly affected by changes in their surroundings resulting from climate changes (Chapin *et. al.*,

1992b); therefore, for its permanent residents, as well as the entire country, it is necessary to understand the current and potential state of the environment in arctic Canada. Chapin *et. al.* (1992b, 450) warn that "…the sensitivity of arctic ecosystems to human activities associated with resource extraction and exploitation will undoubtedly change with changes in vegetation and the thermal balance of the tundra. Thus climatic change could strongly alter the interactions between human populations and their arctic environments." It is for these reasons that the final recommendation is to pave new research directions that adequately account for human/environment interactions, including both scientific and social scientific methods, to most accurately represent the ecological realities with which Inuit must live on a daily basis. These new initiatives become increasingly warranted as Nunavut legislates community approval, and some degree of local participation, in all research projects conducted within the new territory. Jacobs (1991, 6) presents an interesting perspective on the evolving challenges for arctic scientific research:

> Though the scientist may instinctively focus on the relationships of [environmental] problems to the people and the ecosystem of which they are a part, it requires exceptional skill in communication and some understanding of the culture to convince skeptical, pragmatic people who do not share our sometimes unquestioning faith in the inherent usefulness of scientific inquiry. Hope of winning the tolerance if not the enthusiastic support of northerners for the practice of science in the North rests ultimately on the relevance of the research to their situation, demonstrated through communication and education, and on their effective participation in the process.

Because of these changing realities it is foreseeable, and strongly recommended, that new research disciplines are created to bridge the gaps between scientific, social scientific, and local, expertise. This attempt is believed to maximize the contribution of all valid insights, while characterizing tundra environments in a fashion applicable within the broader Canadian and global context.

Bibliography

Analytical Spectral Devices. (2002) *Spectroradiometers/FieldSpec Pro Specs.* URL: http://www.asdi.com/asdi_t2_pr_sp_fsp_s.html. April 7.

Arp J. (2002) Personal Communication. *Discussion on radiance and reflectance calibration for IKONOS imagery*. January 28.

Asner G.P. (1998) Biophysical and biochemical sources of variability in canopy reflectance. *Remote Sensing of Environment*, 64, 234-253.

Asrar G., Myneni, R. B., and Kanemasu, E. T. (1989) Estimation of plant-canopy attributes from spectral reflectance measurements. *Theory and Applications of Optical Remote Sensing.* Eds. Asrar, G. pp. 14-65. John Wiley and Sons, New York.

Barber G., (1988) *Elementary Statistics for Geographers*. The Guilford Press, New York.

Barber G. (2002) Personal Communication. *Linear Regression Discussion.* February 20.

Barbour M.G., Burk, J. H., and Pitts, W. D. (1987) *Terrestrial Plant Ecology*. The Benjamin/Cummings Publishing Company, Inc., Menlo Park. Second Edition.

Baret F., and Guyot, G. (1991) Potentials and Limits of Vegetation Indices for LAI and APAR Assessment. *Remote Sensing of Environment*, 35, 161-173.

Bliss L.C., and Matveyeva, N. V. (1992) Circumpolar Arctic Vegetation. *Arctic Ecosystems in a Changing Climate - An Ecophysiological Perspective.* Eds. Chapin S.F., Jeffries, R.L., Reynolds, J.F., Shaver, G.R. Svoboda, J., and Chu, E.W.), pp. 59-89. Academic Press, Inc., San Diego.

Bliss L.C., and Peterson, K. M. (1992) Plant Succession, Competition, and the Physiological Constraints of Species in the Arctic. In: *Arctic Ecosystems in a Changing Climate - An Ecophysiological Perspective.* Eds. Chapin S.F., Jeffries, R.L., Reynolds, J.F., Shaver, G.R. Svoboda, J., and Chu, E.W.), pp. 111-136. Academic Press, Inc., San Diego.

Boutton T.W., and Tieszen, L. L. (1983) Estimation of plant biomass by spectral reflectance in an east African grassland. *Range Management*, 36, 213-221.

Box E.O., Holben, B. N., and Kalb, H. (1989) Accuracy of the AVHRR vegetation index as a predictor of biomass, primary productivity, and net CO2 flux. *Vegetatio*, 80, 71-89.

Brown J.H. (1984) On the Relationship Between Abundance and Distribution of Species. *The American Naturalist*, 124, 255-279.

Burt P. (1991) *Barrenland Beauties - Showy Plants of the Arctic Coast*. The Northern Publishers, Yellowknife.

Campbell J.B. (1996) *Introduction to Remote Sensing*. The Guilford Press, New York. Second Edition.

Chapin S.F., Jefferies, R. L., Reynolds, J. F., Shaver, G. R., and Svoboda, J. (1992a) Arctic Plant Physiological Ecology: A Challenge for the Future. *Arctic Ecosystems in a Changing Climate - An Ecophysiological Perspective*. Eds. Chapin, S. F., Jefferies, R. L., Reynolds, J. F., Shaver, G. R., Svoboda, J., and Chu, E. W. pp. 3-8. Academic Press, Inc., San Diego.

Chapin S. F., Jeffries., R. L, Reynolds, J. F., Shaver, G. R., and Svoboda, J. (1992b) Arctic Plant Physiological Ecology in an Ecosystem Context. *Arctic Ecosystems in a Changing Climate - An Ecophysiological Perspective*. Eds. Chapin S. F., Jeffries, R. L., Reynolds, J. F., Shaver, G. R. Svoboda, J., and Chu, E. W. pp. 441-451. Academic Press Inc., San Diego.

Chapin S.F., Shaver, G. R., Giblin, A. E., Nadelhoffer, K. J., and Laundre, J. A. (1995) Response of arctic tundra to experimental and observed changes in climate. *Ecology Washington D.C.*, 76, 694-711.

Dancy K.J., Webster, R., and Abel, N. O. J. (1986) Estimating and mapping grass cover and biomass from low-level photographic sampling. *International Journal of Remote Sensing*, 7, 1679-1704.

Davidson A., and Csillag, F. (2001) The Influence of Vegetation Index and Spatial Resolution on a Two-Date Remote Sensing-Derived Relation to C4 Species Coverage. *Remote Sensing of Environment*, 75, 138-151.

de Gruijter J. (1999) Spatial sampling schemes for remote sensing. *Spatial Statistics for Remote* Sensing. Eds. Stein, A. pp. 211-242. Klewer Academic Publishers.

Dey B., and Richards, J. H. (1981) The Canadian North: Utility of Remote Sensing for Environmental Monitoring. *Remote Sensing of Environment*, 11, 57-72.

Dungan J.L. (1995) Geostatistical approaches for spatial estimation of vegetation quantities using ground and image data. *RSS 95: Remote Sensing in Action - Proceedings of the 21st annual conference*, pp. 947-954.

Dyke A.S. (1984) Quaternary Geology of Boothia Peninsula and Northern District of Keewatin, Central Canadian Arctic. *Geological Survey of Canada*, pp. 1-26, Ottawa.

Edlund S.A. (1991) Climate Change and its Effects on Canadian Arctic Plant Communities. In: *Arctic Environment: Past, Present, and Future*. Eds. Woo, M.K, and Gregor, D. J., pp. 121-135. McMaster University, Hamilton.

Edwards E.J., Moody, A., and Walker, D. A. (2000) A Western Alaskan Transect to Examine Interactions of Climate, Substrate, Vegetation, and Spectral Reflectance. pp.58. University of Alaska-Fairbanks, Fairbanks, Alaska. June 22.

ENVI. (2000) *Help Menu.* The Environment for Visualizing Images Software V. 3.4. Boulder, CO, USA.

Environment Canada. (2000) *Boothia Peninsula Plateau.* URL http://www.ec.gc.ca/soer-ree/English/Framework/NarDesc/Region.cfm?region=20. April 12.

Forbes A. (2001) Personal Communication. *Meteorological data for Boothia Peninsula 2001 field season*. February 13.

Galvao L.S., Vitorellow, I., and Pizarro, M. A. (2000) An adequate band positioning to enhance NDVI contrasts among green vegetation, senescent biomass, and tropical soils. *International Journal of Remote Sensing*, 21, 1953-1960.

Gemmell F., and Varjo, J. (1999) Utility of Reflectance Model Inversion Versus Two Spectral Indices for Estimating Biophysical Characteristics in a Boreal Forest Test Site. *Remote Sensing of Environment*, 68, 95-111.

Glaser P.H. (1992) Raised bogs in eastern North America - regional controls for species richness and floristic assemblages. *Journal of Ecology*, 80, 535-554.

Goodall D.W. (1970) Statistical Plant Ecology. *Annual Review of Ecology and Systematics*, 1, 99-124.

Goward S.N., Masek, J. G., Williams, D. L., Irons, J. R., and Thompson, R. J. (2001) The Landsat 7 mission - Terrestrial research and applications for the 21st century. *Remote Sensing of Environment*, 78, 3-12.

Gower S.T., Kucharik, C. J., and Norman, J. M. (1999) Direct and Indirect Estimation of Leaf Area Index, f_{APAR}, and Net Primary Production of Terrestrial Ecosystems. *Remote Sensing of Environment*, 70, 29-51.

Hair J.F.J., Anderson, R. E., Tatham, R. L., and Black, W. C. (1998) *Multivariate Data Analysis.* Prentice Hall, New Jersey. Fifth Edition.

Hansen B.U. (1991) Monitoring natural vegetation in southern Greenland using NOAA AVHRR and field measurements. *Arctic*, 44, 94-101.

Henry G. (1998) Environmental influences on the structure of sedge meadows in the Canadian High Arctic. *Plant Ecology*, 134, 119-129.

Hoekstra T.W., Allen, T. F. H., and Flather, C. H. (1991) Implicit Scaling in Ecological Research. *Bioscience*, 41, 148-154.

Hope A.S., Fleming, J. B., Vourlitis, G., Stow, D. A., Oechel, W. C., Hack, T. (1995) Relating CO2 fluxes to spectral vegetation indices in tundra landscapes: importance of footprint definition. *Polar Record*, 31, 245-250.

Hope A.S., Kimball, J. S., and Stow, D. A. (1993) The relationship between tussock tundra spectral reflectance properties and biomass and vegetation composition. *International Journal of Remote Sensing*, 14, 1861-1874.

Huete A.R. (1988) A Soil-Adjusted Vegetation Index (SAVI). *Remote Sensing of Environment*, 25, 295-309.

Jacobs J.D. (1991) Science and Change in Northern Canada. *Common Ground: Northern Peoples and the Environment*. Eds. Jacobs, J.D, and Montevecchi, W. A., pp. 1-8. Institute of Social & Economic Research, Memorial University, Memorial University, St. John's, Newfoundland.

Jacobsen A., and Hansen, B. U. (1999) Estimation of the soil heat flux/net radiation ratio based on spectral vegetation indexes in high-latitude Arctic areas. *International Journal of Remote Sensing*, 20, 445-461.

Jelinski D.E. (2001) Personal Communication. *Sampling Strategy Discussion*. May 8.

Jelinski D.E., and Wu, J. (1996) The modifiable areal unit problem and implications for landscape ecology. *Landscape Ecology*, 11, 129-140.

Jensen J.R. (1996) *Introductory Digital Image Processing - A Remote Sensing Perspective*. Prentice Hall, New Jersey.

Jensen J.R. (2000) *Remote Sensing of the Environment - An Earth Resource Perspective*. Prentice Hall, New Jersey.

Laidler G.J. (2001) *Investigations into Arctic Tundra Vegetation Ecology and Appropriate Sampling Methods*. Unpublished report, pp. 81. Queen's University, Kingston.

Laidler G.J., and Treitz, P.M. (2001) Biophysical Remote Sensing of Arctic Environments. *Progress in Physical Geography*, in press.

Larsen J.A. (1964) The Role of Physiology and Environment in the Distribution of Arctic Plants. pp. 70. University of Wisconsin.

Lévesque E. (1996) Minimum Area and Cover-Abundance Scales as Applied to Polar Desert Vegetation. *Arctic and Alpine Research*, 28, 156-162.

Lévesque E. (2001) Personal Communication. *Biomass drying methods*. September 13.

Lloyd A.H., Armbruster, S. W., and Edwards, M. E. (1994) Ecology of a steppe-tundra gradient in interior Alaska. *Journal of Vegetation Science*, 5, 897-912.

Lobo A., Moloney, K., Chic, O., and Chiariello, N. (1998) Analysis of fine-scale spatial pattern of a grassland from remotely-sensed imagery and field collected data. *Landscape Ecology*, 13, 111-131.

Longton R.E. (1997) The role of bryophytes and lichens in polar ecosystems. *Ecology of Arctic Environments*. Eds. Woodin, S.J., and Marquiss, M. pp. 69-96. Blackwell Science Limited, Oxford.

McFadden J.P., Chapin, F. S., and Hollinger, D. Y. (1998) Subgrid-scale variability in the surface energy balance of arctic tundra. *Journal of Geophysical Research*, 103, 28,947-28,961.

McMichael C.E., Hope, A. S., Stow, D. A., Fleming, J. B., Vourlitis, G, and Oechel, W. (1999) Estimating CO_2 exchange at two sites in Arctic tundra ecosystems during the growing season using a spectral vegetation index. *International Journal of Remote Sensing*, 20, 683-698.

Merrill E.H., Branble-Brodahl, M. K., Marrs, R. W., and Boyce, M. S. (1993) Estimation of green herbaceous phytomass from Landsat MSS data in Yellowstone National Park. *Journal of Range Management*, 46, 151-157.

Mosbech A., and Hansen, B. U. (1994) Comparison of satellite imagery and infrared aerial photography as vegetation mapping methods in an arctic study area; Jameson Land, East Greenland. *Polar Research*, 13, 139-152.

Mueller-Dombois D., and Ellenberg, H. (1974) *Aims and Methods of Vegetation Ecology*. John Wiley & Sons, Toronto.

Muller S.V., Racoviteanu, A. E., and Walker, D. A. (1999) Landsat MSS-derived land-cover map of northern Alaska: extrapolation methods and a comparison with photo-interpreted and AVHRR-derived maps. *International Journal of Remote Sensing*, 20, 2921-2946.

Murray D.F. (1997) Regional and local vascular plant diversity in the Arctic. *Opera Botanica*, 132, 9-18.

Nadelhoffer K.J., Giblin, A. E., Shaver, G. R., and Linkins, A. E. (1992) Microbial Processes and Plant Nutient Availability in Arctic Soils. *Arctic Ecosystems in a Changing Climate - An Ecophysiological Perspective*. Eds. Chapin S. F., Jeffries, R.L, Reynolds, J. F., Shaver, G. R., Svoboda, J., and Chu, E. W., pp. 261-300. Academic Press, Inc., San Diego.

NASA (2002) *Landsat 7 - Science Data Users Handbook*. URL http://ltpwww.gsfc.nasa.gov/IAS/handbook/handbook_toc.html. January 14.

Nemani R.R., and Running, S. W. (1995) Satellite Monitoring of Global Land Cover Changes and Their Impact on Climate. *Climatic Change*, 31, 395-413.

Neter J., Kutner, M. H., Nachtsheim, C. J., and Wasserman, W. (1996) *Applied Linear Regression Models*. The McGraw-Hill Companies, Inc., Chicago. Third Edition.

Oberbauer S.F., and Dawson, T. E. (1992) Water-Relations of Arctic Vascular Plants. In: *Arctic Ecosystems in a Changing Climate - An Ecophysiological Perspective*. Eds. Chapin S. F., Jefferies, R.L., Reynolds, J. F., Shaver, G. R. Svoboda, J., and Chu, E. W., pp. 259-279. Academic Press, Inc., San Diego.

Oechel W. (1989) Nutrient and water flux in a small arctic watershed: an overview. *Holarctic Ecology*, 12, 29-237.

Oechel W.C., Cook, A. C., Hastings, S. J., and Vourlitis, G. L. (1997) Effects of CO2 and climate change on arctic ecosystems. *Ecology of Arctic Environments*. Eds. Woodin, S. J., and Marquiss, M., pp. 255-273. Blackwell Science Limited, Oxford.

Ostendorf B., and Reynolds, J. F. (1998) A model of arctic tundra vegetation derived from topographic gradients. *Landscape Ecology*, 13, 187-201.

Pielou E.C. (1994) *A Naturalist's Guide to the Arctic*. The University of Chicago Press, Chicago.

Porsild A.E., and Cody, W. J. (1980) *Vascular Plants of Continental Northwest Territories, Canada*. National Museums of Canada, Ottawa.

Purevdorj R., Tateishi, R., Ishiyama, R., and Honda, Y. (1998) Relationships between percent vegetation cover and vegetation indices. *International Journal of Remote Sensing*, 19, 3519-3535.

Qi J., Huete, A. R., Kerr, Y. H., and Sorooshian, S.. (1994) A Modified Soil Adjusted Vegetation Index. *Remote Sensing of Environment*, 48, 119-126.

Radarsat International. (2002) *Products and Resources: Landsat 7*. URL http://www.rsi.ca/.

Rees W.G., Golubeva, E. I., and Williams, M. (1998) Are vegetation indices useful in the Arctic? *Polar Record*, 34, 333-336.

Richardson A.J., and Wiegard, C. L. (1977) Using spectral vegetation indices to estimate rangeland productivity. *Geocarto International*, 1, 63-70.

Rouse J.W., Haas, R. H., Schell, J. A., and Deering, D. W. (1974) Monitoring vegetation systems in the Great Plains with ERTS. *Third Earth Resources Technology Satellite-1 Symposium*. Eds. Freden, S. C, Mercanti, E. P., and Becker, M. A., pp. 309-317. National Aeronautics and Space Administration, Scientific and Technical Information Office, Goddard Space Flight Centre, Washington, D.C. December 10-14.

Schaefer J.A., and Messier, F. (1995) Scale-dependent Correlations of Arctic Vegetation and Snow Cover. *Arctic and Alpine Research*, 27, 38-43.

Sellers P.J., Berry, J. A., Collatz, G. J., Field, C. B., and Hall, F. G. (1992) Canopy reflectance, photosynthesis and transpiration. III. A re-analysis using improved leaf models and a new canopy integration scheme. *Remote Sensing of Environment*, 42, 1-30.

Shapiro S.S., Wilk, M. B., and Chen, H. J. (1968) A Comparative Study of Various Tests for Normality. *Journal of the American Statistical Association*, 63, 1343-1372.

Shaver G.R., and Chapin, S. F. (1991) Production: Biomass Relationships and Element Cycling in Contrasting Arctic Vegetation Types. *Ecological Monographs*, 61, 1-31.

Shaver G.R., and Kummerow, J. (1992) Phenology, Resource Allocation, and Growth of Arctic Vascular Plants. *Arctic Ecosystems in a Changing Climate - An Ecophysiological Perspective*. Eds. Chapin, S. F., Jefferies, R. L., Reynolds, J. F., Shaver, G. R. Svoboda, J., and Chu, E. W., pp. 193-211. Academic Press, Inc., San Diego.

Shaver G.R., Billings, W. D., Chapin, S. F., Giblin, A. E., Nadelhoffer, K. J., Oechel, W. C., and Rastetter, E. B. (1992) Global Change and the Carbon Balance of Arctic Ecosystems. *Bioscience*, 42, 433-441.

Shippert M.M., Walker, D. A., Auerbach, N. A., and Lewis, B. E. (1995) Biomass and leaf-area index maps derived from SPOT images for Toolik Lake and Imnavait Creek areas, Alaska. *Polar Record*, 31, 147-154.

Smithsonian Meteorological Tables. (2002) *Smithsonian Meteorological Tables*. URL http://www.google.com/search?q=cache:2RpszhNDNhUC:edisto.egr.duke.edu/~medina/CE225/ephemer_sun.pdf+smithsonian+meteorological+tables&hl=en. January 23.

SpaceImaging. (2001) *IKONOS Statistics*. URL http://www.spaceimaging.com/aboutus/satellites/IKONOS/ikonos.html#stats. January 16.

Spjelkavik S. (1995) A satellite-based map compared to traditional vegetation map of Arctic vegetation in the Ny-Alesund area, Svalbard. *Polar Record*, 31, 257-269.

STATISTICA Help. (2000) *Shapiro-Wilk statistic*. StatSoft Inc., Tulsa. Version 5.5.

Stonehouse B. (1989) *Polar Ecology*. Blackie and Son Limited, London.

Stow D.A., Burns, B. H., and Hope, A. S. (1989) Mapping Arctic tundra vegetation types using digital SPOT/HRV-XS data - A preliminary assessment. *International Journal of Remote Sensing*, 10, 1451-1457.

Stow D.A., Hope, A. S., and George, R. H. (1993a) Reflectance characteristics of arctic tundra vegetation from airborne radiometry. *International Journal of Remote Sensing*, 14, 1239-1244.

Stow D.A., Burns, B. H., and Hope, A. S. (1993b) Spectral, spatial and temporal characteristics of Arctic tundra reflectance. *International Journal of Remote Sensing*, 14, 2445-2462.

Stow D.A., Daeschner, S., Boynton, W., and Hope, A. (2000) Arctic tundra functional types by classification of single-date and AVHRR bi-weekly NDVI composite datasets. *International Journal of Remote Sensing*, 21, 1773-1779.

Surveys and Mapping Branch. (1978) *District of Franklin, Northwest Territories.* Energy Mines and Resources, Ottawa. NTS map sheets 57F/11, 57F/7, 57F/6, 57F/3, 57F/2.

Tarnocai C., and Netterville, J. A. (1976) Biophysical land classification in Boothia Peninsula and Northwest Keewatin, N.W.T. *Ecological (Biophysical) Land Classification in Canada*, pp. 159-171. Canada Committee on Ecological (Biophysical) Land Classification, Petawawa, Ontario. May 25-28.

Teillet P. (2002) Personal Communication. *Correspondence concerning IKONOS radiometric calibration*. January/February.

Tieszen L.L., Reed, B. C, Bliss, N. B., Wylie, B. K., and Dejong, D. D. (1997) NDVI, C3 and C4 production, and distributions in Great Plains grassland land cover classes. *Ecological Applications*, 7, 59-78.

Treitz P., Howarth, P. J., and Suffling, R. C. (1992) Application of Detailed Ground Information to Vegetation Mapping with High Spatial Resolution Digital Imagery. *Remote Sensing of Environment*, 42, 65-82.

Treitz P.M., and Howarth, P. J. (1999) Hyperspectral remote sensing for estimating biophysical parameters of forest ecosystems. *Progress in Physical Geography*, 23, 359-390.

Trimble Navigation Limited. (1996) *GeoExplorer II - Operation Manual.* Trimble Navigation Limited, California.

Tucker C.J. (1977) Asymptotic nature of grass canopy spectral reflectance. *Applied Optics*, 16, 1151-1157.

Tucker C.J., Vanpraet, C. L., Sharman, M. J., and Van Ittersum, G. (1985) Satellite Remote Sensing of Total Herbaceous Biomass Production in the Senegalese Sahel: 1980 - 1984. *Remote Sensing of Environment*, 17, 233-249.

Turner D.P., Cohen, W. B., Kennedy, R. E., Fassnacht, K. A., and Briggs, J. M. (1999) Relationships between Leaf Area Index and Landsat TM Spectral Vegetation Indices across Three Temperate Zone Sites. *Remote Sensing of Environment*, 70, 52-68.

van Groenewoud H. (1992) The robustness of Correspondence, Detrended Correspondence, and TWINSPAN Analysis. *Journal of Vegetation Science*, 3, 239-246.

Vierling L.A., Deering, D. W., and Eck, T. F. (1997) Differences in arctic tundra vegetation type and phenology as seen using bi-directional radiometry in the early growing season. *Remote Sensing of Environment*, 60, 71-82.

Walker D.A., Acevedo, W., Everett, K. R., Gaydos, L., Brown, J., and Webber, P. J. (1982) Landsat-assisted environmental mapping in the Arctic National Wildlife Refuge, Alaska. pp. 1-70. Colorado University, Institute of Arctic and Alpine Research, Boulder.

Walker D.A. (1995) Toward a New Arctic Vegetation Map: St. Petersburg Workshop. *Arctic and Alpine Research*, 27, 103-104.

Walker D.A., Auerbach, N. A., and Shippert, M. M. (1995) NDVI, biomass, and landscape evolution of glaciated terrain in northern Alaska. *Polar Record*, 31, 169-178.

Walker D.A. (2000) Hierarchical subdivision of Arctic tundra based on vegetation response to climate, parent material and topography. *Global Change Biology*, 6, 19-34.

Walker M.D., Walker, D. A., and Auerbach, N. (1994) Plant communities of a tussock tundra landscape in Brooks Range Foothills, Alaska. *Journal of Vegetation Science*, 5, 843-866.

Wein R.W., and Rencz, A. N. (1976) Plant cover and standing crop sampling procedures for the Canadian High Arctic. *Arctic and Alpine Research*, 8, 139-150.

Wiens J.A. (1989) Spatial scaling in ecology. *Functional Ecology*, 3, 385-397.

Woodcock C.E., and Strahler, A. H. (1987) The Factor of Scale in Remote Sensing. *Remote Sensing of Environment*, 21, 311-332.

Young C.G., Dale, M. R. T., and Henry, G. H. R. (1999) Spatial pattern of vegetation in high arctic sedge meadows. *Ecoscience*, 6, 556-564.

Young S.B. (1994) *To The Arctic*. Wiley Popular Science, Toronto.

Yu R.V. (1994) Snowbed vegetation of far northeastern Asia. *Journal of Vegetation Science*, 5, 829-842.

Appendix 1
Tundra Sub-zones

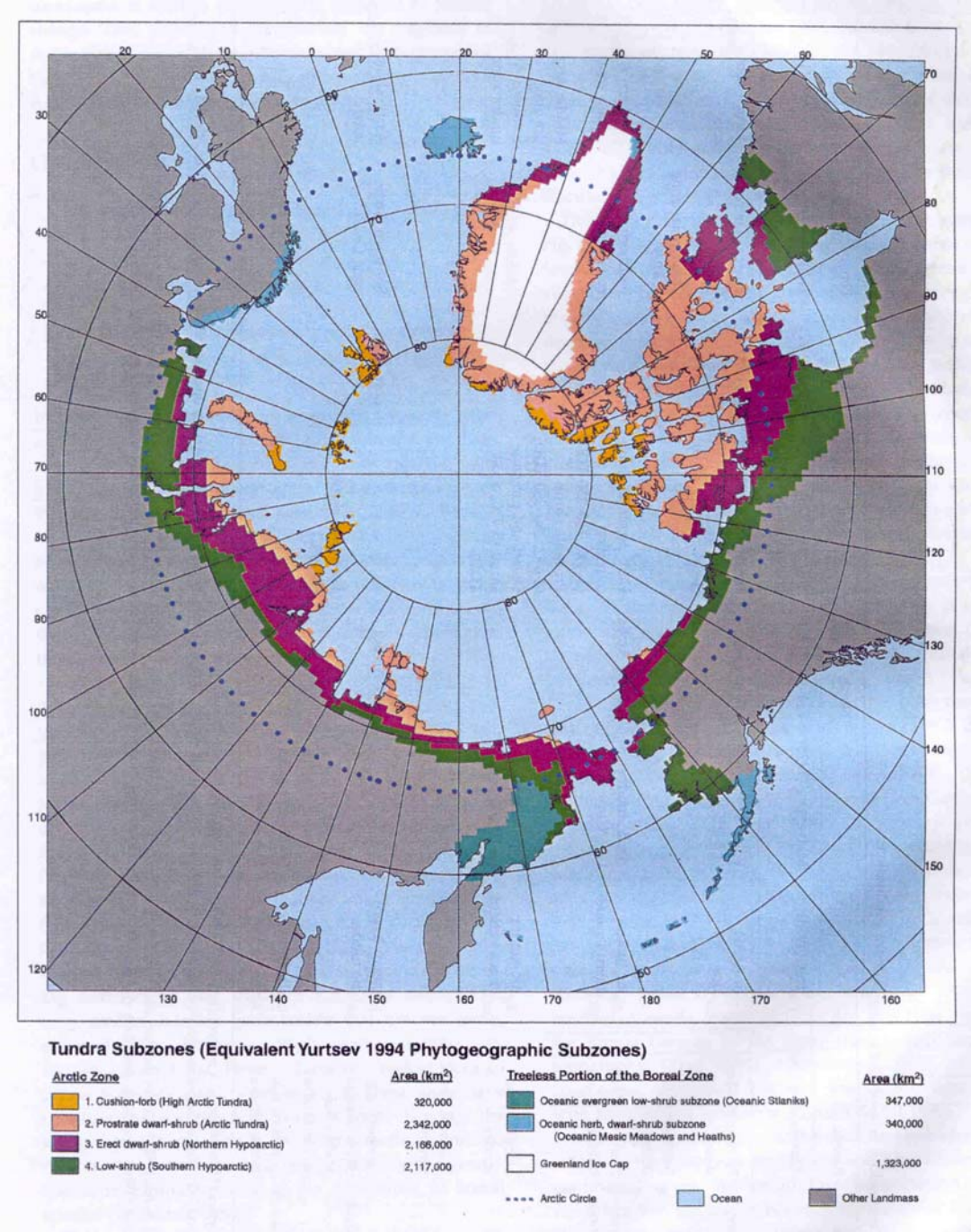

Source: Walker, 2000, 22

Appendix 2
Sedge Meadow Description

Cottongrass, or arctic cotton, (genus *Eriophorum*) is the most important group of sedges (Young, 1994). The "grass" term is actually inaccurate, for sedges are not grasses (Young, 1994), they are a part of the sedge family (*Cyperaceae*) (Pielou, 1994). Often going unnoticed when they are not in flower (Burt, 1991), their characteristic feature is a head (inflorescence) of many tiny flowers that, when aggregated, look like a globular tuft, usually white or light gray in colour (Young, 1994). Different species are found in different conditions defining different kinds of sedge meadows (Young, 1994), but sedges are often associated with marshy or wet areas (Burt, 1991). In many areas, arctic cotton forms a successional stage: tussocks begin on a wet area, or a saturated slope, and mature to create the surface known as tussock tundra (Burt, 1991) (tough, fibrous clumps of *Eriophorum vaginatum* that range in size to a maximum of approximately the size of a human head, connected to the ground by a narrow, flexible, but tough neck (Young, 1994; Pielou, 1994)). Tussock tundra is also favoured by intense frost action (Young, 1994).

Wet tundra is more widespread and less uniform than tussock tundra, as well as being less dependent on a single species (Young, 1994). Cottongrass remains a major component of landcover, especially *Eriophorum angustifolium*, where its best development occurs in flat, marshy areas, usually where standing water remains throughout the majority of summer (Young, 1994). Other *Eriophorum* species dominate in differing amounts of soil moisture and terrain formations. A variety of true sedges (genus *Carex*) comprise the most numerous genera among the *Cyperaceae* family (Pielou, 1994), and they too occur in wet sedge meadows; however, interspecies differentiation may be more difficult than for *Eriophorum* (Young, 1994). In terms of sheer volume (biomass) sedges far outweigh true grasses in most tundra environments. While this is valid information, the difficulty with distinguishing between sedges and grasses necessitates their grouping into the graminoid functional type, so their relative contributions to above-ground biomass may not be quantifiable.

Appendix 3
Common Heath Species

Genus	Species	Name	Description
Ledum	*decumbens*	Labrador Tea	A low shrub with narrow alternate evergreen leaves, seldom exceeding 15cm in height – it ranks with cottongrass as a predictable component of low arctic tundra
Vaccinium	*uliginosum*	Blueberry or Bog Bilberry	The most common blueberry species, a low-growing shrub that is often almost prostrate due to wind pruning, it produces vast quantities of berries over much of the tundra area
Arctostaphylos	*alpina*	Bearberry	A dwarf species of manzanita with large wrinkled leaves, pale green bell-shaped flowers and large, black, tasteless berries
Cassiope	*tetragona*	White Arctic Heather	Tiny white bell-shaped flowers, with needles like evergreen leaves, common on dry, rocky uplands, and they are particularly prevalent in moist coastal mountain regions, prefers sites protected by deep snowbanks for winter
Empetrum	*nigrum*	Crowberry or Blackberry	One of the most important dwarf shrubs, but not in the *Ericaceae* family, a dwarf creeping evergreen shrub with black or dark red berries, common on tundra, beach shores, stony uplands, and all but the most exposed arctic environments

Source: Young, 1994, 195-196; Burt, 1991, 126-136; Pielou, 1994, 150-154

Appendix 4
Lichen Characteristics

Lichens are of great importance in a polar desert environment as this group of primitive plants have adapted amazingly to harsh conditions, where two kinds of plants are actually found living together (i.e. the "thallus" – the main body, a dense tangled mass of threadlike fungal material; and the algae – single-celled organisms encapsulated within the fungal strands, supporting the colony with nutrients) (Young, 1994; Pielou, 1994). Lichens prove difficult to identify, but are generally classified by a series of schemes based on shape, growth habit, colour, reproductive structures, as well as chemical plant constituents (Young, 1994; Pielou, 1994). They are found as a part of almost all tundra vegetation, inhabiting the bare soil between tussocks (if it is dry enough), rocks, and gravel areas (Young, 1994).

Appendix 5
Moss Characteristics

Mosses and lichens are similar mainly in their attributes regarding their lack of roots (Pielou, 194). In contrast though, mosses are simply primitive green plants that contain chlorophyll in their cells to enable them to feed through photosynthesis (Pielou, 1994). Mosses contribute significantly to above-ground production and phytomass in tundra subzones 2 – 4 and production tends to increase with water availability (Longton, 1997). Among the many arctic mosses that are able to grow submerged in water, red moss (*Bryum cryophyllum*) forms great red cushions of incredible brightness, providing splashes of colour in some otherwise quite barren looking landscapes (Pielou, 1994). The most common northern moss is sphagnum, or peat moss (genus *Sphagnum*), where subspecies are hard to differentiate. It is useful, however, to note that all species grow as moist, spongy carpets, made up of thousands of little mound-shaped rosettes. Sphagnum moss is not alone in its peat-producing abilities, and tends to become rarer with increasing latitudes beyond the treeline (Pielou, 1994).

Appendix 6
Potential Influences on the Distribution, Formation, and Composition of Vegetation Communities

External influence	Potential consequences
Permafrost	• Permafrost is perhaps the most obvious arctic environmental characteristic affecting plant growth and spatial distribution at all northern latitudes. • Pielou (1994) states that the Arctic could in fact be called "permafrost country". This term describes permanently frozen ground governing the shape and texture of the ground surface everywhere. This layer of permanently frozen ground may be as deep as 3.5m in the subarctic, or as shallow as 20cm in the High Arctic (Pielou, 1994). • The term "talik" designates the ground below the permafrost layer that remains unfrozen. • The "active layer" is the ground above permafrost, to which all plant roots are confined in the summer, as it is the only layer that thaws. • Permafrost exists, and persists, wherever the average temperature is low enough, and forms a continuous underground layer throughout the whole tundra-covered region. The exceptions are under lakes and rivers big enough and deep enough to avoid freezing to the bottom in winter (Pielou, 1994).
Tundra Polygons (Figure 1)	• A common feature in an arctic landscape, these polygons may range anywhere from 5-50m in diameter. Their shape denotes their formation, as they were formed when the ground cracked as it froze. • A network of ground cracks, outlining tundra polygons, takes decades or even centuries to develop, and they are generally held open and repeatedly enlarged by the growing ice wedges within them (Figure 1) (Pielou, 1994). • **Low-centre polygon** (Figure 2a) – the ice wedge thickens, forcing the soil up on each side into a low shoulder, thus forming a center that is slightly lower than its rim (Figure 2a) (Pielou, 1994). Plants that are able to endure drought and wind exposure tend to grow on the ridges surrounding these polygons (as well as on hummock tops and sometimes the final stage of high-centre polygons once the ground has dried out). The centers of these low polygons are often shallow pools or waterlogged areas dominated by sedges, and sometimes cottongrass (Pielou, 1994). • **High-centre polygon** (Figure 2b) – maintain centers that are waterlogged even when not submerged (Figure 2b). These constitute another plant habitat, where the growth of these various communities may gradually change the landscape causing low-centre polygons to develop, over the very long term, into higher centers (Pielou, 1994). The comparatively damp troughs between polygons and hummocks are habitats for a variety of moisture-loving plants such as knotweed and buttercup, while these troughs also provide arctic white heather the shelter it requires to protect it from strong winds (Pielou, 1994).

Appendix 6 (continued)

Tundra Hummocks (Figure 3)	• One of the most characteristic of all arctic terrains are fields of hummocks, occurring almost everywhere (Pielou, 1994). • A well-developed hummock field displays hummocks of relatively similar size and matching vegetation both on hummock tops and in crevices between (Pielou, 1994). • The resulting pattern appears almost as regular as textured wallpaper, with the hummock size decreasing with increasing latitude. Most commonly found on hummock tops is the arctic dryad, whereas on wetter ground it is the purple saxifrage. The crevices maintain different plants, or are sometimes devoid of plants all together (Pielou, 1994). • Contrary to how they may seem, hummocks are not static: a) flowing water (deepens the channels along hummocks), and wind-born dust (captured on hummock tops and may add to hummock height) can increase the "hummockiness" of the tundra environment b) hummocks drying out (where plants growing on them die, and hummocks may be "sandpapered" flat by wind erosion) and eroding hummocks (stumps appearing as concentric rings) are processes that can decrease the "hummockiness" of the tundra environment) (Pielou, 1994, 49)
Microtopographic Influences on Vegetation Proliferation	• Due to the small stature and specific environmental requirements for plant species in the Arctic, the acknowledgement of the very important role played by microtopography in plant growth and distribution is imperative. • For example, soil moisture (wetness) is controlled more by microtopography than by annual precipitation (Pielou, 1994). This phenomena is resultant from the reality that water on the active layer does not readily disappear because the plants' evaporation, and absorption, of water is slowed by low temperatures – water simply collects in every little hollow and tract of low ground to form wet marshes dotted by numerous tundra ponds (Pielou, 1994). Therefore, the soil's wet and dry pattern is matched by the pattern of plant communities growing on it (Appendix 8). • Microtopography itself may vary in spatial extent, ranging from arrays of big tundra polygons (up to 50m across) to fields of small hummocks (less than 1m) (Pielou, 1994). Plants not only respond to these patterns, they also contribute to their development. In addition, variations in soil fertility, as well as soil distribution, freeze/thaw patterns, animal or human activity, also have visible effects on plants. As demonstrated in the previous subsections, the varied vegetation composition on the landscape surface often highlights the underlying topographic structure (Pielou, 1994). • Snowpatch communities are equally as interesting, and equally as influenced by microtopographical characteristics. These communities are found where winter snowdrifts are able to accumulate to greater than average depth, lasting well into spring and sometimes all through summer (Pielou, 1994). Plants growing in these environments must be able to grow fast, flower, set and seed in an unusually short growing season (even by arctic standards). • Snow provides protection to plants from winter wind and trickles of water throughout the summer drought. Most noticeable in polar desert, these are often the only patches of ground where, due to constant meltwater supply, moss carpets are able to grow. These areas also provide a moist habitat for other plants such as mountain sorrel, snow buttercup, dwarf buttercup, arctic cinquefoil, sibbaldia, and finger lichen (Pielou, 1994).

Appendix 6 (continued)

Figure 1 – Tundra polygons

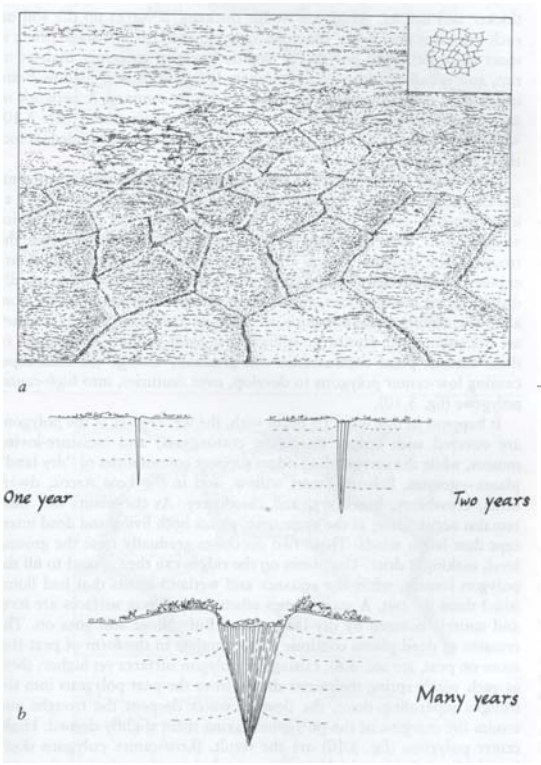

Source: Pielou, 1994, 39

Figure 2 – Low- (a) and high-center (b) polygons

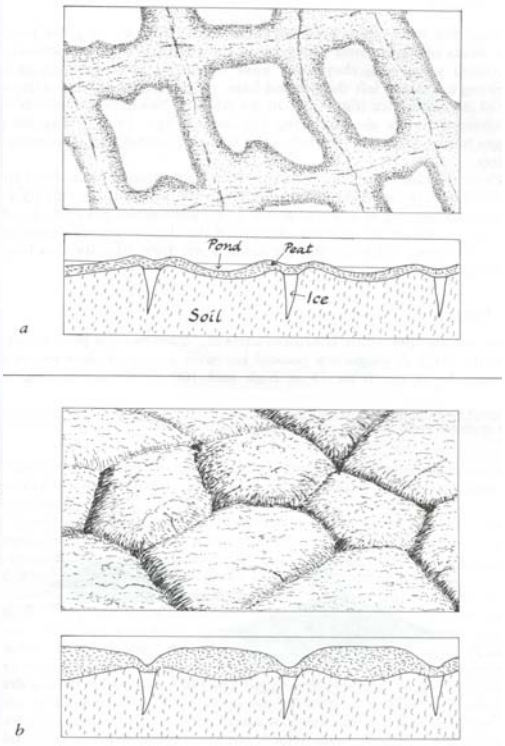

Source: Pielou, 1994, 41

Figure 3 – Tundra hummocks

Photo: Gita Laidler, August 13, 2001

Appendix 7
Patterned Ground Examples

Patterned Ground Design	**Description**
Frost Boils	More or less circular patches of smooth, bare clay, formed where an underground pocket of wet, unfrozen clay or silt (fines) oozes up through a weak spot in the surface
Felsenmeer	Top layer, at the ground surface of stratified stones, where there is a huge expanse of broken, angular rocks, where very few, and generally no, plants may grow
Sorted Circles (Sorted Polygons)	Frost boils outlined by concentric rings of rocks, graded by size where the smallest are closer to the middle
Sorted Patterns	Fines and larger rocks are separated or sorted out
Unsorted Patterns	Discerned where unfrozen fines have oozed in ground devoid of pebbles and rocks, where undisturbed ground between frost boils usually support a modicum of vegetation

Source: Pielou, 1994, 49

Appendix 8
Tundra Communities Described According to Dampness Underfoot

Category	General Land Cover	Characteristics
Dry	Fell fields and barren grounds	➢ widespread in north and restricted to dry uplands in south ➢ expanses of rough, open terrain with virtually ahumic soils ➢ much of the year they appear barren ➢ with summer moisture dried-out cushions and patches of vegetation burst into life, yielding arctic poppies, avens, moss campions, saxifrages
Moist	Shrub and heath lands	➢ central tundra belts are steppe-like plains where low shrubs, sedges, and grasses form a semi-continuous cover of vegetation up to 1m high ➢ in moist lowlands, dense ground cover of short grasses, mosses, lichens and occasional ferns grows from peaty, sometimes waterlogged soils ➢ dwarf willows, birches, and alders form emergent vegetation ➢ better-drained uplands have thinner soils and a ground cover of gray-green lichens, so-called reindeer mosses ➢ tundra is widely grazed by mammals, especially voles and lemmings that burrow in undergrowth
Wet	Mires, marshes, and ponds	➢ undulating coastal plains and other ungraded lowlands, underlain by permafrost, in summer form some of tundra's wettest areas ➢ ponds, marshes and mires fill hollows, alternating with higher ground which emerges first from under snow and dries out in course of summer ➢ from wet, acid, peaty soils with partly-decomposed debris emerge tussock grasses, rich swards of pendent grass and tundra grass, sedges, and rushes, cotton grasses, and dark green, hummock-forming mosses

Source: Stonehouse, 1989, 86-87

Appendix 9

Examples of Ratio-based Indices for Biophysical Studies (adapted from Treitz and Howarth, 1999)

Index	Formula	Description	Origin
Near-IR / Red Reflectance Ratio (Ratio Vegetation Index))	ρ_n/ρ_r	responds to changes in amount of green biomass, chlorophyll content and leaf-water stress	Birth and McVey, 1968; Tucker, 1979
Modified Simple Ratio (MSR)	$\frac{(\rho_n/\rho_r)-1}{(\rho_n/\rho_r)^{1/2}+1}$	MSR is meant to be an improvement over RDVI for linearizing the relationships between the ratio and biophysical parameters.	Chen, 1996
Normalized Difference Vegetation Index (NDVI)	$(\rho_n-\rho_r)/(\rho_n+\rho_r)$	responds to changes in amount of green biomass, chlorophyll content and leaf-water stress	Rouse *et al.*, 1974; Goward *et al.*, 1994
Vegetation Condition Index (VCI)	$\frac{100(NDVI_{ij}-NDVImin_j)}{NDVImax_j-NDVImin_j}$	portrays weather dynamics more effectively than NDVI for non-homogeneous areas by removing the influences of climate, soil, vegetation type and topography	Kogan, 1990
Perpendicular Vegetation Index (PVI)	$\frac{[s(\rho_n)-\rho_r+a]}{[1+(s)^2]^{1/2}}$ where a = soil line intercept s = slope of the soil line	attempts to eliminate differences in soil background and is most effective under conditions of low LAI (arid and semi-arid environments)	Richardson and Wiegand, 1977; Wiegand *et al.*, 1991
Weighted Difference Vegetation Index (WDVI)	$\rho_n-s*\rho_r$ where s = slope of the soil line	WDVI is a mathematically simpler version of PVI, but it has an unrestricted range	Clevers, 1988
Soil Adjusted Vegetation Index (SAVI)	$\frac{(\rho_n-\rho_r)(1+L)}{(\rho_n+\rho_r+L)}$ where $L = 0.5$	L is a correction factor which ranges from 0 for very high vegetation cover to 1 for very low vegetation cover; minimizes soil-brightness induced variations	Huete, 1988; Huete and Tucker, 1991; Qi *et al.*, 1993
Soil and Atmospheric resistant vegetation Index (SARVI2)	$\frac{2.5(\rho_n-\rho_r)}{(1+\rho_n+6\rho_r-7.5/\rho_b)}$	simplification of MNDVI by removing NDVI component	Huete *et al.*, 1997

Appendix 9 (continued)

Index	Landsat TM Equivalent	Description	Origin
Modified SAVI (MSAVI)	$\frac{(\rho_n-\rho_r)(1+L)}{(\rho_n+\rho_r+L)}$ where L = 1-2*s*NDVI*WDVI s = slope of the soil line	this index provides a variable correction factor L which is the product of NDVI and WDVI; the level of vegetation cover does not have to be known *a priori* to calculate L	Qi *et al.*, 1994
Modified SAVI2 (MSAVI2)	$\frac{2\rho_n+1-((2\rho_n+1)^2-8(\rho_n-\rho_r))^{1/2}}{2}$		Qi *et al.*, 1994
Transformed Soil Adjusted Vegetation Index (TSAVI)	$\frac{s[\rho_n-s(\rho_r)-a]}{[a\rho_n+\rho_r-a*s+X*(1+s*s)]}$ where a = soil line intercept s = slope of the soil line X = adjustment factor	modifications of Huete (1988) SAVI to compensate for soil variability due to changes in solar elevation, leaf-angle distribution and LAI	Baret *et al.*, 1989; Baret and Guyot, 1991; Wiegand *et al.*, 1991
Atmospherically Resistant Vegetation Index (ARVI)	$\frac{\rho_n-\rho_{rb}}{\rho_n+\rho_{rb}}$ where $\rho_{rb} = \rho_r-\square(\rho_b-\rho_r)$	minimizes atmospheric-induced variations; utilizes the difference in radiance between the blue and red channels, via a $\square$ function to correct the radiance in the red channel and stabilize the index to variations in aerosol content	Kaufman and Tanré, 1992
Soil and Atmospherically Resistant Vegetation Index (SARVI)	$\frac{\rho_n-\rho_{rb}(1+L)}{\rho_n+\rho_{rb}+L}$ where $\rho_{rb} = \rho_r-\square(\rho_b-\rho_r)$	both atmospheric and canopy background corrections can be combined; minimizes soil and atmospheric noise; results in a more stable NDVI	Kaufman and Tanré, 1992
Soil and Atmospheric resistant vegetation Index (SARVI2)	$\frac{2.5(\rho_n-\rho_r)}{(1+\rho_n+6\rho_r-7.5/\rho_b)}$	simplification of MNDVI by removing NDVI component	Huete *et al.*, 1997
Non-Linear Index (NLI)	$(\rho_n^2-\rho_r)/(\rho_n^2+\rho_r)$	NLI linearizes relationships with surface parameters that tend to be non-linear.	Goel and Qin, 1994
Renormalized Difference Vegetation Index (RDVI)	$(\rho_n-\rho_r)/(\rho_n+\rho_r)^{1/2}$	Developed to linearize relationships with surface parameters that tend to be non-linear.	Roujean and Breon, 1995

Appendix 10
Summary of In Situ Tundra Vegetation Spectral Characteristics

Land Cover	NDVI	Source
Dwarf shrub	0.60	Rees *et al*., 1998
Green fruticose lichen	0.20	
Brown fruticose lichen	0.34	
Acidic dry dwarf-shrub, fruticose-lichen tundra	0.64	Walker *et al*., 1995
Nonacidic dry dwarf-shrub, fruticose-lichen tundra	0.51	
Acidic moist graminoid dwarf-shrub tundra	0.73	
Nonacidic moist graminoid dwarf-shrub tundra	0.64	
Acidic wet graminoid tundra	0.58	
Nonacidic wet graminoid tundra	0.56	
Shrublands	0.82	
Dry heath tundra	0.56	Stow *et al*., 1993b
Moist tussock tundra	0.64	
Wet sedge tundra	0.62	

Appendix 11

Summary of Tundra Vegetation Spectral Characteristics Derived From Satellite Data

Land Cover	Vegetation Index Value Simple Ratio	Vegetation Index Value NDVI	Source
Glaciers	0.53 - 0.67		Spjelkavik, 1995
Young moraines	0.67 - 0.75		
River beds, deltas, and moraines	0.77 - 0.80		
Mountain slopes and stony ground	0.83 - 0.90		
Barren tundra, mostly without vegetation	0.81 - 0.89		
Moist moss tundra dominated by moss Tomentypnum nitens	1.70 & 1.71		
Dechampsia meadows (tundra mires)	1.02		
Dryas heaths	1.33 & 1.16 & 1.28		
Luzula heath	1.14		
Saxifraga oppositifolia - Cetraciella delisei	0.92 - 1.11		
Barren gravel tundra	0.90 - 0.92		
White arctic bell heather		0.57	Mosbech and Hansen, 1994
Blueberry		0.58 - 0.67	
Arctic cottongrass		0.68	
Acidic dry dwarf shrub fruticose-lichen tundra		0.40	Walker *et al*., 1995
Nonacidic dry dwarf shrub fruticose-lichen tundra		0.39	
Acidic moist graminoid dwarf-shrub tundra		0.46	
Nonacidic moist graminoid dwarf-shrub tundra		0.43	
Acidic wet graminoid tundra		0.41	
Nonacidic wet graminoid tundra		0.40	
Shrublands		0.54	
Bare stone tundra		0.36	Rees *et al*., 1998
Partial crustose lichen cover		0.37	
Complete crustose lichen cover		0.69	
Healthy fruticose lichen tundra with some dwarf shrubs		0.71	
Healthy fruticose lichen tundra		0.58	
Damaged fruticose lichen tundra		0.45	
Very damaged fruticose lichen tundra		0.45	
Healthy dwarf shrub tundra		0.71	
Damaged dwarf shrub tundra		0.30	

Appendix 12
Tundra Plant Functional Type Divisions

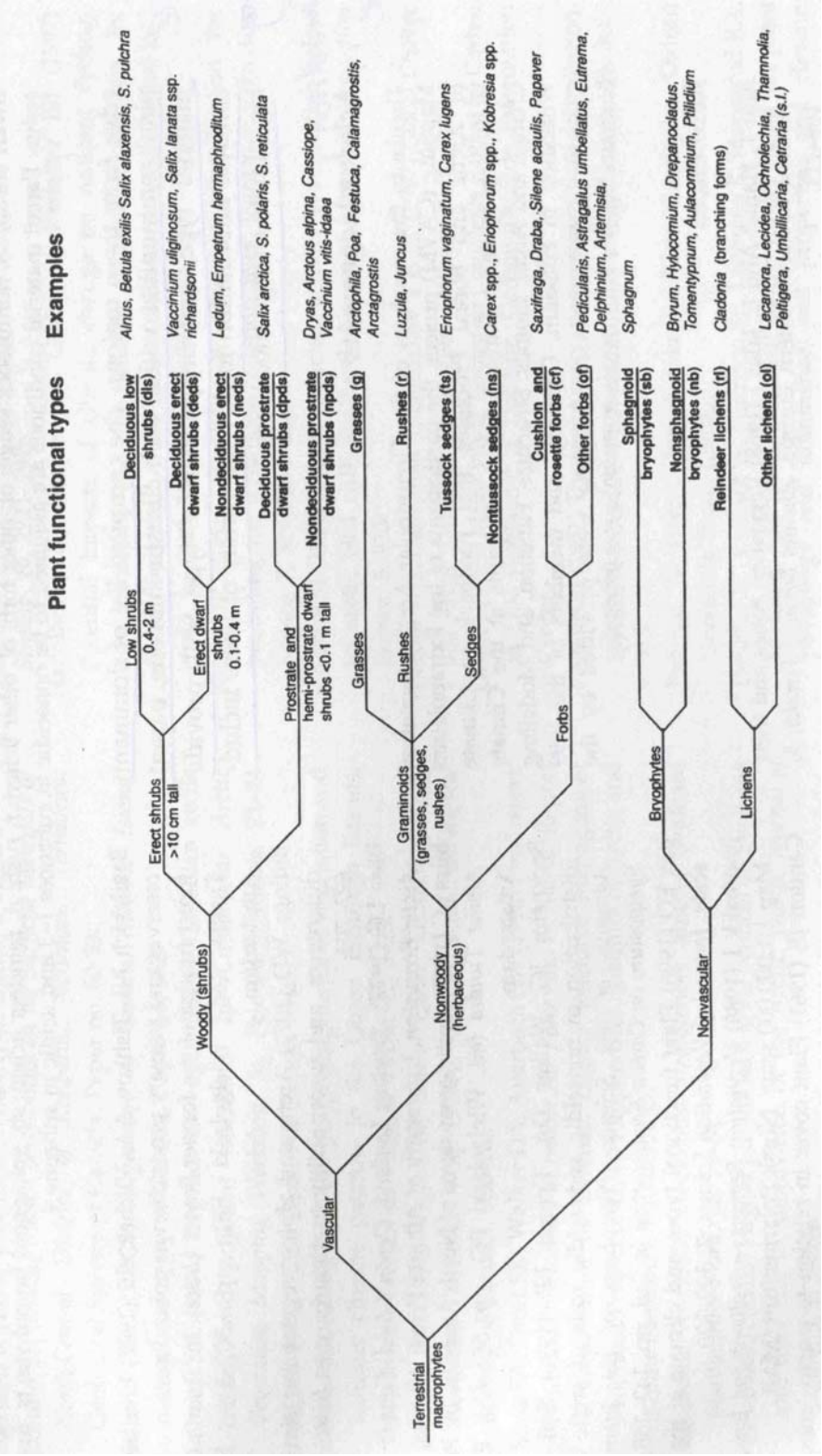

Source: Walker, 2000, 31

Appendix 13
General Geographic Overview of Study Site Location

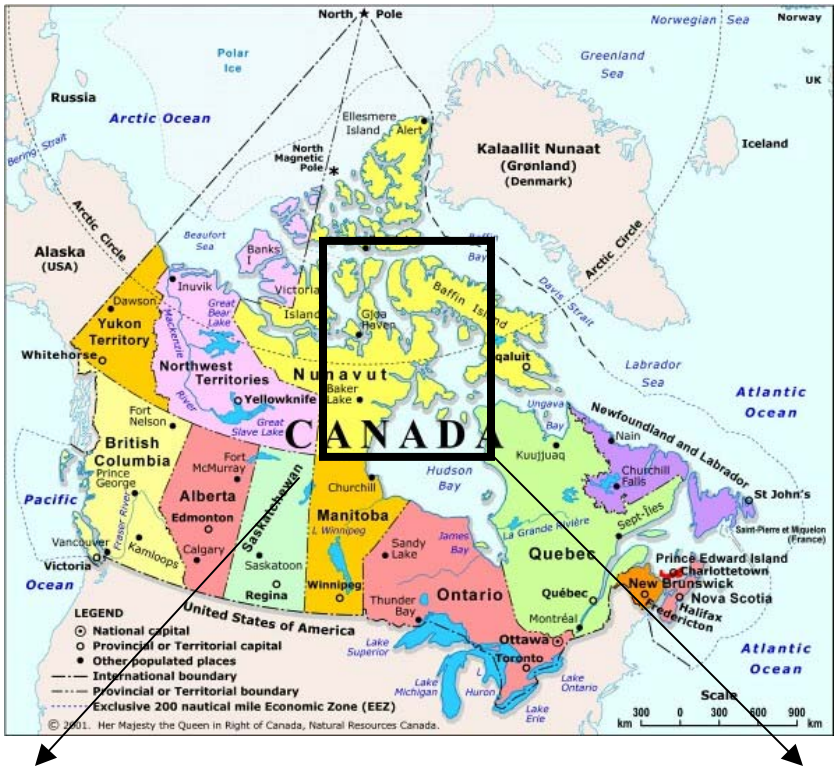

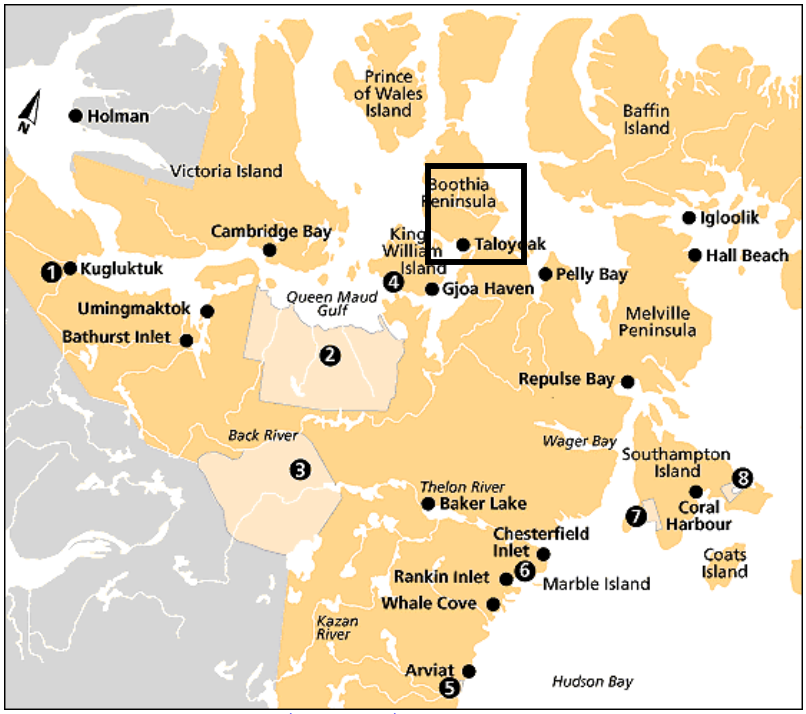

Top: www.canada.gc.ca/canadian/lmap_e.html
Bottom: www.arctictravel.com/maps/bluearea.html

Appendix 14
Tundra Sub-zone General Characteristics

Subzone	Mean July temp. at southern sub-zone boundary (°C) [compromise value][1]	Sum of mean monthly temps above freezing at southern boundary[2] (°C)	Vertical structure of plant cover[3]	Horizontal structure of plant cover[3]	Total phyto-mass[4] (above ground + below ground and live + dead) ($t\,ha^{-1}$)	Net annual production[4] (above ground + below ground) ($t\,ha^{-1}\,y^{-1}$)	Number of vascular plant species in local floras[5]
1. Cushion forb	2–3 [3]	6	Mostly barren. In favourable microsites, 1 lichen or moss layer <2 cm tall, very scattered vascular plants hardly exceeding the moss layer; no woody plants	<5% cover of vascular plants, up to 40% cover by cryptogams mostly associated with cracks in polygonal patterns and protected microsites. No closed root systems	3	0.3	<50
2. Prostrate dwarf shrub	5–7 [6]	12	2 layers, moss layer 3–5 cm thick and herbaceous layer 5–10 cm tall, prostrate and hemi-prostrate dwarf shrubs	5–50% cover of vascular plants, open patchy vegetation	20	2.3	75–125
3. Erect dwarf shrub	8–10 [9]	20	2 layers, moss layer 5–10 cm thick and herbaceous/dwarf-shrub layer 10–40 cm tall	50–80% cover of vascular plants, interrupted closed vegetation	57	3.3	150–250
4. Low shrub	10–12 [12]	35	2–3 layers, moss layer 5–10 cm thick, herbaceous/dwarf-shrub layer 20–50 cm tall, sometimes with low-shrub layer to 80 cm	80–100% cover of vascular plants, closed canopy	107	3.8	200 to >450

[1] Mean July temperatures based on Edlund (1996) and Matveyeva (1998) with a compromise value for global modeling in continental areas.
[2] Sum of mean monthly temperatures from Young (1971).
[3] Vertical and horizontal structure from Chernov & Matveyeva (1997).
[4] Based on Bazilovich & Tishkov (1997) for Russian Arctic.
[5] Number of vascular species in local floras based on Young (1971).

Source: Walker, 2000, 24

Appendix 15
Sample Plot Descriptions

Plot 1*

- low-lying and wet, to moist, sedge meadow
- flats on SSE side of hill near camp
- varies from very wet marshy areas to hummocks, to higher flatter ridges (approximately 30cm)
- not well developed, but overall large low-centre polygons

Facing SE towards convergence of LL and ET

Facing SE towards convergence of LL and ET

*N.B. Plot photos did not turn out therefore these are the closest representations.

Plot 2

- top of the hill, just NW of camp
- elevated ground, fairly dry, similar characteristics for 90% of the area
- gentle slopes in areas
- low trough areas (snowbed accumulation) tend to be wetter where shrub growth thrives (erect and prostrate)

Facing N towards ET

Facing S towards camp and LL

Plot 3

- large flat area
- wetlands with a few higher ridges (50-60cm) near N portion of plot
- just S of ET, NNW from camp

- surrounded by high ridges/hills (10-15m) in a semi-circle formation
- big pond to E of plot
- low land in general
- hummocks interspersed throughout

Facing N towards ET

Facing SSE towards camp and LL

Overview of P3 from W ridge (facing E)

Plot 4

- very flat surface
- broad flat/high centre polygons with small, shallow troughs
- dry rocky surface
- vegetation interspersed with stones/pebbles
- quite homogenous

Appendix 15 (continued)

Facing NNE towards ET

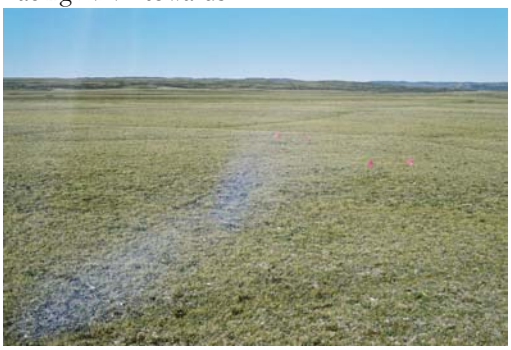

Facing SSE towards LL

Plot 5

- hills to the SSW of the plot
- gently sloping foot/toe sloe (NNE towards ET)
- perhaps drainage flats
- irregular surface features
- very unique vegetation combinations
- deceiving moisture (i.e. seems dry but damp underneath, likely due to runoff direction)
- pretty rocky, lots of underlying moss

Facing N towards ET

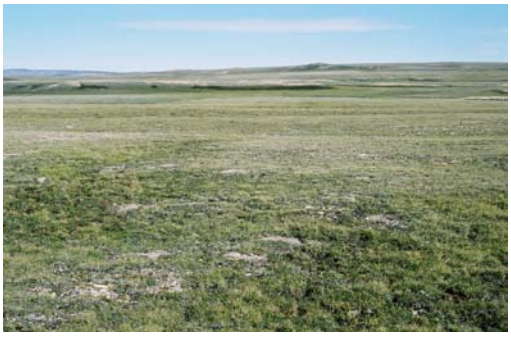

Facing SSW towards LL

Plot 6

- very gentle S slope towards LL
- unique vegetation patterns
- interspersed with distinct circular patches of gravel/soil and vegetation
- sorted and non-sorted circles
- similar cover to P7, but different vegetation spatial aggregration

Appendix 15 (continued)

Facing NE towards ET

Facing S towards LL

Plot 7

- a raised area, sloping gently SSW towards LL
- sorted and non-sorted stripe formations (interspersed vegetation and rocks)
- as side slope extends down towards river, stripes become much less pronounced

Facing SSW towards LL

Plot 8

- low-lying flat area surrounded by hills/ridges
- vague stripe formations
- damp to moist environment, a little hummocky, lots of sedges
- pond near the S corner

Facing N towards ET

Facing SSW towards LL

Appendix 15 (continued)

Plot 9

- deep valley with hills/ridges to NW and SE
- small catchment for snow meltwater, draining into ET
- central area is a series of high-centre polygons, where troughs can be up to 0.5m deep and the equivalent of small streams
- quite lush vegetation, moist to wet, but much drier in polygon centres and on plot edges
- on either side near the footslopes drier surface and less dense/lush vegetation
- quite heterogeneous environment, but unique community and the only noticeable water track large enough to sample

Facing NNE towards ET

Facing SSW towards LL

From SE ridge, looking N towards ET

Plot 10

- lowland, wetland, but not as wet as first perceived
- moist to wet sedge meadow
- fairly flat, on the SW side of high ridges (towards LL)

Appendix 15 (continued)

Facing N towards ET

Facing S towards LL

Plot 11

- similar to Plot 7 but with less prominent stripes
- quite high elevation, but relatively flat local topography (plateau)
- lots of rock interspersed with vegetation
- deceiving soil moisture, more moist than first perceived

Facing NE towards ET

Facing SW towards LL

Plot 12

- highest elevation of all plots
- N-sloping ridge, towards ET
- quite barren, predominantly rock cover with a few isolated clumps of vegetation

Facing NE towards ET

Facing S towards LL

Appendix 16
Original Sampling Plots

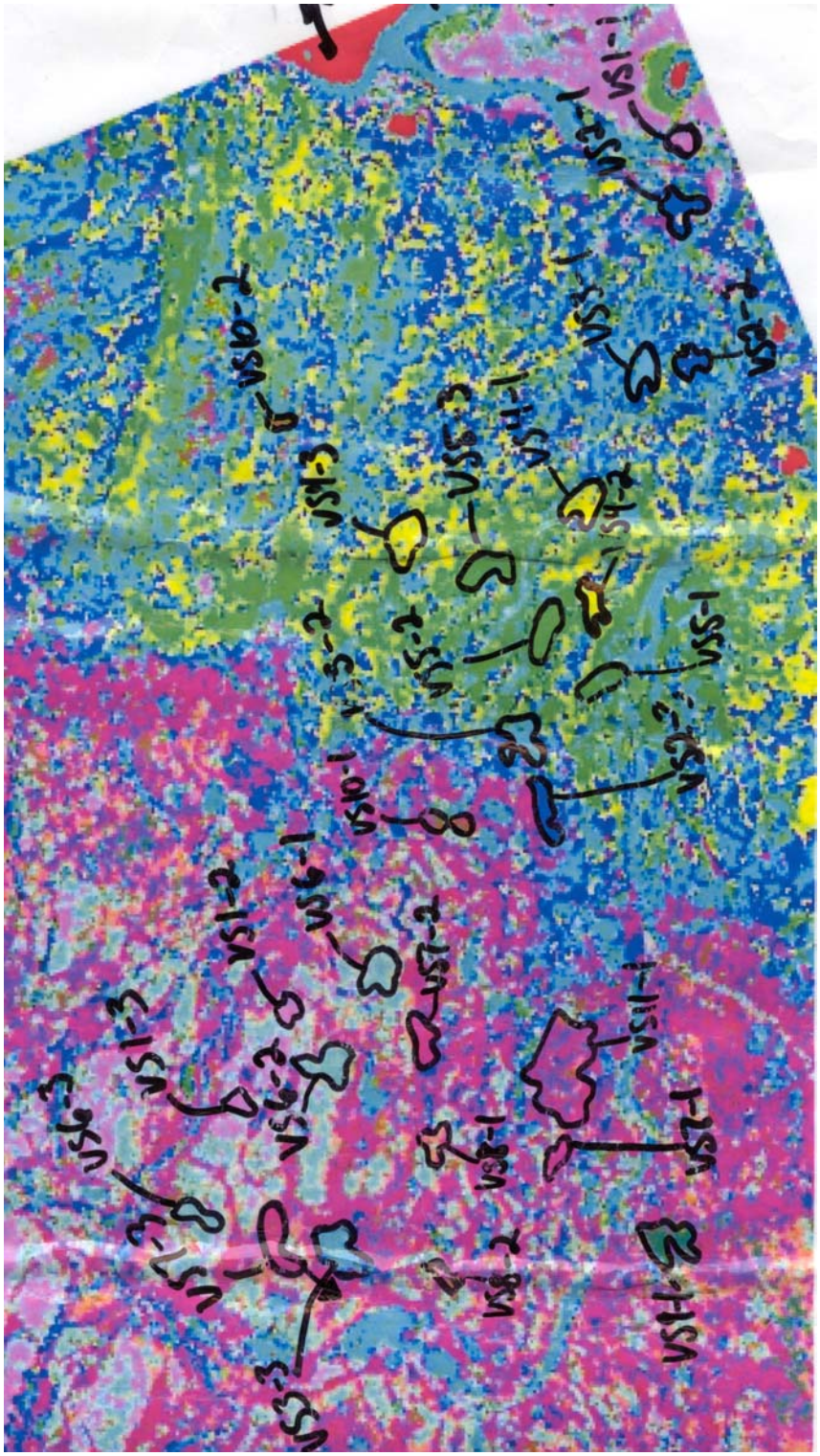

Appendix 17
Sample Plot Locations

Corners	UTM Easting	UTM Northing
Vs 1-2 (P12)		
C1	465775.4	7793605.5
C2	465839.6	7793529.3
C3	465752.2	7793436.1
C4	465701.3	7793518.3
Centre	465774	7793530.6
Vs 2-1 (P2)		
C1	471662.7	7787095.9
C2	471764.1	7787074.8
C3	471691.6	7786940.2
C4	471617.5	7787006.2
Centre	471689.4	7787029.3
VS 2-3 (P8)		
C1	466728.1	7790489
C2	466791.4	7790410.8
C3	466705.4	7790350.8
C4	466646.3	7790430.9
Centre	466719	7790415.4
VS 4-2 (P6)		
C1	468388.3	7788943.7
C2	468442.8	7788859.4
C3	468377.2	7788785.4
C4	468305.8	7788887.9
Centre	468375.1	7788876.9
VS 5-1 (P7)		
C1	467746.1	7789711.9
C2	467806.7	7789631.8
C3	467723.3	7789578.2
C4	467661.7	7789658.4
Centre	467733.1	7789644.6
VS 5-2 (P5)		
C1	468413.1	7789658.5
C2	468479.1	7789583.5
C3	468427.9	7789503.7
C4	468347.1	7789583.8
Centre	468407.4	7789581.8

Corners	UTM Easting	UTM Northing
VS 6-1 (P11)		
C1	465834.1	7792589.3
C2	465896.2	7792511.2
C3	465836.4	7792430.3
C4	465773.1	7792508.5
Centre	465833.9	7792512.7
VS 7-2 (P10)		
C1	464670.9	7792605.4
C2	464726.1	7792528.1
C3	464648.4	7792463.4
C4	464583.3	7792560
Centre	464658.9	7792542.2
VS 10-1 (P9)		
C1	466809.6	7791579.5
C2	466869.2	7791521.2
C3	466787.7	7791418.2
C4	466701.7	7791472.7
Centre	466797.4	7791495.2
VS 12-1 (P4)		
C1	470405.9	7787773.5
C2	470452.8	7787683.2
C3	470376.8	7787617.7
C4	470328.4	7787706.2
Centre	470388.8	7787691.9
VS 15-1 (P1)		
C1	471767.3	7786834.4
C2	471832.1	7786761.0
C3	471746.8	7786706.5
C4	471681.1	7786782.9
Centre	471756.9	7786772.6
VS 16-1 (P3)		
C1	471498.7	7787198.0
C2	471594.3	7787169.1
C3	471556.9	7787083.0
C4	471461.8	7787105.4
Centre	471532.5	7787134.2

Appendix 18
Plot Setup (not to scale)

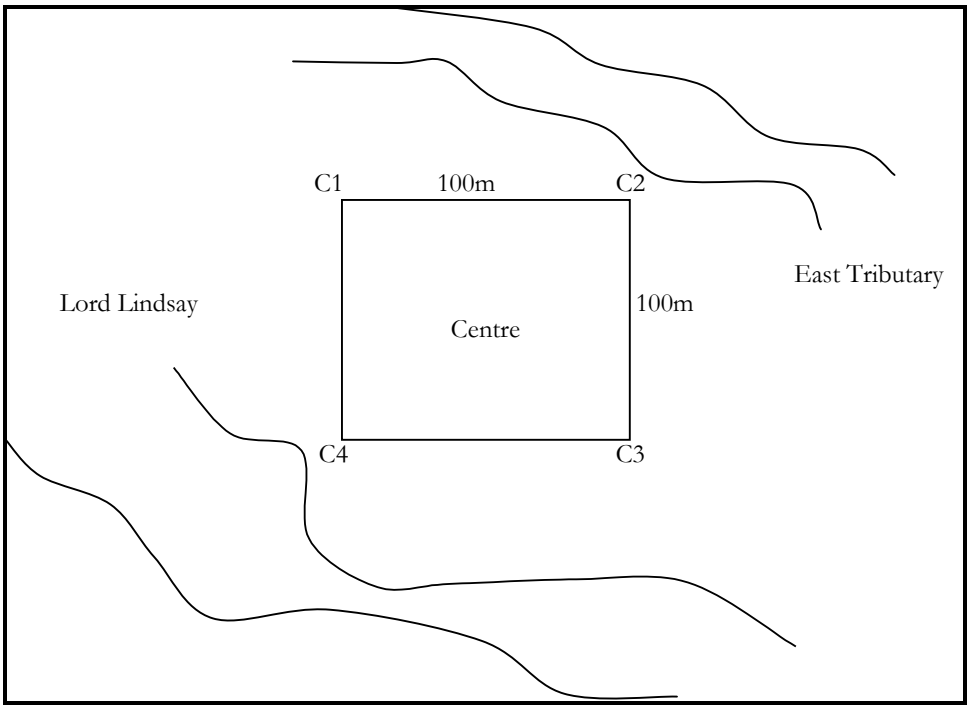

Appendix 19
GPS Characteristics

For plot corner/centre coordinates, and later quadrat positions, a GPS (coordinates expressed in Universal Transverse Mercator (UTM) projection, zone 15, and North American Datum 1927 (NAD27)) was employed to determine locational position (+/- 5m). The accuracy of these measurements was derived from a user-specified average of 500 (plot corners/centres) and 150 (quadrats) point collections. Plot locations were more important, thus explaining the larger number of points collected; also, time was a limiting factor for quadrat positions because many more coordinates had to be collected within plots. The GPS unit incorporates a satellite triangulation method, which increases the accuracy of the averaged location by taking into account each satellite's location (4 total) relative to the other satellites in the constellation (24 possible) to predict the accuracy of positions obtained within that constellation (Trimble Navigation Limited, 1996). While the GeoExplorer II receiver automatically uses the constellation with the lowest position dilution of precision (PDOP), PDOP maximum was set at 6 to further enhance confidence in the acquired coordinates and ensure acceptable positioning accuracy (Trimble Navigation Limited, 1996). Interestingly, time of day was a constraining factor on the accuracy of GPS measurements, as the PDOP tended to be very high (and thus inadequate for coordinate measurement) between noon and 1pm each day. This limitation was later worked into the sampling scheme as the predictability of this phenomenon was confirmed.

Appendix 20
Sampling Consideration Issues

Issues	Consideration	Reasoning
Practical	Avoid undue complexity	• it may introduce unforeseen operation difficulties during fieldwork • complexities introduced may complicate statistical analysis and increase computation time
Practical	Allow for unexpected delay in fieldwork	• there are always factors that arise that are out of the researcher's control (e.g. mobility limitations in June/July) – allow for approximately 20% of the total time for fieldwork
Practical	Include a test phase if necessary	• if there is significant uncertainty about fieldwork logistics or spatial variability, a preliminary test phase is always worth the extra effort (a test phase locally even prior to leaving may also be useful)
Practical	Evaluate the scheme beforehand	• it is prudent to quantitatively predict the cost of operation of the scheme and the accuracy of the result, prior to fieldwork
Scientific	Protocol for fieldwork	• fieldwork rules usually concern the physical act of taking samples and measurements in the field • they should also describe what to do if a sample is inaccessible or falls outside target area • poor protocol may seriously affect quality of results • protocol should be: complete, unambiguous, practically feasible, and scientifically sound • all details concerning the acquisition of necessary field equipment should be addressed well in advance of the departure date
Scientific	Protocol for data recording	• prior to fieldwork prescribed codes for data recording should be established, as well as accountability for same concerns as fieldwork protocol • data input sheets should be designed ahead of time
Statistical	Prior information on spatial variability	• should attempt to gain prior information on spatial variability in order to design most appropriate sampling method (satellite images, aerial photos, and thematic maps should help) • once on site, the variability around sample sites should also be investigated
Statistical	Modes of sample point selection	• point selection should include considerations such as: conveniences sampling, purposive sampling, and probability sampling
Statistical	Sources of error	• accuracy may be affected by sampling error, sample treatment, measurement and 'non-response' (a situation where for some reason no data can be obtained from a sample element)

Adapted from: de Gruijter, 1999, 214-216

Appendix 21
Random Quadrat Sampling Procedures

Directional Component:

- use two full decks of playing cards including all suits ranging from numbers 1 – 8
- shuffle thoroughly
- for each quadrat record the revealed card indicates the direction to travel to locate the area of interest
    - 1 = North
    - 2 = North East
    - 3 = East
    - 4 = South East
    - 5 = South
    - 6 = South West
    - 7 = West
    - 8 = North West

Locational Component:

- use two full decks of playing cards including all suits ranging from 1 – King, and 4 Jokers
- each numbered card represents that number of paces to travel
- Jack = 11 paces, Queen = 12 paces, King = 13 paces, Joker = 20 paces
- for each quadrat record the revealed number of paces (in the pre-determined direction) to travel to locate the quadrat position

Plot Coverage Component:

- to ensure that the entire plot was covered, the 100x100m area was divided into four quadrants (Figure A)
- once all the locational components were determined, the remaining cards were continually revealed until 1 – 4 had been revealed, and the order they appeared was the order that quadrants were to be sampled
- each quarter of the plot was to have 12, 13, 12, 13 quadrats sampled within their bounds, respectively
- where the direction and paces placed quadrats across quadrant boundaries this was accepted
- where the direction and paces placed quadrats outside plot boundaries, this was not accepted and directions were altered by 90° to turn back into the plot
- within each quadrant both direction and paces were initiated from the centre of the plot quarter, and from there each subsequent quadrat location was determined from the current one completed

Figure A – Quadrant Locations

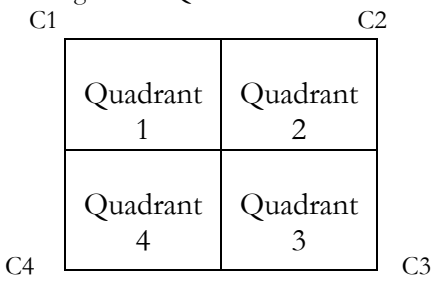

Appendix 22
Summary of Qualitative Quadrat Descriptives

Microsites (MI)

Code	*Description*
1	Frost scar element
2	Inter-frost scar element
3	Hummock
4	Flark, interstrang, or interhummok area
5	Polygon centre
6	Polygon trough
7	Polygon rim
8	Stripe element
9	Inter-stripe element
10	Point bar (raised element)
11	Slough (wet element) - moist to wet/moss cover
12	Hilltop
13	Lowland with raises and depressions (hummocks in areas)
14	Interspersed stone circles with level terrain

Modified from (Edwards *et al.*, 2000)

Topographic Position (TP)

Code	*Description*
1	Hill crest or shoulder
2	Side slope
3	Footslope or toeslope
4	Flat
5	Drainage channel
6	Depression
7	Lake or pond
8	Hummocky flats

Modified from (Edwards *et al.*, 2000)

Exposure

Code	*Description*
1	Protected from winds
2	Moderate exposure to winds
3	Exposed to winds
4	Very exposed to winds

Source: Edwards *et al.,* 2000

Appendix 23
Tundra Plant Species, Codes, and References

Species	Common Name	Code	Reference	Page	Inuit Name	Photo	Plant Press*	Display # **
Arctagrostis latifolia	Polar grass	PG	Porsild and Cody, 1980	75		11/5, 38/4, 38/5	1	6
Armeria maritima	Thrift	AM	Burt, 1991	144		11/22	19	1
Brassica sp.	Mustard species	BS	Porsild and Cody, 1980	339		11/16	13, 23, 54	29
Cardamine digitata	Cuckoo-flower	CD	Burt, 1991	72		11/19	16	
Cardamine pratensis	Cuckoo-flower	CP	Burt, 1991	72		17/14	28	
Cardamine sp.	Cuckoo-flower	CS	Burt, 1991	72		18/19	35	9
Carex aqualitis	wetland sedge	CG	Porsild and Cody, 1980	129		11/11	6	32
Carex bigelowii	dryland sedge	LG	Porsild and Cody, 1980	129		13/20	22	34
Carex sp.	Sedge species		Porsild and Cody, 1980	129		11/13	8	10
Cassiope tetragona	White Arctic Heather	CA	Burt, 1991	130	iksut	11/24	20	25
Chrysanthemum integrifolium	Arctic daisy	CI, SP	Burt, 1991	184	hongaoyak	17/10, 17/17	25	
?	Circular leaf plant	CR					43	
Cladina sp.	Reindeer moss	CL	Burt, 1991	20	quayaut	13/19	21	37
Dryas integrifolia	Mountain aven	DI	Burt, 1991	88	kokiuyaq	11/7, 38/10	3	15
Equistem variegatum	Horsetail	EV	Burt, 1991	28			24	
Erect Salix	indistinguishable	EW	Burt, 1991	50				
Eriophorum sp.	Cottongrass	ESP	Burt, 1991	36	kangyuq			
Eriophorum augustifolium	Cottongrass	EA, RG	Burt, 1991	36	kangyuq	17/21	31, 41	
Eriophorum scheuchzeri	Cottongrass	ES	Burt, 1991	36	kangyuq	17/15, 38/11	29	11
Grasses	indistinguishable grass/sedge	GR						
Lesquerella arctica	Arctic bladderpod	LA	Burt, 1991	74		11/20	17	2
Lycopodium sp.	Club moss (or finger lichen?)	LS						
Melandrium apelatum	Purple bladder-campion	MA	Burt, 1991	62		11/15, 21/4	11, 40	14, 14b
Moss	Indistinguishable species	MO			urruk			
Mushroom		MU			puyuqtuq			17
Oxytropis arctobia	Arctic Oxytrope	OA	Burt, 1991	122		17/20, 19/17	10	3

Appendix 23 (continued)

Species	Common Name	Code	Reference	Page	Inuit Name	Photo	Plant Press*	Display #**
Oxytropis maydelliana	Yellow Oxytrope	OM	Burt, 1991	120	iraq	11/6	2	30
Oxyria digyna	Mountain sorrel	OD	Burt, 1991	58	hirnuq	11/14	9	16
Papaver radicatum	Arctic poppy	PR	Burt, 1991	84		11/21	18	4
Pedicularis capitata	Capitate lousewort	PC	Burt, 1991	172		11/8	4	7
Pedicularis lanata	Woolly lousewort	PL	Burt, 1991	174	anguvak	11/10	5	27
Pedicularis sudetica	Sudetan lousewort	PS	Burt, 1991	176		11/18	15	22
Potentialla vahliana	Cinquefoil	Y6	Porsild and Cody, 1980	409		21/8	39	28
Prostrate Salix	indistinguishable	PW	Burt, 1991	48-50		11/23, 17/13	26	18, 19
?	Rock tripe	RT	Burt, 1991	?				
Salix herbacea	Least willow	SH	Burt, 1991	52				
Salix reticulata	Net-veined willow	SR	Burt, 1991	50			27	
Saxifraga hirculus	Yellow marsh saxifrage	SX	Burt, 1991	110		11/16	12	29
Saxifraga oppositifolia	Purple mountain saxifrage	SO			hukahinnaq	3/16, 3/20	52	20, 20b
Stellaria longipes	Star Chickweed	PP, WF	Burt, 1991	60	taijuhiit	20/5	38, 42	
Stellaria sp.	Star Chickweed	TF	Burt, 1991	60		11/9	36	23
Thamnolia subliformis sp.	Worm lichen	TS	Burt, 1991	20		13/19	21	
?	Undifferentiated leaves	UL				18/14, 18/19		35
?	Yellow lichen	YL	Burt, 1991	20	quayaut	13/19	21	37
Xanthoria elegans	Jewel lichen	JL	Burt, 1991	22	quayaut	3/11		13

Non-Vegetated Cover Type	Code
Dark ground/bare soil	DS
Exposed soil	ES
Rock/gravel	RK
Water	WA

*N.B. Wherever possible, a plant species specimen was collected for both reference and verification purposes at later stages in analysis. Thus, each plant press number corresponds to a physical species example stored carefully in a wood and paper plant press.

** Display numbers correspond to reference photos in following figures.

Appendix 23 (continued)

#1 – *Armeria maritime* (Thrift)

#2 – *Lesquerella arctica* (Arctic bladderpod)

#3 – *Oxytropis arctobia* (Arctic oxytrope)

#4 – *Papaver radicatum* (Arctic poppy)

Appendix 23 (continued)

#5 – *Dryas integrifolia* (Mountain aven… in seed)

#6 – *Arctagrostis latifolia.* (Polar grass)

#7 – *Pedicularis capitata* (Capitate lousewort)

#8 – *Cardamine digitata* (Cuckoo-flower)

Appendix 23 (continued)

#9 – *Cardamine sp.* (Cuckoo-flower)

#10 – *Carex sp.* (type of sedge)

#11 – *Eriophorum scheuchzeri* (Arctic cotton/Cottongrass)

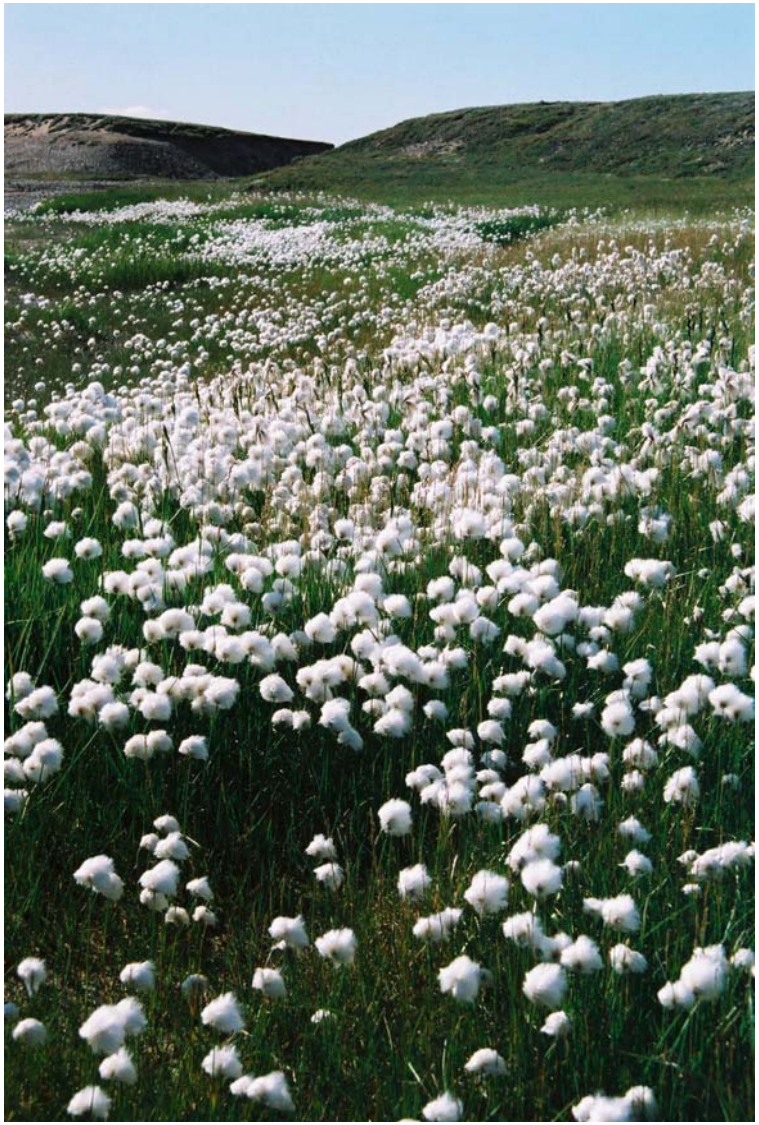

Appendix 23 (continued)

#12 – *Epilobium latifolium* (Dwarf fireweed)

#13 – *Xanthoria elegans* (Jewel lichen)

#14 – *Mellandrium apelatum* (Purple bladder-campion)

#14b – *Mellandrium apelatum* (Purple bladder-campion)

Appendix 23 (continued)

#15 – *Dryas integrifolia* (Mountain aven)

#16 – *Oxyria Digyna* (Mountain sorrel)

#17 – Mushroom species

#18 – *Salix sp.* (Prostrate willow species)

Appendix 23 (continued)

#19 – *Salix sp.* (Prostrate willow species)

#20 – *Saxifraga oppositifolia* (Purple mountain saxifrage)

#20b – *Saxifraga oppositifolia* (Purple mountain saxifrage)

#21 – *Saxifraga tricuspidata* (Prickly saxifrage)

Appendix 23 (continued)

#22 – *Pedicularis sudetica* (Sudetan lousewort)

#23 – *Stellaria sp.* (Star Chickweed)

#24 – Unknown species

#25 – *Cassiope tetragona* (White arctic heather)

Appendix 23 (continued)

#26 – *Cerastium alpinum* (Mouse-ear Chickweed)

#27 – *Pedicularis lanata* (Woolly lousewort)

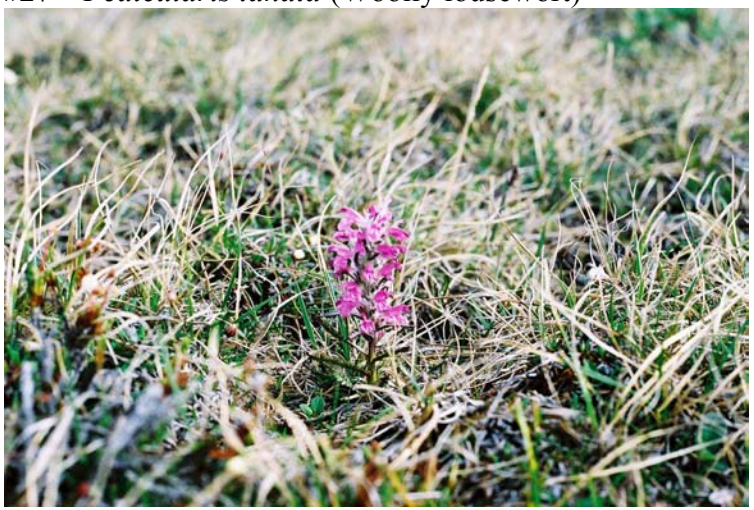

#28 – *Potentilla vahliana* (Cinquefoil)

#29 – *Brassica sp.* (Mustard) and *Saxifraga hirculus* (Yellow marsh saxifrage – larger, near front)

Appendix 23 (continued)

#30 – *Oxytropis maydelliana* (Yellow Oxytrope)

#31 – Unknown yellow species

#32 – *Carex aqualitis* (wetland sedge)

#33 – *Parrya arctica* (Mustard species)

Appendix 23 (continued)

#34 – *Carex bigelowii* (dryland sedge)

#35 – Undifferentiated Leaves (just below middle)

#36 – *Eriophorum augustifolium* (Cottongrass)

#37 – *Cladina sp.* (Reindeer moss), (Yellow lichen), and *Thamnolia subliformia sp.* (Worm lichen)

Appendix 24
Summary of Qualitative Plot Descriptives

Landforms (LA)

Code	*Description*
1	Hills (kames and moraines too)
2	Talus slope
3	Colluvial basin
4	Glaciofluvial and other fluvial terraces
5	Marine Terrace
6	Floodplains
7	Drained lakes and flat lake margins
8	Abandoned point bars and sloughs
9	Estuary
10	Lake or pond
11	Stream
12	Sea bluff
13	Lake bluff
14	Stream bluff
15	Sand dunes
16	Beach
17	Disturbed

Source: Edwards *et al.,* 2000

Surficial Geomorphology (SG)

Code	*Description*
1	Frost scars
2	Wetland hummocks
3	Turf hummocks
4	Gelifluction features
5	Strangmoor or aligned hummocks
6	High- or flat-centered polygons
7	Mixed high- and low-centered polygons
8	Sorted and non-sorted stripes
9	Palsas
10	Thermokarst pits
11	Featureless or < 20% frost scars
12	Well-developed hillslope water tracks and small streams >50cm deep
13	Poorly developed hillslope water tracks <50cm deep
14	Gently rolling or irregular microrelief
15	Stony surface
16	Lakes and ponds
17	Disturbed

Source: Edwards *et al.,* 2000

Appendix 25
Example Field Book Data Entries for VS 5-1 (P7)

No. Random Site Selection for next plot
Date July 22, 2001 Page 64

Q#	Direction	Paces	Q#	Direction	Paces
1	NE	6	24	SW	1
2	N	5	25	E	3
3	W	2	26	S	11
4	SE	13	27	N	7
5	N	13	28	W	11
6	SE	13	29	S	20
7	SE	10	30	NW	12
8	W	13	31	E	7
9	SE	20	32	NE	3
10	SW	1	33	W	8
11	S	5	34	NW	4
12	E	1	35	S	1
13	SE	2	36	W	4
14	E	20	37	SE	4
15	NE	8	38	W	2
16	NE	5	39	NW	13
17	W	11	40	W	9
18	SW	12	41	N	1
19	NW	3	42	S	13
20	N	7	43	NE	9
21	SW	6	44	NW	8
22	S	9	45	SE	4
23	NW	2	46	N	7

No.
Date 22/07/01 Page 65

Q#	Direction	Paces
47	S	10
48	E	9
49	NW	10
50	NW	10

Order of quadrants: 2, 3, 4, 1

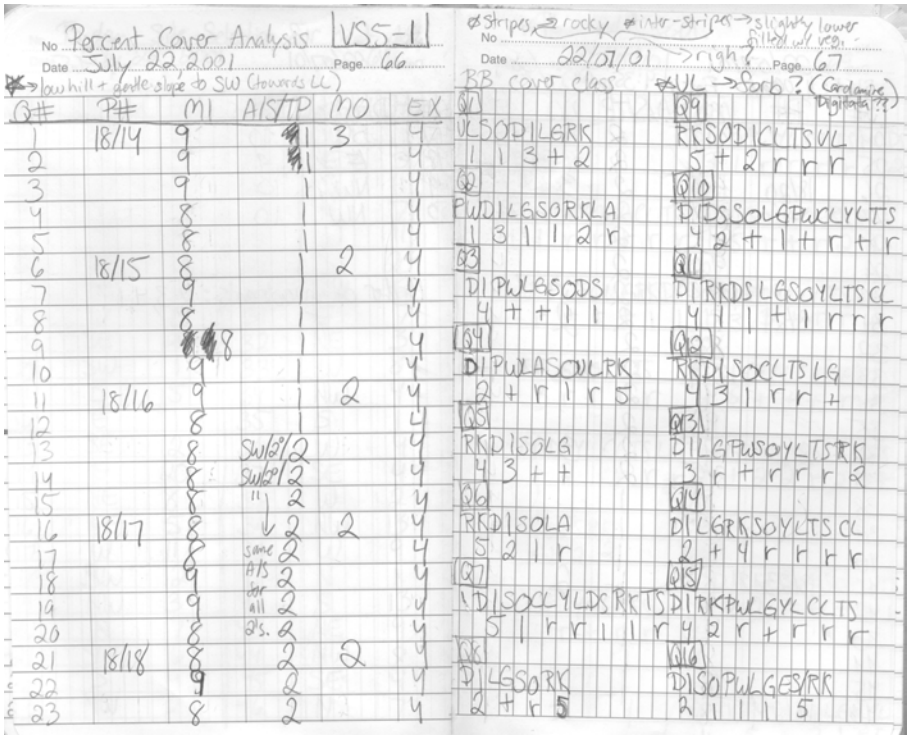

No. Percent Cover Analysis VS5-1
Date July 22, 2001 Page 66
low hill + gentle slope to SW (towards LL)

Q#	P#	MI	AI/TP	NO	EX
1	18/14	9	1	3	4
2		9	1		4
3		9	1		4
4		8	1		4
5		8	1		4
6	18/15	8	1	2	4
7		9	1		4
8		8	1		4
9		8	1		4
10		9	1		4
11	18/16	9	1	2	4
12		8	1		4
13		8	SW/2/2		4
14		8	SW/2/2		4
15		8	" 2		4
16	18/17	8	↓ 2	2	4
17		8	same 2		4
18		9	#'s 2		4
19		9	for 2		4
20		8	all 2		4
21	18/18	8	#'s. 2	2	4
22		9	2		4
23		8	2		4

Ø Stripes → rocky Ø inter-stripes → slightly lower silty w/ veg.
No.
Date 22/07/01 → righ? Page 67
BB cover class Ø VL → Sorb ? (Cardamine Digitata ??)

Q1: VLSODILGRK | 1 1 3 + 2
Q2: PWDILGSORKLA | 1 3 1 1 2 r
Q3: DIPWLGSODS | 4 + + 1 1
Q4: DIPWLASOLRK | 2 + r 1 r 5
Q5: RKDISOLG | 4 3 + +
Q6: RKDISOLA | 5 2 1 r
Q7: DISOCLYLDSRKTS | 5 1 1 r r 1 1 r
Q8: DILGSORK | 2 + r 5
Q9: RKSODICLTSVL | 5 + 2 r r r
Q10: DDSSOLGPWCLYCLTS | 4 2 + 1 + r + r
Q11: DIRKDSLGSOYLTSCL | 4 1 1 + 1 r r r
Q12: RKDISOCLTSLG | 4 3 1 r r +
Q13: DILGPWSOYLTSRK | 3 r + r r r 2
Q14: DILGRKSOYLTSCL | 2 + 4 r r r r r
Q15: DIRKPWLGYLCLTS | 4 2 r + r r r
Q16: DISOPWLGESRK | 2 1 1 1 1 5

Appendix 25 (continued)

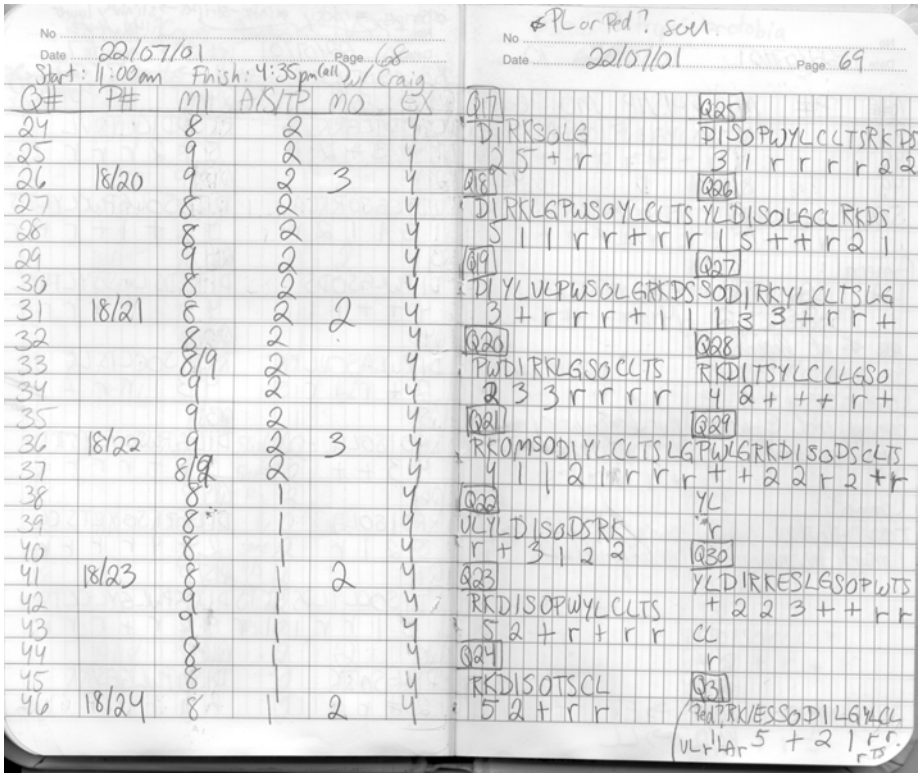

Q#	P#	ML	AX/TP	MO	EX
24		8	2		4
25		9	2		4
26	18/20	9	2	3	4
27		8	2		4
28		8	2		4
29		9	2		4
30		8	2		4
31	18/21	8	2	2	4
32		8	2		4
33		8/9	2		4
34		9	2		4
35		9	2		4
36	18/22	9	2	3	4
37		8/9	2		4
38		8	1		4
39		8	1		4
40		8	1		4
41	18/23	8	1	2	4
42		9	1		4
43		9	1		4
44		8	1		4
45		8	1		4
46	18/24	8	1	2	4

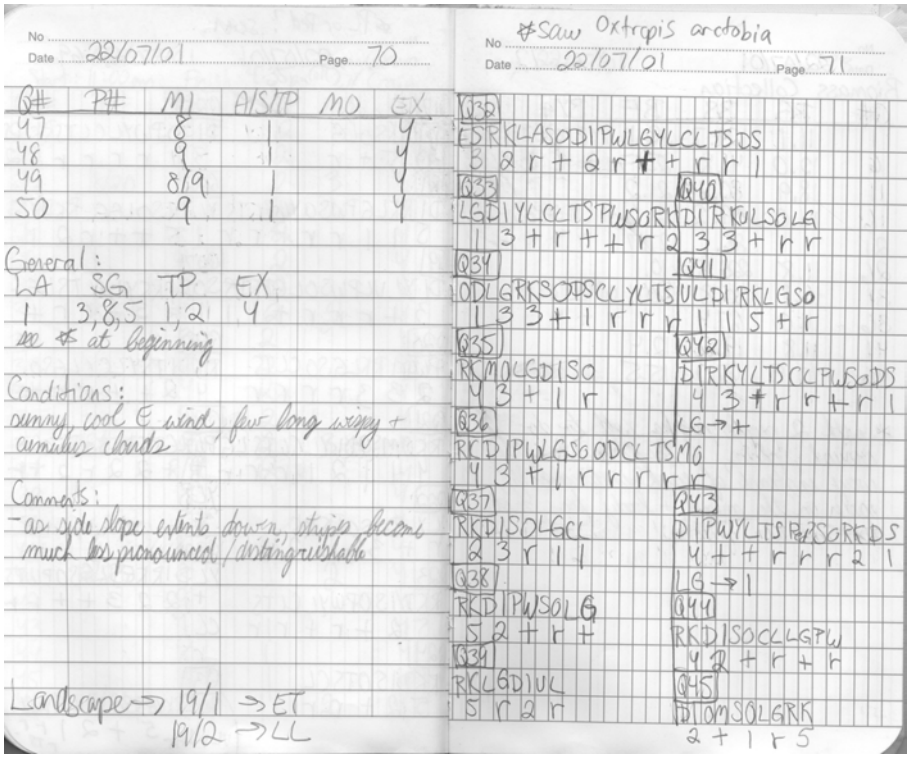

Q#	P#	ML	AX/TP	MO	EX
47		8	1		4
48		9	1		4
49		8/9	1		4
50		9	1		4

General:

LA	SG	TP	EX
1	3,8,5	1,2	4

see # at beginning

Conditions:
sunny, cool & wind, few long wispy + cumulus clouds

Comments:
- ax side slope extends down, stripe becomes much less pronounced / distinguishable

Landscape → 19/1 → ET
19/2 → LL

Appendix 25 (continued)

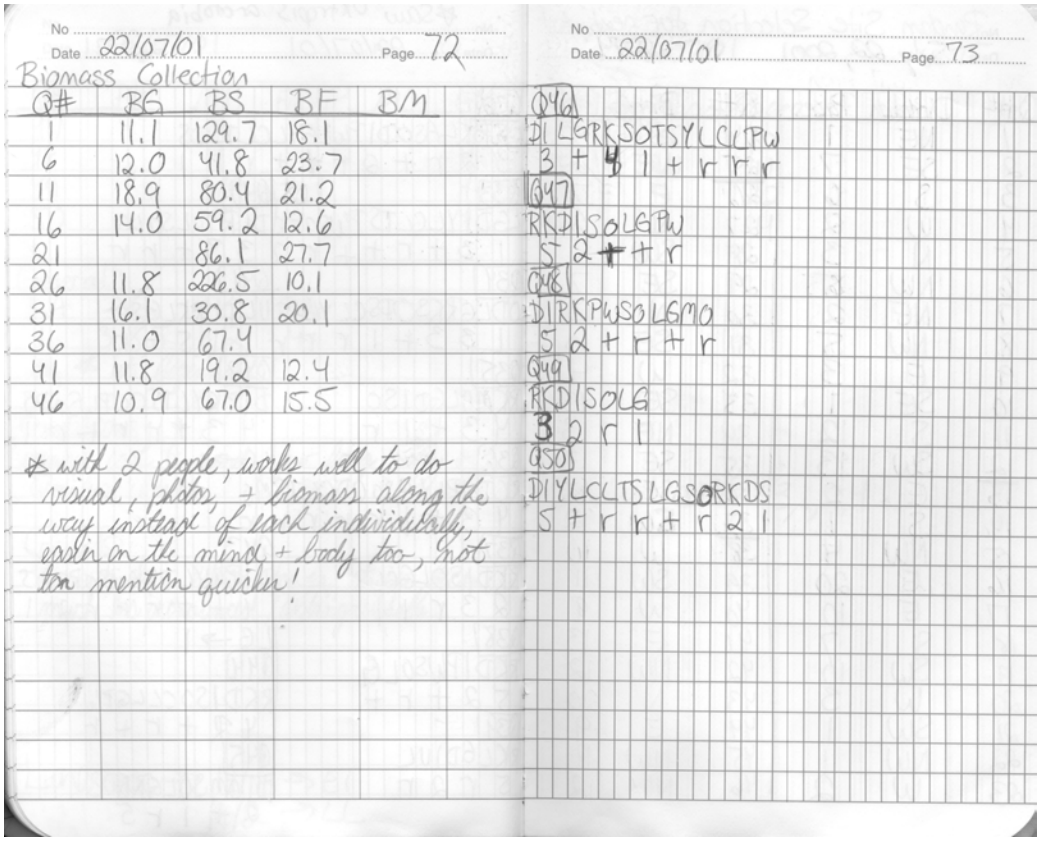

No
Date 22/07/01 Page 72

Biomass Collection

Q#	BG	BS	BF	BM
1	11.1	129.7	18.1	
6	12.0	41.8	23.7	
11	18.9	80.4	21.2	
16	14.0	59.2	12.6	
21		86.1	27.7	
26	11.8	226.5	10.1	
31	16.1	30.8	20.1	
36	11.0	67.4		
41	11.8	19.2	12.4	
46	10.9	67.0	15.5	

* with 2 people, works well to do visual, photos, + biomass along the way instead of each individually, easier on the mind + body too, not to mention quicker!

No
Date 22/07/01 Page 73

Q46
DILGRKSOTSYLCLTPW
3 + 4 1 + r r r

Q47
RKDISOLGPW
5 2 + + r

Q48
DIRKPWSOLGMO
5 2 + r + r

Q49
RKDISOLG
3 2 r 1

Q50
DIYLCLTSLGSORKDS
5 + r r + r 2 1

Appendix 26
Ground Control Point (GCP) Distribution

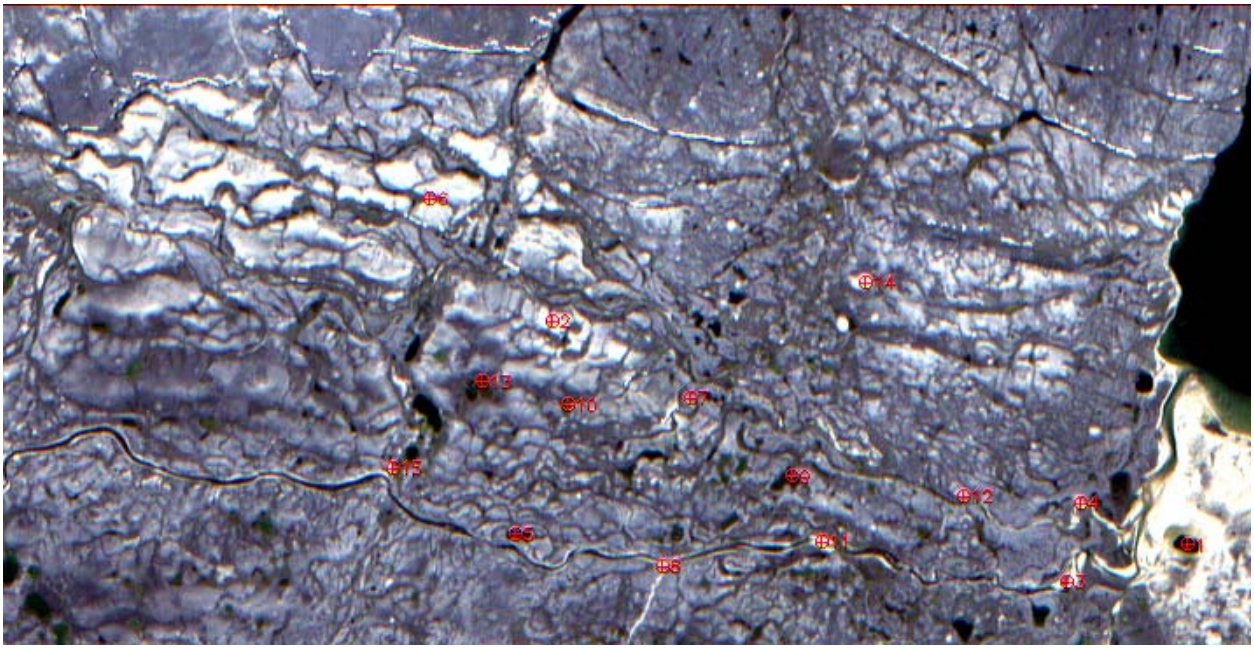

Subset of Landsat 7 ETM+ image showing GCP location

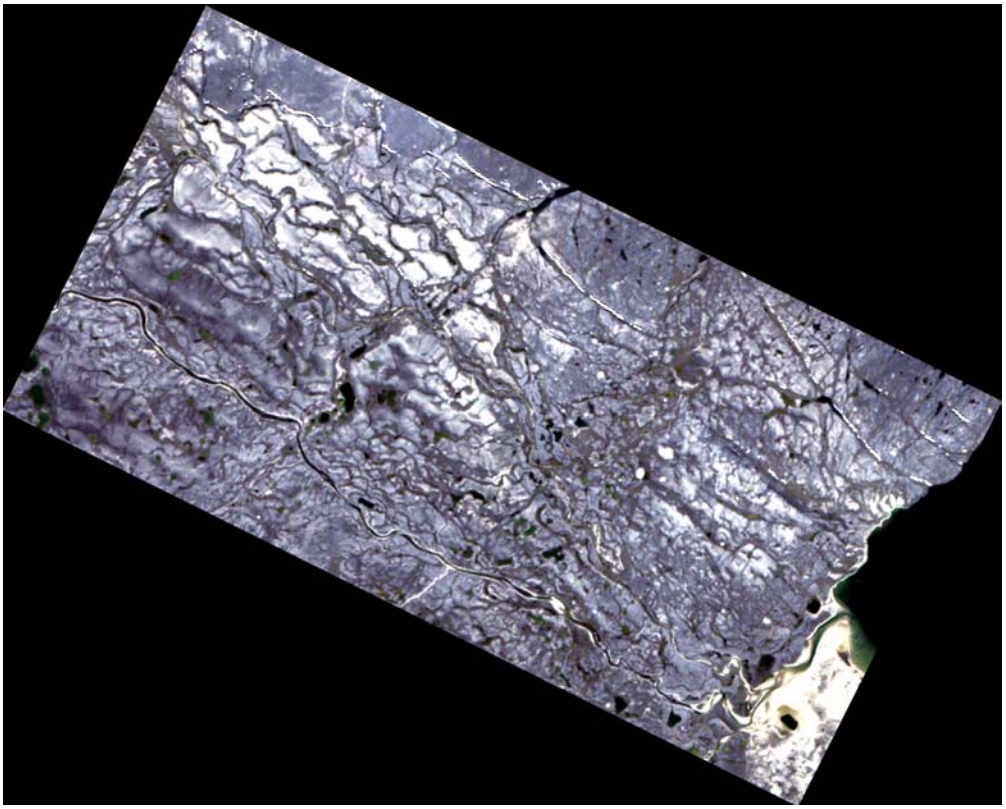
Resulting warped (georectified) Landsat image

N

Appendix 27
Landsat Radiometric Calibration Parameters

Band	Gain	Offset	Mean solar exoatmospheric irradiance
1 (blue)	0.775686	-6.20000	1969
2 (green)	0.795686	-6.39999	1840
3 (red)	0.619216	-5.00000	1551
4 (nir)	0.637255	-5.10001	1044
5 (mir)	0.125725	-0.99999	225.7
6 (mir2)	0.043726	-0.35000	82.07

Appendix 28

Spectral Quadrat and Plot Similarities for Calculating Plot Surface Spectral VIs

ASD Q#	A1	A2	A3	A4	A5	A6	A7	A8	A9	A10	A11	A12	A13	A14	A15	A16	A17	A18
VS Plot	VS 15-1	VS 15-1	VS 15-1	VS 2-1	VS 2-1	VS 2-1	VS 16-1	VS 16-1	VS 12-1	VS 12-1	VS 5-2	VS 5-2	VS 5-2	VS 5-2	VS 4-2	VS 4-2	VS 10-1	VS 10-1
Total G	62.5	2.5	2.5	2.5	2.5	0	87.6	2.5	15	15	2.5	0.1	15	62.5	0	2.5	15	37.5
Total F	0	0	0	2.5	2.5	0	0.2	0	5	2.5	0.3	0.1	0	0	0	0	0	0
Total S	40	0	62.5	62.5	62.5	0	0	0	37.5	37.5	17.5	2.6	90	37.5	0	62.6	90	0
Total Br	0	87.5	37.5	0	0	0	2.5	37.5	0	0	0	0	0	0	0	15	0	0
Total L	0	0	0	0.2	0.2	0	0	0	0.3	0.3	0	0	0	0	0	0	0	0
Total Veg Cover	102.5	90	102.5	67.7	67.7	0	90.3	40	57.8	55.3	20.3	2.8	105	100	0	80.1	105	37.5
Total NV	0	0	0	15.1	0	87.6	0	62.5	2.5	15	65	102.5	2.6	0	102.5	17.5	0	87.5

Plot	4-2	1-2	5-1	6-1	12-1	2-1	5-2	15-1	16-1	10-1	2-3	7-2
Total G	0.57	0.1	1.3	0.3	10.01	11.5	7.77	22.11	39.96	26.01	30.22	56.9
	1.07	1.6	1.03	1.33	3.51	2.47	2.51	0.96	0.1	0.27	0.89	0.22
	31.87	17.3	34.32	44.37	40.36	52.7	38.18	28.92	20.79	39.42	17.27	2.95
	7.1	0	0.75	2.85	0	2.8	11.65	42.6	40	19.85	14.6	11.3
	0.07	0.1	0.19	0.07	0.18	0.06	0.05	0.01	0	0.11	0	0
	40.68	19	36.55	48.92	54.06	69.5	60.17	94.61	100.85	85.66	62.98	71.38
	47.95	79.1	48.15	46.85	21.45	13.4	26.3	8.85	3.55	7.45	19.76	20.95

Surface Spectral Similarities	
4-2	A15+16(40/60)
1-2	A4+6+15(20/40/40)
5-1	A4+A10+15+12(20/28/22/30)
6-1	A4+6+12(50/25/25)
12-1	A10(100)
2-1	A5+4+6+17(80/10/5/5)
5-2	A11+12+13+14(10/5/55/30)
15-1	A1+2+3(60/20/20)
16-1	A7+17(60/40)
10-1	A17+18(50/50)
2-3	A7+13+11(60/25/15)
7-2	A7+11(75/25)

Appendix 29

Unsupervised Classification Input Parameters for Both Satellite Images

Parameter	Classification #1	Classification #2	Classification #3
Min classes	5 (default)	5 (default)	5 (default)
Max classes	10	15	20
Max iterations	60	60	60
Change threshold %	5 (default)	5 (default)	5 (default)
Min # of pixels in class	50	50	50
Max class stdv	1 (default)	1 (default)	1 (default)
Min class stdv	5 (default)	5 (default)	5 (default)
Max # of merge pairs	2 (default)	2 (default)	2 (default)
Max stdv from mean	- (default)	- (default)	- (default)
Max distance error	- (default)	- (default)	- (default)
Saved as	unsuper_10	unsuper_15	unsuper_20

Appendix 30
Plot Species Richness

Plot	Graminoids	Forbs	Shrubs	Lichens	Mosses	Non-Vegetated
P1	LG, CG, PG, GR, EV	SO, PC, PED?, PS, CS, SX, PL, MA	DI, PW, EW, CA, SR	CL, TS, YL	MO	DS, WA, ES
P2	LG, CG, PG	SO, PC, PED?, OM, OA, PS, OD, LA, PL, CP	DI, SH, PW, EW, CA	JL, CL, TS, YL	MO	DS, ES, RK
P3	LG, CG, PG, GR, EV, EA, ESP	SO, PED?, PS, SX, WF, PC, BS	DI, PW, EW	-	MO	ES, RK, WA
P4	LG	SO, PED?, OM, OD, CI, TF, LA, MA, UL	CA, PW, DI, SR	CL, TS, YL, RT	-	RK
P5	CG, LG, EV	SO, LA, PED?, OM, PL, OD, UL, CI, TF, SP, MA, PC, PP	PW, DI	CL, TS, YL	MO, MU	DS, ES, RK
P6	LG	SO, PED?, UL, CI, PR, OD, LA	DI, PW, CA	CL, TS, YL	MO	DS, ES, RK
P7	LG	SO, PED?, OM, OD, UL, OA, LA	DI, PW	CL, TS, YL	MO	DS, ES, RK
P8	PG, GR, EV, EA, LG, ESP	CR, AM, UL, CI TF, WF, MA, SX, CS, OD, SO, PC	DI, PW, EW	TS	MO	RK, DS, ES
P9	LG, PG, GR, EA, ESP	PL, PED?, PS, PC, MA, CS, SX, CR, WF	CA, PW, DI	CL, TS, YL	MO, LS?	RK, ES, WA, DS
P10	PG, EV, EA, RG	PED?, SX, SP, WF, CS, SS, CR, MA	DI, PW, EW	-	MO	RK, DS
P11	LG	SO, PED?, OM, UL, LA, MA, PR	DI, PW	CL, TS, YL, JL	MO	DS, ES, RK
P12	LG	SO, LA, Y6, MA, UL	DI, PW	CL, TS, YL, JL	-	RK

Appendix 31
Species Percent Cover vs. Frequency Plots

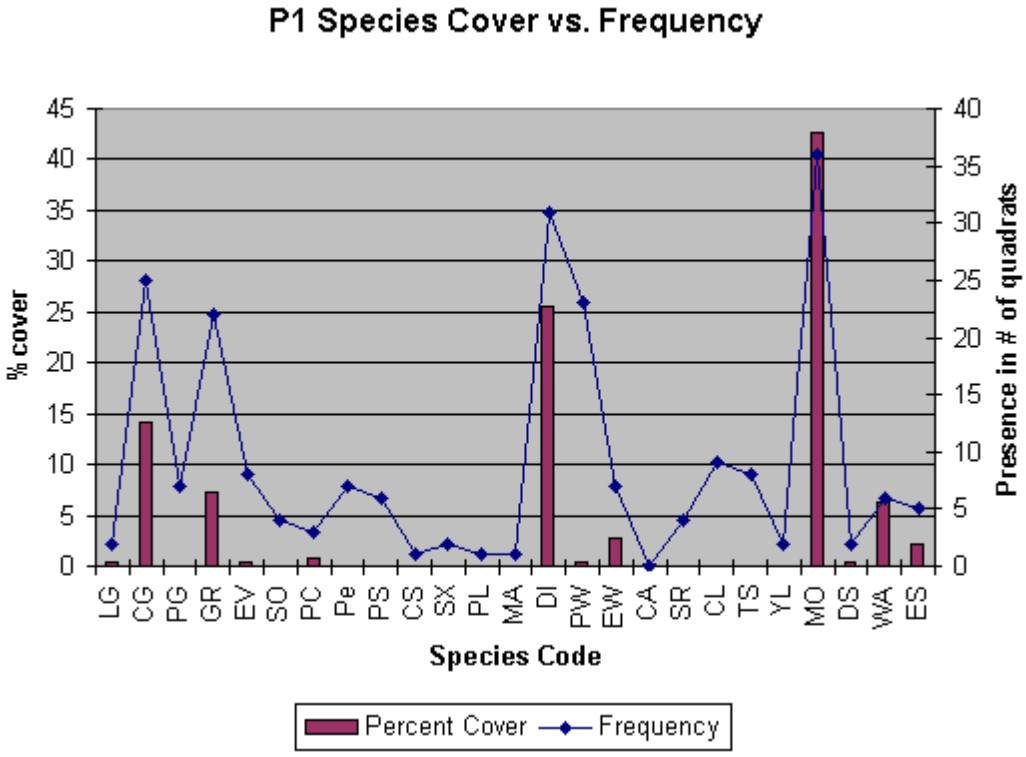

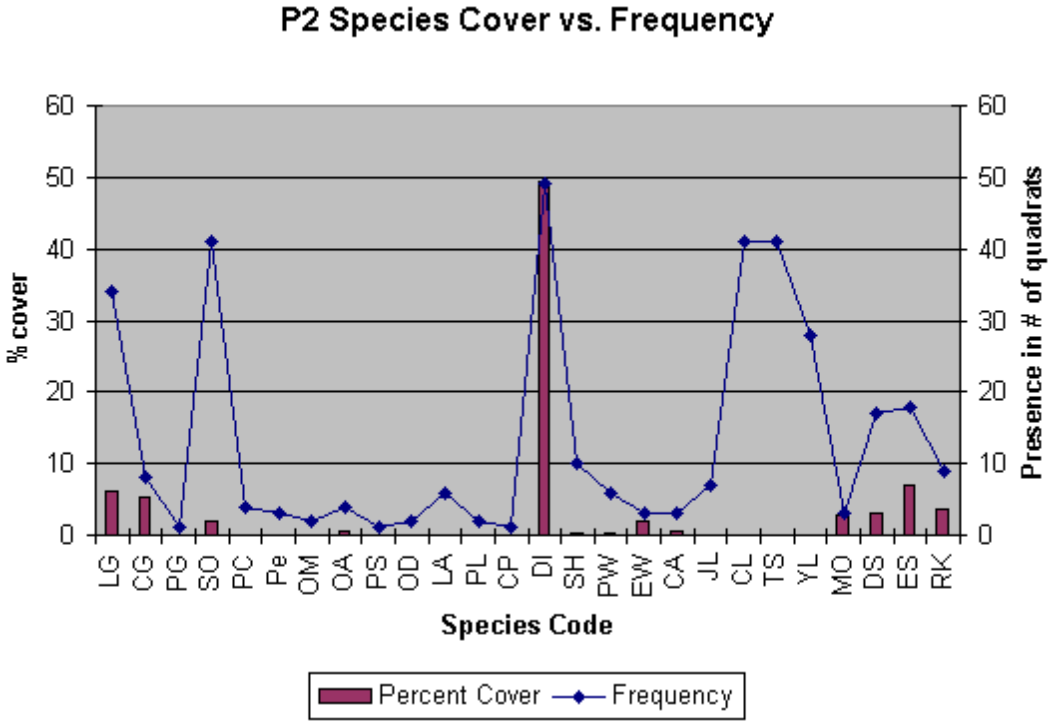

Appendix 31 (continued)

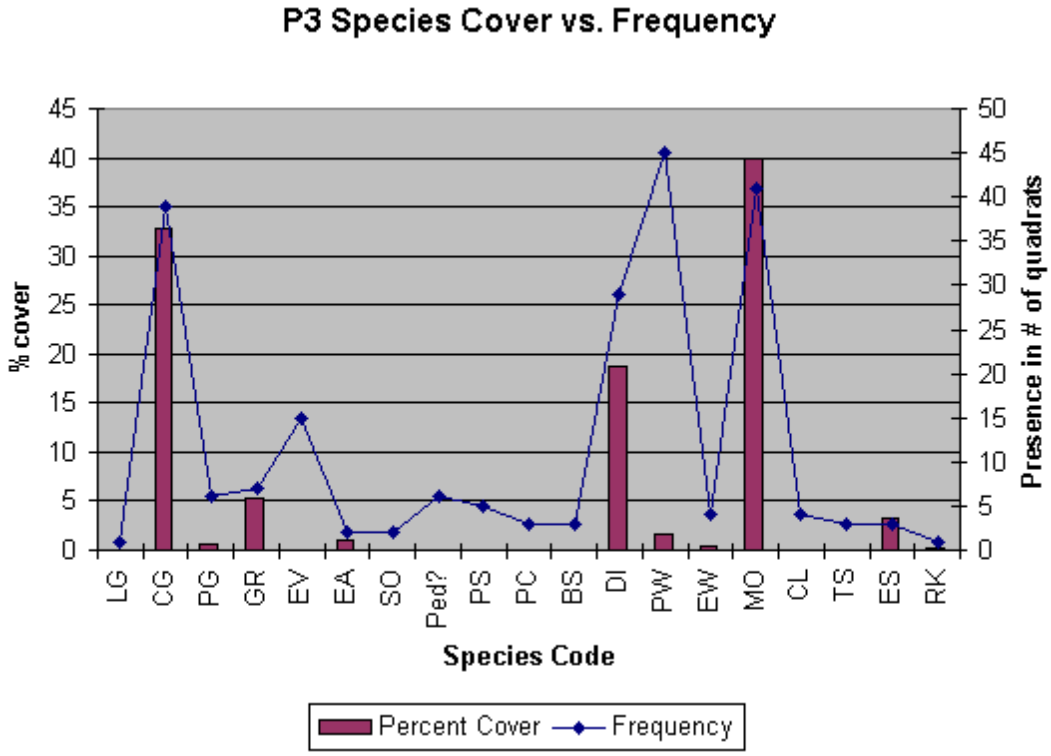

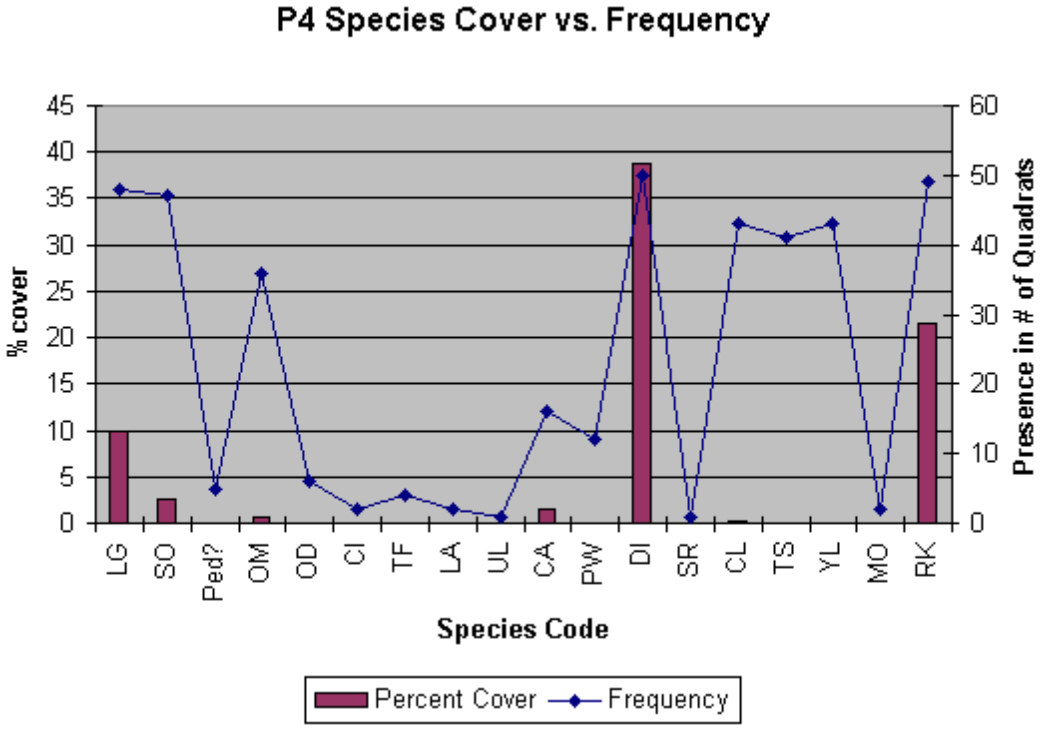

Appendix 31 (continued)

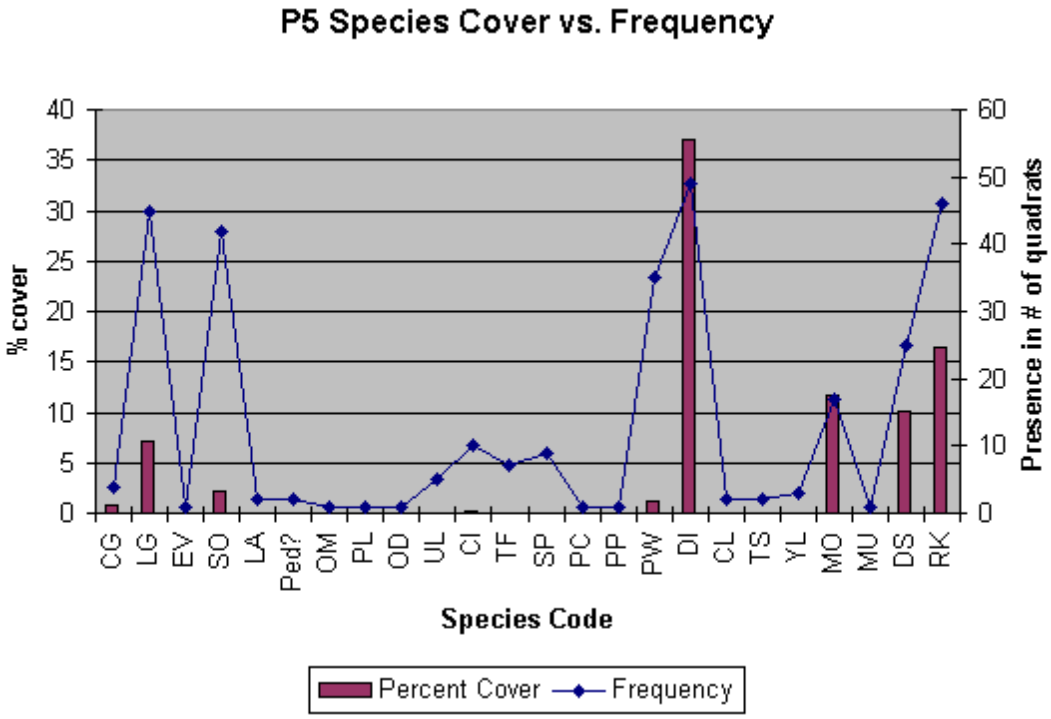

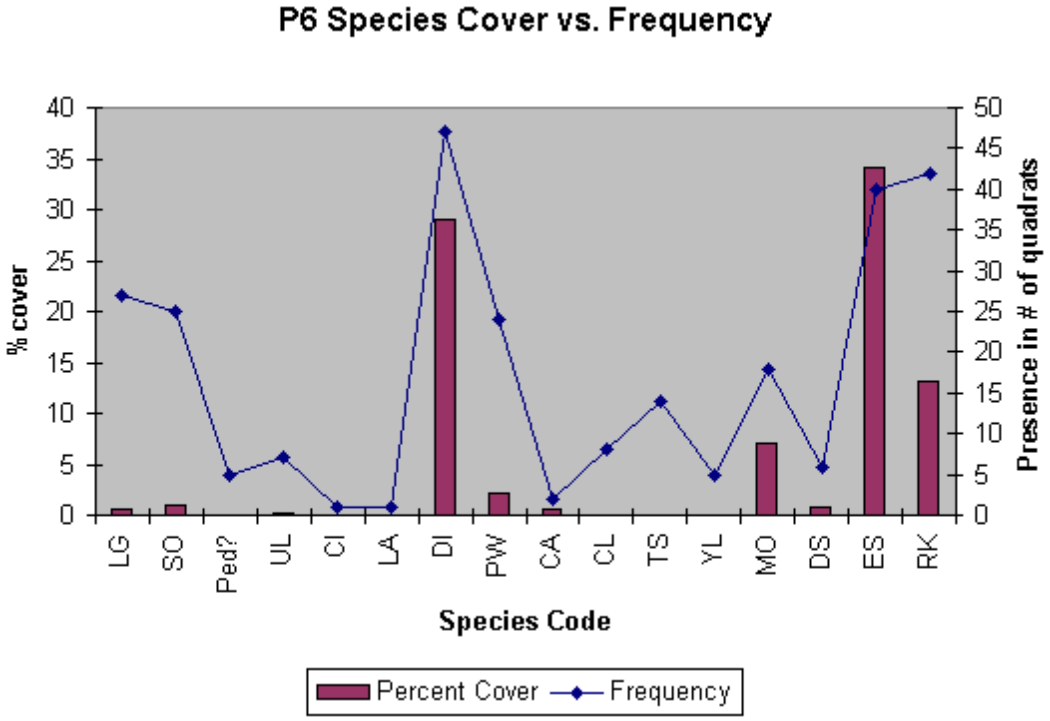

Appendix 31 (continued)

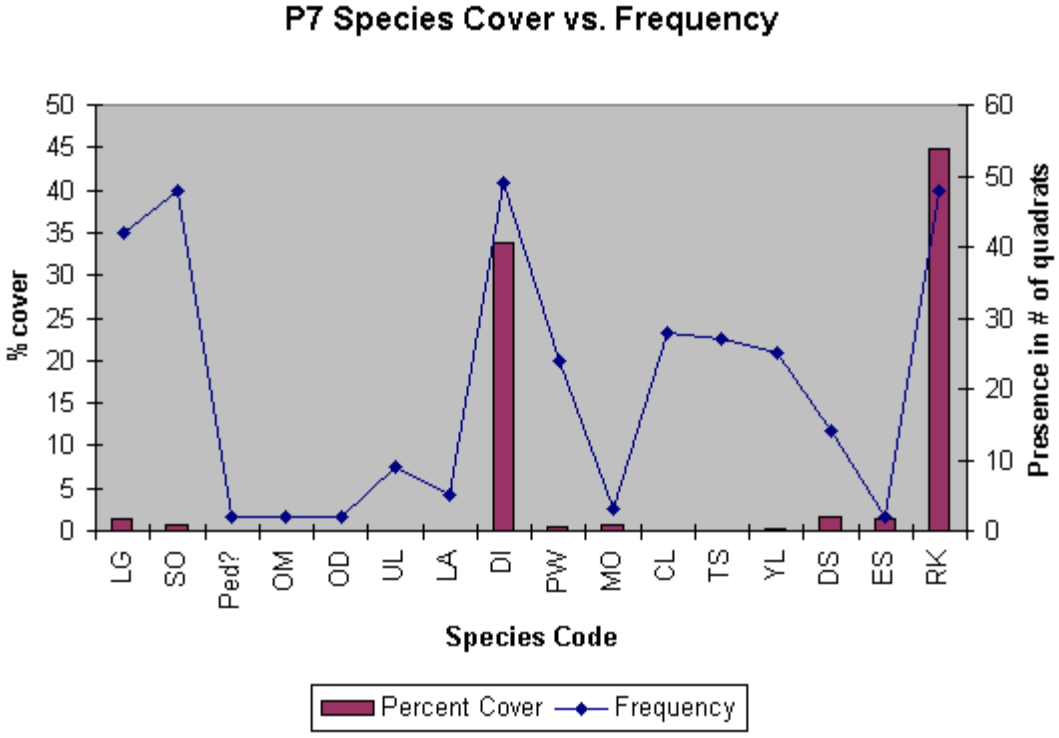

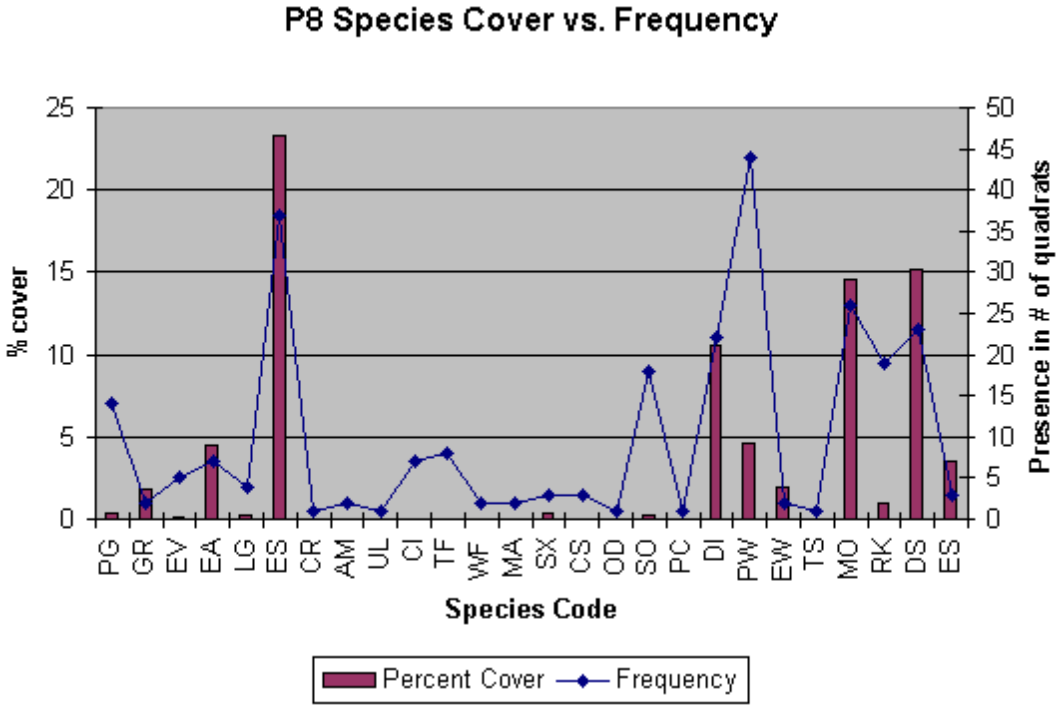

Appendix 31 (continued)

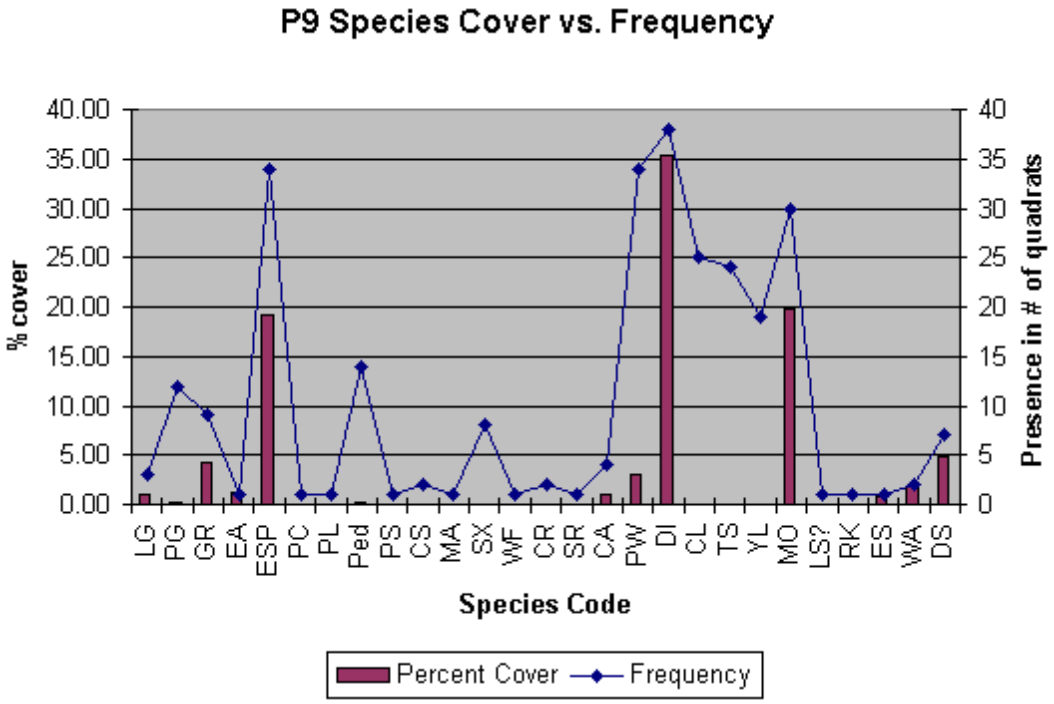

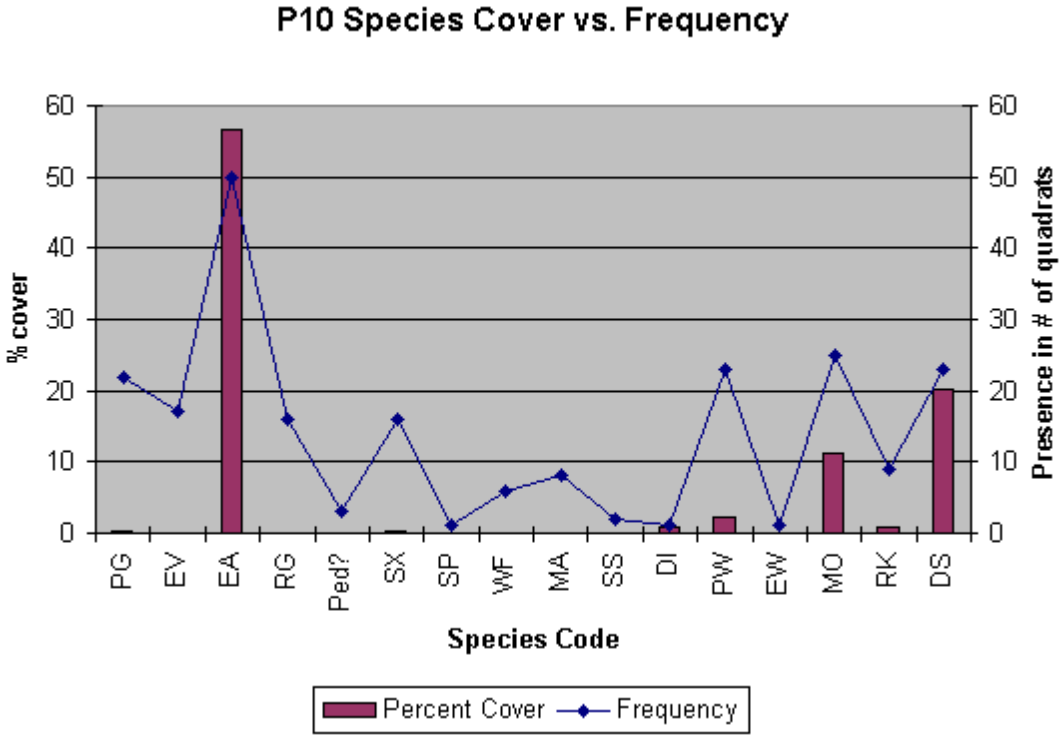

Appendix 31 (continued)

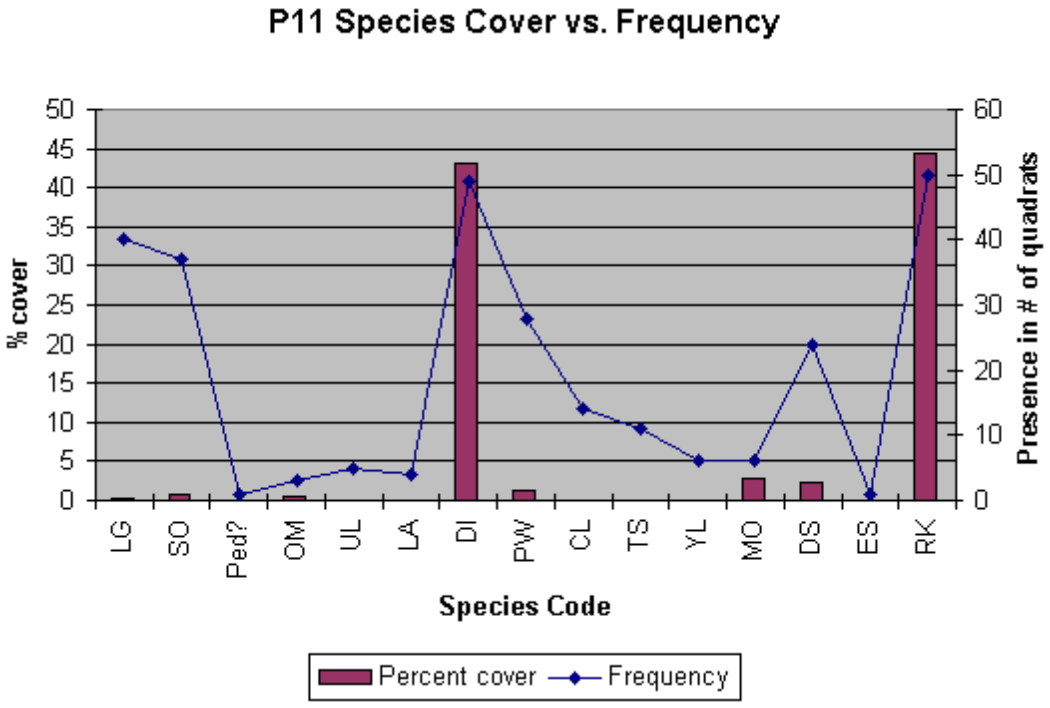

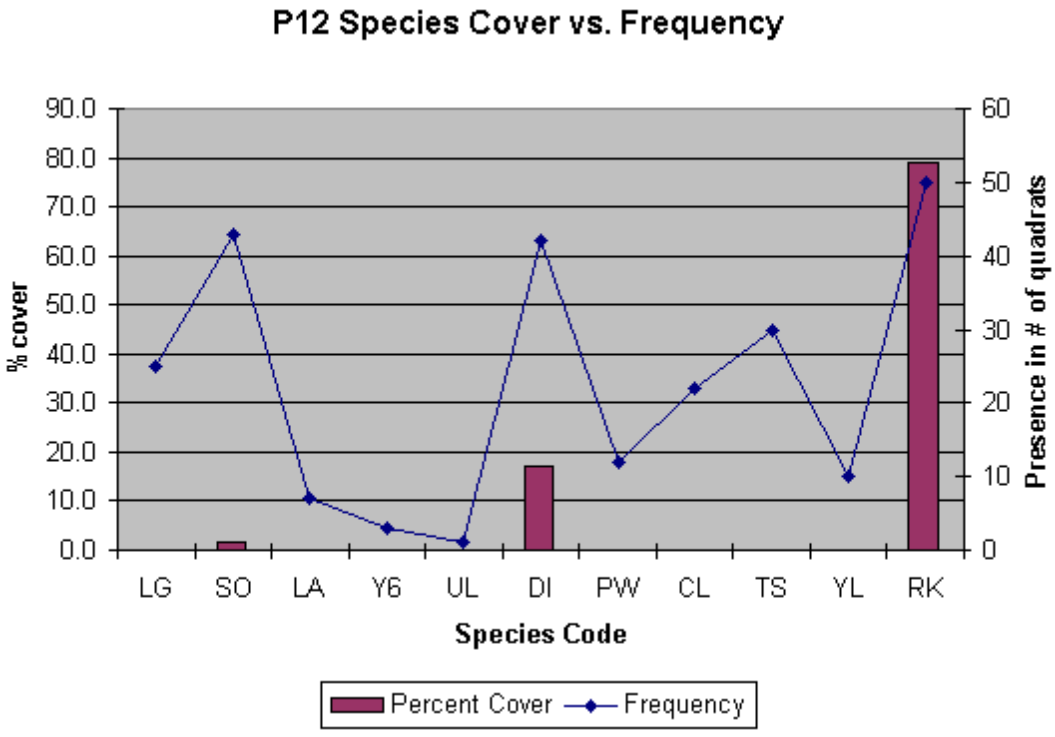

Appendix 32
Relationships Between Species Percent Cover and Frequency

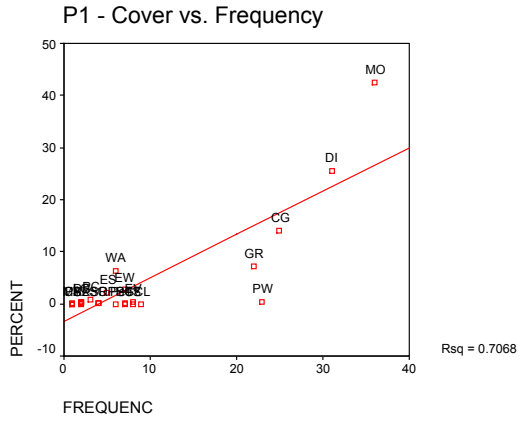

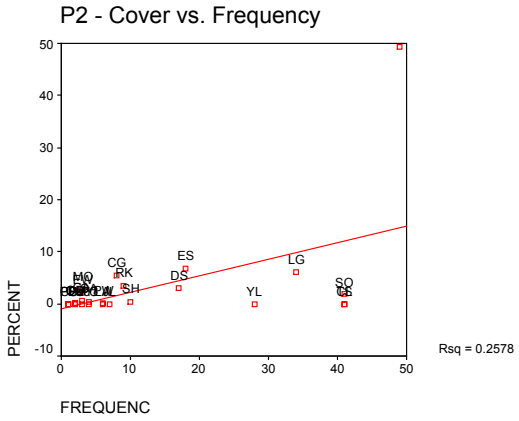

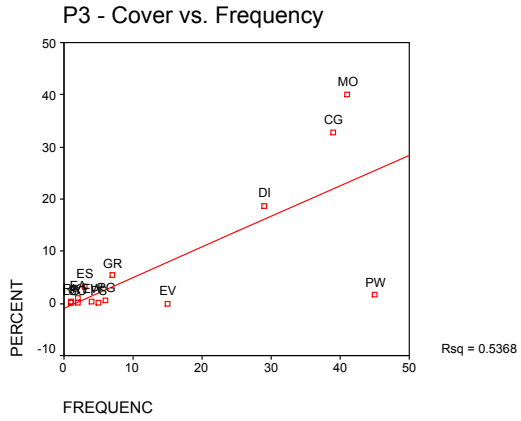

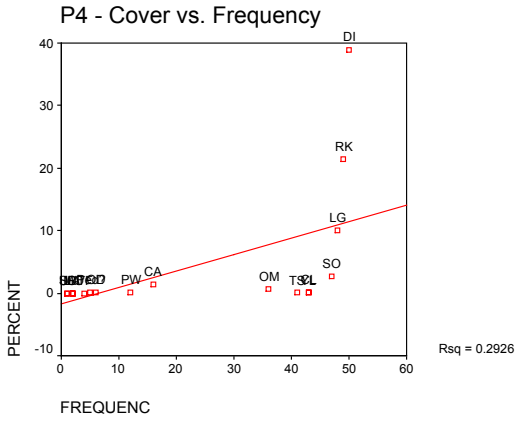

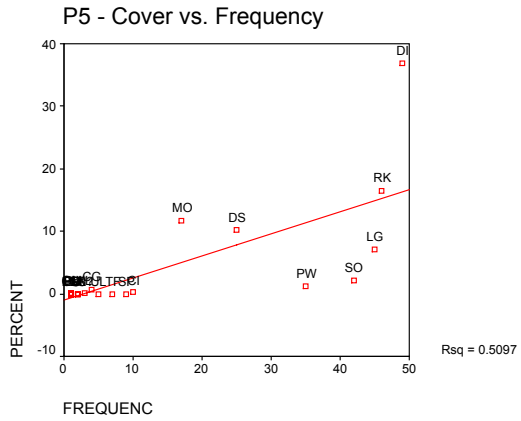

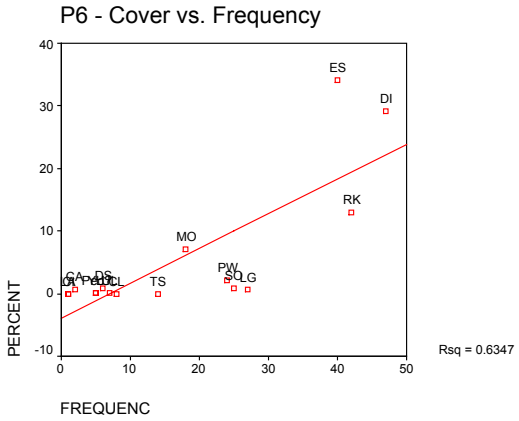

Appendix 32 (continued)

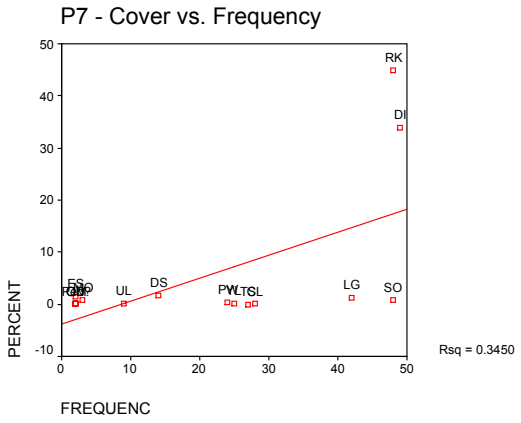

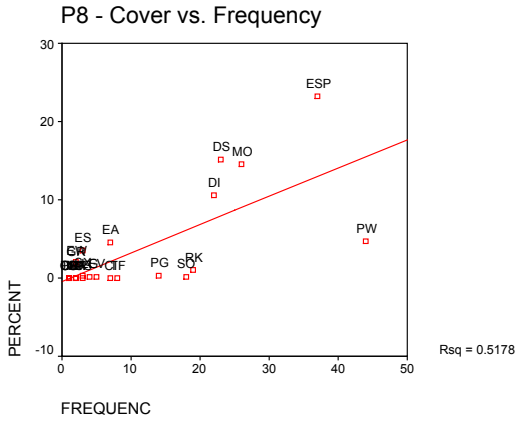

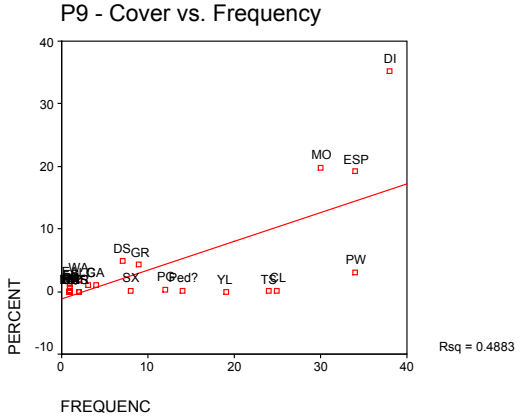

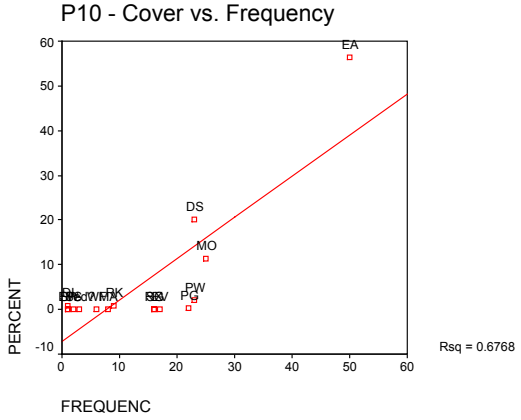

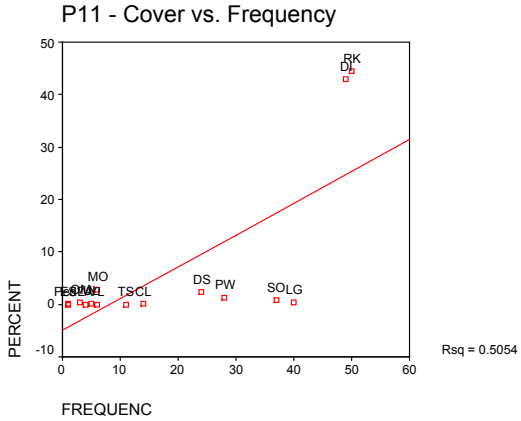

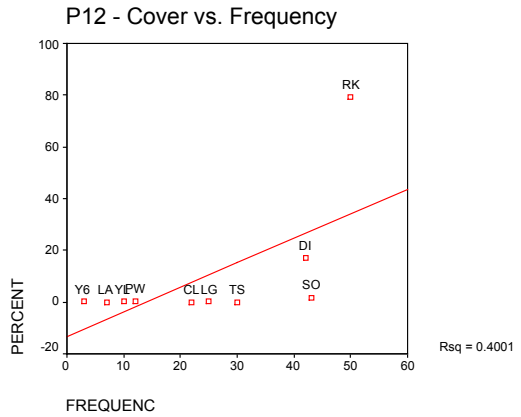

Appendix 33
Regression Results for Percent Cover of 10 vs. 50 Quadrats

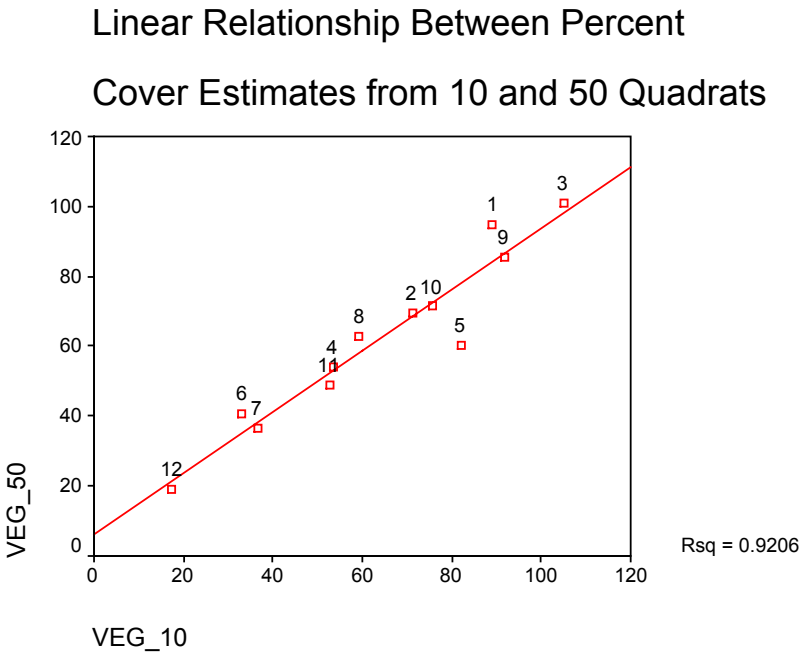

Regression Results for Percent Cover Estimates

Model	R	R Square	Adjusted R Square	Std. Error of the Estimate
1	.959	.921	.913	7.1645

a Predictors: (Constant), VEG_10
b Dependent Variable: VEG_50

Coefficients

		Unstandardized Coefficients		Standardized Coefficients	t	Sig.	95% Confidence Interval for B	
Model		B	Std. Error	Beta			Lower Bound	Upper Bound
1	(Constant)	5.936	5.604		1.059	.314	-6.551	18.423
	VEG_10	.877	.081	.959	10.769	.000	.696	1.059

a Dependent Variable: VEG_50

Casewise Diagnostics

Case Number	PLOT	Std. Residual	VEG_50	Predicted Value	Residual
	5	-2.486	60.17	77.9844	-17.8144

a Dependent Variable: VEG_50

ANOVA
%cover (10) and %cover (50)

	Sum of Squares	df	Mean Square	F	Sig.
Between Groups	21.603	1	21.603	.033	.857
Within Groups	14198.417	22	645.383		
Total	14220.020	23			

Appendix 34
Plot Percent Cover Mean and Standard Deviation

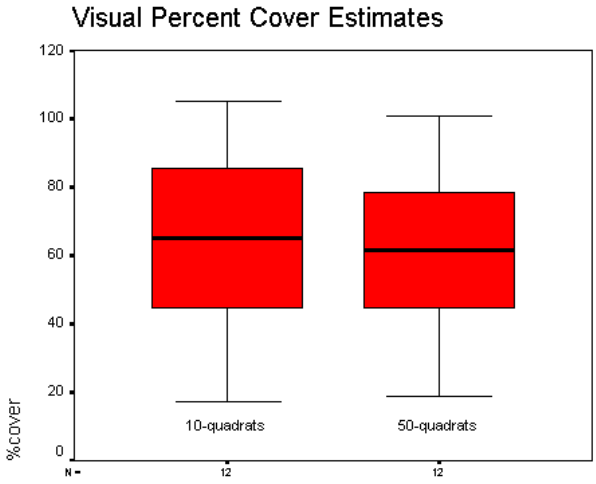

Appendix 35
Plot Percent Cover Results

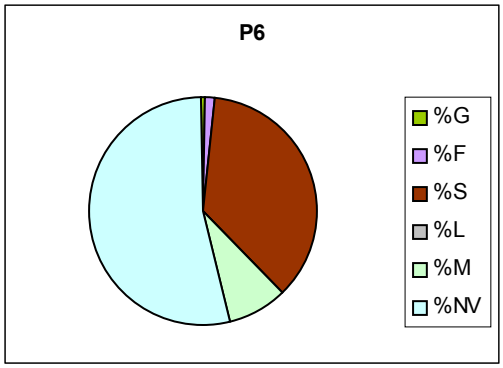

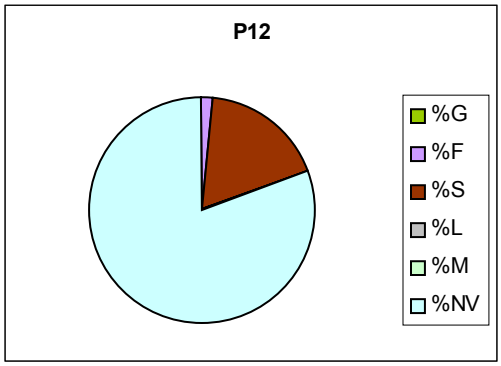

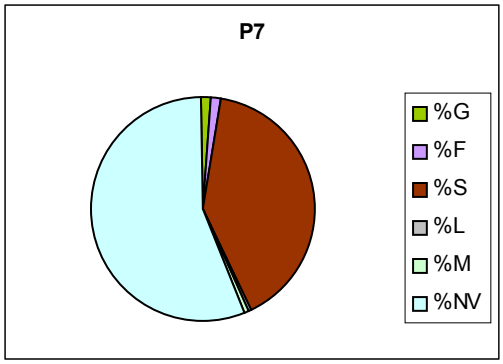

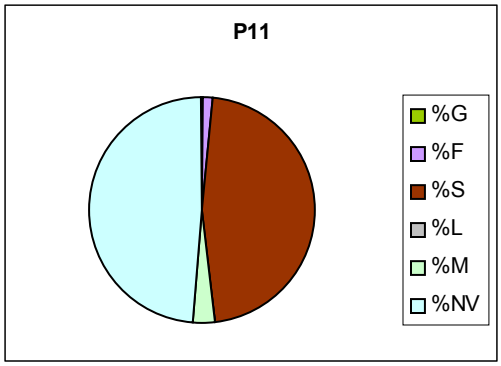

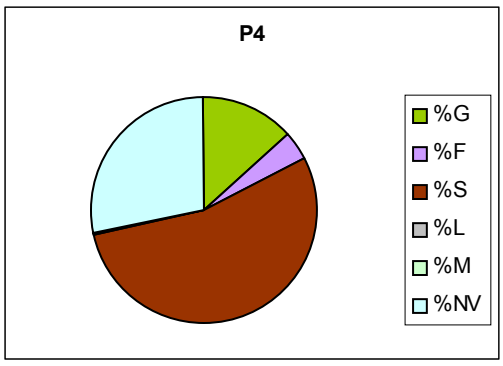

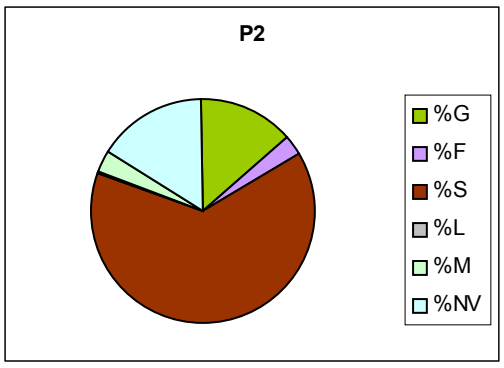

Appendix 35 (continued)

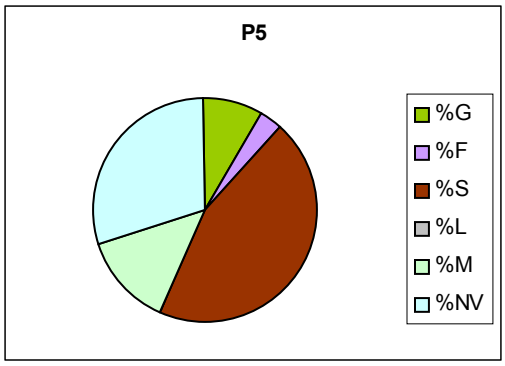

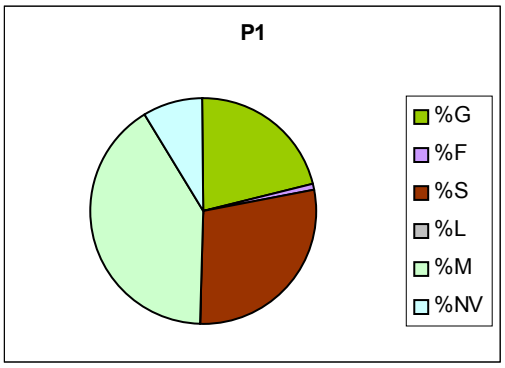

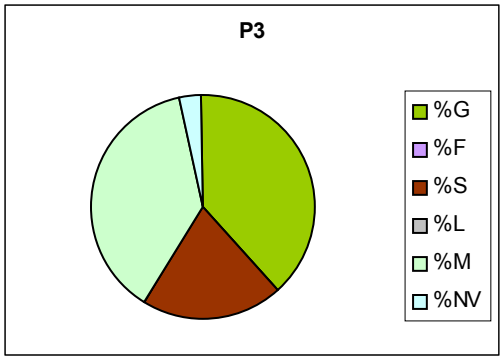

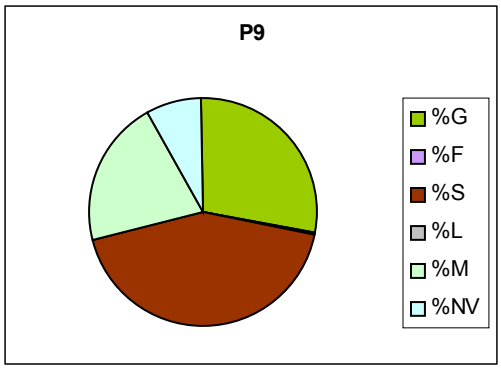

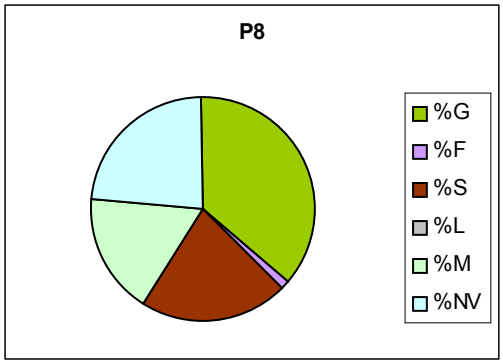

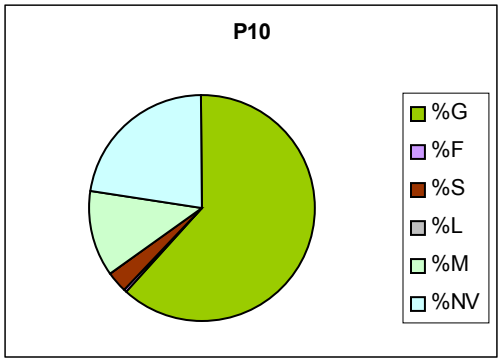

Where:
%G = graminoid cover
%F = forb cover
%S = shrub cover
%L = lichen cover
%M = moss cover
%NV = non-vegetated cover

Appendix 36
Bryophyte Biomass Mean and Standard Deviation Graphs

Figure A – Mean bryophyte biomass

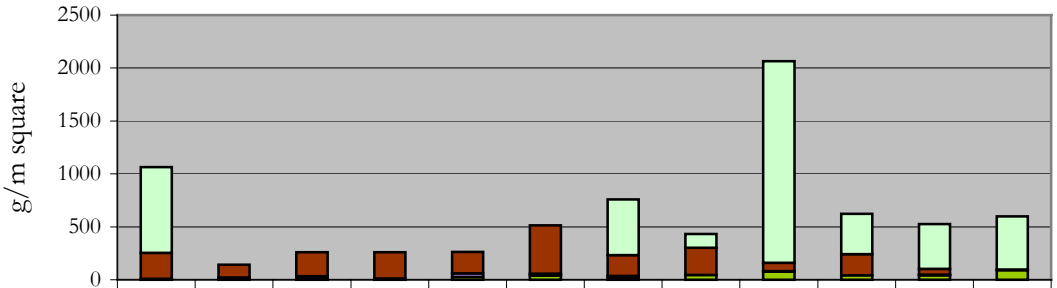

	P6	P12	P7	P11	P4	P2	P5	P1	P3	P9	P8	P10
BM	808.89	0	0	0	0	0	525.07	129.82	1905.24	380.89	424.44	502.13
BS	245.44	121.28	225.6	247.28	201.6	456.76	196.44	259.56	78.8	199.64	55.04	5.08
BF	6.48	19.84	21.88	9.44	33.64	18.4	13.24	0	2.16	0.96	6.68	0.48
BG	1.88	1.12	11.96	3.88	27.72	39	24.16	43.88	79.68	41.76	41	91.12

Plot #

Where, BM = Moss biomass
BS = Shrub biomass
BF = Forb biomass
BG = Graminoid biomass

Figure b

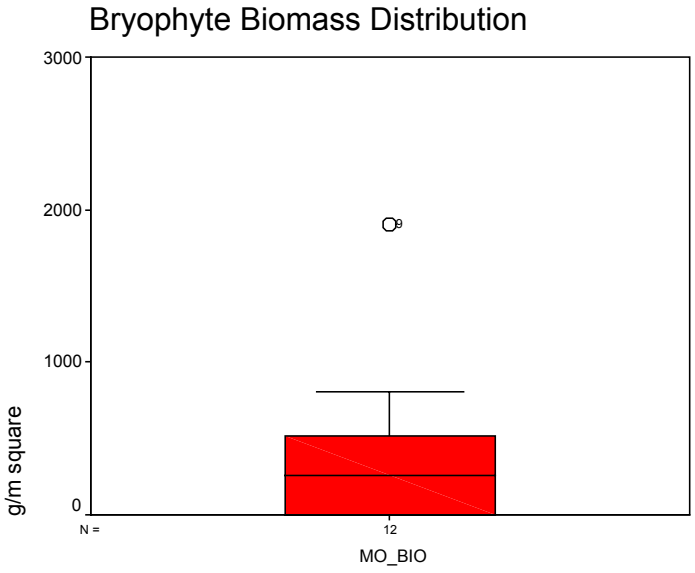

Appendix 37
Vascular Plant Biomass Mean and Standard Deviation

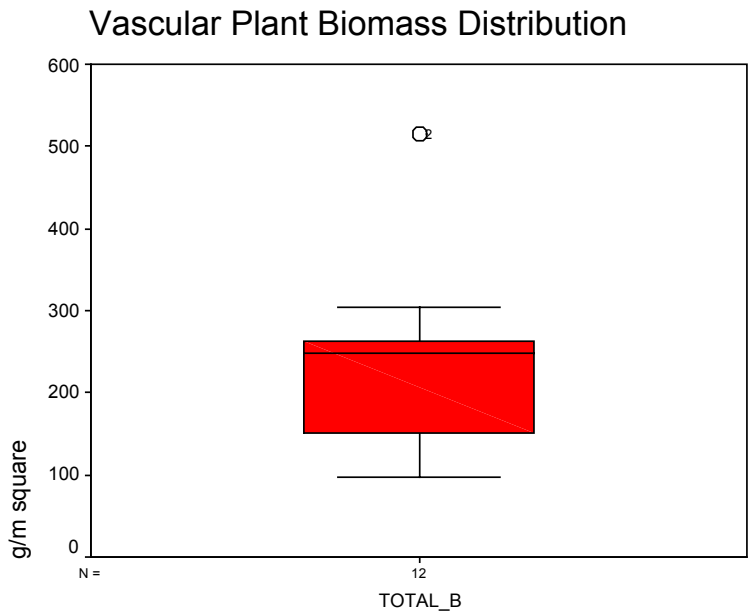

Appendix 38

Surface Spectral Response Curves and Quadrat Photos

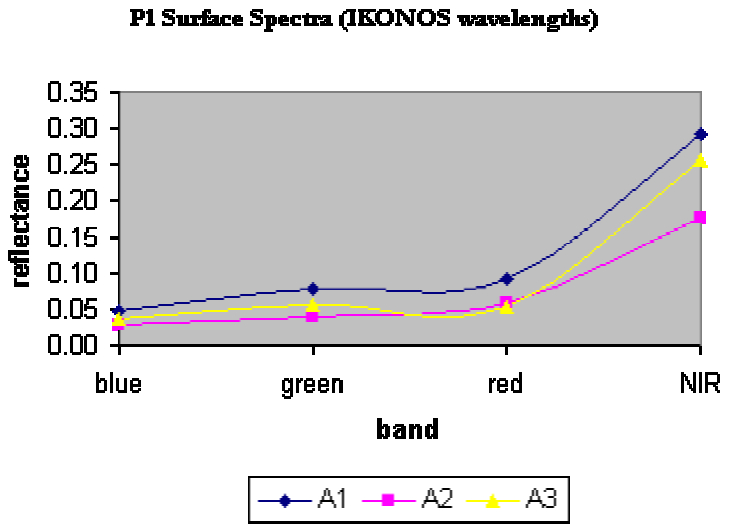

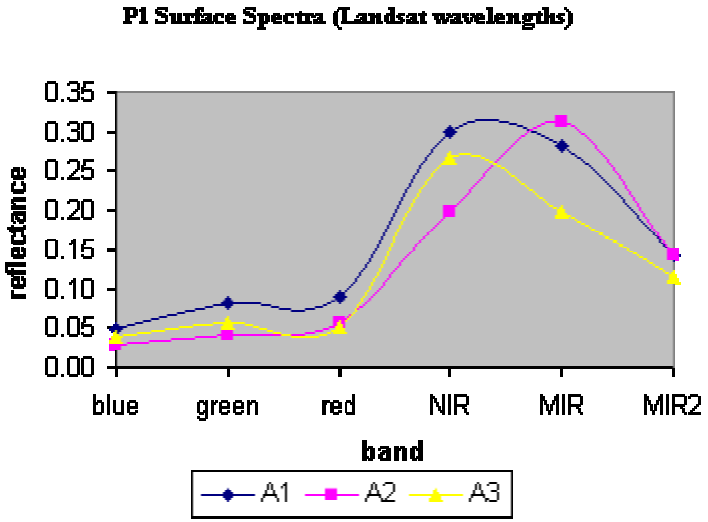

A1

A2

A3

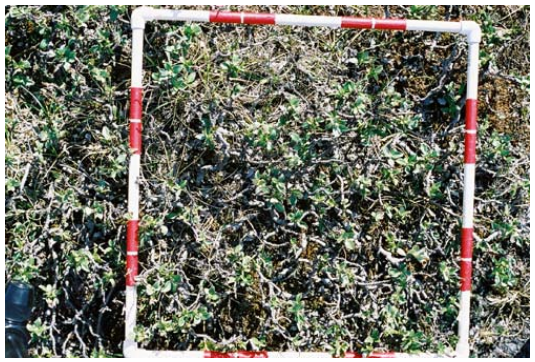

Appendix 38 (continued)

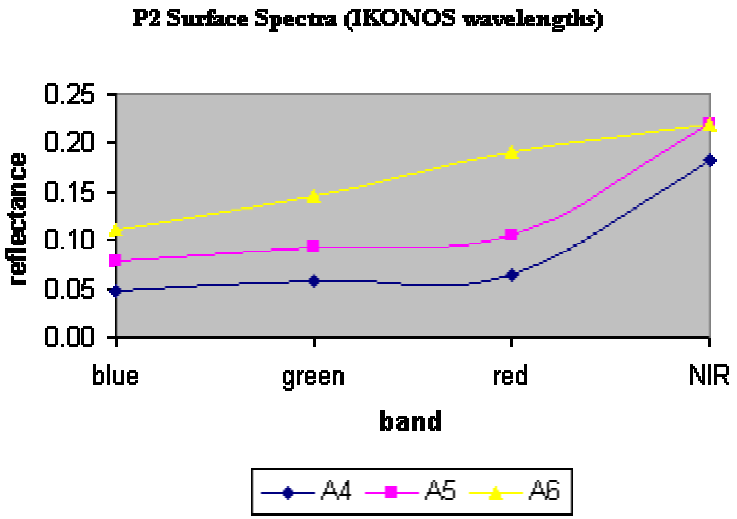

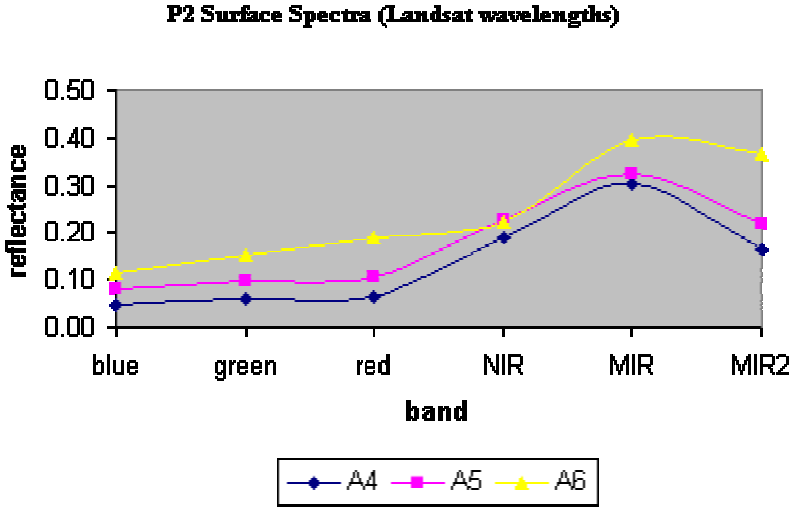

A4

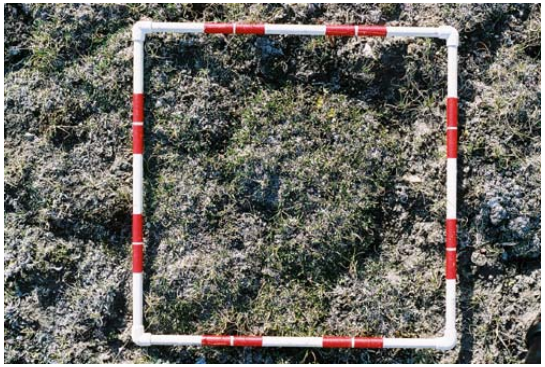

A5

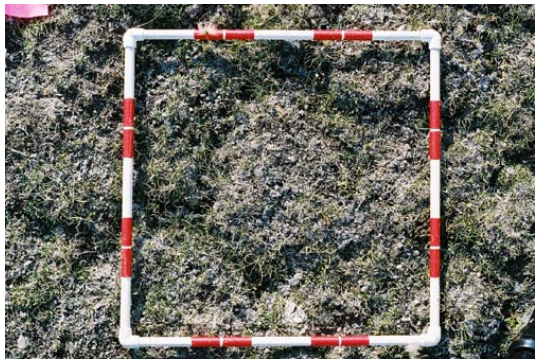

A6

Appendix 38 (continued)

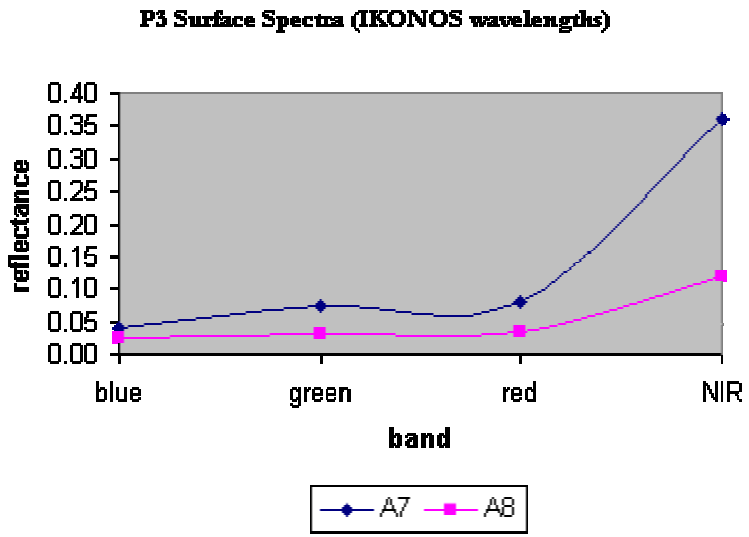

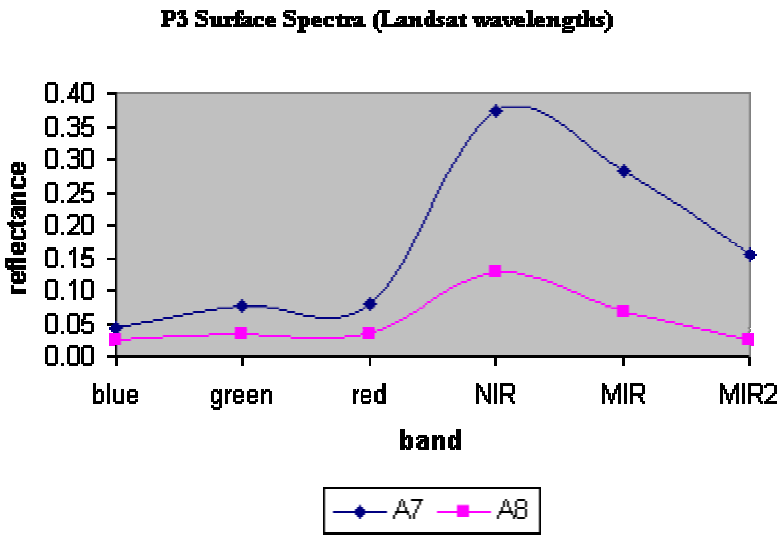

A7

A8

Appendix 38 (continued)

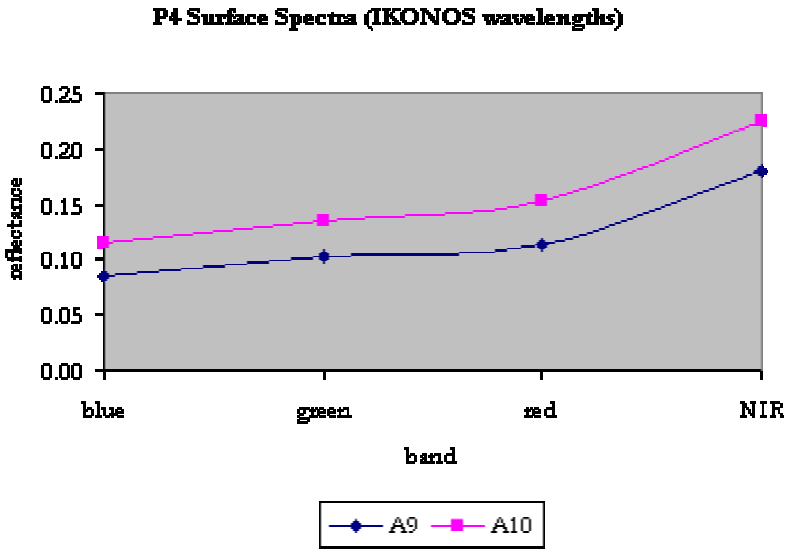

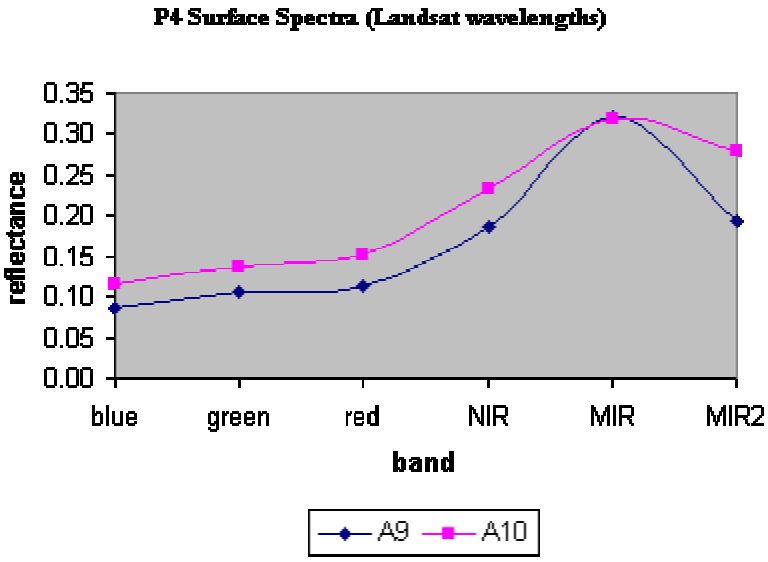

A9

A10

Appendix 38 (continued)

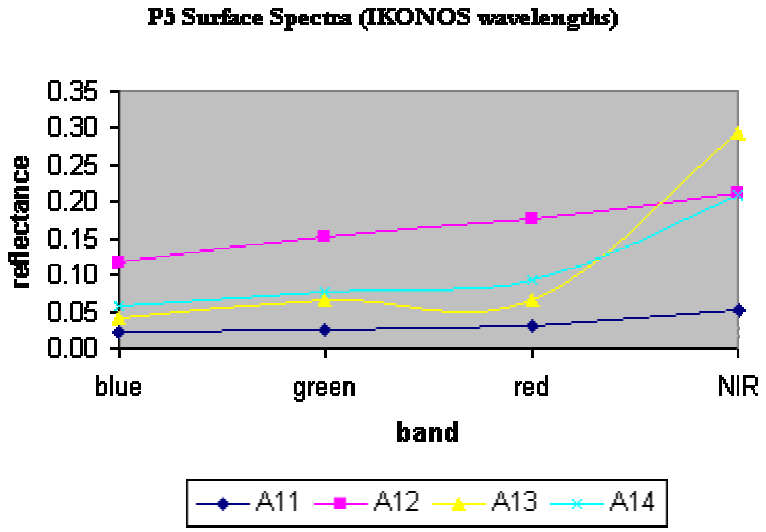

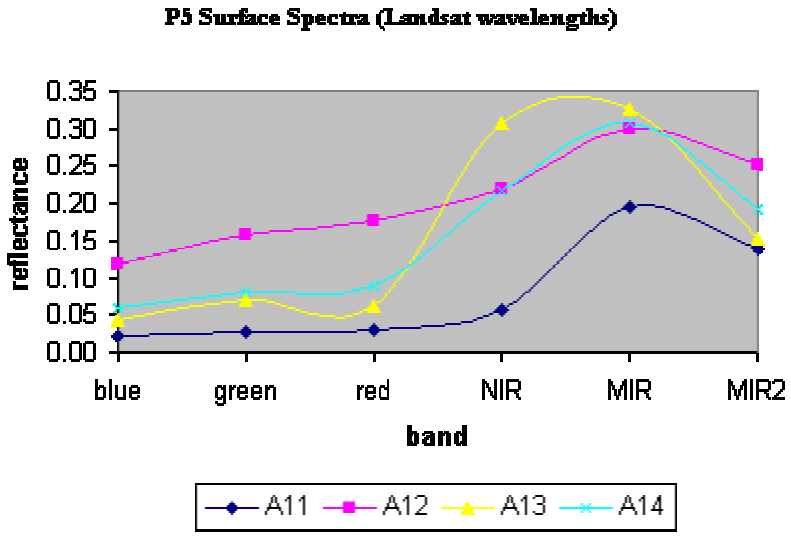

A11

A12

A13

A14

Appendix 38 (continued)

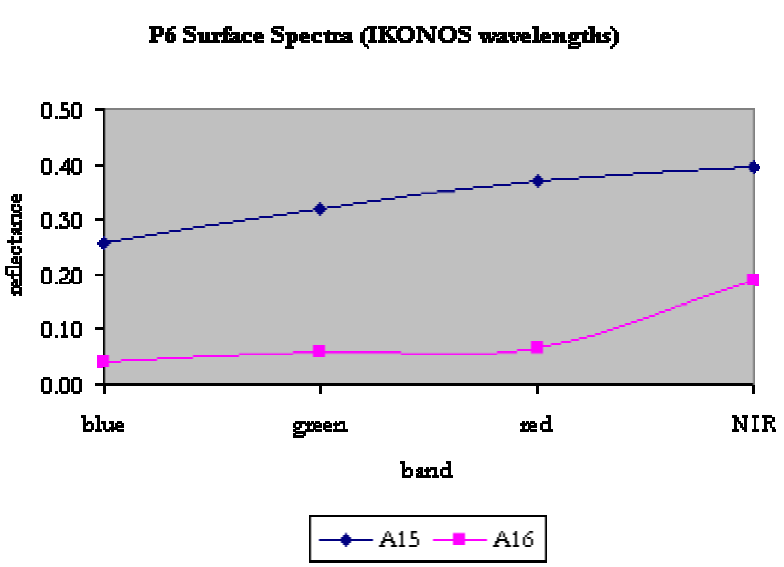

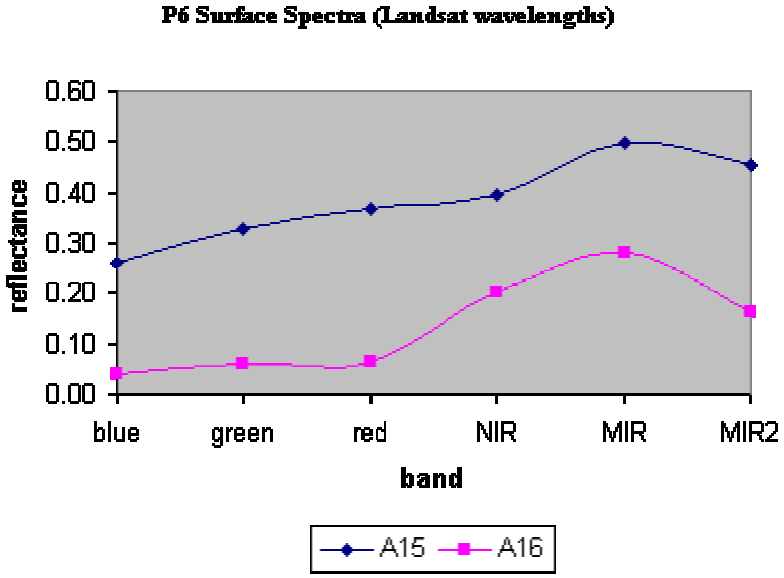

A15

A16

Appendix 38 (continued)

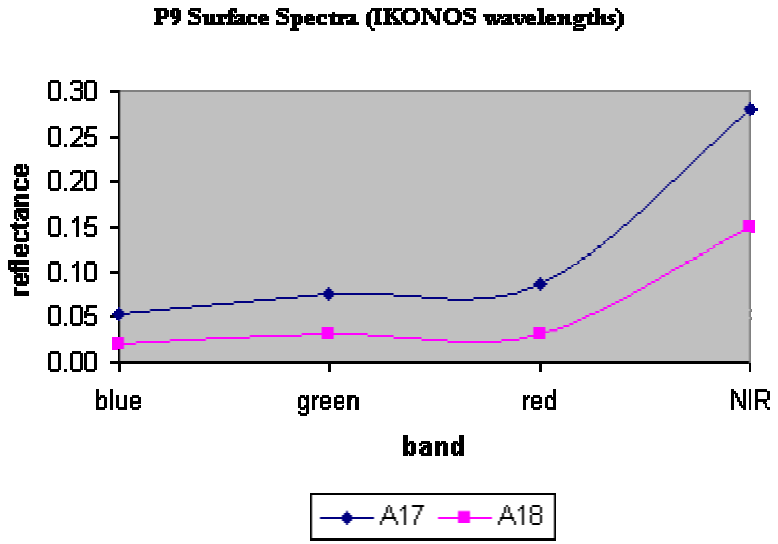

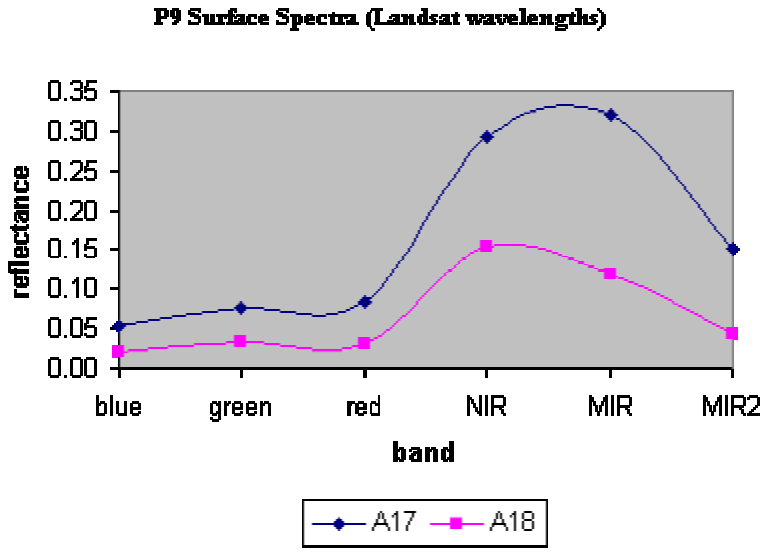

A17

A18

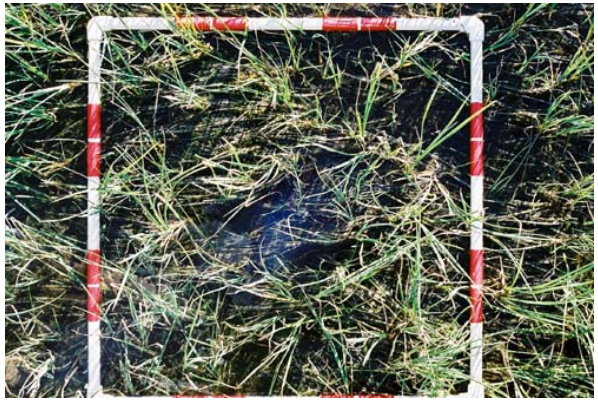

Appendix 39
*Plot ROI Separability Results**

IKONOS ROIs
Region #9:
Region #12: 1.99999951
Region #4: 1.99688372
Region #1: 1.08368666
Region #3: 1.01381851
Region #2: 0.76123721
Region #8: 1.04666475
Region #6: 1.97748382
Region #7: 1.99611648
Region #5: 1.13207289
Region #11: 1.97343393
Region #10: 0.82013642

Region #12:
Region #9: 1.99999951
Region #4: 2.00000000
Region #1: 2.00000000
Region #3: 2.00000000
Region #2: 1.99998755
Region #8: 2.00000000
Region #6: 1.90175317
Region #7: 1.96674583
Region #5: 1.99999998
Region #11: 1.94962985
Region #10: 2.00000000

Region #4:
Region #9: 1.99688372
Region #12: 2.00000000
Region #1: 1.99988173
Region #3: 1.99994650
Region #2: 1.77161217
Region #8: 1.99996777
Region #6: 1.99907644
Region #7: 1.55648830
Region #5: 1.96229376
Region #11: 1.19373733
Region #10: 1.99997344

IKONOS ROIs
Region #1:
Region #9: 1.08368666
Region #12: 2.00000000
Region #4: 1.99988173
Region #3: 0.45738469
Region #2: 1.66276237
Region #8: 0.95700382
Region #6: 1.99999999
Region #7: 1.99999422
Region #5: 1.24361361
Region #11: 1.99995318
Region #10: 0.54305769

Region #3:
Region #9: 1.01381851
Region #12: 2.00000000
Region #4: 1.99994650
Region #1: 0.45738469
Region #2: 1.69808313
Region #8: 1.00455543
Region #6: 1.99999961
Region #7: 1.99997943
Region #5: 1.35129808
Region #11: 1.99978939
Region #10: 0.49789334

Region #2:
Region #9: 0.76123721
Region #12: 1.99998755
Region #4: 1.77161217
Region #1: 1.66276237
Region #3: 1.69808313
Region #8: 1.78606769
Region #6: 1.94893337
Region #7: 1.89445765
Region #5: 1.08890118
Region #11: 1.74574754
Region #10: 1.66700717

IKONOS ROIs
Region #8:
Region #9: 1.04666475
Region #12: 2.00000000
Region #4: 1.99996777
Region #1: 0.95700382
Region #3: 1.00455543
Region #2: 1.78606769
Region #6: 2.00000000
Region #7: 1.99999995
Region #5: 1.10440375
Region #11: 1.99999618
Region #10: 0.38220294

Region #6:
Region #9: 1.97748382
Region #12: 1.90175317
Region #4: 1.99907644
Region #1: 1.99999999
Region #3: 1.99999961
Region #2: 1.94893337
Region #8: 2.00000000
Region #7: 0.84564453
Region #5: 1.99670465
Region #11: 1.64246858
Region #10: 2.00000000

Region #7:
Region #9: 1.99611648
Region #12: 1.96674583
Region #4: 1.55648830
Region #1: 1.99999422
Region #3: 1.99997943
Region #2: 1.89445765
Region #8: 1.99999995
Region #6: 0.84564453
Region #5: 1.93638218
Region #11: 0.33636442
Region #10: 1.99999984

Appendix 39 (continued)

IKONOS ROIs
Region #5:
- Region #9: 1.13207289
- Region #12: 1.99999998
- Region #4: 1.96229376
- Region #1: 1.24361361
- Region #3: 1.35129808
- Region #2: 1.08890118
- Region #8: 1.10440375
- Region #6: 1.99670465
- Region #7: 1.93638218
- Region #11: 1.84091537
- Region #10: 1.62850162

Region #11:
- Region #9: 1.97343393
- Region #12: 1.94962985
- Region #4: 1.19373733
- Region #1: 1.99995318
- Region #3: 1.99978939
- Region #2: 1.74574754
- Region #8: 1.99999618
- Region #6: 1.64246858
- Region #7: 0.33636442
- Region #5: 1.84091537
- Region #10: 1.99999310

Region #10:
- Region #9: 0.82013642
- Region #12: 2.00000000
- Region #4: 1.99997344
- Region #1: 0.54305769
- Region #3: 0.49789334
- Region #2: 1.66700717
- Region #8: 0.38220294
- Region #6: 2.00000000
- Region #7: 1.99999984
- Region #5: 1.62850162
- Region #11: 1.99999310

Landsat ROIs
Region #9:
- Region #12: 2.00000000
- Region #4: 2.00000000
- Region #1: 1.56034337
- Region #3: 1.94489750
- Region #2: 1.84886780
- Region #8: 1.99443616
- Region #6: 1.99989311
- Region #7: 1.99999994
- Region #5: 1.97239896
- Region #11: 1.99791411
- Region #10: 1.99128267

Region #12:
- Region #9: 2.00000000
- Region #4: 2.00000000
- Region #1: 2.00000000
- Region #3: 2.00000000
- Region #2: 2.00000000
- Region #8: 2.00000000
- Region #6: 1.99959634
- Region #7: 1.99999976
- Region #5: 2.00000000
- Region #11: 1.99999946
- Region #10: 2.00000000

Region #4:
- Region #9: 2.00000000
- Region #12: 2.00000000
- Region #1: 2.00000000
- Region #3: 2.00000000
- Region #2: 2.00000000
- Region #8: 2.00000000
- Region #6: 1.99999999
- Region #7: 1.99956819
- Region #5: 1.99999988
- Region #11: 1.97860557
- Region #10: 2.00000000

Landsat ROIs
Region #1:
- Region #9: 1.56034337
- Region #12: 2.00000000
- Region #4: 2.00000000
- Region #3: 1.32528938
- Region #2: 1.99603364
- Region #8: 1.81270189
- Region #6: 2.00000000
- Region #7: 2.00000000
- Region #5: 1.99995242
- Region #11: 2.00000000
- Region #10: 1.97977053

Region #3:
- Region #9: 1.94489750
- Region #12: 2.00000000
- Region #4: 2.00000000
- Region #1: 1.32528938
- Region #2: 1.99999826
- Region #8: 1.81205631
- Region #6: 2.00000000
- Region #7: 2.00000000
- Region #5: 2.00000000
- Region #11: 2.00000000
- Region #10: 1.99428794

Region #2:
- Region #9: 1.84886780
- Region #12: 2.00000000
- Region #4: 2.00000000
- Region #1: 1.99603364
- Region #3: 1.99999826
- Region #8: 2.00000000
- Region #6: 1.99999903
- Region #7: 1.99999276
- Region #5: 1.99753069
- Region #11: 1.98166573
- Region #10: 2.00000000

Appendix 39 (continued)

Landsat ROIs
Region #8:
- Region #9: 1.99443616
- Region #12: 2.00000000
- Region #4: 2.00000000
- Region #1: 1.81270189
- Region #3: 1.81205631
- Region #2: 2.00000000
- Region #6: 2.00000000
- Region #7: 2.00000000
- Region #5: 1.99999650
- Region #11: 2.00000000
- Region #10: 1.72522921

Region #6:
- Region #9: 1.99989311
- Region #12: 1.99959634
- Region #4: 1.99999999
- Region #1: 2.00000000
- Region #3: 2.00000000
- Region #2: 1.99999903
- Region #8: 2.00000000
- Region #7: 1.29739943
- Region #5: 1.99999992
- Region #11: 1.76427548
- Region #10: 2.00000000

Region #7:
- Region #9: 1.99999994
- Region #12: 1.99999976
- Region #4: 1.99956819
- Region #1: 2.00000000
- Region #3: 2.00000000
- Region #2: 1.99999276
- Region #8: 2.00000000
- Region #6: 1.29739943
- Region #5: 1.99998253
- Region #11: 1.27188697
- Region #10: 2.00000000

Landsat ROIs
Region #5:
- Region #9: 1.97239896
- Region #12: 2.00000000
- Region #4: 1.99999988
- Region #1: 1.99995242
- Region #3: 2.00000000
- Region #2: 1.99753069
- Region #8: 1.99999650
- Region #6: 1.99999992
- Region #7: 1.99998253
- Region #11: 1.99883280
- Region #10: 1.97413524

Region #11:
- Region #9: 1.99791411
- Region #12: 1.99999946
- Region #4: 1.97860557
- Region #1: 2.00000000
- Region #3: 2.00000000
- Region #2: 1.98166573
- Region #8: 2.00000000
- Region #6: 1.76427548
- Region #7: 1.27188697
- Region #5: 1.99883280
- Region #10: 2.00000000

Region #10:
- Region #9: 1.99128267
- Region #12: 2.00000000
- Region #4: 2.00000000
- Region #1: 1.97977053
- Region #3: 1.99428794
- Region #2: 2.00000000
- Region #8: 1.72522921
- Region #6: 2.00000000
- Region #7: 2.00000000
- Region #5: 1.97413524
- Region #11: 2.00000000

* highlighted numbers indicate separable ROIs (i.e. > 1.7)

Appendix 40

Preliminary Class Descriptions For Unsupervised Classification

IKONOS Unsupervised Classification Results

Class #	Cover Type	Rationale	Cover Type	Rationale
2	**Ponds and river (mid-depth water)**	Low visible DNs, declining consistently through to nir – location in middle of ponds and certain river sections	**Ponds and river (mid-depth water)**	Low visible DNs, declining consistently through to nir (lowest DNs of all classes) – limited extent in middle of ponds and certain river sections
3	**Ponds, lake and river (mid – deep water)**	Low visible DNs, declining consistently through to nir (almost identical to Class 10) – location in middle of ponds, certain river sections, and Sanagak Lake	**Ponds and river (mid-depth water)**	Low visible DNs, declining consistently through to nir – limited extent in middle of ponds and certain river sections
4	**Shallow water (river/ lake/pond shores)**	Low DNs, but only slight decrease from visible to nir wavelengths – location of rings around ponds and certain river sections, may represent saturated moss communities	**Ponds and river (mid-depth water)**	Low visible DNs, declining consistently through to nir (higher than Class 2 & 3) – location in middle of ponds and certain river sections
5	**Moist sedge meadow**	mid-range DNs with most distinct vegetation curve – spatial distribution based on study area familiarity	**Shallow water (river/ lake/pond shores)**	Low DNs, but only slight decrease from visible to nir wavelengths – location of rings around ponds and particular river sections
6	**Dwarf-shrub heath**	Higher DNs than Class 5, less distinct spectral curve suggesting senescent or more sparse vegetation – spatial distribution based on study area familiarity	**Water-track vegetation**	Visible DN range similar to water classes, yet higher nir response indicates increasing presence of vegetation – localized distribution, ponds/lakes drainage paths, accumulate in narrow ridge valleys
7	**Barren/ Sandy**	Highest DNs, constant spectral response through visible and nir wavelengths – location along rivers, areas known to be sand bars and very sparsely vegetated ridge tops	**Moist sedge meadow**	mid-range DNs with most distinct vegetation curve – spatial distribution based on study area familiarity
8	**Rivers**	Highest DNs of water classes, but same spectral trend downwards towards nir – location mainly in rivers but also in some ponds	**Dwarf-shrub heath**	Higher DNs than Class 7, less distinct spectral curve suggesting senescent or more sparse vegetation – spatial distribution based on study area familiarity
9	**Shallow water**	Similar spectral response to Class 8, but lower DNs – location mainly in river and ponds, and shallow areas of Sanagak Lake	**Barren/ Sandy**	Highest DNs, constant spectral response through all wavelengths – location along rivers, areas known to be sand bars and very sparsely vegetated ridge tops
10	**Ponds and river (mid-depth water)**	Low visible DNs, declining consistently through to nir (only slightly higher than Class 2) – location in middle of ponds and certain river sections	**Rivers**	Highest DNs of water classes, but same spectral trend downwards towards nir – location mainly in rivers but also in some ponds
11	n/a	n/a	**Snowbed vegetation**	Higher DNs than Class 6, but lower than other vegetation classes, less distinct vegetation spectral response due to higher water content – spatial distribution along the base of ridges and greater prominence on north-slope bases (i.e. later melting)
12	n/a	n/a	**Shallow water**	Similar spectral response to Class 8, but lower DNs – location mainly in river and ponds, and shallow areas of Sanagak Lake
13	n/a	n/a	**Ponds and river (mid-depth water)**	Low visible DNs, declining consistently through to nir (higher than Class 2 & 3, and higher than Class 4 in nir wavelengths) – location in middle of ponds and certain river sections
14	n/a	n/a	**Ponds and river (mid-depth water)**	Low visible DNs, declining consistently through to nir (second lowest DNs of all classes) – limited extent in middle of ponds and certain river sections

Appendix 40 (continued)

Landsat Unsupervised Classification Results

Class #	Cover Type	Rationale	Cover Type	Rationale
2	**Deep water**	Lowest DNs, and consistent response through visible, nir, and mir wavelengths – location in middle of ponds and Sanagak Lake	**Deep water**	Lowest DNs, and consistent response through visible, nir, and mir wavelengths – location in middle of ponds and Sanagak Lake
3	**Ponds and river (mid-depth water)**	Low visible DNs, declining consistently through to mir – location ponds, certain river sections, and near edges of Sanagak Lake	**Ponds and river (mid-depth water)**	Low visible DNs, declining consistently through to mir – location ponds, certain river sections, and near edges of Sanagak Lake
4	**Shallow river/lake/ pond shores**	Consistent low DNs, but higher than Class 2 & 3 indicates increased vegetation – location on river/lake/ pond edges	**Deep river and ponds**	High visible DNs (for water), but drops through nir and mir wavelengths – location in middle of river, middle of ponds, and edge of Sanagak Lake
5	**Water-track/ snowbed vegetation**	Lower DNs than other vegetation types due to increased water content – surrounds ponds, wet areas, likely saturated communities	**Shallow river/pond shores**	Consistent low DNs, but higher than Class 2 & 3 indicates increased vegetation – location on river/pond edges
6	**Moist sedge meadow**	mid-range DNs with most distinct vegetation curve – spatial distribution based on study area familiarity	**Shallow river/pond shores**	Only slightly higher response than Class 5, perhaps indicates more presence of vegetation – location on river/pond edges
7	**Dwarf-shrub heath**	Higher DNs than Class 6, less distinct spectral curve suggesting senescent or more sparse vegetation – spatial distribution based on study area familiarity	**Water-track/ snowbed vegetation**	Lower DNs than other vegetation types due to increased water content – surrounds ponds, wet areas, likely saturated communities
8	**Barren/ Sandy**	Highest DNs, constant spectral response through visible wavelengths, slight decrease for nir and increasing again in mir – location along rivers, areas known to be sand bars and very sparsely vegetated ridge tops	**Moist sedge meadow**	mid-range DNs with most distinct vegetation curve – spatial distribution based on study area familiarity
9	**Shallow rivers and ponds**	Highest water DNs and slight decline through nir and mir wavelengths – location along river edges, likely underlain by sand/rock	**Sedge meadow**	mid-range DNs with distinct vegetation curve, higher visible and mir DNs, but same nir DNs, as Class 8 – spatial distribution based on study area familiarity
10	**Deep rivers and ponds**	High visible DNs (for water), but drops through nir and mir wavelengths – location in middle of river, middle of ponds, and edge of Sanagak Lake	**Dwarf-shrub heath**	Higher DNs than Class 9, less distinct spectral curve suggesting senescent or more sparse vegetation – spatial distribution based on study area familiarity
11	n/a	n/a	**Barren/ Sandy**	Highest DNs, constant spectral response through visible wavelengths, slight decrease for nir and increasing again in mir – location along rivers, areas known to be sand bars and very sparsely vegetated ridge tops
12	n/a	n/a	**Shallow rivers and ponds**	Highest water DNs and slight decline through nir and mir wavelengths – location along river edges, likely underlain by sand/rock
13	n/a	n/a	**Shallow rivers and ponds**	Slightly lower DNs than Class 12, same curve shape – location along river edges, perhaps deeper areas underlain by sand/rock
14	n/a	n/a	**Shoreline/ water-saturated vegetation**	Higher DNs than Class 7, but less distinct vegetation spectral curve – location along river and pond shorelines
15	n/a	n/a	**Deep rivers and ponds**	High visible DNs (for water), but drops through nir and mir wavelengths – location in middle of river, middle of ponds, and edge of Sanagak Lake

Appendix 41
Surface Quadrat VI Results

ASD Q#	NDVI	SAVI (0.5)	SAVI (1)	MSAVI
A1	0.547	0.358	0.306	0.336
A2	0.559	0.283	0.227	0.248
A3	0.678	0.394	0.326	0.370
A4	0.504	0.254	0.204	0.220
A5	0.377	0.225	0.187	0.198
A6	0.085	0.057	0.050	0.050
A7	0.654	0.465	0.407	0.458
A8	0.596	0.215	0.163	0.175
A9	0.241	0.135	0.111	0.114
A10	0.212	0.138	0.118	0.121
A11	0.314	0.068	0.049	0.050
A12	0.104	0.069	0.059	0.060
A13	0.666	0.424	0.359	0.407
A14	0.416	0.237	0.195	0.208
A15	0.037	0.033	0.032	0.032
A16	0.516	0.268	0.2167	0.235
A17	0.553	0.356	0.3027	0.332
A18	0.676	0.273	0.2107	0.231

Appendix 42
Plot VI Results

NDVI

Study plot	**Surface NDVI**	Std. Dev. Surface NDVI	**IKONOS NDVI**	Std. Dev. IKONOS NDVI	**Landsat NDVI**	Std. Dev. Landsat NDVI
P6	0.229	0.131	0.178	0.076	0.198	0.052
P12	0.149	0.045	0.060	0.021	0.083	0.014
P7	0.199	0.040	0.197	0.043	0.224	0.039
P11	0.299	0.132	0.203	0.041	0.246	0.026
P4	0.212	0.000	0.234	0.018	0.253	0.013
P2	0.384	0.138	0.310	0.042	0.353	0.022
P5	0.528	0.164	0.356	0.039	0.397	0.029
P1	0.576	0.119	0.382	0.027	0.426	0.028
P3	0.613	0.121	0.408	0.033	0.439	0.025
P9	0.614	0.044	0.400	0.070	0.431	0.056
P8	0.606	0.175	0.391	0.031	0.448	0.018
P10	0.570	0.291	0.405	0.032	0.436	0.029

SAVI (L=0.5)

Study plot	**Surface SAVI**	Std. Dev. Surface SAVI	**IKONOS SAVI**	Std. Dev. IKONOS SAVI	**Landsat SAVI**	Std. Dev. Landsat SAVI
P6	0.127	0.062	0.184	0.067	0.180	0.036
P12	0.087	0.019	0.067	0.022	0.083	0.013
P7	0.118	0.019	0.203	0.037	0.200	0.026
P11	0.159	0.064	0.207	0.037	0.217	0.019
P4	0.138	0.000	0.236	0.017	0.216	0.009
P2	0.226	0.083	0.308	0.040	0.296	0.017
P5	0.315	0.108	0.337	0.033	0.310	0.019
P1	0.351	0.086	0.362	0.035	0.332	0.029
P3	0.421	0.097	0.384	0.032	0.337	0.023
P9	0.314	0.029	0.385	0.066	0.345	0.038
P8	0.395	0.137	0.377	0.033	0.353	0.016
P10	0.366	0.235	0.396	0.037	0.340	0.022

SAVI (L = 1)

Study plot	**Surface SAVI(1)**	Std. Dev. Surface SAVI(1)	**IKONOS SAVI(1)**	Std. Dev. IKONOS SAVI(1)	**Landsat SAVI(1)**	Std. Dev. Landsat SAVI(1)
P6	0.106	0.048	0.187	0.063	0.172	0.030
P12	0.073	0.015	0.070	0.023	0.083	0.013
P7	0.098	0.015	0.206	0.035	0.190	0.022
P11	0.129	0.051	0.210	0.035	0.205	0.017
P4	0.118	0.000	0.237	0.017	0.201	0.008
P2	0.188	0.069	0.307	0.039	0.275	0.015
P5	0.264	0.091	0.329	0.031	0.280	0.016
P1	0.294	0.075	0.353	0.039	0.299	0.030
P3	0.365	0.087	0.374	0.03	0.302	0.023
P9	0.256	0.032	0.378	0.065	0.314	0.032
P8	0.341	0.120	0.370	0.034	0.319	0.015
P10	0.317	0.207	0.392	0.040	0.306	0.020

Appendix 42 (continued)

MSAVI

Study plot	**Surface MSAVI**	Std. Dev. Surface MSAVI	**IKONOS MSAVI**	Std. Dev. IKONOS MSAVI	**Landsat MSAVI**	Std. Dev. Landsat MSAVI
P6	0.113	0.053	0.187	0.064	0.175	0.032
P12	0.077	0.016	0.070	0.023	0.083	0.013
P7	0.103	0.016	0.205	0.036	0.193	0.024
P11	0.137	0.056	0.209	0.036	0.209	0.018
P4	0.121	0.000	0.237	0.017	0.206	0.009
P2	0.200	0.073	0.308	0.039	0.285	0.017
P5	0.294	0.104	0.334	0.033	0.295	0.019
P1	0.325	0.082	0.358	0.037	0.317	0.032
P3	0.408	0.100	0.381	0.033	0.321	0.025
P9	0.281	0.036	0.383	0.066	0.333	0.038
P8	0.384	0.136	0.375	0.034	0.339	0.017
P10	0.356	0.234	0.394	0.038	0.325	0.023

Appendix 43
Qualitative Spatial Analysis of Satellite NDVI

The advantages of high spatial resolution data become evident upon closer investigation of satellite images. Increasingly isolating an area of interest highlights the delineation of IKONOS fine-scale detail (Figure A), while Landsat transforms into an increasingly pixilated appearance (Figure B). Comparing specific areas portrayed by the letters overlaid on the images, reinforces IKONOS' enhanced mapping capabilities:

A. Landsat cannot resolve a small stream that runs off the East Tributary of the Lord Lindsay River.

B. Wetland areas with lush mosses and prominent sedges that surround a semi-circle of small lakes is barely differentiated by Landsat. Furthermore, the boundaries between the three small lakes are dissolved in Figure B.

C. Small drainage streams and ponds are depicted in Figure A, but are non-existent in Figure B.

D. Locally raised surfaces just to the right of D are bisected by a small water track of lush vegetation, likely fed by the small ponds above, and to both sides below (Figure A). In Figure B these important microsites are aggregated to form a relatively uniform NDVI response.

Appendix 43 (continued)

Figure A – Close-up IKONOS NDVI

Figure B – Close-up Landsat NDVI

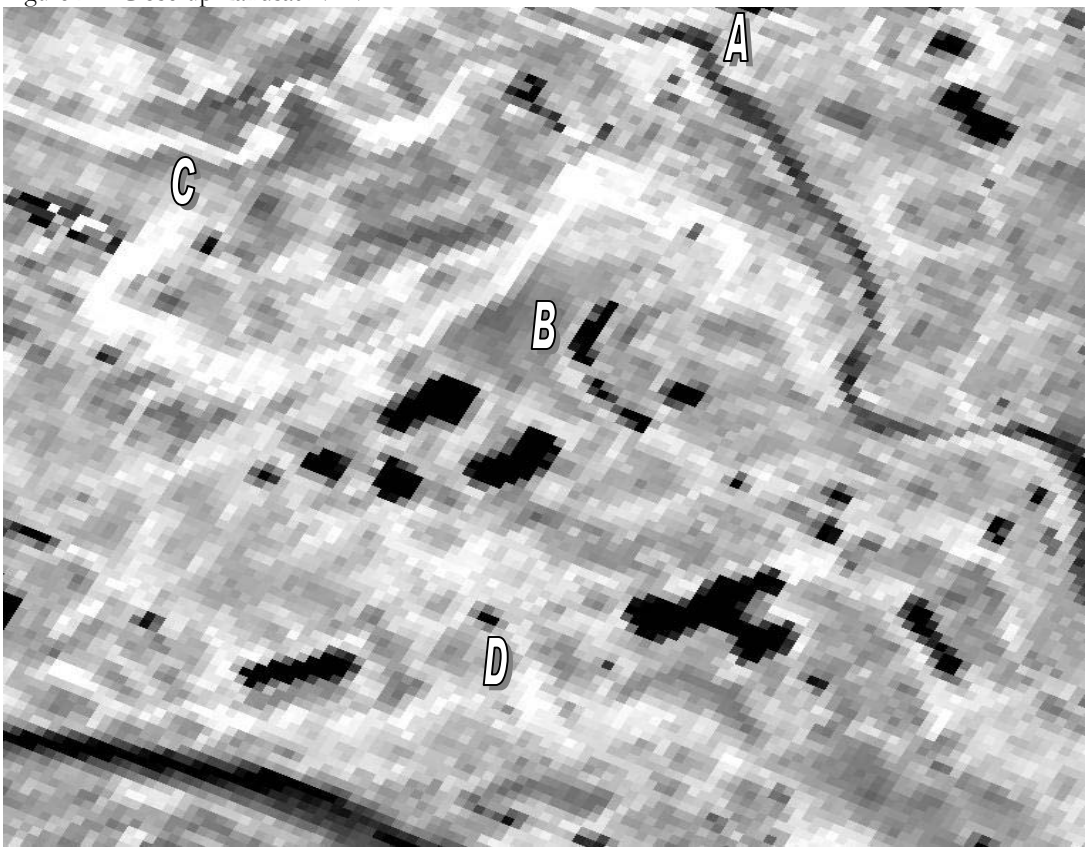

Appendix 44
Histograms of Data Normality

Total Vascular Plant Biomass
Shapiro-Wilk W=.86227, p<.0522

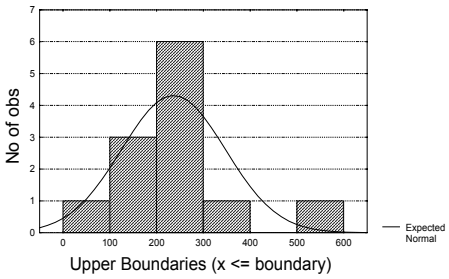

Visual Percent Vegetation Cover (50 quadrats)
Shapiro-Wilk W=.98347, p<.9939

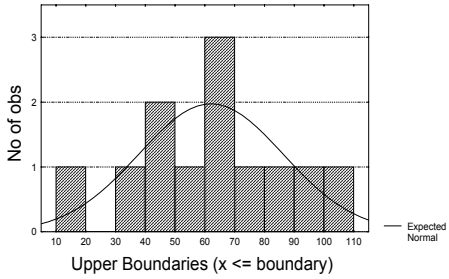

Surface NDVI
Shapiro-Wilk W=.84073, p<.0283

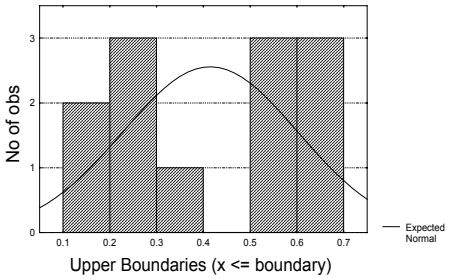

IKONOS NDVI
Shapiro-Wilk W=.87307, p<.0715

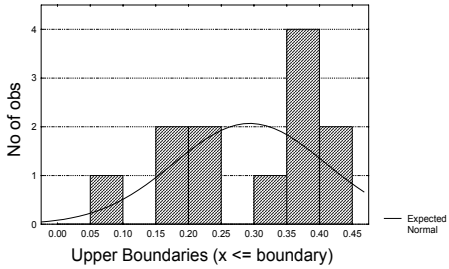

Landsat NDVI
Shapiro-Wilk W=.86400, p<.0549

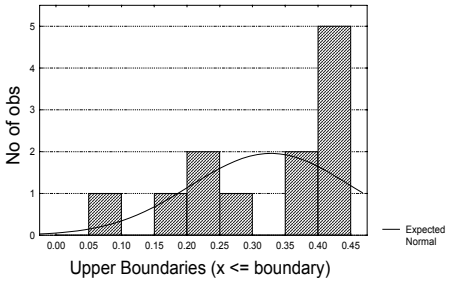

Surface SAVI
Shapiro-Wilk W=.89673, p<.1439

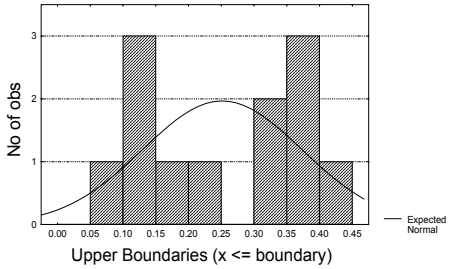

IKONOS SAVI
Shapiro-Wilk W=.88238, p<.0940

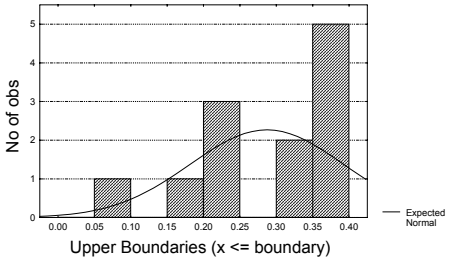

Landsat SAVI
Shapiro-Wilk W=.86451, p<.0557

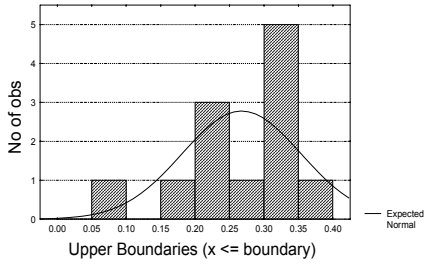

Appendix 44 (continued)

Surface SAVI (1)
Shapiro-Wilk W=.90401, p<.1787

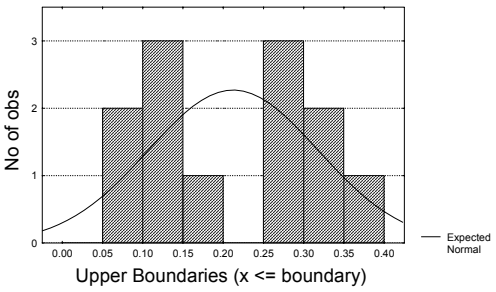

IKONOS SAVI (1)
Shapiro-Wilk W=.88889, p<.1140

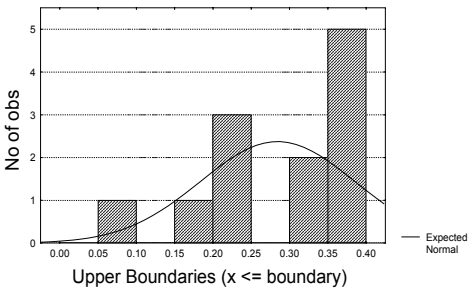

Landsat SAVI (1)
Shapiro-Wilk W=.86495, p<.0564

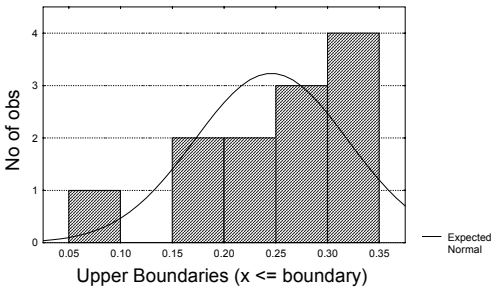

Surface MSAVI
Shapiro-Wilk W=.89884, p<.1532

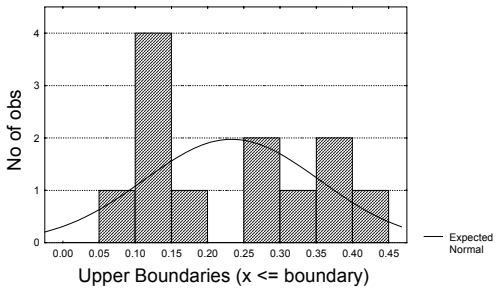

IKONOS MSAVI
Shapiro-Wilk W=.88555, p<.1033

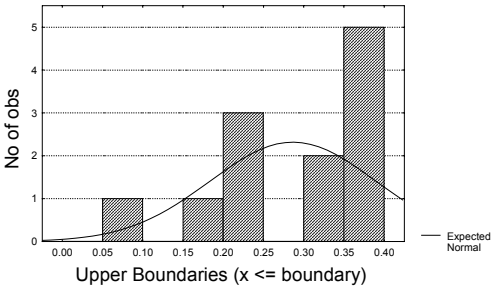

Landsat MSAVI
Shapiro-Wilk W=.87027, p<.0659

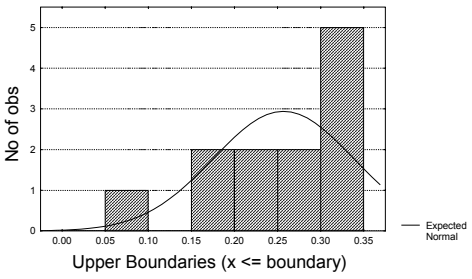

Surface GVI
Shapiro-Wilk W=.90994, p<.2130

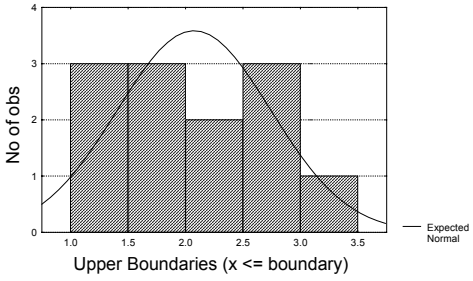

Landsat GVI
Shapiro-Wilk W=.88719, p<.1084

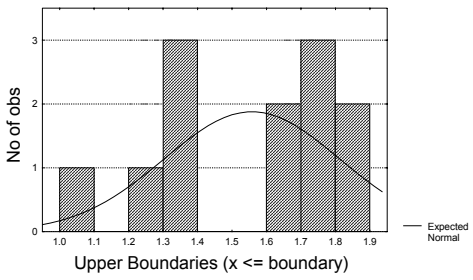

Species Richness
Shapiro-Wilk W=.88011, p<.0879

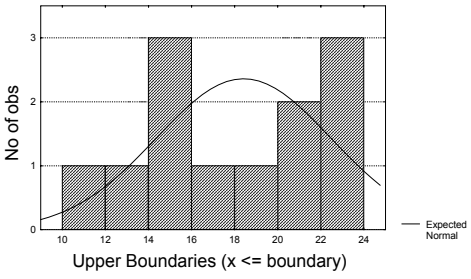

Appendix 45
Residual Plots

Surface VI and %cover residual scattergraphs

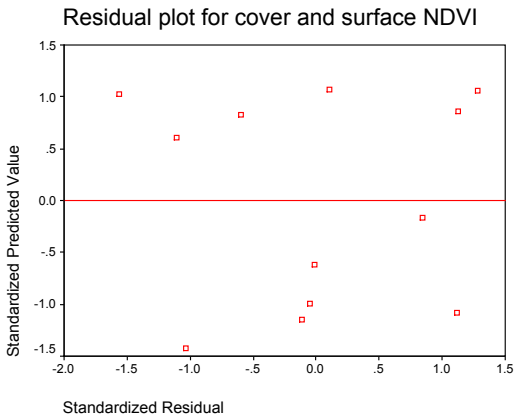

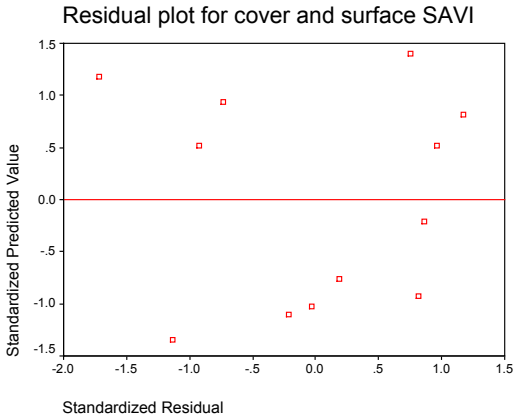

IKONOS VI and %cover residual scattergraphs

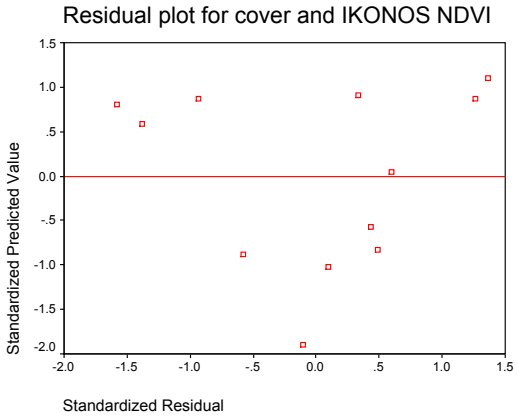

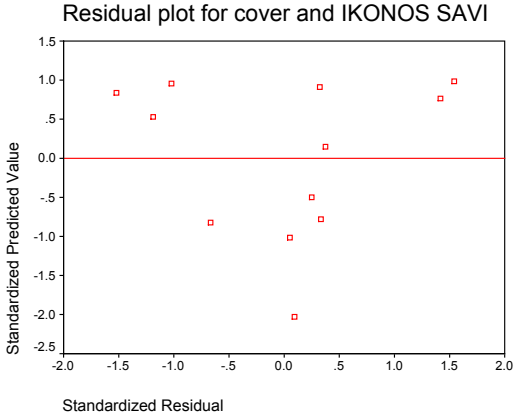

Landsat VI and %cover residual scattergraphs

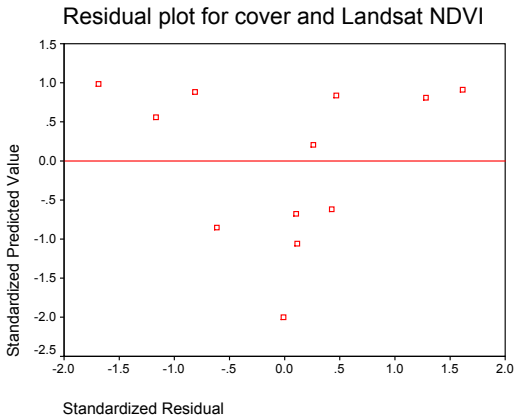

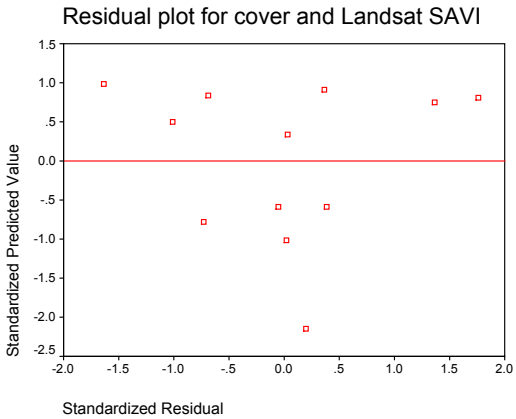

Vita

Name:	Gita Joan Laidler
Place and Year of Birth:	Toronto, 1977
Education:	Nepean High School, 1991 – 1996
	York University, 1996 – 2000 B.E.S. (Honours, Environmental Studies) 2000
	Queen's University, 2000 – 2002 M.Sc. 2002
Experience:	Research Assistant, 05/1999 – 08/1999, Earth Observations Laboratory, Centre for Research in Earth and Space Technology, Toronto
	Research Assistant, 11/1999 – 08/2000, Department of Psychology, York University
	Teaching Assistant**,** 09/2000 – 04/2001, Department of Geography, Queen's University GPHY 242 and 342 (Introductory and intermediate remote sensing)
	Teaching Assistant, 09/2001 – 04/2002, Department of Geography, Queen's University GPHY 210 (Introduction to climate change and global ecosystems) and GPHY 249 (Generation, display, and analysis of geographic information)
Awards:	Entrance Scholarship, York University, 1996 – 1997
	Sport and Recreation Student Award, York University, 1998 – 1999
	Continuing Scholarship, York University, 1998 – 1999
	Yeowomen Volleyball Excellence Award, York University, 1998 – 1999
	FES Undergraduate Achievement Award, York University, 1999 – 2000
	FES Senior Honours Work Award of Distinction, York University, 1999 – 2000
	FES Dean's Honour Roll, York University, 1996 – 2000

Canadian Interuniversity Sport Academic All-Canadian, York University, 1996 – 2000

Faculty of Graduate Studies Dean's Honour Roll, Queen's University, 2000 – 2001

Northern Scientific Training Program Research Funding, Queen's University, 2000 – 2001

Natural Resources Canada (NRCan) Earth Science NSERC Supplement, Queen's University, 2000 – 2001

National Science and Engineering Research Council (NSERC) PGS A Scholarship, Queen's University, 2000 – 2002

Ontario University Athletics East Division Women's Volleyball First Team All-Star, Queen's University, 2001 – 2002

Publications:

Reeves, R., Elder, J., and Laidler, G. (2000) Accuracy of the Canadian Digital Elevation Data and the National Topographic Database in the Gatineau Region of Québec. *Geomatica*. 51,1: 57-64.

Laidler, G. and Treitz, P. (2001) Biophysical Remote Sensing in Arctic Environments. *Progress In Physical Geography*. In press.

Conference Presentations:

Laidler, G. and Treitz, P. (2001) *A Preliminary Investigation into the Utility of Spectral Vegetation Indices for Estimating Biomass in an Arctic Tundra Environment.* Annual General Meeting of the Canadian Association of Geographers, McGill University, Montréal, Québec. May, 30.

Laidler, G. 2001. *Information Requirements for Impact Assessment of Hydro-electric Development.* Annual General Meeting of the Canadian Association of Geographers, McGill University, Montréal, Québec. May, 31.

Laidler, G. 2000. *Merging Traditional Ecological Knowledge with Scientific Investigation – A Remote Sensing Perspective.* The 2nd Annual Aboriginal Issues Symposium, Queen's University, Kingston, Ontario. November, 5.